



Ministério da
Ciência e Tecnologia



INPE-00000-TDI/0000

**STUDYING SIGNATURES OF ALTERNATIVE
COSMOLOGIES IN THE COSMIC MICROWAVE
BACKGROUND**

Dennis Fernandes Alves Bessada

Tese de Doutorado do Curso de Pós-Graduação em Astrofísica, orientada pelo Dr. Oswaldo Duarte Miranda, e com a colaboração do Prof. Dr. William H. Kinney (SUNY/Buffalo) aprovada em 19 de Fevereiro de 2010.

Original document registry:
<<http://urlib.net/xxx>>

INPE
São José dos Campos
2010

PUBLISHED BY:

Instituto Nacional de Pesquisas Espaciais - INPE

Gabinete do Diretor (GB)

Serviço de Informação e Documentação (SID)

Caixa Postal 515 - CEP 12.245-970

São José dos Campos - SP - Brasil

Tel.:(012) 3945-6911/6923

Fax: (012) 3945-6919

E-mail: pubtc@sid.inpe.br

EDITORIAL COMMITTEE:**Chairperson:**

Dr. Gerald Jean Francis Banon - Coordenação Observação da Terra (OBT)

Members:

Dr^a Maria do Carmo de Andrade Nono - Conselho de Pós-Graduação

Dr. Haroldo Fraga de Campos Velho - Centro de Tecnologias Especiais (CTE)

Dr^a Inez Staciari Batista - Coordenação Ciências Espaciais e Atmosféricas (CEA)

Marciana Leite Ribeiro - Serviço de Informação e Documentação (SID)

Dr. Ralf Gielow - Centro de Previsão de Tempo e Estudos Climáticos (CPT)

Dr. Wilson Yamaguti - Coordenação Engenharia e Tecnologia Espacial (ETE)

DIGITAL LIBRARY:

Dr. Gerald Jean Francis Banon - Coordenação de Observação da Terra (OBT)

Marciana Leite Ribeiro - Serviço de Informação e Documentação (SID)

Jefferson Andrade Ancelmo - Serviço de Informação e Documentação (SID)

Simone A. Del-Ducca Barbedo - Serviço de Informação e Documentação (SID)

DOCUMENT REVIEW:

Marciana Leite Ribeiro - Serviço de Informação e Documentação (SID)

Marilúcia Santos Melo Cid - Serviço de Informação e Documentação (SID)

Yolanda Ribeiro da Silva Souza - Serviço de Informação e Documentação (SID)

ELECTRONIC EDITING:

Viveca Sant´Ana Lemos - Serviço de Informação e Documentação (SID)



Ministério da
Ciência e Tecnologia



INPE-00000-TDI/0000

**STUDYING SIGNATURES OF ALTERNATIVE
COSMOLOGIES IN THE COSMIC MICROWAVE
BACKGROUND**

Dennis Fernandes Alves Bessada

Tese de Doutorado do Curso de Pós-Graduação em Astrofísica, orientada pelo Dr. Oswaldo Duarte Miranda, e com a colaboração do Prof. Dr. William H. Kinney (SUNY/Buffalo) aprovada em 19 de Fevereiro de 2010.

Original document registry:
<<http://urlib.net/xxx>>

INPE
São José dos Campos
2010

Cataloging in Publication Data

Sobrenome, Nomes.

Cutter Studying Signatures of Alternative Cosmologies in the Cosmic Microwave Background / Dennis Fernandes Alves Bessada. – São José dos Campos : INPE, 2010.

xxiv + 188 p. ; (INPE-00000-TDI/0000)

Dissertação ou Tese (Mestrado ou Doutorado em Nome do Curso) – Instituto Nacional de Pesquisas Espaciais, São José dos Campos, AAAA.

Orientador : José da Silva.

1. Cosmology. 2. Inflation 3. Non-inflationary models of the early universe. 4. Cosmic Microwave Background Radiation. 5. Alternative Cosmologies I. Título.

CDU 000.000

Copyright © 2010 do MCT/INPE. Nenhuma parte desta publicação pode ser reproduzida, armazenada em um sistema de recuperação, ou transmitida sob qualquer forma ou por qualquer meio, eletrônico, mecânico, fotográfico, reprográfico, de microfilmagem ou outros, sem a permissão escrita do INPE, com exceção de qualquer material fornecido especificamente com o propósito de ser entrado e executado num sistema computacional, para o uso exclusivo do leitor da obra.

Copyright © 2010 by MCT/INPE. No part of this publication may be reproduced, stored in a retrieval system, or transmitted in any form or by any means, electronic, mechanical, photocopying, recording, microfilming, or otherwise, without written permission from INPE, with the exception of any material supplied specifically for the purpose of being entered and executed on a computer system, for exclusive use of the reader of the work.

**ATENÇÃO! A FOLHA DE
APROVAÇÃO SERÁ INCLU-
IDA POSTERIORMENTE.**

Mestrado ou Doutorado em Nome do
Curso

To my parents Cida and António (in memoriam).

ACKNOWLEDGEMENTS

These acknowledgments are divided into two parts: first, to the Portuguese-speaking people, and second, to the English-speaking ones.

Meus profundos agradecimentos vão, primeiramente, à minha mãe, Aparecida, que permitiu, com a educação que me proporcionou, chegar a este ponto. Agradeço também à Elaine, que me acompanhou durante este período repleto de trabalho e de importantes desafios.

Agradeço também ao meu orientador, Professor Oswaldo Duarte Miranda, que me presenteou com o projeto de pesquisa que culmina nesta tese de doutorado. Muito obrigado pela paciência e cuidadosa orientação. Agradeço também ao Professor Raul Abramo, do Instituto de Física da USP (IFUSP), por suas valiosas contribuições neste projeto. Agradeço também à CAPES pelo apoio financeiro tanto no Brasil quanto nos Estados Unidos, sem o qual a realização desta tese seria impossível. Agradeço também à FAPESP que, por meio do Projeto Temático do Grupo Gráviton, do INPE, financiou minha participação em muitos eventos no Brasil e no exterior.

Também gostaria de agradecer aos meus orientadores do passado, cujo importante auxílio foi fundamental na minha preparação para realizar este trabalho: Professor Gerson Francisco, do Instituto de Física Teórica (IFT-UNESP), que me orientou na segunda fase de meu mestrado; Professor Nathan Berkovits do IFT-UNESP, que me orientou na iniciação científica e na primeira fase do mestrado; Professor Abraham Hirsz Zimmerman, também do IFT-UNESP, que me aceitou como aluno de iniciação científica ainda em meu primeiro ano de graduação. Também agradeço imensamente ao Professor Henrique Fleming, do IFUSP, cuja orientação em meus primeiros meses do curso de graduação foram fundamentais para minha formação como físico.

Agradeço também aos Professores Nelson Pinto-Neto, do Centro Brasileiro de Pesquisas Físicas (CBPF), ao Professor Jailson Alcaniz, do Observatório Nacional (ON), e aos Professores Carlos Alexandre Wuensche de Souza e José Carlos Neves de Araujo (ambos da Divisão de Astrofísica do INPE) que me honraram ao aceitar participar de minha banca de doutoramento.

Gostaria de agradecer também aos Professores José Antônio de Freitas Pacheco, José Carlos Neves de Araujo, Odylio Denys de Aguiar, Carlos Alexandre Wuensche de Souza, Thyrso Villela e Armando Bernui, da DAS-INPE, pelas discussões fundamentais acerca da primeira fase deste trabalho. Também agradeço aos amigos Claudio Brandão e César Costa, que muito me auxiliaram com a parte computacional desta tese.

Para finalizar, gostaria de agradecer aos amigos aqui do INPE, que tornam a DAS um excelente local para se trabalhar: Douglas Barzon, Chico (o arauto!!), Márcio, Claudio, César, Karleyne, Mariana, Camila, Marina, Cristiane, Germán, Leonardo, Julio, Eder, Thiago, Tereza, Danielle, Sônia, Valdirene, Nilda, Valéria, Reitano, Néri, Alan e o Edinho. Também agradeço a amizade dos Professores da DAS: Ana Zodi, Joaquim, Cláudia, Cecatto, Reinaldo Carvalho, Hugo, e Francisco Jablonski.

Now, I would like to thank Will Kinney for having me at SUNY Buffalo, and for collaborating deeply in this work. Without his guidance half of this work would have not been possible. I also wish to thank Dejan Stojkovic and John Wang for the great talks and meetings we had during my stay at Buffalo. I have learnt a lot from you! It was really great to work together!

ABSTRACT

In the present thesis we study the signatures of four alternative cosmological models in the Cosmic Microwave Background: Massive Gravity, the Modified Fierz-Pauli model (MFP), DBI inflation and Tachyacoustic Cosmology. The first two models are studied as alternatives to the Friedmann-Robertson-Walker cosmology, and we showed that both models lead to the same results for tensor perturbations, whereas for vector modes the MFP model leads to non-decaying amplitudes, unlike Massive Gravity and General Relativity (GR), where such modes are washed out by the expansion of the universe. We calculated the vector and tensor contributions to the Sachs-Wolfe (SW) effect, and derived the corresponding Boltzmann equations, arguing qualitatively that vector modes in the MFP model would leave a distinct signature in CMB polarization. Also, we calculated the power spectrum for CMB anisotropies induced by the tensor modes in Massive Gravity, and showed that such massive modes would leave a clear signature for low multipoles, $\ell < 30$. We derived new solutions for DBI inflation, and showed that they encompass *all* the well-known inflationary potentials found in the canonical model. We also worked out a particular case, a non-canonical model with large-field potentials, and compared our predictions with the current available data, showing that our solutions in DBI are in good agreement with observations. A distinguishing feature of our solutions is the production of large amplitudes of non-gaussianity, which can be a powerful observable to discriminate among inflationary models. We also propose an alternative to inflation, the tachyacoustic model, in which we do obtain a nearly scale-invariant spectrum of primordial perturbations and solve the horizon problem in a *decelerating* universe. These goals are achieved by a k-essence model with superluminal speed of sound, which is causally self-consistent. The tachyacoustic model does not solve entirely the flatness problem, but a work in progress is being conducted to tackle this issue.

STUDYING SIGNATURES OF ALTERNATIVE COSMOLOGIES IN THE COSMIC MICROWAVE BACKGROUND

RESUMO

Estudamos, na presente tese de doutoramento, assinaturas de quatro modelos cosmológicos alternativos na Radiação Cósmica de Fundo em Microondas (CMB), a saber: Gravitação Massiva, Modelo de Fierz-Pauli modificado (MFP), inflação DBI e cosmologia Taquiacústica. Os dois primeiros modelos foram estudados como alternativas à cosmologia usual, descrita pela métrica de Friedmann-Robertson-Walker, e demonstramos que ambos os modelos fornecem os mesmos resultados no tocante a perturbações tensoriais, ao passo que o modelo MFP produz amplitudes de modos vetoriais que não decaem com a expansão do universo, diferentemente da Gravitação Massiva e da Relatividade Geral, onde tais modos simplesmente desaparecem com a respectiva expansão. Calculamos as contribuições dos modos vetoriais e tensoriais para o efeito Sachs-Wolfe (SW), e derivamos as equações de Boltzmann correspondentes, argumentando qualitativamente que os modos vetoriais deixariam uma assinatura distinta na polarização da CMB. Também calculamos o espectro de potências de anisotropias da CMB induzido por modos tensoriais na Gravitação Massiva, e mostramos que tais modos massivos deixariam uma clara assinatura para baixos multipolos, ou seja, $\ell < 30$. Derivamos novas soluções para a inflação DBI, e mostramos que as mesmas incluem *todos* os bem-conhecidos potenciais encontrados na teoria de inflação canônica. Dentre as soluções encontradas, aprofundamos-nos numa em particular, que consiste em um modelo não-canônico com potencial do tipo “*large-field*”, e comparamos nossas previsões com os dados disponíveis, mostrando que nossas soluções no modelo DBI estão em pleno acordo com as observações. Uma característica distinta de nossas soluções se refere à produção de largas amplitudes de não-gaussianidade, que consiste em um observável eficiente para se testar e selecionar diferentes modelos inflacionários. Propomos, também, um modelo alternativo à inflação, que denominamos modelo *taquiacústico*, o qual fornece um espectro quase-invariante de escala para perturbações escalares e soluciona o problema do horizonte no contexto de um universo *deflacionário*, ou seja, com expansão desacelerada. Tais resultados são obtidos por meio de um modelo de k-essência cuja velocidade de propagação de perturbações é superluminal, sem, no entanto, violar qualquer princípio de causalidade. O modelo taquiacústico não soluciona totalmente o problema da planura do universo, mas um trabalho em andamento visa remover este obstáculo.

LIST OF FIGURES

	<u>Pág.</u>
2.1 The major events in the very early universe. Figure borrowed from (BAUMANN, 2009).	21
4.1 The solution to the horizon problem in the inflationary cosmology. Source: Baumann (2009).	44
4.2 Large-field polynomial potentials.	50
4.3 Small-field polynomial potentials.	52
4.4 Hybrid potentials.	53
5.1 Interactions taking place at recombination. Adapted from (DODELSON, 2003).	69
5.2 Coordinate system for the photon momentum \vec{p}	74
5.3 The time evolution of the normalized GW amplitudes $h_n(\tau)/h_n(\tau_r)$. Compare with Figure 1 of (BASKARAN et al., 2006).	86
5.4 Temperature anisotropies induced by GWs in GR.	88
5.5 CMB polarization power spectra. Figure adapted from (BOCK,2008).	88
6.1 The time evolution of the normalized GW amplitudes for $n = 5$	100
6.2 For $n = 10$	100
6.3 For $n = 50$	101
6.4 For $n = 100$	101
6.5 For $n = 500$	102
6.6 For $n = 1000$	102
6.7 The “tail of Figure 6.4 zoomed in, showing the phase difference in the tensor modes at very low redshifts for both massless and massive gravitons.	103
6.8 The correlation functions C_ℓ^{TT} for GR and Massive Gravity. Note that the massive gravitons leave a signature on the spectrum for low multipoles.	108
6.9 The low-multipole “tail” in the TT correlation function. Note the quite distinct signatures for $\ell < 30$ for the mass range selected.	109
7.1 The observables n_s (left), r (right) as a function of the exponent of the speed of sound β for each value of p ($V(\phi) \propto \phi^p$) for $N = 46$	129
7.2 The observables n_s (left), r (right) as a function of the exponent of the speed of sound β for each value of p ($V(\phi) \propto \phi^p$) for $N = 60$	130

7.3	The observable f_{NL} as a function of the exponent of the speed of sound β (left) for each value of p ($V(\phi) \propto \phi^p$) for $N = 46$. On right is depicted the behavior of f_{NL} compared to r	131
7.4	The observable f_{NL} as a function of the exponent of the speed of sound β (left) for each value of p ($V(\phi) \propto \phi^p$) for $N = 60$. On right is depicted the behavior of f_{NL} compared to r	131
7.5	68 % (black) and 95 % C.L. (red) on the n_s and r parameter space for WMAP5 alone. In each panel we plot the values of n_s and r for a specific potential $V(\phi) \propto \phi^p$ according to the exponent β of the speed of sound.	132
C.1	The six possible polarization modes for an arbitrary metric theory of gravitation. In terms of the NP amplitudes, we have the following: (a) $\text{Re } \Psi_4$; (b) $\text{Im } \Psi_4$; (c) Φ_{22} ; (d) Ψ_2 ; (e) $\text{Re } \Psi_3$; (f) $\text{Im } \Psi_3$. Figure adapted from (WILL, 2005).	162

LIST OF TABLES

	<u>Pág.</u>
1.1 The structure of the SCM.	3
1.2 The structure of the Alternative Cosmologies.	3
2.1 The basic constituents of the universe.	18
7.1 The sign rule for models with $\alpha + \beta = -2$ and $\phi > 0$ (BESSADA et al., 2009).	117
7.2 The sign rule for models with $\alpha + \beta \neq -2$, $\alpha < 0$, and $\phi > 0$ (BESSADA et al., 2009).	118
7.3 The sign rule for models with $\alpha + \beta \neq 0$, $\alpha > 0$ and $\phi > 0$ (BESSADA et al., 2009).	118
7.4 A summary of the distinct models discussed in this work.	128

LIST OF ABBREVIATIONS

CMB	–	Cosmic Microwave Background
DBI	–	Dirac-Born-Infeld
FRW	–	Friedmann-Robertson-Walker
GR	–	General Relativity
GW(s)	–	Gravitational Wave(s)
Λ CDM	–	A FRW model with Cold Dark Matter and Dark Energy represented by a cosmological constant Λ
MFP	–	Modified Fierz-Pauli Model
PGW(s)	–	Primordial Gravitational Wave(s)
QFT	–	Quantum Field Theory
SCM	–	Standard Cosmological Model

LIST OF SYMBOLS

$\{\alpha, \beta, \dots\} = \{0, 1, 2, 3\}$	– Spacetime coordinates
$\{i, j, \dots\} = \{1, 2, 3\}$	– Spatial coordinates
$\eta_{\alpha\beta} = \text{diag}\{+, -, -, -\}$	– Signature of the Minkowski metric
$\dot{f} = \frac{df}{dt}$	– Derivatives with respect to the cosmic time
$f' = \frac{df}{d\eta}$	– Derivatives with respect to the conformal time
$f' = \frac{df}{d\phi}$	– From Chapter 7 on, a prime indicates a derivative with respect to the scalar field ϕ
$M_P = 1/\sqrt{8\pi G}$	– Reduced Planck mass
z	– Redshift; from Chapter 4 on, indicates the Mukhanov variable
$c = \hbar = 1$	– Natural units adopted, except in Chapters 5 and 6

CONTENTS

	<u>Pág.</u>
1 INTRODUCTION	1
1.1 Why Alternative Cosmologies?	1
1.1.1 A modified model for gravitation: Massive Gravity	4
1.1.2 A non-canonical model of inflation: DBI Inflation	4
1.1.3 A non-inflationary model: Tachyacoustic Cosmology	6
1.2 Why look for Signatures in the CMB?	7
1.3 Organization of the present thesis	8
2 THE HOMOGENEOUS AND ISOTROPIC UNIVERSE	9
2.1 The Friedmann-Robertson-Walker Metric	9
2.2 Cosmological Distances and Horizons	11
2.3 Cosmological Dynamics: The Friedmann and Raychaudhuri Equations	13
2.4 The Energy and Matter Content of the Universe	17
2.5 The Birth of CMB: Recombination and Decoupling	19
3 THE THEORY OF COSMOLOGICAL PERTURBATIONS	23
3.1 Disturbing the smoothness of the universe	23
3.1.1 Metric fluctuations	23
3.1.2 Density Perturbations	27
3.2 Gauge Symmetries for Cosmological Perturbations	30
3.3 Einstein equations for Cosmological Perturbations	35
4 THE INFLATIONARY UNIVERSE	39
4.1 The Cosmic Puzzles	39
4.1.1 The Flatness Problem	39
4.1.2 The Horizon Problem	40
4.2 The Inflationary Paradigm	41
4.3 Flow Hierarchy in Inflation	45
4.4 Inflationary Potentials	50
4.4.1 Large-Field Inflationary Potentials	50
4.4.2 Small-field polynomial potentials	51
4.4.3 Hybrid potentials	52

4.4.4	Exponential potentials - Power-law Inflation	53
4.5	Quantum Fluctuations from Inflation	54
4.5.1	Introducing Perturbations	54
4.5.2	Evolution of the Scalar Modes	55
4.5.3	Evolution of the Tensor Modes	57
4.5.4	Quantizing the Modes	57
4.6	Solutions to the Mode Equation	59
4.6.1	Slow-Roll Solutions	60
4.6.2	The Power-Law Solution	61
4.6.3	The de Sitter Solution	63
4.7	Power Spectrum	63
5	THEORY OF CMB ANISOTROPIES AND POLARIZATION GENERATED BY PRIMORDIAL TENSOR MODES	67
5.1	Boltzmann Equations in Cosmology	67
5.2	Radiative Transfer induced by Tensor Modes	69
5.3	The T, E and B-Modes	78
5.4	The Solutions to the Boltzmann Equations	82
5.5	Correlation functions	84
6	SIGNATURES OF MASSIVE GRAVITONS IN THE CMB	89
6.1	Theories of Gravity with Massive Gravitons	89
6.1.1	The Modified Fierz-Pauli Model	90
6.1.2	Massive Gravity	92
6.2	Cosmological Perturbations in Massive Theories of Gravity	94
6.2.1	Cosmological Perturbations in the MFP Model	95
6.2.2	Cosmological Perturbations in Massive Gravity	96
6.3	Primordial Massive Tensor Modes	97
6.4	Boltzmann Equations for Massive Gravitons	104
6.4.1	The Sachs-Wolfe effect induced by Massive Gravitons	104
6.4.2	The Basis for Thomson Scattering	105
6.4.3	The Full Boltzmann Equations	106
6.5	CMB Anisotropies induced by Massive Tensor Modes	107
7	SIGNATURES OF DBI INFLATION IN THE CMB	111
7.1	DBI Inflation - An Overview	111
7.2	The Model	113

7.2.1	The General Setting	113
7.2.2	The Solutions $\alpha + \beta = -2$	116
7.2.3	The Solutions $\alpha + \beta \neq -2$	117
7.3	Classes of inflationary potentials in DBI inflation	119
7.3.1	Large-field polynomial potentials	119
7.3.2	Small-field polynomial potentials	122
7.3.3	Hybrid potentials	125
7.3.4	Exponential potentials	126
7.4	An Application of Non-Canonical Large-Field Polynomial Models	128
8	SIGNATURES OF TACHYACOUSTIC COSMOLOGY IN THE	
	CMB	133
8.1	Tachyacoustic Cosmology	133
8.2	Cosmological solutions for constant flow parameters	136
8.3	Reconstructing the Action	139
8.3.1	$n = 0$: A Cuscuton-like model	140
8.3.2	$n = 3$: The DBI model	142
8.4	Cosmological Perturbations for constant flow parameters	143
8.5	Boundary Action	146
9	CONCLUSIONS AND PERSPECTIVES	149
	APPENDIX A - BASIC DEFINITIONS OF GR	153
A.1	Some key tensors in GR	153
	APPENDIX B - GAUGE TRANSFORMATIONS IN GR	155
B.1	Infinitesimal Coordinate Transformations in GR	155
B.2	Application: Weak Gravitational Fields in GR - Gravity Waves	155
	APPENDIX C - POLARIZATION STATES FOR AN ARBI-	
	TRARY METRIC THEORY OF GRAVITATION	159
C.1	The Newman-Penrose Formalism	159
C.2	Polarization of GWs	160
C.2.1	The general setting	161
C.2.2	Polarization of GWs in GR	165
	APPENDIX D - SCALAR FIELD THEORIES - K-ESSENCE	167
D.1	k-Essence Dynamics	167

D.2	Flow Hierarchy for k-Essence models	170
D.3	Cosmological Perturbations in k-Essence Models	172
D.4	Causal Structure of k-Essence Models	174
	REFERENCES177

1 INTRODUCTION

The best way to introduce a subject is through its title. If the author is fortunate enough to come up with the right title, then it would guide us through the main motivations of the work as the Sibyl guided Aeneas¹ or Virgil guided Dante Alighieri² in the deepest darkness of the underworld.

In our case, the title says *Studying Signatures of Alternative Cosmologies in the Cosmic Microwave Background*. As scientists, we must ask questions, and the following ones seem to be the most appropriate:

- Why Alternative Cosmologies?
- Why look for Signatures in the CMB?

A sketch of the answers is provided below. We hope they suffice!

1.1 Why Alternative Cosmologies?

The flat homogeneous and isotropic universe became the most successful cosmological paradigm proposed so far. The great success of this model lays on three fundamental predictions: the expansion of the universe, as shown by Edwin Hubble, the *primordial nucleosynthesis*, which establishes the abundances of light nuclei formed in the first three minutes of the universe (ALPHER et al., 1948)³, and the generation of the *Cosmic Microwave Background*, a relic radiation emerging from the formation process of the first neutral atoms of the universe, which took place around 380.000 years after the Big Bang (DICKE et al., 1965; PEEBLES, 1968). All such predictions had been successfully borne out by high-precision experiments thanks to the great technological leaps achieved in the past three decades. However, the same experiments that endorsed the homogeneous and isotropic universe also uncovered another problems; among them, it is worth mentioning the problems of the cosmological horizon and flatness, of the “missing matter”, and the problem of present-day acceleration of the universe. To tackle these issues, three main theoretical ideas have been pushed forward to a certain degree of success: the mechanism of *Cosmological Inflation* to provide the answers to the problems of the early universe (GUTH,

¹See *The Aeneid*, one of the jewels of Ancient Literature.

²See Dante Alighieri’s *The Divine Comedy*, the monument of the Pre-Renaissance Literature.

³See reference (IOCCO et al., 2009) for an updated account of this subject.

1981; LINDE, 1982; ALBRECHT; STEINHARDT, 1982), the existence of *Dark Matter* (DM)⁴ and *Dark Energy* (DE)⁵ as components in the cosmic inventory. These three ingredients (with the cosmological constant Λ playing the role of DE), associated with a flat, isotropic and homogeneous description of the universe make up what we call today the *Standard Cosmological Model* (SCM, also called *inflation plus Λ CDM model*), the most widely accepted paradigm to understand the universe as a whole.

However, even being supported by the current experiments, there is a plethora of open questions which still "haunts" the standard paradigm:

1. Cosmological Inflation, in its current form, does not solve the key problem of the initial singularity. Also, it predicts density perturbations with *nearly* Gaussian correlations, which might not be true: WMAP5 results suggest that such correlations are likely non-Gaussian (KOMATSU et al., 2009).
2. What is the nature of DM? Is the missing mass problem an indication that GR needs some modification on cosmological scales?
3. What is the nature of DE? Is the present-day acceleration of the universe driven by this exotic component, or does GR fail on large scales, demanding a modification?

These unanswered questions in the SCM framework clearly indicate that our current cosmological paradigm cannot be the ultimate model of the whole universe (or the best possible approximation to). The SCM provides a good starting point, but further steps should be taken. The quest for such additional steps motivates the study of *Alternative Cosmologies*. However, how would such modified models look like?

Our starting point is the SCM itself. It starts with the inflationary phase after the Big Bang, whose end is characterized by the decay of its scalar field (the *inflaton*) into ultra-relativistic particles (the reheating process - see (BASSETT et al., 2006) for a review), and hence initiating the radiation-dominated phase. From this point on,

⁴See (EINASTO, 2009) for the astrophysical evidence of DM, (BERTONE et al., 2005) for a review of Particle DM and (TAOSO et al., 2008) for the requirements that must be fulfilled by the DM candidates.

⁵See (COPELAND et al., 2006) and (FRIEMAN et al., 2008) for a review of the problems and the candidates for DE.

the standard FRW model with DM and DE comes into play and drives the expansion of the universe. Therefore, the structure of the SCM model is composed of an initial phase at the early universe (canonical inflation), then followed by a transition epoch (reheating), which bridges the first with the third phase characterized, among other well-known phenomena, by the primordial nucleosynthesis, recombination, and the present-day acceleration. We summarize this structure in Table 1.1.

TABLE 1.1 - The structure of the SCM.

Model	Initial phase (Prelude)	Transition epoch (Interlude)	Final phase (Postlude)
SCM	Canonical Inflation	Reheating	FRW model with DM and DE

Following the structure shown above, we could knit together different models to build up an alternative cosmology. In Table 1.2 we summarize all the possibilities obtained by changing the structure delineated in Table 1.1.

TABLE 1.2 - The structure of the Alternative Cosmologies.

Alternative Model	Prelude	Interlude	Postlude
1.	Canonical Inflation	Reheating	Modified FRW model to mimic DM and/or DE
2.	Modified Inflation	Field decay	FRW model
3.	Non-inflationary phase	Field decay	FRW model
4.	Non-inflationary phase	Field decay	Modified FRW model to mimic DM and/or DE

We could have set up other structures for the alternative cosmologies, but the four ones introduced seem to be the simplest to start with, in particular the first three. By the way, analogy with well grounded theories and simplicity will be the guiding principles of this work. They will be also leading principles to choose among the the models to be studied in this thesis, which we briefly outline below.

1.1.1 A modified model for gravitation: Massive Gravity

Let us take a deeper look at the possible constructions proposed in Table 1.2. The first class of models preserves canonical inflation, but requests a modified FRW model. This model should, in turn, be a cosmological solution to a modified theory of gravitation, in the same way as the usual FRW model is a particular solution to the Einstein equations. Then, what is the simplest modification that can be made to GR in order to derive such cosmological model? Quantum Field Theory (QFT) provides a precious clue.

In QFT the simplest models are related to massless and neutral free fields. The next degree of complexity is implemented by adding mass and charge to the field. Then, more complex constructions can be made by adding interactions, and so forth. Since GR deals with classical gravitational fields, whose “quanta” are *massless* spin-2 particles (the *gravitons*), the next natural step toward a modified version of gravity is the inclusion of *massive* spin-2 particles into the theory, analogously to what is done in the realm of QFT. Therefore, it seems that the simplest generalization of GR is a theory of gravitation with *massive gravitons*. There are several attempts to introduce massive gravitons in GR, but in this thesis we will address two particular models: the *modified Fierz-Pauli* model, as studied in (FINN; SUTTON, 2002), and *Massive Gravity*, as developed in (RUBAKOV, 2004) and (DUBOVSKY, 2004). We shall investigate the cosmological consequences of massive gravitons (BESSADA; MIRANDA, 2009b; BESSADA; MIRANDA, 2009a) as representatives of the alternative cosmologies in the Class 1 of Table 1.2.

1.1.2 A non-canonical model of inflation: DBI Inflation

The second class of models presented in Table 1.2 includes models with modified inflationary phases and the standard FRW cosmology. What would be the simplest modification to be done in the canonical inflationary model? As we shall discuss later on, the kinetic term of the canonical inflaton is proportional to the time derivative of the field squared; then, what makes a single-field inflationary model differ from any other is its potential term, for different potentials lead to different inflationary pictures (DODELSON et al., 1997). Then, an interesting option left for modification is the mathematical form of the kinetic term, which gives rise to the so-called *k-inflation* (ARMENDARIZ-PICON et al., 1999). A particular form of k-inflation, called *DBI inflation* (SILVERSTEIN; TONG, 2004), (ALISHAHIHA et al., 2004) (see (MCALLISTER;

(SILVERSTEIN, 2008) for a review), where DBI stands for Dirac, Born and Infeld, may give answers that canonical inflation cannot do ⁶. As an example, canonical inflation is phenomenological in character, and a fundamental explanation of it is still missing; in other words, canonical inflation was simply “put by hand” to solve the cosmological puzzles at the early universe, and does not seem to be derived from any fundamental physical theory. DBI inflation, on the other hand, is a low-energy solution in String theory, which is one of the candidates to be such fundamental theory of the Nature. String theory predicts a broad class of scalar fields associated with the compactification of extra dimensions and the configuration of lower-dimensional branes moving in a higher-dimensional bulk space. This fact gave rise to some phenomenologically viable inflation models, such as the KKLMMT scenario (KACHRU et al., 2003), Racetrack Inflation (BLANCO-PILLADO et al., 2004), Roulette Inflation (BOND et al., 2007), alongside with DBI scenario. But why DBI inflation, and not any other of the models mentioned above?

First of all, DBI inflation is a particular case of a wider class of scalar-field models, the so-called k-inflation, which is characterized by a far-reaching feature: they possess a varying speed of sound. General k-inflationary models possess a complex flow hierarchy (AFSHORDI et al., 2007b), which depends on the derivatives with respect to the number of e-folds N of the Hubble parameter H , of the speed of sound c_s , and of \mathcal{L}_X , the derivative of the k-essence Lagrangian with respect to the canonical kinetic term X . In the case of DBI inflation, the flow hierarchy is simplified due to the property that $\mathcal{L}_X \equiv c_s^{-1}$; also, DBI inflation admits several exact solutions to the flow equations (SPALINSKI, 2007a; CHIMENTO; LAZKOZ, 2008; SPALINSKI, 2008; KINNEY; TZIRAKIS, 2008; TZIRAKIS; KINNEY, 2009). Another important feature is connected to the fact that a low sound speed leads to substantial non-Gaussianity (ALISHAHIHA et al., 2004; CHEN et al., 2007; SPALINSKI, 2007a; BEAN et al., 2008a; LOVERDE et al., 2008), which would be a distinguishing signature of such non-canonical inflationary model.

Therefore, due to this wealth of possible solutions and results, DBI inflation is a potential candidate to provide better responses to the current open questions in the canonical inflationary scenario. We shall investigate the consequences of new

⁶The original work of Born and Infeld is related to a non-linear extension of classical electrodynamics (BORN; INFELD, 1934), which was later reformulated by Dirac (DIRAC, 1960). It became convenient to dub DBI the low-energy version of the string model due to the similarities between its Lagrangian and the original one.

solutions of DBI inflation (BESSADA et al., 2009) as representatives of the alternative cosmologies in the Class 2 of Table 1.2.

1.1.3 A non-inflationary model: Tachyacoustic Cosmology

Last, but not least, let us say some words about the third class of models presented in Table 1.2. They have a non-inflationary model to drive the cosmological phenomena at the very early universe. But, why should we look for non-inflationary models? The answer is quite simple: inflation is *not* the unique way to solve the cosmological puzzles of the very early universe. Also, it is not the only mechanism to generate a nearly scale-invariant spectrum as observed today. Actually, any model in which the comoving Hubble radius *shrinks* will not only solve the horizon problem, but will generate the desired spectrum of perturbations. Another alternatives are the models with a contracting phase, like the Bouncing cosmologies (see (NOVELLO; BERGLIAFFA, 2008) for a review) and the Ekpyrotic scenario (GRATTON et al., 2004) to construct a cosmology consistent with observations. It is also possible to decouple the horizon and flatness problems, for example in theories with a varying speed of light, so that the causal horizon is much larger than the Hubble length (ALBRECHT; MAGUELJO, 1999). It is also possible to solve the horizon problem by a universe which is much older than a Hubble time as in string gas cosmology (BRANDENBERGER, 2009) or island cosmology (DUTTA; VACHASPATI, 2005; DUTTA, 2006), or by the inclusion of extra dimensions (STARKMAN et al., 2001b; STARKMAN et al., 2001a). However, it has been argued that inflation, ekpyrosis and some bouncing models are the *only* mechanisms for generating a scale-invariant spectrum of perturbations (GRATTON et al., 2004; KHOURY; PIAZZA, 2009; PETER et al., 2007).

Therefore, there is enough room for more alternative non-inflationary models. We propose a new alternative, the *Tachyacoustic Cosmology* (BESSADA et al., 2009), in which we solve the horizon problem and generate a nearly scale-invariant spectrum of the fluctuations. The flatness problem is not yet solved, but a work in progress is striving for tackling this issue. We shall investigate the cosmological consequences of the Tachyacoustic model as a representative of the alternative cosmologies in the Class 3 of Table 1.2.

1.2 Why look for Signatures in the CMB?

In the paragraphs above we have outlined some possible theoretical alternatives to tackle the problems found in the SCM. However, it seems quite natural to expect that the laws of Nature emerge from a *single* theory, not from *many*. How can we distinguish among the candidates? At this point it is quite appropriate to quote Feynman's words:

"It doesn't matter how beautiful your theory is, it doesn't matter how smart you are. If it doesn't agree with experiment, it's wrong".

Then, we must find some "laboratory" in the universe to probe the predictions made by such alternative cosmologies. Since we are interested in the physical processes that took place in the very early universe, it is quite natural to search for signatures of such alternative cosmologies in some observable that has been generated back then. But what is the cosmological observable that has been generated so far in the past? Primordial gravity waves (PGW) are by far the best, since they could probe the Big Bang (or whatever model that claims to replace it) itself. However, this task has been not yet accomplished experimentally (see (SATHYAPRAKASH; SCHUTZ, 2009) for the current status of GW Astronomy), and only in the near future PGW could be used as a probe of the very early universe.

The next candidate is CMB. This relic radiation, released around 380.000 after the Big Bang, after the physical processes called *recombination* and *decoupling*, is the oldest "snapshot" of the early universe available. Although recombination took place a long time after inflation (or whatever drove the very early stages of the universe), CMB anisotropies and polarization encode the imprints of the very early universe since classical density perturbations at recombination grew out of quantum fluctuations produced during this period. Such imprints are so powerful that even with the current technological limitations, WMAP5 data acted as a "razor" on the inflationary models, ruling out many of them (KINNEY et al., 2008). Then, future measurements are promising, and the satellite Planck⁷, launched in 2009, is likely to bring great news in the upcoming months.

These are the points that motivate us to look for signatures of alternative cosmologies in the CMB.

⁷<http://www.rssd.esa.int/index.php?project=planck>

1.3 Organization of the present thesis

In order to achieve the goals mentioned in the former two sections, the present thesis is organized as follows: in Chapter 2 we discuss the basic ideas underlying the homogeneous and isotropic universe, whereas in Chapter 3 we introduce the theory of cosmological perturbations. In Chapter 4 we review the main ideas of the inflationary universe, and in Chapter 5 we discuss the generation of CMB anisotropies and polarization in the realm of GR, which concludes the introductory part of the text. In Chapter 6 we start our analysis of alternative cosmologies, focussing the signatures of massive gravitons in the CMB. In Chapter 7 we discuss our solutions in DBI inflation, and study their signatures. In Chapter 8 we introduce the main ideas of the tachyacoustic model, and in the Conclusions we summarize the results obtained throughout this work.

2 THE HOMOGENEOUS AND ISOTROPIC UNIVERSE

In this chapter we summarize the key features of the homogeneous, isotropic and expanding universe as first proposed by Alexander Friedmann in 1922 and 1924. We follow closely (MUKHANOV, 2005), (WEINBERG, 2008), (KINNEY, 2009) and (BAUMANN, 2009).

2.1 The Friedmann-Robertson-Walker Metric

The first ingredient to build a cosmological model rests on the so-called *Cosmological Principle*, which states that the universe is *homogeneous* (*i.e.*, looks the same in every point) and *isotropic* (that is, looks the same in all directions) on the largest scales (larger than 100 or 200 Mpc). In addition to this assumption, which is in agreement with observations, we also consider the fact that the universe is *expanding*, as discovered by Edwin Hubble in the late 1920s. Given such empirical facts, let us now consider a spacetime characterized by a manifold \mathcal{M} and a metric $g_{\alpha\beta}$, whose line element is expressed as

$$ds^2 = g_{00}dt^2 + 2g_{0i}dtdx^i + g_{ij}dx^i dx^j \quad (2.1)$$

for some coordinate chart $\{x^\alpha\}$. The Cosmological Principle demands an isotropic spatial section of \mathcal{M} , which implies that the displacements $+dx^i$ and $-dx^i$ give exactly the same contribution; hence, the terms $dtdx^i$ cannot appear in (2.1), which is consistent only if $g_{0i} = 0$. The vanishing of g_{0i} allows for a foliation of the manifold into spatial 3-surfaces Σ of constant time; as a result, any observer sitting on Σ measures the same time t , the so-called *cosmic time*. If we demand that Σ be homogeneous, the component g_{00} must be constant, otherwise two points on two spatial sections Σ_1 and Σ_2 at times t_1 and t_2 would be distinguishable, which violates the requirement of homogeneity. Since we can get rid of g_{00} by a time redefinition, we simply take the normalization $g_{00} = 1$ for the sake of simplicity. It can be proved (WEINBERG, 1972) that isotropy at all points of Σ implies homogeneity, so that Σ is a *maximally symmetric subspace* of \mathcal{M} , and then

$$ds^2 = dt^2 - a(t)^2 \left[\frac{dr^2}{1 - Kr^2} + r^2 (d\theta^2 + \sin^2 \theta d\varphi^2) \right], \quad (2.2)$$

where $a(t)$ is the *scale factor*, which characterizes the relative size of the spacelike hypersurfaces Σ at different times, and we have adopted the spherical coordinates

r, θ, φ to characterize this spatial section. The *curvature* parameter K takes the values $-1, 0$ or $+1$, for a negatively, flat or positively curved Σ , respectively. The quantity defined by

$$H(t) \equiv \frac{\dot{a}(t)}{a(t)}, \quad (2.3)$$

also called *Hubble parameter*, measures the expansion rate of the universe, and it is one of the key cosmological parameters. The metric (2.2) is called *Friedmann-Robertson-Walker* (FRW) metric.

It is convenient to cast the FRW metric into a more symmetric form, which can be done by means of cartesian coordinates; the result is

$$ds^2 = dt^2 - a(t)^2 \left[\frac{dx^2 + dy^2 + dz^2}{(1 + Kr^2/4)^2} \right], \quad (2.4)$$

where

$$r^2 = x^2 + y^2 + z^2. \quad (2.5)$$

Also, we can write the FRW metric (2.4) as

$$ds^2 = dt^2 - a(t)^2 \gamma_{ij} dx^i dx^j, \quad (2.6)$$

where γ_{ij} is the metric of the hypersurface Σ , given by

$$\gamma_{ij} = \frac{1}{(1 + Kr^2/4)^2} \delta_{ij}. \quad (2.7)$$

Since every hypersurface Σ is described by a static spatial metric γ_{ij} , we can set up a very convenient coordinate system to describe the physical variables in an expanding universe. This static property establishes that every distance $\Delta \mathbf{x}$ measured by means of the spatial metric (2.7) on a given hypersurface is constant, not evolving with time; this would correspond to the coordinate system attached to an observer at rest relative to expansion. A physical separation \mathbf{x}_{phys} between such points evolves in time, so that it is clear from (2.2) that it obeys

$$\Delta \mathbf{x}_{phys} = a(t) \Delta \mathbf{x}. \quad (2.8)$$

The coordinate system (t, \mathbf{x}) attached to an observer at rest relative to expansion

is called a *comoving* coordinate system. The same idea can be applied to the time coordinate; defining the *conformal time* τ as

$$d\tau \equiv \frac{dt}{a(t)}, \quad (2.9)$$

the FRW metric becomes

$$ds^2 = a(\tau)^2 [d\tau^2 - \gamma_{ij} dx^i dx^j], \quad (2.10)$$

that is, the introduction of a conformal time factorizes the FRW metric into a static metric multiplied by a conformal factor $a(\tau)$.

Conformal time is a "clock" that slows down with the expansion of the universe, and it is specially useful in measuring cosmological distances, which we address in the next section.

2.2 Cosmological Distances and Horizons

Once we are given a metric that describes the cosmological spacetime, we can now take a further step and use it to measure cosmological distances. To do so, let us first rewrite the spatial section of the FRW metric in spherical coordinates,

$$d\ell^2 \equiv d\chi^2 + \Phi_K(\chi^2) (d\theta^2 + \sin^2 \theta d\varphi^2), \quad (2.11)$$

where

$$r^2 \equiv \Phi_K(\chi^2) = \begin{cases} \sinh^2 \chi & K = -1 \\ \chi^2 & K = 0 \\ \sin^2 \chi & K = +1, \end{cases} \quad (2.12)$$

so that

$$ds^2 = a(\tau)^2 (d\tau^2 - d\ell^2). \quad (2.13)$$

If a photon is emitted from a given source at a time t_i , and an observer detects it at the instant t , we have, along the line of sight (that is, with θ, φ constant), that

$$d\chi = \pm d\tau, \quad (2.14)$$

since photons travel on null geodesics, $ds^2 = 0$. Equation (2.13) has a twofold im-

portance; first, its integration gives

$$\chi(\tau) = \pm\tau + \text{const.}, \quad (2.15)$$

which, in a $\tau - \chi$ plane, correspond to straight lines, preserving the light cone structure of a Minkowski spacetime (but notice that the FRW spacetime is curved). Second, integrating equation (2.14) using (2.9), we see that the quantity

$$d_p^{\text{com}}(t) \equiv \tau - \tau_i = \int_{t_i}^t \frac{d\tilde{t}}{a(\tilde{t})} \quad (2.16)$$

represents the maximum comoving distance that a photon can propagate from its emission at a time t_i up to its detection at the time t . The physical or *proper* distance d_p between such two points comes from (2.8), that is,

$$d_p = a(t)d_p^{\text{com}}. \quad (2.17)$$

If we take $t_i = 0$, equation (2.16) gives the maximum comoving distance that a photon can travel from the ‘initial time’ (assuming that the universe had one) up to a given time t . This defines the *comoving cosmological horizon* as the conformal time lapse between 0 and t :

$$\tau = \int_0^t \frac{d\tilde{t}}{a(\tilde{t})}. \quad (2.18)$$

Using the definition of the Hubble parameter (2.3), we can rewrite the definition (2.18) in terms of the scale factor a ,

$$\tau = \int_0^t d \ln \tilde{a} \, d_H(\tilde{a}), \quad (2.19)$$

where

$$d_H(a) \equiv \frac{1}{aH} \quad (2.20)$$

is the so-called *comoving Hubble radius*. The difference between the comoving horizon and the comoving Hubble radius is the following (quoting (DODELSON, 2003)): *if the particles are separated by distances greater than τ , they never could have communicated with one another; if they are separated by distances greater than $(aH)^{-1}$, they cannot talk to each other now!*

Therefore, if any comoving scale λ is *larger* than d_H , it is *outside the horizon*, that is, cannot be in causal contact with a given observed scale, whereas if λ is *smaller* than d_H it is *inside* the horizon. Since we normally deal with wavenumbers $k \propto \lambda^{-1}$ rather than λ itself, we can say whether a scale is inside or outside the horizon by means of the following rule:

$$\frac{k}{aH} \ll 1 \implies \text{Scale } \lambda \text{ is outside the horizon (Superhorizon Scale)} \quad (2.21)$$

$$\frac{k}{aH} \gg 1 \implies \text{Scale } \lambda \text{ is inside the horizon (Subhorizon Scale)} \quad (2.22)$$

These concepts play a crucial role in the discussion on quantum fluctuations generated by inflation, as we shall see in Section 4.5.

Along with the notion of cosmological horizons to discuss physical scales in the very early universe, there is another way to accomplish this goal, by means of the so-called *curvature scale* (MUKHANOV, 2005), specially useful for analyzing bouncing models.

2.3 Cosmological Dynamics: The Friedmann and Raychaudhuri Equations

Once we have discussed the basic features of the FRW metric, let us now derive the dynamical equations that rule the Friedmann cosmological model. We first discuss the Hubble parameter in terms of the conformal time, which is simply given by

$$H = \frac{a'}{a^2}, \quad (2.23)$$

where a prime denotes a derivative with respect to the conformal time, and we have used

$$\frac{d}{d\tau} = a \frac{d}{dt}. \quad (2.24)$$

Defining

$$\mathcal{H} \equiv \frac{a'}{a}, \quad (2.25)$$

it follows that

$$H = \frac{\mathcal{H}}{a}. \quad (2.26)$$

Using the definition of conformal time (2.9) and the metric (2.10), it follows that

the Christoffel symbol of the second kind is given by

$$\Gamma_{\alpha\beta}^0 = \mathcal{H} \begin{pmatrix} 1 & 0 \\ 0 & \gamma_{ij} \end{pmatrix}, \quad \Gamma_{\alpha\beta}^k = \begin{pmatrix} 0 & \mathcal{H}\delta^k_i \\ \mathcal{H}\delta^k_i & -\frac{Kf}{2} [x_{(i}\delta^k_{j)} - x^k\gamma_{ij}] \end{pmatrix}, \quad (2.27)$$

where we have defined

$$f = \frac{1}{(1 + Kr^2/4)^2}. \quad (2.28)$$

From (2.27) and using (A.7) we calculate the Ricci tensor, whose components are

$$R^0_0 = -3a^{-2}\mathcal{H}', \quad R^0_i = 0, \quad R^i_j = -a^{-2} (\mathcal{H}' + 2\mathcal{H}^2 + 2K) \delta^i_j, \quad (2.29)$$

and the scalar curvature, given by (A.8)

$$R = -6a^{-2} (\mathcal{H}' + \mathcal{H}^2 + K). \quad (2.30)$$

Substituting expressions (2.29) and (2.30) into (A.9) we find the components of the Einstein tensor,

$$G^0_0 = 3a^{-2} (\mathcal{H}^2 + K), \quad G^0_i = 0, \quad G^i_j = -a^{-2} (2\mathcal{H}' + \mathcal{H}^2 + K) \delta^i_j. \quad (2.31)$$

Since the Einstein equation relates the geometry to the energy-matter content, let us now drop a few words on the stress energy-tensor to source this geometry. The assumption of a homogeneous and isotropic universe demands that its energy and matter content also be homogeneous and isotropic; hence, we can approximate them as perfect fluids. We first consider a family of fundamental observers whose worldlines are tangent to the timelike four-vector

$$u^\alpha \equiv \frac{dx^\alpha}{d\bar{\tau}}, \quad (2.32)$$

where $\bar{\tau}$ is the proper time of the observer, and satisfies

$$g_{\alpha\beta} u^\alpha u^\beta = 1. \quad (2.33)$$

The fluid is then written as

$$T_{\alpha\beta} = (\rho + P) u_\alpha u_\beta - P g_{\alpha\beta}, \quad (2.34)$$

where P is the pressure of the fluid and ρ is its energy density in the rest frame. Since the cosmic time is measured by the observers' clocks at rest with respect to the matter content of the universe, we take the four-velocity in the comoving frame $u^\alpha = (1, 0, 0, 0)$, so that

$$T^0_0(x) = \rho(t), \quad T^0_i(x) = 0, \quad T^i_j(x) = -P(t) \delta^i_j, \quad (2.35)$$

(homogeneity implies that the pressure and density are functions of the cosmic time only).

The energy or matter content of the universe is also assumed to satisfy an *equation of state* of the form

$$P(\rho) = w\rho, \quad (2.36)$$

where w is the *equation of state parameter*.

Since the stress energy-momentum energy tensor is conserved, $T^{\alpha\beta}{}_{;\alpha} = 0$, it follows from (2.35) the *continuity equation*

$$\dot{\rho} = -3H(\rho + P), \quad (2.37)$$

or, in terms of the conformal time,

$$\rho' = -3\mathcal{H}(\rho + P). \quad (2.38)$$

The dynamical equations for the scale factor can be obtained by plugging (2.31) and (2.35) into (A.10), yielding

$$\left(\frac{a'}{a}\right)^2 = \frac{a^2}{3M_P^2}\rho - K, \quad (2.39)$$

where

$$M_P^2 \equiv \frac{1}{8\pi G} \quad (2.40)$$

is the so-called *reduced Planck mass*, and G is Newton's gravitational constant. In terms of the conformal time τ we have

$$\frac{a''}{a} = \frac{1}{6M_P^2}(\rho - 3P)a^2, \quad (2.41)$$

whereas in terms of the cosmic time t , equations (2.39) and (2.41) become

$$\left(\frac{\dot{a}}{a}\right)^2 = \frac{1}{3M_P^2}\rho - \frac{K}{a^2}, \quad (2.42)$$

and

$$\frac{\ddot{a}}{a} = -\frac{1}{6M_P^2}(\rho + 3P). \quad (2.43)$$

Expressions (2.39) and (2.42) are two versions of the *Friedmann equation*, whereas expressions (2.41) and (2.43) are two versions of the *Raychaudhuri equation*. There is a third version of each of the above equations, which encompasses the so-called *cosmological constant*, denoted by Λ , and can be understood as follows. We know from tensor calculus that the Einstein tensor satisfies the contracted Bianchi identity $\nabla_\alpha G^{\alpha\beta} = 0$; in addition to that, the stress-energy tensor also satisfies a conservation law, $\nabla_\alpha T^{\alpha\beta} = 0$. Since the covariant derivative of the metric tensor also vanishes, $\nabla_\alpha g^{\alpha\beta} = 0$, we see that a modified Einstein equation like

$$G_{\alpha\beta} - \Lambda g_{\alpha\beta} = \frac{1}{M_P^2}T_{\alpha\beta} \quad (2.44)$$

also satisfies the Bianchi and energy conservation constraints. In this case, in terms of the Hubble parameter defined as functions of the cosmic (2.3) and of the conformal (2.25) times, the Friedmann and Raychaudhuri equations read:

$$H^2 = \frac{1}{3M_P^2}\rho + \frac{\Lambda}{3} - \frac{K}{a^2}, \quad (2.45)$$

$$\dot{H} + H^2 = -\frac{1}{6M_P^2}(\rho + 3P) + \Lambda. \quad (2.46)$$

$$\mathcal{H}^2 = \frac{a^2}{3M_P^2}\rho + \frac{a^2\Lambda}{3} - K, \quad (2.47)$$

$$\mathcal{H}' + \mathcal{H}^2 = \frac{1}{3M_P^2}(\rho - 3P)a^2 + a^2\Lambda, \quad (2.48)$$

where

$$\frac{\ddot{a}}{a} = \dot{H} + H^2, \quad (2.49)$$

$$\frac{a''}{a} = \mathcal{H}' + \mathcal{H}^2. \quad (2.50)$$

2.4 The Energy and Matter Content of the Universe

The simplest equation to be solved in cosmology is the continuity equation, (2.37). It relates the energy or matter content of the universe, given by their density ρ , with its expansion, given by the scale factor a . To solve this equation for a given component, we simply substitute (2.36) into (2.37), which gives

$$\rho(a) = \rho_0 \left(\frac{a}{a_0} \right)^{-3(1+w)}. \quad (2.51)$$

For the sake of simplicity, let us consider for a moment that the universe has a single component characterized by an equation of state parameter w ; then, substituting (2.51) into the Friedmann equation (2.42) for $K = 0$, we find

$$a(t) = a_0 \left(\frac{t}{t_0} \right)^{2/3(1+w)} \quad (2.52)$$

for $w \neq -1$. a_0 and t_0 are integration constants; we shall always take these quantities at present time (unless otherwise stated), and reserve the subscript "0" to denote them. For the rest of this chapter we normalize the present time value of the scale factor as $a_0 = 1$; however, other normalizations can be adopted, as we shall see in Section 5.2.

The solution $w = -1$ is of special interest, since it is related to the cosmological constant. To see this, let us solve the Friedmann equation (2.45) in the vacuum ($\rho = 0$): in this case, the Hubble parameter is constant, and given by

$$H^2 = \frac{\Lambda}{3}, \quad (2.53)$$

so that the dynamical evolution of the scale factor in the presence of a cosmological constant is given by

$$a(t) = a_0 e^{H(t-t_0)}. \quad (2.54)$$

Also, from (2.53), we see that Λ plays the role of an energy density, for, defining

$$\rho_\Lambda \equiv M_P^2 \Lambda, \quad (2.55)$$

we see that equation (2.45) is equivalent to the Friedmann equation without a cosmological constant, (2.42). Since ρ_Λ is constant, as defined in expression (6.15), from

the continuity equation (2.37) we see that $\rho'_\Lambda = 0$ implies $\rho_\Lambda + P_\Lambda = 0$, which is satisfied only if

$$\rho_\Lambda = -P_\Lambda \implies w = -1. \quad (2.56)$$

This empty spacetime filled with a cosmological constant is called *de Sitter space*.

The three usual values for the equation of state parameter, as well as the corresponding solutions for ρ , a and H are summarized in Table 2.1.

TABLE 2.1 - The basic constituents of the universe.

Component	w	$\rho(a)$	$a(t)$	$a(\tau)$	$H(t)$
Photons	1/3	a^{-4}	$t^{1/2}$	τ	$1/t$
Matter	0	a^{-3}	$t^{2/3}$	τ^2	$1/t$
Λ	-1	<i>const.</i>	e^{Ht}	$-\tau^{-1}$	<i>const.</i>

It is obvious that a single-component universe is just an idealized picture, since it is clearly multi-component; however, when a given species *dominates* over the others, that is, its density contribution is much larger than the other contributions, we can approximate the solution of the Friedmann and Raychaudhuri equations by a single-component universe. In the general case, with a plethora of constituents, the total density and pressure are given by

$$\rho = \sum_i \rho_i, \quad P = \sum_i P_i. \quad (2.57)$$

It is convenient to introduce a dimensionless quantity to describe the densities of the species ρ . This quantity, which we call *density parameter*, and denote by Ω , is simply written as the energy density of a given species normalized by the *critical density*, which is defined as the energy density of the universe in the case where $\Lambda = K = 0$,

$$\rho_c \equiv 3M_P^2 H^2; \quad (2.58)$$

then, for each species i , and the total content of the universe, the density parameter are given by

$$\Omega_i \equiv \frac{\rho_i}{\rho_c}, \quad \Omega \equiv \sum_i \Omega_i. \quad (2.59)$$

From equation (2.42) and the definitions (2.59) we deduce an important expression,

$$\Omega(a) = 1 - \frac{K}{(aH)^2}. \quad (2.60)$$

The current observations of CMB and the large-scale structure favor a cosmological model composed of baryonic matter (subscript B), *dark matter* (subscript DM), and a vacuum energy that plays the role of the *dark energy* (subscript Λ), in the following proportions today (KOMATSU et al., 2009):

$$\Omega_B \sim 0.04, \quad \Omega_{DM} \sim 0.23 \quad \Omega_\Lambda \sim 0.72, \quad (2.61)$$

which indicates that the universe is nearly flat today, $\Omega_0 \sim 1$. This observationally-favored model is called the Λ CDM or *cosmic concordance* model. Together with the inflationary paradigm, the Λ CDM model makes up the widely accepted model to describe the universe, the SCM.

2.5 The Birth of CMB: Recombination and Decoupling

Let us now briefly comment on the history of the universe since its early days. We have seen in Section 2.4 that the energy density of the photons goes like $\rho_\gamma \propto a^{-4}$ (Table 2.1); then, using the well known Stefan-Boltzmann law $\rho_\gamma \propto T^4$, we easily find that

$$T \propto \frac{1}{a} = 1 + z, \quad (2.62)$$

where z is a quantity called *redshift*. Then, the universe was very hot in the past, and went on cooling down as it expanded; by reaching a temperature around $T \sim 10^{10}$ K, the first nuclei were formed by primordial nucleosynthesis, so that the universe became filled with an ionized plasma of light nuclei, electrons and photons. The universe was opaque, that is, the mean free path of the photons were too small to allow for free propagation; they were almost immediately absorbed after being emitted. The amount of radiation was much larger than the amount of matter, so the universe was dominated by radiation. For the sake of simplicity, assuming that the matter content of the universe were composed solely of hydrogen at early times, eventually a proton could capture an electron and form a neutral hydrogen atom by means of the radiative recombination reaction,



however, the high temperature of the plasma were far above the ionization energy of the hydrogen, so that the high-energy photons ionized these atoms by means of the reaction



Therefore, hydrogen atoms formed even in the radiation-dominated period, but they were extremely short-lived, and were dissociated by photo-ionization. As the universe cooled down, more matter were formed, and the photon energies dropped; then at the temperature $T \sim 9730\text{K}$, the energy densities of radiation and matter became equal, thus inaugurating the era of *radiation-matter equality*. Thereafter, more and more atoms of hydrogen were formed since less photon were sufficiently energetic to photo-ionize the neutral atoms. When the number density of the neutral atoms became nearly equal to the number density of the ions, the *recombination process* took place: the ionization fraction of the universe dropped quickly, so that more free electrons were captured to form neutral atoms. At this time, the rate of the interaction photon-electron Γ were larger than the expansion rate of the universe H ; then, by the time of equality $\Gamma = H$, the photon-electron scattering *froze-out*, that is, photons no longer interacted with the electrons and then free-streamed in the universe when $\Gamma < H$. This event is called *decoupling*, and took place around

$$\boxed{\text{Decoupling : } z_{dec} \simeq 1100, \quad T_{dec} \simeq 3000\text{K}}. \quad (2.65)$$

After decoupled, the photons were scattered for the last time by the electrons, and this event makes up what is called the *last scattering surface* (LSS)¹. A summary of the key events in the very early universe is given in Figure 2.1.

Then, after the LSS, the CMB is born!

¹To be more precise, the LSS should be dubbed LSL, *last scattering layer*, for not all the photons are last-scattered at the same time!

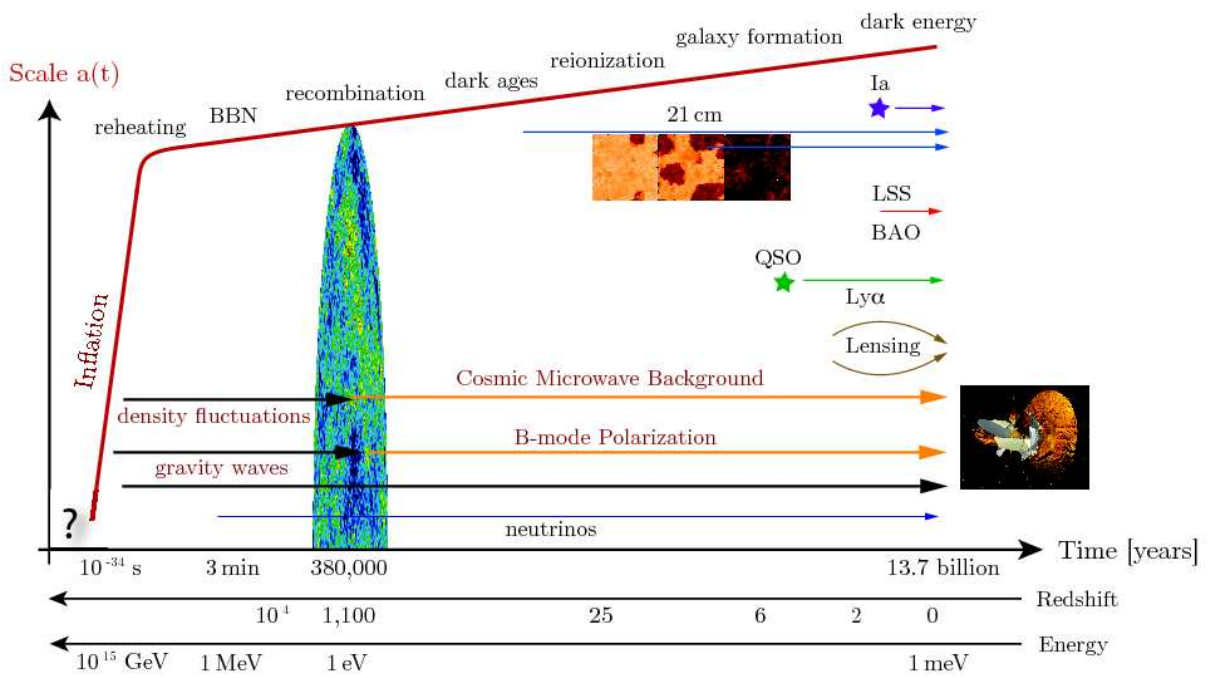


FIGURE 2.1 - The major events in the very early universe. Figure borrowed from (BAUMANN, 2009).

3 THE THEORY OF COSMOLOGICAL PERTURBATIONS

In the Chapter 2 we have discussed the key ingredients of a homogeneous, isotropic and expanding universe. In what follows we shall add fluctuations to the metric and to the energy-momentum tensor, which is going to play an essential role in the theory of CMB anisotropies and polarization. We follow closely (MUKHANOV et al., 1992), (KODAMA; SASAKI, 1984), (MUKHANOV, 2005), (WEINBERG, 2008)) and (GIOVANNINI, 2005).

3.1 Disturbing the smoothness of the universe

3.1.1 Metric fluctuations

Let us consider a general metric $g_{\alpha\beta}$ describing such inhomogeneous and anisotropic spacetime. To first-order, this metric can be split up into two pieces¹,

$$g_{\alpha\beta} = {}^{(0)}g_{\alpha\beta} + \delta g_{\alpha\beta}, \quad (3.1)$$

with the supplementary condition

$$|\delta g_{\alpha\beta}| \ll 1 \quad (3.2)$$

where ${}^{(0)}g_{\alpha\beta}$ plays the role of a *background metric* (the FRW metric, for example), and $\delta g_{\alpha\beta}$ represents the metric fluctuations. Since $\delta g_{\alpha\beta}$ is symmetric, we must have ten independent components in four dimensions, which can be written in terms of independent scalar (S), vector (V), and tensor (T) fields. As usual, the spacetime \mathcal{M} is foliated into ‘smooth’ hypersurfaces of constant time Σ , and each perturbation is defined on Σ . Such decomposition is written as

$$\delta g_{\alpha\beta} = \delta_S g_{\alpha\beta} + \delta_V g_{\alpha\beta} + \delta_T g_{\alpha\beta}, \quad (3.3)$$

where the condition $|\delta_I g_{\alpha\beta}| \ll 1$, $I = S, V, T$, must be fulfilled in order to guarantee that the fluctuations are independent. The expressions for $\delta_I g_{\alpha\beta}$ are given below.

• Scalar Perturbations

¹It is important to stress that the equality symbol $=$ here means that such approximation is valid only up to first-order. For the sake of simplicity we keep this symbol henceforth, but bearing in mind that this is a weak equality.

The component δg_{00} is a pure scalar, whereas the vector components δg_{0i} can be built from first-order derivatives of a scalar field. As to tensor perturbations, there are two ways to construct a tensor from a scalar: either we multiply a scalar by the 3-metric γ_{ij} on Σ , or take second-order derivatives of it. Since the fields are defined on Σ , we only care about the spatial components of covariant derivatives. Therefore, scalar perturbations are given by (MUKHANOV et al., 1992)

$$\delta_S g_{\alpha\beta} = a(\tau)^2 \begin{pmatrix} 2\varphi & -B_{|i} \\ -B_{|i} & 2(\psi\gamma_{ij} - E_{|ij}) \end{pmatrix}, \quad (3.4)$$

where φ , B , ψ and E are scalar fields, and the subscript “ $|i$ ” indicates a covariant derivative on a spacelike hypersurface Σ . Such scalar fields contribute with four independent components to the metric perturbations.

• Vector Perturbations

We know from classical electrodynamics that a massless vector field A_α satisfies a Maxwell-like equation

$$\partial_\alpha W^{\alpha\beta} = J^\beta, \quad (3.5)$$

where $W_{\alpha\beta} \equiv A_{\alpha,\beta} - A_{\beta,\alpha}$ and J^β is the analog of a current density. The Maxwell tensor $W_{\alpha\beta}$ is invariant under gauge transformations

$$\tilde{A}_\alpha = A_\alpha - \partial_\alpha \xi, \quad (3.6)$$

where ξ is an arbitrary function. Then, using this gauge freedom, we can eliminate some degrees of freedom of the vector field A_α by imposing some constraint as, for example, the Lorentz condition

$$\partial_\alpha A^\alpha = 0. \quad (3.7)$$

In the cosmological context, δg_{00} gives no vector contribution, since it is scalar, but δg_{0i} does, since it is a vector. The tensor part δg_{ij} can be also constructed from vectors by taking covariant derivatives of them. Therefore, putting these facts together, we have, for vector perturbations,

$$\delta_V g_{\alpha\beta} = -a(\tau)^2 \begin{pmatrix} 0 & -S_i \\ -S_i & F_{i|j} + F_{j|i} \end{pmatrix}. \quad (3.8)$$

where S_i and F_i are vector fields. These fields must satisfy Maxwell-like equations as (3.5) which also allows for a gauge choice. We impose the analog of the Lorentz gauge (3.7),

$$S^i{}_{|i} = F^i{}_{|i} = 0, \quad (3.9)$$

since the vectors are constructed on Σ . Hence, each vector has two independent components, and, altogether, contribute with four independent components to the metric perturbations.

• Tensor Perturbations

Tensor perturbations can be constructed as

$$\delta_T g_{\alpha\beta} = -a(\tau)^2 \begin{pmatrix} 0 & 0 \\ 0 & h_{ij} \end{pmatrix}, \quad (3.10)$$

where h_{ij} is a tensor defined on Σ . We can also fix the number of components of h_{ij} by means of gauge transformations in analogy with the weak-field approximation (see Appendix C.2.2 for details); we then impose

$$h^i{}_{j|i} = h^i{}_i = 0, \quad (3.11)$$

which means that h_{ij} is a transverse trace-free (TTF) tensor (B.19). Therefore, tensor perturbations contribute with two independent components.

Adding up the contributions of S (4), of V (4) and of T (2), we get the ten independent contributions to the metric perturbations, given by

$$\delta g_{\alpha\beta} = a(\tau)^2 \begin{pmatrix} 2\varphi & S_i - B_{|i} \\ S_i - B_{|i} & -F_{i|j} - F_{j|i} + 2\psi\gamma_{ij} - 2E_{|ij} - h_{ij} \end{pmatrix}. \quad (3.12)$$

The corresponding perturbations to the fundamental tensors of GR can be deduced as follows. We start with the inverse metric $g^{\alpha\beta}$ which, to first order, is given by

$$g^{\alpha\beta} = {}^{(0)}g^{\alpha\beta} - \delta g^{\alpha\beta}. \quad (3.13)$$

Substituting relations (3.1) and (3.13) into the usual equation

$$g^{\alpha\gamma}g_{\gamma\beta} = \delta^\alpha_\beta, \quad (3.14)$$

it can be shown that

$$\delta g^{\alpha\beta} = -^{(0)}g^{\alpha\kappa}g^{\beta\lambda}\delta g_{\kappa\lambda}. \quad (3.15)$$

Due to the linear character of the perturbations, the Christoffel symbol of first kind reads

$$\Gamma_{\kappa\beta\gamma} = {}^{(0)}\Gamma_{\kappa\beta\gamma} + \delta\Gamma_{\kappa\beta\gamma}; \quad (3.16)$$

notice that the linearity property of the perturbations makes the ‘ δ ’ symbol ‘act’ like a linear differential operator; then, we could have used this “operator”² instead of algebraic manipulations performed. From (A.2), we have that

$$\delta\Gamma_{\kappa\beta\gamma} = \frac{1}{2}[\partial_\gamma\delta g_{\kappa\beta} + \partial_\beta\delta g_{\gamma\kappa} - \partial_\kappa\delta g_{\beta\gamma}]. \quad (3.17)$$

From the definition of the Christoffel symbol of second kind, (A.3), we find

$$\Gamma^\alpha_{\beta\gamma} = {}^{(0)}\Gamma^\alpha_{\beta\gamma} + \delta\Gamma^\alpha_{\beta\gamma}, \quad (3.18)$$

where

$$\delta\Gamma^\alpha_{\beta\gamma} = {}^{(0)}g^{\alpha\kappa}\delta\Gamma_{\kappa\beta\gamma} + \delta g^{\alpha\kappa}{}^{(0)}\Gamma_{\kappa\beta\gamma}, \quad (3.19)$$

which leads to

$$\delta\Gamma^\alpha_{\beta\gamma} = \frac{1}{2}{}^{(0)}g^{\alpha\kappa}[\nabla_\gamma\delta g_{\kappa\beta} + \nabla_\beta\delta g_{\gamma\kappa} - \nabla_\kappa\delta g_{\beta\gamma}], \quad (3.20)$$

where we have used expression (A.2).

The linearity property also allows us to write down the Ricci tensor (A.7) as

$$R_{\alpha\beta} = {}^{(0)}R_{\alpha\beta} + \delta R_{\alpha\beta}, \quad (3.21)$$

²Strictly speaking, δ is not a differential operator, since the perturbation expansion stops at first-order; however, the similarity between a differential operator and the algebraic result as shown in (3.16) due to the first-order expansion allows for its use as if it were an operator.

where

$$\begin{aligned}\delta R_{\alpha\beta} &= \partial_\kappa \delta \Gamma^\kappa_{\alpha\beta} - \partial_\beta \delta \Gamma^\kappa_{\alpha\kappa} + {}^{(0)}\Gamma^\kappa_{\alpha\beta} \delta \Gamma^\lambda_{\kappa\lambda} + \delta \Gamma^\kappa_{\alpha\beta} {}^{(0)}\Gamma^\lambda_{\kappa\lambda} \\ &- {}^{(0)}\Gamma^\kappa_{\alpha\lambda} \delta \Gamma^\lambda_{\kappa\beta} - \delta \Gamma^\kappa_{\alpha\lambda} {}^{(0)}\Gamma^\lambda_{\kappa\beta}.\end{aligned}\quad (3.22)$$

Rewriting the derivatives of the perturbed Christoffel symbols in terms of their covariant derivatives (A.2), we see that

$$\delta R_{\alpha\beta} = \nabla_\kappa \Gamma^\kappa_{\alpha\beta} - \nabla_\beta \Gamma^\kappa_{\alpha\kappa}.\quad (3.23)$$

Using the same techniques, the mixed tensor δR^α_β , the scalar curvature δR and the Einstein tensor $\delta G_{\alpha\beta}$ read

$$\delta R^\alpha_\beta = {}^{(0)}g^{\alpha\gamma} \delta R_{\gamma\beta} + \delta g^{\alpha\gamma} {}^{(0)}R_{\gamma\beta},\quad (3.24)$$

$$\delta R = {}^{(0)}g^{\alpha\gamma} \delta R_{\gamma\alpha} + \delta g^{\alpha\gamma} {}^{(0)}R_{\gamma\alpha},\quad (3.25)$$

$$\delta G_{\alpha\beta} = \delta R_{\alpha\beta} - \frac{1}{2} [\delta g_{\alpha\beta} {}^{(0)}R + {}^{(0)}g_{\alpha\beta} \delta R].\quad (3.26)$$

3.1.2 Density Perturbations

As discussed in Chapter 2, the energy and matter content of the universe can be treated as a perfect fluid, whose expression is given by (2.34). To first-order, we can decompose the stress-energy tensor into its background contribution, ${}^{(0)}T_{\alpha\beta}$, described by the expression (2.34), and a perturbation $\delta T_{\alpha\beta}$, so that

$$T_{\alpha\beta} = {}^{(0)}T_{\alpha\beta} + \delta T_{\alpha\beta}.\quad (3.27)$$

The same linearity argument accounts for similar decompositions for the elements of (3.27), that is,

$$u^\alpha = {}^{(0)}u^\alpha + \delta u^\alpha,\quad (3.28)$$

$$P = P_0 + \delta P,\quad (3.29)$$

$$\rho = \rho_0 + \delta \rho,\quad (3.30)$$

where P_0 , ρ_0 stand for the background values of the pressure and energy density, respectively. Then, substituting (3.28), (3.29) and (3.30) into (3.27), and using ‘ δ ’

as a linear differential operator, it follows that

$$\begin{aligned}\delta T_{\alpha\beta} &= (\delta\rho + \delta P) {}^{(0)}u_\alpha {}^{(0)}u_\beta + [\rho_0 + P_0] [\delta u_\alpha {}^{(0)}u_\beta + {}^{(0)}u_\alpha \delta u_\beta] \\ &- {}^{(0)}g_{\alpha\beta} \delta P - P_0 \delta g_{\alpha\beta}.\end{aligned}\tag{3.31}$$

Expression (3.31) is not yet the most general way to produce small inhomogeneities and anisotropy in a perfect background fluid; we can also introduce the *anisotropic stresses* in the spatial components of $\delta T_{\alpha\beta}$, represented by the quantity Π_{ij} , which can be decomposed exactly in the same fashion as in the metric (3.3):

$$\Pi_{ij} = \Pi^S_{ij} + \Pi^V_{ij} + \Pi^T_{ij},\tag{3.32}$$

where

$$\Pi^S_{ij} = \Pi_{|ij} - \frac{1}{3} \gamma_{ij} \nabla^2 \Pi,\tag{3.33}$$

$$\Pi^V_{ij} = \frac{1}{2} (\Pi_{i|j} + \Pi_{j|i}),\tag{3.34}$$

$$\Pi^T_{ij} = \Pi_{ij},\tag{3.35}$$

subject to the constraints

$$\Pi^i_{\ |i} = 0, \quad \Pi^i_{\ j|i} = \Pi^i_{\ i} = 0,\tag{3.36}$$

exactly as in (3.9) and (3.11). Notice that, by construction, the full anisotropic stress tensor is traceless, as it should be. Anisotropic stresses arise, for example, in the neutrino free-streaming.

We can calculate every component of $\delta T_{\alpha\beta}$ as follows: since ${}^{(0)}u_\alpha = (1, 0, 0, 0)$ for the background fluid, we have, in conformal units,

$${}^{(0)}u_\alpha(\tau) = (a(\tau), 0, 0, 0);\tag{3.37}$$

then, using δ as an operator, it follows from (2.33) that

$${}^{(0)}g_{\alpha\beta} {}^{(0)}u^\beta \delta u^\alpha = -\frac{1}{2} {}^{(0)}u^\alpha {}^{(0)}u^\beta \delta g_{\alpha\beta}.\tag{3.38}$$

Next, plugging the 00 component of (3.12), and (3.37) into (3.38), we get

$$\delta u^0 = -\frac{\varphi}{a}. \quad (3.39)$$

However, the component δu^i cannot be determined by means of expression (3.38), since this equality is identically zero on both sides for the $0i$ component of the background metric and the i component of the four-velocity. We then introduce a new vector field, which we define to be

$$\delta u^i \equiv \frac{v^i}{a}, \quad (3.40)$$

where v^i is the 3-velocity of matter defined with respect to the spatial coordinates x^i . The covariant version of δu^i is

$$\delta u_i = a (S_i - B_{|i} - v_{|i}), \quad (3.41)$$

where we have used

$$\delta u_\alpha = \delta g_{\alpha\beta} {}^{(0)}u^\beta + {}^{(0)}g_{\alpha\beta} \delta u^\beta, \quad (3.42)$$

which is the ‘‘perturbed version’’ of the usual expression to raise indices.

Once we have the components of the four-velocity perturbation, we can easily evaluate the components of $\delta T_{\alpha\beta}$ as given in (3.31) and (3.33-3.35)

$$\begin{aligned} \delta T_{00} &= a^2 [\delta\rho + 2\rho_0\varphi], \\ \delta T_{i0} &= a^2 [-(\rho_0 + P_0)v_i + \rho_0(S_i - B_{|i})], \\ \delta T_{ij} &= a^2 \left\{ -\left(\delta P - 2P_0\psi - \frac{1}{3}\nabla^2\Pi\right)\gamma_{ij} + (2P_0E + \Pi)_{|ij} \right. \\ &\quad \left. + 2[P_0F_{(i|j)} + 2\Pi_{(i|j)}] + P_0h_{ij} + \Pi_{ij} \right\}. \end{aligned} \quad (3.43)$$

In general, the pressure depends not only on the energy density ρ , but also on the entropy per baryon ratio S ; then,

$$\delta P = \left(\frac{\partial P}{\partial\rho}\right)_S \delta\rho + \delta P_{nad} \quad (3.44)$$

$$\equiv c_s^2\delta\rho + \delta P_{nad}, \quad (3.45)$$

where the first term on the right-hand side represents an *adiabatic process*, *i.e.*,

with constant entropy, and the second one stands for a non-adiabatic process. For hydrodynamical matter, c_s plays the role of the the speed of sound, given by (D.15), in plain analogy with the propagation of acoustic waves in a material medium.

3.2 Gauge Symmetries for Cosmological Perturbations

As discussed in the Appendix B, gauge transformations play a fundamental role in GR; they allow the existence of GWs, for example. In cosmology they also play a fundamental role, and are extremely important for all the investigations that we will undertake in this thesis. This is why we shall discuss this issue in some detail.

To begin with, we assume the FRW metric in Cartesian coordinates (2.10) as our background metric, where γ_{ij} is the metric on the 3-spaces Σ , given by (2.7). As we have earlier discussed, such subspaces are maximally symmetric, and hence the background metric is *form-invariant*, that is (WEINBERG, 1972)

$${}^{(0)}\tilde{g}_{\alpha\beta}(\tilde{x}) = {}^{(0)}g_{\alpha\beta}(\tilde{x}). \quad (3.46)$$

Property (3.46) implies that

$$\tilde{a}(\tilde{\tau}) = a(\tilde{\tau}), \quad (3.47)$$

and

$$\tilde{\gamma}_{ij}(\tilde{x}) = \gamma_{ij}(\tilde{x}). \quad (3.48)$$

In the cosmological context the local coordinate transformations (B.2) are slightly different due to the adoption of the conformal time τ as our evolution parameter. Hence, these coordinate transformations read

$$\tilde{\tau} = \tau + \xi^0, \quad \tilde{x}^i = x^i + \xi^i; \quad (3.49)$$

in the same way, we can show that the metric transformation (3.1), given by equation (B.5), changes slightly,

$$\delta\tilde{g}_{\alpha\beta} = \delta g_{\alpha\beta} - \nabla_{\alpha}\epsilon_{\beta} - \nabla_{\beta}\epsilon_{\alpha}, \quad (3.50)$$

where $\epsilon_{\alpha} = a(\tau)^2(\xi_0, -\xi_i)$. It is convenient to decompose the spatial part of ξ_{α} into a vector and a scalar component,

$$\xi_i = \xi_{|i} + \zeta_i, \quad (3.51)$$

where ζ_i is a divergenceless vector, $\zeta_i{}^{|i} = 0$. This constraint eliminates one of the components of ζ_i , leaving just two independent quantities which, together with the scalar ξ , make up the three components of ξ_i , hence validating the decomposition (3.51).

With these vectors we are now in position to derive the gauge transformations for the metric fluctuations. Taking each component of the metric (3.12) in the coordinate system \tilde{S} , and substituting it into the equation (3.50), we find

$$\begin{aligned}\delta\tilde{g}_{00} &= 2\tilde{a}(\tilde{\tau})^2\tilde{\varphi} \\ &= 2a(\tau)^2\varphi - 2\xi'_0 - 2\mathcal{H}\xi_0,\end{aligned}\tag{3.52}$$

$$\begin{aligned}\delta\tilde{g}_{0i} &= -\tilde{a}(\tilde{\tau})^2\tilde{B}_{|i} + \tilde{a}(\tilde{\tau})^2\tilde{S}_i \\ &= a(\tau)^2[-B_{|i} + S_i - \xi_{0|i} + \xi'_{|i} + \zeta'_i],\end{aligned}\tag{3.53}$$

$$\begin{aligned}\delta\tilde{g}_{ij} &= \tilde{a}(\tilde{\tau})^2[2\tilde{\psi}\gamma_{ij} - 2\tilde{E}_{|ij} - \tilde{F}_{i|j} - \tilde{F}_{j|i} + \tilde{h}_{ij}] \\ &= a(\tau)^2[2(\psi - \mathcal{H}\xi_0)\gamma_{ij} - 2(E - \xi)_{|ij} - (F_i - \zeta_i)_{|j} - (F_j - \zeta_j)_{|i} \\ &\quad + h_{ij}].\end{aligned}\tag{3.54}$$

Therefore, reassembling the variables in (3.52), (3.53) and (3.54), we find all the gauge transformations for the metric fluctuations:

a) Gauge transformations for scalar perturbations

$$\tilde{\varphi} = \varphi - \xi'_0 - \mathcal{H}\xi_0,\tag{3.55}$$

$$\tilde{B} = B + \xi_0 - \xi',\tag{3.56}$$

$$\tilde{\psi} = \psi + \mathcal{H}\xi_0,\tag{3.57}$$

$$\tilde{E} = E - \xi,\tag{3.58}$$

b) Gauge transformations for vector perturbations

$$\tilde{S}_i = S_i + \zeta'_i,\tag{3.59}$$

$$\tilde{F}_i = F_i - \zeta_i,\tag{3.60}$$

c) Gauge transformations for tensor perturbations

$$\tilde{h}_{ij} = h_{ij}. \quad (3.61)$$

We now turn to the gauge transformations for the energy-matter sector. Since $T_{\alpha\beta}$ is a second rank tensor, it transforms as (B.1) under the local transformations (3.49). After some algebra we can show that

$$\begin{aligned} \delta\tilde{T}^\alpha{}_\beta(\tilde{x}) &= \delta T^\alpha{}_\beta(x) - {}^{(0)}T^\alpha{}_\gamma(x)\xi^\gamma{}_{|\beta} + {}^{(0)}T^\gamma{}_\beta(x)\xi^\alpha{}_{|\gamma} \\ &\quad - {}^{(0)}T^\alpha{}_{\beta|\gamma}(x)\xi^\gamma; \end{aligned} \quad (3.62)$$

then, raising one of the indices of (3.43) and substituting into (3.62), we find

$$\delta\tilde{\rho}(\tilde{x}) = \delta\rho(x) - \xi_0\rho'_0(x), \quad (3.63)$$

$$\delta\tilde{P}(\tilde{x}) = \delta P(x) - \xi_0 P'_0(x), \quad (3.64)$$

$$\tilde{v}_i(\tilde{x}) = v_i(x) + \xi'_i + \zeta'_i. \quad (3.65)$$

In particular, decomposing the velocity field v_i in the same way as we did in (3.51),

$$v_i = v_{|i} + \omega_i, \quad (3.66)$$

where $\omega_i{}^{|i} = 0$, and using (3.51) we see that

$$\tilde{v} = v + \xi', \quad (3.67)$$

$$\tilde{\omega}_i = \omega_i + \zeta'_i. \quad (3.68)$$

Once we have established the gauge transformations for the metric components, let us now analyze the gauge-fixing procedure for the parameters ξ^0 and ξ . From (3.58) it follows that

$$\xi = E - \tilde{E}; \quad (3.69)$$

then, from (3.56) and (3.69),

$$\xi_0 = (\tilde{B} - \tilde{E}') - (B - E'). \quad (3.70)$$

Substituting (3.70) into (3.55), we find

$$\tilde{\varphi} = \varphi - (\tilde{B} - \tilde{E}')' + (B - E')' - \mathcal{H} \left[(\tilde{B} - \tilde{E}') - (B - E') \right]. \quad (3.71)$$

Defining the scalar field

$$\Phi \equiv \varphi + \mathcal{H}(B - E') + (B - E')', \quad (3.72)$$

it is clear from expression (3.71), that the field Φ is *invariant* under the gauge transformations (3.55) and (3.58). Likewise, substituting (3.70) into (3.57), we find

$$\tilde{\psi} = \psi + \mathcal{H} \left[(\tilde{B} - \tilde{E}') - (B - E') \right]; \quad (3.73)$$

then, defining the scalar field

$$\Psi \equiv \psi - \mathcal{H}(B - E'), \quad (3.74)$$

it is also clear that Ψ is also invariant under the gauge transformations (3.55) and (3.58). The fields Φ and Ψ are called *Bardeen potentials* (BARDEEN, 1980).

As to vector fields, we can fix the gauge ζ_i by means of equation (3.60),

$$\zeta_i = F_i - \tilde{F}_i, \quad (3.75)$$

which, together with (3.59), ends up being

$$\tilde{S}_i = S_i + (F_i - \tilde{F}_i)'; \quad (3.76)$$

then, defining the vector field

$$W_i \equiv S_i + F_i', \quad (3.77)$$

it follows that the vector field W_i is invariant under the gauge transformations (3.59) and (3.60).

As for tensor perturbations, expression (3.61) shows immediately that the tensor field h_{ij} is invariant under gauge transformations,

$$\tilde{h}_{ij} = h_{ij}. \quad (3.78)$$

We can also construct gauge-invariant quantities in the matter sector. Plugging (3.70) into (3.63) and (3.64), it is immediate to see that the quantities

$$\delta\rho^{(GI)} \equiv \delta\rho + \rho'_0(B - E'), \quad (3.79)$$

$$\delta P^{(GI)} \equiv \delta P + P'_0(B - E') \quad (3.80)$$

are also invariant under the the same transformations. As to the 3-velocity of the fluid, from (3.69), we conclude that the quantity

$$\mathcal{V} \equiv v + E' \quad (3.81)$$

is invariant under the coordinate transformations (3.49). Also, from (3.75) and (3.76), the quantities

$$\mathcal{F}_i \equiv \omega_i + F_i \quad (3.82)$$

$$\mathcal{S}_i \equiv \omega_i - S_i \quad (3.83)$$

are invariant under the transformations (3.68).

Along with the gauge-invariant variables defined above, we can also use the gauge-fixing procedure to write down the Einstein equations for the cosmological perturbations in more convenient coordinate systems. A special gauge is particularly convenient for computations, the so-called *longitudinal gauge* or *conformal Newtonian gauge*, which we next discuss. We take $B = E = 0$ in this gauge, which fixes completely the coordinates. Then, in the coordinate system S the potentials Φ and Ψ take the form

$$\Phi = \varphi_L, \quad \Psi = \psi_L, \quad (3.84)$$

where the subscript L stands for conformal Newtonian. In this gauge, the fields φ_L and ψ_L coincide with their corresponding invariant potentials. Also, in this case, the line element takes the simplified form

$$ds^2 = a(\tau)^2 [(1 + 2\Phi) d\tau^2 - (1 - 2\Psi) \gamma_{ij} dx^i dx^j], \quad (3.85)$$

which bears resemblance to the Newtonian line element in GR. The difference lies in the fact that, in Newtonian approximation in GR, $\Phi = \Psi$. The physical interpretation of Φ is immediate in this analogy: it acts as a gravitational potential. To see the physical interpretation of Ψ , let us calculate the fluctuations in the spatial cur-

vature, $\delta R^{(3)}$. A convenient gauge to do such calculation is the *comoving orthogonal gauge*, in which an observer sits on a given hypersurface. In this case, for scalar perturbations, the perturbation to the fluid 3-velocity δu_i is zero, so that, from (3.41) and (3.66), we have

$$\delta u_i^{(\text{com})} = 0 \implies v_{(\text{com})} + B_{(\text{com})} = 0, \quad (3.86)$$

where the subscript (com) stands for ‘‘comoving’’. In this gauge, using the definition of the curvature of a hypersurface, $R^{(3)} = g^{ij} R_{ij}^{(3)}$, and expression (3.25), we find that

$$\delta R^{(3)} = \frac{4}{a^2} \nabla^2 \psi_{(\text{com})} \quad (3.87)$$

in the comoving gauge. Hence, $\psi_{(\text{com})}$ plays the role of a curvature perturbation. Therefore, in (3.85) the Bardeen variable Φ plays the role of a Newtonian potential, whereas Ψ is associated with curvature perturbations.

We can connect $\psi_{(\text{com})}$ with any other gauge by means of expressions (3.56), (3.57) and (3.67),

$$\psi = \psi_{(\text{com})} + \mathcal{H}(v + B), \quad (3.88)$$

where we have used relation (3.86). Plugging (3.74) and (3.81) into (3.88) we find

$$\psi_{(\text{com})} = \Psi - \mathcal{H}\mathcal{V}. \quad (3.89)$$

The gauge-invariant variable

$$\mathcal{R} \equiv -[\Psi - \mathcal{H}\mathcal{V}] \quad (3.90)$$

represents the *comoving curvature perturbation*, and will be of fundamental importance to discuss the generation of quantum fluctuations during inflation in Section 4.5.

3.3 Einstein equations for Cosmological Perturbations

Using the techniques introduced in Section 3.1 we see that the Einstein equation for the fluctuations (A.10) takes the form

$$\delta G_{\alpha\beta} = \frac{1}{M_P^2} \delta T_{\alpha\beta}. \quad (3.91)$$

Substituting the metric (3.12) into expression (3.15), and using the corresponding expressions for the background (2.10) and (2.27), and plugging this result into expression (3.16) first, and then into (3.17) in the sequel, we find all the components of the perturbed Christoffel symbol of second kind. Then, plugging them into expression (3.23), and so forth, we derive the components of the Einstein tensor by means of equation (3.26) and the background expressions discussed in Chapter 2, Section 2.3. For a flat universe, with $K = 0$, we have

$$\delta G_{00} = 2\nabla^2\Psi - 6\mathcal{H}\psi', \quad (3.92)$$

$$\begin{aligned} \delta G_{0i} &= -(\mathcal{H}^2 + 2\mathcal{H}') (B_{,i} - S_i) + 2(\Psi' + \mathcal{H}\Phi)_{,i} + \frac{1}{2}\nabla^2 W_i \\ &+ (\mathcal{H}' - \mathcal{H}^2) (B - E')_{,i}, \end{aligned} \quad (3.93)$$

$$\begin{aligned} \delta G_{ij} &= \{2\Psi'' + 2(\mathcal{H}^2 + 2\mathcal{H}')(\Phi + \Psi) + 2\mathcal{H}(\Phi' + 2\Psi') + \nabla^2(\Phi - \Psi) \\ &+ 2(\mathcal{H}'' + \mathcal{H}\mathcal{H}') (B - E')\} \delta_{ij} + [\Psi - \Phi - 2(\mathcal{H}^2 + 2\mathcal{H}') E]_{,ij} \\ &+ \left[\frac{1}{2}W'_i + \mathcal{H}W'_i - (\mathcal{H}^2 + 2\mathcal{H}') F_i \right]_{,j} + (i \leftrightarrow j) \\ &+ \frac{1}{2} [h''_{ij} + 2\mathcal{H}h'_{ij} - \nabla^2 h_{ij} - 2(\mathcal{H}^2 + \mathcal{H}') h_{ij}]. \end{aligned} \quad (3.94)$$

From expressions (3.43) and (3.91-3.94) we finally find the Einstein equations for cosmological perturbations for the gauge-invariant quantities (3.72), (3.74) and (3.77-3.83). For scalar perturbations, the Einstein equations are

$$\nabla^2\Psi - 3\mathcal{H}(\Psi' + \mathcal{H}\Phi) = \frac{a^2}{2M_P^2} \delta\rho^{(GI)}, \quad (3.95)$$

$$(\Psi' + \mathcal{H}\Phi)_{,i} = -\frac{a^2}{2M_P^2} (\rho_0 + P_0) \mathcal{V}_{,i}, \quad (3.96)$$

$$\begin{aligned} &\Psi'' + \mathcal{H}(\Phi' + 2\Psi') + (\mathcal{H}^2 + 2\mathcal{H}')\Phi + \frac{1}{2}\nabla^2(\Phi - \Psi) \\ &= \frac{a^2}{2M_P^2} \left(\delta P^{(GI)} - \frac{1}{3}\nabla^2\Pi \right), \end{aligned} \quad (3.97)$$

$$\nabla^2(\Phi - \Psi) = -\frac{a^2}{M_P^2} \nabla^2\Pi. \quad (3.98)$$

The Einstein equations for vector perturbations are

$$\nabla^2 W_i = -\frac{2a^2}{M_P^2} (\rho_0 + P_0) \mathcal{S}_i, \quad (3.99)$$

$$W_i' + 2\mathcal{H}W_i = \frac{2a^2}{M_P^2} \Pi_i, \quad (3.100)$$

whereas for tensor perturbations

$$h_{ij}'' - \nabla^2 h_{ij} + 2\mathcal{H}h_{ij}' = \frac{2a^2}{M_P^2} \Pi_{ij}. \quad (3.101)$$

In the absence of anisotropic stresses the solution to equation (3.100) is

$$W_i = \frac{C_i}{a^2}, \quad (3.102)$$

where C_i is a constant vector. Therefore, vector perturbations decay quickly as the universe expands, and we do not expect them to endure up to the time of recombination. This is the reason why vector perturbations are completely neglected in the current cosmological paradigm.

From the evolution equations for the scalar modes we can recast the definition of the curvature on comoving hypersurfaces (3.90) into a very useful form, as we shall see in Chapter 4. First, subtracting $-2\mathcal{H}^2$ on both sides in equation (2.48), and using equation (2.47), we have, for $K = \Lambda = 0$,

$$\mathcal{H}^2 - \mathcal{H}' = \frac{a^2}{2M_P^2} (\rho_0 + P_0); \quad (3.103)$$

then, plugging equations (3.96) and (3.103) into (3.90) we see that \mathcal{R} becomes

$$\mathcal{R} = -\Psi - \frac{\mathcal{H}(\mathcal{H}\Phi + \Psi')}{\mathcal{H}^2 - \mathcal{H}'}. \quad (3.104)$$

4 THE INFLATIONARY UNIVERSE

In this chapter we introduce the inflationary cosmology. We follow closely (KINNEY, 2009), (BAUMANN, 2009), and (RIOTTO, 2002), together with (MUKHANOV, 2005) and (WEINBERG, 2008), and references therein.

4.1 The Cosmic Puzzles

The Λ CDM model has a number of successes in explaining the structure of the universe from primordial nucleosynthesis up to large scales. However, when applied to the very early universe, to the tiny fractions of time right after the initial singularity (as the standard lore has it¹), the standard paradigm failed completely. Basically, the standard FRW has four problems when applied to the very early universe²:

- a) The Flatness problem
- b) The Horizon problem
- c) The Entropy problem
- d) The Monopole problem.

In particular, we briefly review the first two problems in the subsections below, to see how the inflationary “miracle” works.

4.1.1 The Flatness Problem

As we have discussed in Section 2.4, the current observations favor a flat universe today, $\Omega_0 \sim 1$. However, was the universe nearly flat throughout all its history? The answer can be understood as follows. Using the Friedmann equation in the form (2.60), and taking its derivative with respect to the logarithm of the scale factor, it follows that

$$\frac{d|\Omega - 1|}{d \ln a} = (1 + 3w) \Omega |\Omega - 1|, \quad (4.1)$$

where we have used the equation of state (2.36). If the universe is flat, it remains flat at all times; however, if there is a slight deviation from flatness, the term $(1 + 3w)$

¹Despite we do not discuss non-singular models here and stick to the current Big Bang picture, it is worth mentioning that the initial singularity is completely absent in some cosmological models; see (NOVELLO; BERGLIAFFA, 2008) for a review.

²Not to mention the initial singularity, the worst of the SCM problems, where *all* physical laws *do* fail!

is positive for a radiation- or matter-dominated universe, which means that a flat universe is *unstable* for

$$\frac{d|\Omega - 1|}{d \ln a} > 0; \quad (4.2)$$

hence, small deviations from flatness at early times would grow due to the expansion of the universe and, as a result, the universe today would be *anything* but flat. Since the primordial nucleosynthesis limit is $|\Omega_{nuc} - 1| \leq 10^{-12}$, it is clear that such minute deviation from flatness would diverge at late times. The situation is even worse at the Planck epoch, since $|\Omega_{Pl} - 1| \leq 10^{-61}$; then, the FRW universe filled with radiation or matter cannot explain the present-time flatness of the universe due to the instability presented in equation (4.2). This is the so-called *flatness problem*.

4.1.2 The Horizon Problem

As we have seen in Section 2.2, the comoving cosmological horizon is defined as the maximum comoving distance travelled by a photon since the initial singularity up to a time t , and it is given by the conformal time τ (2.18); also, any physical distance in cosmology is related to a comoving length by means of the scale factor (2.8). In particular, for a radiation- or matter-dominated universe, the scale factor evolves as $a(t) \propto t^n$, where $n = 1/2$ for radiation or $n = 2/3$ for matter; then, using expressions (2.18) and (2.20), it follows that

$$a(t) \propto t^n \implies \tau \propto t^{1-n} \sim d_H. \quad (4.3)$$

Since for both radiation- or matter-dominated universe $1 - n$ is always positive, we conclude that the comoving cosmological horizon grows with time, and is *finite*; also, in this case, the comoving cosmological horizon coincides with the Hubble radius (2.20). Comoving scales entering the horizon today were outside the horizon at LSS, which means that they were not in causal contact. An accurate calculation shows that in the standard FRW universe two photons separated by an angular distance larger than around 1° were not in causal contact (RIOTTO, 2002). This fact would imply a very inhomogeneous temperature in the microwave sky; however, observational evidence shows exactly the opposite: the temperature is homogeneous up to 10^{-5} K even for angular separations larger than 1° ! This apparent lack of causal connection among primordial scales due to the finite horizon is called the *horizon problem*.

Both the flatness and the horizon problems are related. Using the fact that the Hubble parameter is $H(t) \propto t^{-1}$ for $a(t) \propto t^n$ (see Table 2.1), together with relations (2.18) and (2.60), the ratio between a comoving scale λ and the comoving horizon is a constant, given by

$$\left(\frac{\lambda}{d_H}\right)^2 |\Omega - 1| \equiv \kappa = \text{const.} \quad (4.4)$$

Taking the derivative of (4.4) with respect of $\ln a$, and using (4.1), we have

$$\frac{d}{d \ln a} \left(\frac{\lambda}{d_H}\right) = -\frac{\kappa}{2} \frac{1}{|\Omega - 1|^{3/2}} \frac{d|\Omega - 1|}{d \ln a}, \quad (4.5)$$

which is negative for $(1 + 3w) > 0$, since relation (4.2) holds:

$$\frac{d}{d \ln a} \left(\frac{\lambda}{d_H}\right) < 0. \quad (4.6)$$

The inequality (4.6) shows that the comoving horizon size grows with time, so that certain scales become causally connected only at later times. Equation (4.5) is the link between the flatness problem and the horizon problem.

4.2 The Inflationary Paradigm

The key to solve both the flatness and the horizon problem is term $(1 + 3w)$ in (4.1): if it is positive, as we have seen, both problems arise; if it is *negative*, though,

$$\frac{d|\Omega - 1|}{d \ln a} < 0, \quad \frac{d}{d \ln a} \left(\frac{\lambda}{d_H}\right) > 0, \quad (4.7)$$

which means that the point $\Omega = 1$ is *stable*, that is, the universe evolves toward flatness, and that the cosmological horizon *shrinks* in comoving units, so that a given scale would be *inside* the horizon at early times. Then, a fluid with an equation of state parameter satisfying $w < -1/3$ would solve both cosmological puzzles. Notice that, from the Raychaudhuri equation (2.43), such fluid would cause a period of *acceleration* in the early universe:

$$w < -\frac{1}{3} \implies \frac{\ddot{a}}{a} = -\frac{1}{6M_P^2} \rho (1 + 3w) > 0. \quad (4.8)$$

This period of accelerated expansion at the very early universe is called *inflation* (see Figure 2.1 to see when inflation takes place). Inflation solves not only the flatness and horizon problems, but also the other two, namely the entropy and the monopole problems, as shown in (RIOTTO, 2002).

Once we have a solution to the cosmological puzzles by means of an accelerated expansion, the next task is: how to implement inflation? Scalar fields provide the simplest way to do the job. We define the scalar field ϕ , which we call *inflaton*, to be the responsible to drive inflation. The dynamics of general scalar field theories is described by the action (D.1), whose simplest form is given by the Lagrangian density

$$\mathcal{L}[X, \phi] = X - V(\phi), \quad (4.9)$$

X being the kinetic term defined in (D.2), and $V(\phi)$ is the potential that describes the self-interactions of the field. The equation of motion for the inflaton field follows from (4.9) and (D.4),

$$\frac{1}{\sqrt{-g}} \partial_\alpha (\sqrt{-g} \partial^\alpha \phi) + V_{,\phi} = 0, \quad (4.10)$$

where we have defined

$$V_{,\phi} \equiv \frac{dV}{d\phi}. \quad (4.11)$$

For a flat FRW metric (2.6) and a homogeneous scalar field, $\phi(t, \mathbf{x}) = \phi(t)$ - which we assume to be the case throughout this Section, unless otherwise stated -, the equation of motion (4.10) becomes

$$\ddot{\phi} + 3H\dot{\phi} + V_{,\phi} = 0. \quad (4.12)$$

Equation (4.12) is basically a Klein-Gordon equation in an expanding spacetime. The extra contribution $3H\dot{\phi}$ is a friction term due to the expansion of the universe.

The hydrodynamic approach is set up as follows. First, the stress-energy momentum for the inflaton is obtained by plugging (4.9) into (D.9),

$$T_{\alpha\beta} = \phi_{,\alpha} \phi_{,\beta} - g_{\alpha\beta} \left[\frac{1}{2} g^{\kappa\lambda} \phi_{,\kappa} \phi_{,\lambda} - V(\phi) \right]. \quad (4.13)$$

The energy density and pressure for the inflaton field are derived by substituting

(4.9) into (D.10) and (D.11), which, for a flat FRW metric (2.6), gives

$$\rho_\phi = \frac{\dot{\phi}^2}{2} + V(\phi), \quad (4.14)$$

$$P_\phi = \frac{\dot{\phi}^2}{2} - V(\phi). \quad (4.15)$$

The corresponding Friedmann equation for the inflaton field is given by plugging (4.9) into (D.17),

$$H^2 = \frac{1}{3M_P^2} \left[\frac{\dot{\phi}^2}{2} + V(\phi) \right]. \quad (4.16)$$

From the definition of the equation of state (2.36), and expressions (4.14) and (4.15), we find

$$w_\phi = \frac{\dot{\phi}^2 - 2V(\phi)}{\dot{\phi}^2 + 2V(\phi)}; \quad (4.17)$$

hence, when the potential term dominates the kinetic term,

$$V(\phi) \gg \dot{\phi}^2, \quad (4.18)$$

that is, when the inflaton is slowly rolling down the potential - this is why this condition is called *slow-roll* limit -, it follows that

$$P_\phi \simeq -\rho_\phi, \quad (4.19)$$

and then $1+3w < 0$, which implements the accelerated expansion. Expression (4.19) is called *de Sitter* limit, in analogy to the corresponding solution obtained for an empty universe filled with a cosmological constant as discussed in Section 2.4. From the continuity equation (2.37) and the de Sitter limit (4.19), we deduce that $\rho'_\phi \simeq 0$, and then ρ_ϕ is nearly constant. This fact implies that H is also nearly constant, since Friedmann equation states that $H^2 \propto \rho_\phi$. Therefore, the inflationary spacetime is approximately de Sitter, and the universe expands quasi-exponentially according to expression (2.54),

$$a(t) \sim e^{Ht}. \quad (4.20)$$

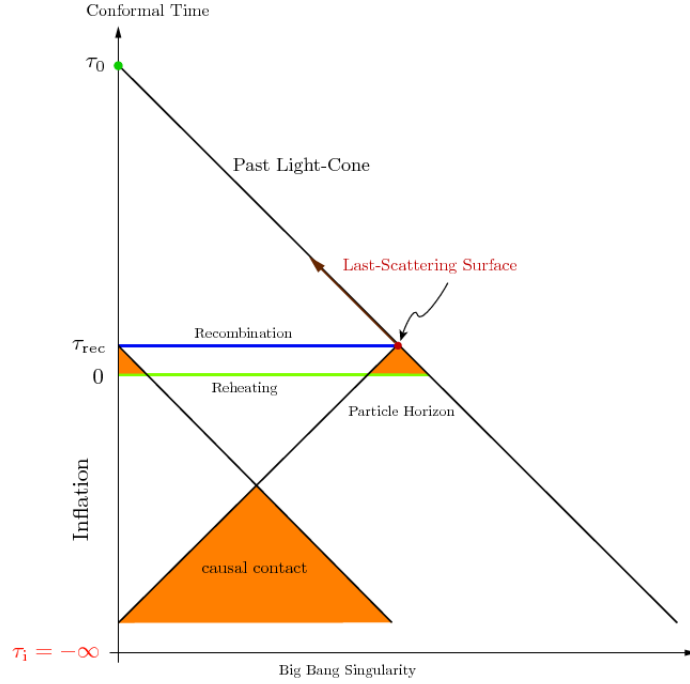


FIGURE 4.1 - The solution to the horizon problem in the inflationary cosmology. Source: Baumann (2009).

The conformal time for a quasi-de Sitter expansion is (Table 2.1)

$$\tau \sim -\frac{1}{aH}, \quad (4.21)$$

so that conformal time is *negative* during inflation, and tends to zero at late times. This means that if inflation took place *before* the radiation-dominated phase, its negative conformal time could be arbitrarily pushed back toward $-\infty$ depending on the duration of inflation. The time $\tau = 0$ represents the transition from the inflationary expansion to radiation domination. In this case, the past light cones of two events taking place at CMB would intersect thanks to such “extrapolation” to negative conformal times due to inflation. This overlap of the past light cones causally connects the events, solving the horizon problem. The conformal diagram depicted in Figure (4.1) illustrates how this mechanism work.

The duration of inflation can be parameterized conveniently by the introduction of a new variable. Integrating the equation that defines the Hubble parameter, (2.3)

between a given instant t and the end t_e of inflation, we have

$$a(t) = a_e \exp \left[- \int_t^{t_e} dt' H(t') \right]; \quad (4.22)$$

defining the *number of e-folds*, N as

$$dN \equiv -H dt, \quad (4.23)$$

and choosing the value of N at the end of inflation as $N_e = 0$, expression (4.22) reads

$$a(N) = a_e e^{-N}. \quad (4.24)$$

The definition of N looks awkward, since it goes backward in time; however, since we have observational access only to the end of inflation (KINNEY, 2009), it is convenient to assume $N_e = 0$ by the same reason that we take the initial time as $t_{in} = 0$: simplicity. The number of e-folds required for inflation ranges from $N = 46$ to $N = 60$ (see (LIDDLE; LEACH, 2003) for a discussion on these limits). However, we still can have inflation when $N \gg 60$ (for example, in exponential models, as we shall see).

Therefore, the inflationary solution in the slow-roll approximation provides a very successful solution to the mentioned cosmological puzzles. In the next section we discuss in more detail the consequences of slow-roll approximation, and derive a full set of parameters that will become fundamental to our investigations.

4.3 Flow Hierarchy in Inflation

As we have seen in the previous Section, in the slow-roll limit (4.18) the potential term dominates over the kinetic term, so that the Friedmann equation can be described as

$$H^2 \simeq \frac{1}{3M_P^2} V(\phi); \quad (4.25)$$

since the Hubble parameter is nearly constant, equation (4.25) implies that the potential is *approximately flat*; such condition can be formalized as

$$V_{,\phi} \ll V. \quad (4.26)$$

Since $\dot{\phi}$ slowly varies with time, its derivative $\ddot{\phi}$ must be negligible, so that the equation of motion (4.12) becomes

$$\dot{\phi} \simeq -\frac{V_{,\phi}}{3H}. \quad (4.27)$$

Then, in the slow-roll limit the time evolution of the inflaton field depends on the variation of the potential with respect to the field itself. Since $V(\phi)$ is a function of ϕ , with no explicit time dependence, equation (4.27) suggests that all the time evolution can be replaced by evolution in ϕ if it is a monotonic function in time. In this sense, the field ϕ acts as a ‘‘clock’’. This property works well for the slow-roll approximation, but is it valid in the general case? To answer this question let us take the derivative of the Hubble parameter in (4.16) with respect to ϕ and use its equation of motion (4.12); the result is

$$\dot{\phi} = -2M_P^2 H_{,\phi}, \quad (4.28)$$

which shows that we can express the Hubble parameter as a function of ϕ , $H = H(\phi)$. Plugging equation (4.28) into (4.16) we have that

$$\left[\frac{d}{d\phi} H(\phi) \right]^2 - \frac{3}{2M_P^2} H(\phi)^2 - \frac{1}{2M_P^4} V(\phi) = 0. \quad (4.29)$$

Equations (4.28) and (4.29) are called *Hamilton-Jacobi* equations for inflation (MUSLIMOV, 1990), (SALOPEK; BOND, 1990). The Hamilton-Jacobi equation describes the evolution of the Hubble parameter entirely in terms of the inflaton field, which is very convenient for computational purposes.

From equation (4.28) we can express the time derivative of the Hubble parameter H in terms of ϕ solely,

$$\dot{H} = -2M_P^2 H_{,\phi}^2; \quad (4.30)$$

then, from equations (2.49) and (4.30), we see that the acceleration of the universe can be expressed in terms of ϕ -dependent functions,

$$\frac{\ddot{a}}{a} = H^2 [1 - \epsilon(\phi)], \quad (4.31)$$

where we have defined the *flow parameter* ϵ as

$$\epsilon \equiv 2M_P^2 \left(\frac{H_{,\phi}}{H} \right)^2. \quad (4.32)$$

In terms of the flow parameter ϵ , the Hamilton-Jacobi equation (4.29) becomes

$$H(\phi)^2 \left[1 - \frac{1}{3}\epsilon(\phi) \right] = \frac{1}{3M_P^2} V(\phi), \quad (4.33)$$

whereas the equation of state for the inflaton field reads

$$P_\phi = \left[\frac{2}{3}\epsilon(\phi) - 1 \right] \rho_\phi, \quad (4.34)$$

where we have substituted into expression (4.17) the relations (4.28) for $\dot{\phi}$ and the Hamilton-Jacobi equation (4.33) for V , and used definition (4.32).

We can also rewrite higher-order time derivatives of ϕ in terms of $H(\phi)$ and its derivatives. In particular, $\ddot{\phi}$ reads

$$\ddot{\phi} = -2M_P^2 H_{,\phi\phi} \dot{\phi}, \quad (4.35)$$

so that the equation of motion (4.12) can be completely written in terms of $\dot{\phi}$:

$$(3 - \eta) H \dot{\phi} + V_{,\phi} = 0, \quad (4.36)$$

where we have defined the second flow parameter η as

$$\eta \equiv 2M_P^2 \frac{H_{,\phi\phi}}{H}. \quad (4.37)$$

Notice that the value of the flow parameter ϵ literally *controls* inflationary expansion:

$$\boxed{\ddot{a} > 0 \iff \epsilon < 1}, \quad (4.38)$$

so that inflation lasts as long as the flow parameter ϵ is less than one. Also, both parameters ϵ and η *dictate* the slow-roll approximation: taking $\epsilon \ll 1$, the equation

of state (4.34) becomes

$$P_\phi \simeq -\rho_\phi, \quad (4.39)$$

in agreement with (4.19), whereas the Hamilton-Jacobi (4.33) reads

$$\epsilon \ll 1 \implies H^2 \simeq \frac{1}{3M_P^2} V(\phi), \quad (4.40)$$

which coincides with expression (4.25), (the consequence of the slow-roll approximation (4.18)). In turn, taking $\eta \ll 1$, equation (4.36) becomes

$$\eta \ll 1 \implies \dot{\phi} \simeq -\frac{V_{,\phi}}{3H}, \quad (4.41)$$

which coincides with relation (4.27), (the consequence of the approximate flatness of the potential, given by (4.26)).

Hence, the flow parameters ϵ and η play a decisive role to determine the conditions for inflation and slow-roll. In particular, if ϵ varies with time (it can be a constant, as we shall see in the next Section), inflation ends when ϕ reaches the value $\phi = \phi_e$,

$$\boxed{\text{End of inflation : } \epsilon(\phi_e) = 1}. \quad (4.42)$$

If ϵ is constant, additional physics must be introduced to enforce inflation to end.

Along with the flow parameters ϵ and η we can derive a whole hierarchy of higher-order parameters as follows. First of all, we adopt the convention that the sign of $\sqrt{\epsilon}$ is the same of $H_{,\phi}$,

$$\sqrt{\epsilon} \equiv +\sqrt{2}M_P \frac{H_{,\phi}}{H}; \quad (4.43)$$

then, taking the derivative of the parameter η , for example, we get

$$\frac{d\eta}{d\phi} = 2M_P^2 \frac{H_{,\phi\phi\phi}}{H} - \frac{\eta\sqrt{\epsilon}}{\sqrt{2}M_P}, \quad (4.44)$$

which may be simplified by defining

$$\xi^2 \equiv (2M_P^2)^2 \frac{H_{,\phi}H_{,\phi\phi\phi}}{H^2}, \quad (4.45)$$

leading to

$$\frac{d\eta}{d\phi} = \frac{\xi^2 - \epsilon\eta}{\sqrt{2\epsilon}M_P}, \quad (4.46)$$

and so forth. Proceeding this way, the ℓ -th parameter, with $\ell = 3, \dots, \infty$, is given by (KINNEY, 2002)

$${}^\ell\lambda = (2M_P^2)^\ell \left(\frac{H_{,\phi}}{H}\right)^{\ell-1} \frac{1}{H} \frac{d^{\ell+1}}{d\phi^{\ell+1}} H. \quad (4.47)$$

In particular, we can get rid of the extra factors appearing in (4.46) by simply changing the variable ϕ to the number of e-folds, N , defined in (4.23), so that

$$\frac{d}{d\phi} = \frac{1}{\sqrt{2\epsilon}M_P} \frac{d}{dN}, \quad (4.48)$$

and then

$$\frac{d\eta}{dN} = \xi^2 - \epsilon\eta. \quad (4.49)$$

In terms of N , the flow parameter ϵ assume the following equivalent (and simpler) form

$$\epsilon = \frac{1}{H} \frac{dH}{dN}. \quad (4.50)$$

The flow parameters (4.32), (4.37), (4.45) and (4.47) satisfy an infinite set of first-order differential equations, the so-called *flow hierarchy*

$$\begin{aligned} \frac{d\epsilon}{dN} &= \epsilon(2\eta - 2\epsilon), \\ \frac{d\eta}{dN} &= \xi^2 - \epsilon\eta, \\ &\vdots \\ \frac{d^\ell\lambda}{dN} &= -{}^\ell\lambda[\ell\epsilon - (\ell-1)\eta] + {}^{\ell+1}\lambda. \end{aligned} \quad (4.51)$$

Solutions to this infinite hierarchy of flow equations are equivalent to solutions of the scalar field equation of motion.

4.4 Inflationary Potentials

Inflation acquires different properties depending on the shape of the scalar potential $V(\phi)$. We summarize below the different classes of inflationary potentials according to the classification pushed forward by (DODELSON et al., 1997). All figures are adapted from (KINNEY, 2003).

4.4.1 Large-Field Inflationary Potentials

In these models, the inflaton field is displaced far from its minimum to a value $\phi \sim \mu$ (several times the value M_P), and then rolls down toward its minimum at the origin on a potential

$$V(\phi) = \Lambda^4 \left(\frac{\phi}{\mu} \right)^p, \quad (4.52)$$

where Λ is the energy scale of inflation, and $p > 1$ (Figure 4.2). In this case, $\phi > \phi_e$, and then inflation occurs when the inflaton field strength is larger than its minimum.

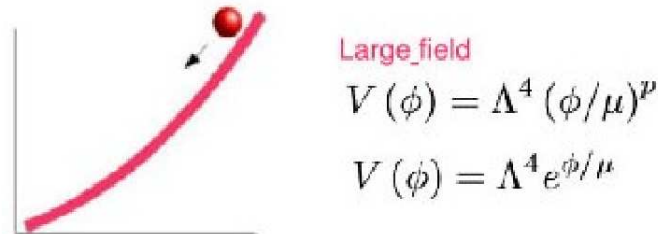


FIGURE 4.2 - Large-field polynomial potentials.

The flow parameters are given by

$$\epsilon(\phi) = \frac{p^2 M_P^2}{2 \phi^2}, \quad (4.53)$$

$$\eta(\phi) = \frac{p(p-2)}{2} \frac{M_P^2}{\phi^2}, \quad (4.54)$$

whereas inflation ends when

$$\frac{\phi_e^c}{M_P} = \frac{p}{\sqrt{2}}. \quad (4.55)$$

4.4.2 Small-field polynomial potentials

Small-field polynomial potentials in canonical inflation arise from a spontaneous symmetry breaking in the presence of a “false” vacuum in unstable equilibrium with nonzero vacuum energy density and a “physical” vacuum, for which the classical expectation value of the scalar field is nonzero, $\langle\phi\rangle \neq 0$ (KINNEY; MAHANTHAPPA, 1996). A typical potential of this form arises in the so-called “natural” inflation models (FREESE *et al.*, 1990). These models are characterized by an effective symmetry-breaking scale $\mu \propto \langle\phi\rangle$ such that $\phi \ll \mu \ll M_P$, the field rolls down from an unstable equilibrium at the origin toward μ ; hence, for positive ϕ we have always $\dot{\phi} > 0$, see Figure 4.3.

$$V(\phi) = \Lambda^4 \left[1 - \frac{1}{p} \left(\frac{\phi}{\mu} \right)^p \right], \quad (4.56)$$

where μ is the effective symmetry-breaking scale given by (KINNEY; MAHANTHAPPA, 1996)

$$\mu = \left[\frac{(m-1)! V(\phi)}{|d^m V/d\phi^m|} \right]^{1/m} \Bigg|_{\phi=0}, \quad (4.57)$$

and m is the order of the lowest nonvanishing derivative of the potential at the origin. Potential (4.56) has to be regarded as the lowest-order term in a Taylor expansion, since higher order terms can be neglected due to the smallness of ϕ in comparison to μ . In the canonical small-field scenario the initial unstable equilibrium state is characterized by the vacuum energy density Λ^4 , which is the height of the potential at the origin, $\Lambda^4 = V(0)$.

The flow parameter ϵ assumes the form

$$\epsilon(\phi) = \frac{M_P}{\mu\sqrt{2}} \left(\frac{\phi}{\mu} \right)^{2(p-1)}, \quad (4.58)$$

whereas from (4.58) we see that inflation ends at

$$\frac{\phi_e}{\mu} = \left[\frac{\mu}{M_P} \sqrt{2} \right]^{1/(p-1)}. \quad (4.59)$$

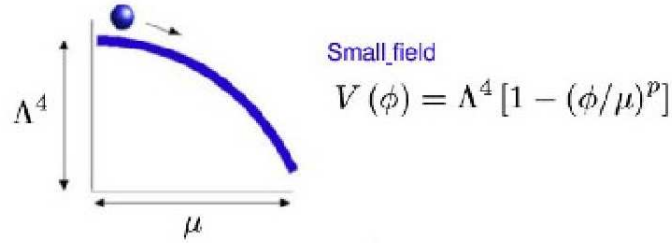


FIGURE 4.3 - Small-field polynomial potentials.

4.4.3 Hybrid potentials

This family of inflationary models is characterized by two scalar fields: one field ϕ drives inflation, whereas the other ψ makes inflation end. The original hybrid potential was pushed forward by Linde, (LINDE, 1994; LINDE, 1991)

$$V(\phi) = \frac{m^2}{2}\phi^2 + \frac{\lambda'}{2}\psi^2\phi^2 + \frac{\lambda}{4}(M^4 - \psi^2)^2, \quad (4.60)$$

where M is a given energy scale, and m , λ and λ' coupling constants. For $\phi > \phi_c = \lambda M^2/\lambda'$, that is, its critical value, the potential for ψ has a minimum at $\psi_{\min} = 0$, which occurs during inflation. The field ψ is kept at this minimum, so that ϕ slowly rolls down the effective potential

$$V(\phi) = \frac{\lambda M^4}{4} + \frac{m^2}{2}\phi^2, \quad (4.61)$$

until it reaches the critical value ϕ_c , which shifts the minimum of ψ to $\psi_{\min} = \pm M$. The field ψ then rolls down toward one of these minima, enforcing inflation to end.

In general, the effective potentials for hybrid models are of the form

$$V(\phi) \sim \Lambda^4 \left[1 + \left(\frac{\phi}{\mu} \right)^p \right], \quad (4.62)$$

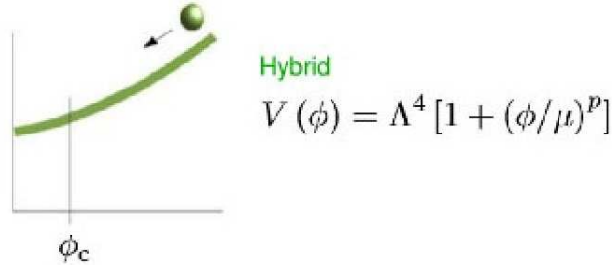


FIGURE 4.4 - Hybrid potentials.

where, again, expression above is the lowest-order term of a Taylor expansion. The behavior of the inflaton field on the hybrid potential is depicted in Figure 4.4.

4.4.4 Exponential potentials - Power-law Inflation

Exponential potentials make up a very important class of inflationary models, and are characterized by

$$V(\phi) = \Lambda^4 \exp \left[\sqrt{\frac{2}{p}} \left(\frac{\phi}{M_P} \right)^2 \right], \quad (4.63)$$

where $p > 0$. In this case, the Hubble parameter also has an exponential form, and then leads to a scale factor with power-law dependence on t , $a \propto t^p$. This class of inflationary models were studied by Lucchin and Matarrese under the name *power-law inflation* (LUCCHIN; MATARRESE, 1985). One of the most important features of these models is that the flow parameters are constant:

$$\epsilon(\phi) = \eta(\phi) = \frac{1}{p}; \quad (4.64)$$

also, the Hubble parameter is inversely proportional to t ,

$$H = \frac{1}{\epsilon t}. \quad (4.65)$$

The inflaton in this class of models behaves exactly as large-field models, as depicted in Figure 4.2.

4.5 Quantum Fluctuations from Inflation

Once we have introduced the fundamental ideas concerning the dynamics of inflation, let us now discuss one of the most fundamental results of the inflationary cosmology: the generation of nearly scale-invariant spectrum of perturbations, which seeds the structure formation of the universe. We have introduced perturbations in Chapter 3, but a question remains unanswered: what created such tiny primordial fluctuations? Inflation is a mechanism that provides this answer³. Instead of a classical inflaton field evolving classically on a potential $V(\phi)$, as we have considered so far, small *quantum* fluctuations $\delta\phi$ around its classical trajectory couple to the spacetime curvature, originating then the primordial density fluctuations. Such quantum fluctuations evolve during inflation, until they exit the horizon and become classically "frozen", and only much time later they re-enter the horizon and act as the classical seeds to the small inhomogeneities that will grow into structure by gravitational instability. Therefore, inflation solves in a very elegant and physically rich way the problem of the generation of the small fluctuations in the universe.

In the next section we treat in detail the generation of such small fluctuations provided by inflation. We drop the subscript $,\phi$ to indicate derivatives in the sequel, and simply write it as ϕ .

4.5.1 Introducing Perturbations

To see how the inflaton fluctuations couple with the inhomogeneities discussed in Chapter 3, let us derive first the equation of motion (4.10) for the perturbations. To do so, we take the metric in the longitudinal gauge (3.85) with tensor perturbations,

$$ds^2 = a(\tau)^2 \left\{ (1 + 2\Phi) d\tau^2 - [(1 - 2\Psi) \delta_{ij} + h_{ij}] dx^i dx^j \right\}, \quad (4.66)$$

and use δ as an "operator" on (4.10), whose result is

$$\delta\phi'' + 2\mathcal{H}\delta\phi' - \nabla^2\delta\phi - \phi'(\Phi' + 3\Psi') + 2a^2\Phi V_\phi + a^2V_{\phi\phi}\delta\phi = 0. \quad (4.67)$$

³Although other proposals do also provide an answer. See the Introduction and Chapter 8.

Proceeding the same way for the stress energy-momentum tensor (4.13), we have

$$\begin{aligned}\delta T_{00} &= \phi' \delta \phi' + 2a^2 \Phi V + a^2 V_\phi \delta \phi, \\ \delta T_{i0} &= \phi' \delta \phi, \\ \delta T_{ij} &= \left[-(\Phi + \Psi) \phi'^2 + \phi' \delta \phi + a^2 (2\Psi V - V_\phi \delta \phi) \right] \delta_{ij};\end{aligned}\quad (4.68)$$

next, using expressions (3.92-3.94) for the Einstein tensor, and (4.68) for the energy-momentum tensor, the Einstein equations (3.91) read

$$\nabla^2 \Psi - 3\mathcal{H}(\Psi' + \mathcal{H}\Phi) = \frac{1}{2M_P^2} (\phi' \delta \phi' - \phi'^2 \Phi + a^2 V_\phi \delta \phi), \quad (4.69)$$

$$\Psi' + \mathcal{H}\Phi = \frac{1}{2M_P^2} \phi' \delta \phi, \quad (4.70)$$

$$\begin{aligned}\Psi'' + \mathcal{H}(\Phi' + 2\Psi') + (\mathcal{H}^2 + 2\mathcal{H}')\Phi \\ = -\frac{1}{2M_P^2} (\Phi \phi'^2 - \phi' \delta \phi' + a^2 V_\phi \delta \phi).\end{aligned}\quad (4.71)$$

The equation for the tensor perturbations is identical to (3.101) without anisotropic stresses, and is given by

$$h''_{ij} - \nabla^2 h_{ij} + 2\mathcal{H}h'_{ij} = 0. \quad (4.72)$$

Equations (4.69-4.71) show the coupling between the inflaton perturbation $\delta\phi$ and the scalar modes Φ and Ψ , whereas tensor modes do not couple. Despite tensor modes will not play any role in the density perturbations at the time of recombination, they do generate CMB temperature anisotropies by inducing a gravitational redshift on the photons frequency using the same mechanism of horizon exit and re-entry. More on this topic will be discussed in Chapter 5.

4.5.2 Evolution of the Scalar Modes

Equation (4.70) shows that the comoving curvature perturbation (3.104) is connected to the perturbation of the inflaton field, $\delta\phi$; to see this, we first substitute the expressions for the energy density (4.14) and for the pressure (4.15) into expression (3.103); then, going to conformal time, we get $\dot{\phi} = \phi'/a$, and

$$\mathcal{H}^2 - \mathcal{H}' = \frac{1}{2M_P^2} \phi'^2, \quad (4.73)$$

so that, from (3.104), (4.70) and (4.73), we find

$$\mathcal{R} = -\Psi - \mathcal{H} \frac{\delta\phi}{\phi'}. \quad (4.74)$$

Therefore, the small fluctuations of the inflaton field induce curvature perturbations by means of equation (4.74). In particular, taking the derivative of equation (4.74), and using (4.69) and (4.71), we find

$$\mathcal{R}' = -\frac{2M_P^2 \mathcal{H}}{\phi'} \nabla^2 \Psi; \quad (4.75)$$

then, defining the variable z as

$$z(\tau) \equiv \frac{a\phi'}{\mathcal{H}}, \quad (4.76)$$

and using again (4.69), (4.71) together with (4.75) and (4.76), we find

$$\mathcal{R}'' + 2\frac{z'}{z}\mathcal{R}' - \nabla^2 \mathcal{R} = 0. \quad (4.77)$$

Introducing the *Mukhanov-Sasaki* potential u as

$$u \equiv z\mathcal{R}, \quad (4.78)$$

equation (4.77) turns to

$$u'' - \nabla^2 u - \frac{z''}{z}u = 0. \quad (4.79)$$

Expanding the Mukhanov-Sasaki potential u in its Fourier modes,

$$u(\tau, x) = \int \frac{d^3k}{(2\pi)^{3/2}} u_{\mathbf{k}}(\tau) e^{i\mathbf{k}\cdot\mathbf{x}}, \quad (4.80)$$

we obtain the *mode equation for curvature perturbations*,

$$\boxed{u_k'' + \left(k^2 - \frac{z''}{z}\right) u_k = 0}, \quad (4.81)$$

which shows that the mode functions u_k depend only upon the magnitude of the comoving wave vector \mathbf{k} .

4.5.3 Evolution of the Tensor Modes

We now turn our attention to the equation for tensor perturbations, given by (4.72). We first go to the Fourier space, expanding the tensor h_{ij} according to (C.28) and (C.29), and following the discussion in Section C.2.2,

$$h_{ij}(\tau, x) = \int \frac{d^3k}{(2\pi)^{3/2}} \left[h_{\mathbf{k}}^{(+)}(\tau) \varepsilon_{ij}^{(+)}(\mathbf{k}) + h_{\mathbf{k}}^{(\times)}(\tau) \varepsilon_{ij}^{(\times)}(k) \right] e^{i\mathbf{k}\cdot\mathbf{x}}, \quad (4.82)$$

where $\varepsilon_{ij}^{(+,\times)}$ are the polarization tensors given by (C.33). Plugging expansion (4.82) into equation (4.72), we get

$$h_k'' + 2\mathcal{H}h_k' + k^2 h_k = 0, \quad (4.83)$$

for both modes $+$ and \times , whence we deduce that the tensor modes h_k depend only on the magnitude of the modes \mathbf{k} (see Appendix C). Defining the quantity (GRISHCHUK, 1975),

$$\mu_k(\tau) \equiv \frac{M_P}{2} a(\tau) h_k(\tau), \quad (4.84)$$

we obtain the *mode equation for tensor perturbations*

$$\boxed{\mu_k'' + \left[k^2 - \frac{a''}{a} \right] \mu_k = 0}, \quad (4.85)$$

which has the same functional form as the corresponding equation for the curvature fluctuations (4.81).

4.5.4 Quantizing the Modes

Before undertaking the task of solving the mode equations (4.81) and (4.85) for scalar and tensor perturbations, it is important to gain some insight by studying the asymptotic behavior of the mode functions u_k and μ_k . Since these equations have the same functional form, we solve for the function u_k first, and then write down the similar solutions for μ_k . The asymptotic limits are discussed below.

- **Short-wavelength limit: Subhorizon scales**

This limit is characterized by

$$k^2 \gg \frac{z''}{z}, \quad (4.86)$$

so that the mode equation (4.81) becomes

$$u_k'' + k^2 u_k = 0. \quad (4.87)$$

This is the equation of a simple harmonic oscillator, whose solution is given by

$$u_k(\tau) = \frac{A_k e^{ik\tau} + B_k e^{-ik\tau}}{\sqrt{2k}}. \quad (4.88)$$

• **Long-wavelength limit: Superhorizon scales**

In this case,

$$k^2 \ll \frac{z''}{z}, \quad (4.89)$$

and so equation (4.81) yields

$$u_k'' - \frac{z''}{z} u_k = 0, \quad (4.90)$$

whose solution is

$$\frac{u_k''}{u_k} = \frac{z''}{z} \implies u_k(\tau) \propto z(\tau). \quad (4.91)$$

The arbitrary normalization constants can be fixed as follows. We first expand $u(\tau, \mathbf{x})$ as a quantum operator,

$$u(\tau, \mathbf{x}) = \int \frac{d^3 \mathbf{k}}{(2\pi)^{3/2}} \left[u_k(\tau) e^{i\mathbf{k}\cdot\mathbf{x}} \hat{a}_{\mathbf{k}} + u_k^*(\tau) e^{-i\mathbf{k}\cdot\mathbf{x}} \hat{a}_{\mathbf{k}}^\dagger \right], \quad (4.92)$$

where $\hat{a}_{\mathbf{k}}$ and $\hat{a}_{\mathbf{k}}^\dagger$ are respectively the annihilation and creation operators, and satisfies the well known commutation relations

$$\left[\hat{a}_{\mathbf{k}}, \hat{a}_{\mathbf{k}'}^\dagger \right] = \delta^{(3)}(\mathbf{k} - \mathbf{k}'), \quad (4.93)$$

and, for the vacuum state $|0\rangle$,

$$\hat{a}_{\mathbf{k}}|0\rangle = 0. \quad (4.94)$$

Inverting the operators $\hat{a}_{\mathbf{k}}$ and $\hat{a}_{\mathbf{k}}^\dagger$ to express them in the configuration space, after a hard work we can show that (4.93) implies the Wronskian condition

$$u_k u_k^{*'} - u_k^* u_k' = i. \quad (4.95)$$

Substituting expression (4.92) into (4.95), we obtain

$$|A_k|^2 - |B_k|^2 = 1, \quad (4.96)$$

which is the normalization condition. The second condition that provides a way to fix one of the constants is the choice of the quantum vacuum. In quantum field theory, the vacuum is defined as the a zero-particle state as seen by an inertial observer in the Minkowski spacetime, where a quantum state representing a particle with momentum \mathbf{k} can be built from the creation operators $\hat{a}_{\mathbf{k}}^\dagger$. In the case of quantum cosmological fluctuations, the vacuum choice must be performed on subhorizon scales, since all the comoving scales were deep inside the Hubble horizon and then in causal contact. Subhorizon scales correspond to the short-wavelength limit, where the mode equation switches to a harmonic oscillator-like equation (4.87), whose solutions lead to a Minkowski vacuum as long as k is time-independent. To ensure a Minkowski vacuum we must set

$$A_k = 1, \quad B_k = 0, \quad (4.97)$$

which guarantees that $\hat{a}_{\mathbf{k}}|0\rangle = 0$, as desired. Choice (4.97) is called the *Bunch-Davies* vacuum. Using conditions (4.96) and (4.97) we completely fix the constants A_k and B_k .

As for superhorizon scales, (4.91), it follows from the definition of the mode u_k , equation (4.78), that

$$\mathcal{R}_k = \frac{u_k}{z} \simeq \text{const.}; \quad (4.98)$$

hence, modes with wavelengths larger than the horizon have constant nonzero amplitude for the curvature on comoving hypersurfaces. That is, the quantum amplitudes of the long wavelength modes, outside the horizon, asymptote to a constant nonzero amplitude. This is the well known phenomenon of *mode freezing*, which allows for a quantum fluctuation to exit the horizon as a perturbation with constant amplitude and re-enter the horizon as a classical inhomogeneity that seeds the future structure formation.

4.6 Solutions to the Mode Equation

Once we have discussed the main features of the asymptotic limits of the quantum fluctuations, we next work out some full solutions to the mode equations.

4.6.1 Slow-Roll Solutions

Let us now study the slow-roll solution to the mode equation (4.81). One of the key ingredients to finding such solutions is provided by the flow parameters (4.32), (4.37) and (4.45); they come into play through equation (4.28), from which we have

$$\frac{\dot{\phi}}{H} = \frac{\phi'}{\mathcal{H}} = -\sqrt{2M_{\text{P}}^2\epsilon}, \quad (4.99)$$

so that the variable z becomes

$$z = -a\sqrt{2M_{\text{P}}^2\epsilon}. \quad (4.100)$$

Next, using definitions (2.24) and (4.23), we get

$$\frac{d}{d\tau} = -aH \frac{d}{dN}, \quad (4.101)$$

so that the acceleration term z''/z turns to (KINNEY, 2002)

$$\frac{z''}{z} \equiv a^2 H^2 F(\epsilon, \eta, \xi^2), \quad (4.102)$$

where

$$F \equiv 2 + 2\epsilon - 3\eta + 2\epsilon^2 - 4\epsilon\eta + \eta^2 + \xi^2, \quad (4.103)$$

and then the mode equation (4.81) becomes

$$\frac{1}{aH} \frac{d^2 u_k}{d\tau^2} + \left[\left(\frac{k}{aH} \right)^2 - F \right] u_k = 0. \quad (4.104)$$

Note that the ratio $k/(aH)$ appearing in equation (4.104) determines whether a given wavelength is in- or outside the horizon (2.21-2.22); then, it is convenient to introduce a new variable (KINNEY, 2005)

$$y \equiv \frac{k}{aH}, \quad (4.105)$$

such that $y \ll 1$ for superhorizon and $y \gg 1$ for subhorizon scales. In terms of y ,

the derivative with respect to the conformal time reads

$$\frac{d^2}{d\tau^2} = a^2 H^2 \left[(1 - \epsilon)^2 y^2 \frac{d^2}{dy^2} + G(\epsilon, \eta) y \frac{d}{dy} \right], \quad (4.106)$$

where

$$G = -2\epsilon\eta + 2\epsilon^2. \quad (4.107)$$

Therefore, the mode equation (4.104) becomes

$$(1 - \epsilon)^2 y^2 \frac{d^2 u_k}{dy^2} + (-2\epsilon\eta + 2\epsilon^2) y \frac{du_k}{dy} + [y^2 - F] u_k = 0, \quad (4.108)$$

so that to first order in slow-roll, it turns to

$$(1 - 2\epsilon) y^2 \frac{d^2 u_k}{dy^2} + [y^2 - 2 - 2\epsilon + 3\eta] u_k = 0, \quad (4.109)$$

whose solution is

$$u_k(y) = y^{1/2} \left[\alpha H_\nu^{(1)} \left(\frac{y}{1 - \epsilon} \right) + \beta H_\nu^{(2)} \left(\frac{y}{1 - \epsilon} \right) \right], \quad (4.110)$$

where α and β are constants and $H_\nu^{(1)}$, $H_\nu^{(2)}$ are Hankel functions of first and second kind, respectively, and

$$\nu = \frac{3}{2} + 2\epsilon - \eta. \quad (4.111)$$

Using the normalization condition established by the Wronskian (4.95) and fixing the Bunch-Davies vacuum (4.97), we have $\beta = 0$, so that we find from (4.110) the normalized solution

$$u_k(y) = \frac{1}{2} \sqrt{\frac{\pi}{k}} \left(\frac{y}{1 - \epsilon} \right) H_\nu^{(1)} \left(\frac{y}{1 - \epsilon} \right). \quad (4.112)$$

4.6.2 The Power-Law Solution

The power-law solution is characterized by *constant* slow-roll parameters, and give rise to inflationary exponential models like (4.63). For $\epsilon = \text{const.}$, from definition

(4.76) we have

$$\frac{z''}{z} = \frac{a''}{a}, \quad (4.113)$$

so that the same solution works for both tensor and curvature modes. Equations (2.49) and (4.31) yield

$$\frac{a''}{a} = a^2 (2 - \epsilon) H^2; \quad (4.114)$$

then, using the definition of conformal time, (2.9) and (4.65), we find

$$\tau = -\frac{1}{1 - \epsilon} \frac{1}{aH}. \quad (4.115)$$

From the definition of the variable y , (4.105), and (4.115), it follows that

$$y = -\frac{k\tau}{1 - \epsilon}, \quad (4.116)$$

so that the mode equation (4.81) and (4.85) become

$$(1 - \epsilon)^2 y^2 \frac{d^2 u_k}{dy^2} + [y^2 - (2 - \epsilon)] u_k = 0. \quad (4.117)$$

The solution to equation (4.117) is given by

$$u_k(y) = y^{1/2} \left[\alpha H_\nu^{(1)} \left(\frac{y}{1 - \epsilon} \right) + \beta H_\nu^{(2)} \left(\frac{y}{1 - \epsilon} \right) \right], \quad (4.118)$$

where now

$$\nu = \frac{3 - \epsilon}{2(1 - \epsilon)}. \quad (4.119)$$

From the normalization condition established by the Wronskian (4.95) and fixing the Bunch-Davies vacuum (4.97), we have $\beta = 0$, so that from (4.116) and (4.118) we find the normalized solution

$$u_k(y) = \frac{1}{2} \sqrt{\frac{\pi}{k} \left(\frac{-k\tau}{1 - \epsilon} \right)} H_\nu^{(1)} \left(\frac{-k\tau}{1 - \epsilon} \right), \quad (4.120)$$

which is an exact solution to *all* wavelengths.

4.6.3 The de Sitter Solution

For the de Sitter solution, $H = \text{const.}$, so that $\epsilon = 0$. The mode equation is the same as (4.117) for $\epsilon = 0$, so that the de Sitter solutions (4.118) read

$$u_k(\tau) = \sqrt{-k\tau} \left[\alpha H_{3/2}^{(1)}(-k\tau) + \beta H_{3/2}^{(2)}(-k\tau) \right], \quad (4.121)$$

where we have used the result $\nu = 3/2$ from (4.119). Using the expressions for the Hankel functions $H_{3/2}$ (see, *e.g.*, (ABRAMOWITZ; STEGUN, 1972)), and using the asymptotic limits $-k\tau \rightarrow 0$ and $k\tau \rightarrow \infty$ to apply the Bunch-Davies vacuum condition, and normalizing the modes as we did in the previous subsection, we find that (4.121) becomes

$$u_k(\tau) = \frac{1}{\sqrt{2k}} \left(1 - \frac{i}{k\tau} \right) e^{-ik\tau}, \quad (4.122)$$

which is valid for all wavelengths, and is an exact solution.

4.7 Power Spectrum

Once we have found solutions to the mode equations (4.81) and (4.85) the next important step is the computation of the amplitude of the quantum fluctuations. For a generic function $f(\tau, \mathbf{x})$ (which can be either the Mukhanov-Sasaki potential or the tensor amplitude), the two-point correlation function is defined as

$$\xi(\tau, r) \equiv \langle 0 | f(\tau, \mathbf{x}) f(\tau, \mathbf{x} + \mathbf{r})^* | 0 \rangle, \quad (4.123)$$

where ξ depends on $r = |\mathbf{r}|$ by isotropy. Expanding f in Fourier modes as in (4.80), we find from (4.123) that

$$\xi(\tau, r) = \int \frac{d^3k}{(2\pi)^{3/2}} \frac{d^3k'}{(2\pi)^{3/2}} \langle 0 | f_{\mathbf{k}}(\tau) f_{\mathbf{k}'}^*(\tau) | 0 \rangle e^{i\mathbf{k}\cdot\mathbf{r}}; \quad (4.124)$$

assuming that the Fourier modes $f_{\mathbf{k}}$ are normally distributed, we define the *power spectrum* $P(k)$ as

$$\langle 0 | f_{\mathbf{k}} f_{\mathbf{k}'}^* | 0 \rangle = \frac{2\pi^2}{k^3} P(k) \delta^{(3)}(\mathbf{k} - \mathbf{k}'), \quad (4.125)$$

where the normalization $2\pi^2/k^3$ has been chosen to render the power spectrum dimensionless. Therefore,

$$\langle |f(\tau, \mathbf{x})|^2 \rangle = \int \frac{dk}{k} P(k). \quad (4.126)$$

For curvature perturbations, from the definition of the Mukhanov-Sasaki potential we have $\mathcal{R}_k = u_k/z$, so that the corresponding power spectrum (4.126) is

$$P_{\mathcal{R}}(k) = \frac{k^3}{2\pi^2} \left| \frac{u_k}{z} \right|^2. \quad (4.127)$$

As we have seen in Section 4.5.4, on superhorizon scales the curvature perturbation (4.98) is nearly constant, so that we can approximate the mode function u_k by a de Sitter solution (4.122) which, on superhorizon scales $-k\tau \rightarrow 0$, yields

$$u_k(\tau) \simeq -\frac{1}{\sqrt{2k}} \frac{i}{k\tau}; \quad (4.128)$$

next, using the expression for the conformal time given by (4.115) with $\epsilon \ll 0$, that is, $\tau \sim -1/(aH)$, it follows from (4.128) that

$$u_k(\tau) \simeq \frac{iaH}{\sqrt{2k^3}}. \quad (4.129)$$

Next, using (4.100), (4.127) and (4.129), we find, at the *horizon exit* $k = aH$,

$$\boxed{P_{\mathcal{R}}^{1/2} = \frac{1}{8\pi^2} \frac{H^2}{M_P^2 \epsilon} \Big|_{k=aH}}. \quad (4.130)$$

For tensor perturbations, the power spectrum is given by

$$P_T(k) = \frac{k^3}{\pi^2} |h_k|^2, \quad (4.131)$$

where the factor 2 accounts for the two polarization states of the graviton. In the slow-roll limit, the solution for μ is given by (4.129) on superhorizon scales,

$$\mu_k(\tau) \simeq \frac{iaH}{\sqrt{2k^3}}; \quad (4.132)$$

then, substituting (4.84) and (4.132) into (4.131), we find, at the horizon exit,

$$P_T = \frac{2}{\pi^2} \frac{H^2}{M_P^2} \Big|_{k=aH}. \quad (4.133)$$

Another important quantity, whose upper bound is measured by CMB satellites, is the tensor-to-scalar ratio, r , which is nothing but the tensor power spectrum normalized to its scalar counterpart, that is,

$$r \equiv \frac{P_T}{P_{\mathcal{R}}}. \quad (4.134)$$

We can usually approximate both the scalar and tensor power spectra on k by a power-law, $P(k) \propto k^n$; then, the *spectral scalar index*, n_s , and the *tensor spectral index* can be evaluated by means of the expressions

$$\begin{aligned} n_s - 1 &\equiv \frac{d(\ln P_{\mathcal{R}})}{d(\ln k)}, \\ n_T &\equiv \frac{d(\ln P_T)}{d(\ln k)}, \end{aligned} \quad (4.135)$$

respectively. The spectral indices measure the scale dependence of the power spectrum on the Fourier mode k . In the slow-roll limit, we have

$$\begin{aligned} n_s - 1 &= -4\epsilon + 2\eta, \\ n_T &= -2\epsilon. \end{aligned} \quad (4.136)$$

5 THEORY OF CMB ANISOTROPIES AND POLARIZATION GENERATED BY PRIMORDIAL TENSOR MODES

In this Section we discuss the basic mechanism for generating small anisotropies and polarization in CMB. Unlike the previous chapters, in the present we will keep the usual constants c , h and k_B . In what follows we shall use the terms "tensor modes" and "PGWs" indistinguishably.

5.1 Boltzmann Equations in Cosmology

As we have briefly discussed in Section 2.5, CMB photons freely propagate after decoupling. They move along geodesics, and we can treat this photon gas using the techniques of statistical mechanics, namely, the Liouville equation

$$\frac{df}{d\tau} = 0, \quad (5.1)$$

where $f = f(x^\alpha, p^\alpha)$ is the photon distribution function, and p^α is the photon four-momentum, given by

$$p^\alpha = \frac{dx^\alpha}{d\lambda}, \quad (5.2)$$

where λ parameterizes the photon's trajectory. Equation (5.1) is also called *collisionless Boltzmann equation*. Since the photon four-momentum satisfies the mass-shell condition

$$g_{\alpha\beta} p^\alpha p^\beta = 0, \quad (5.3)$$

the phase-space of the photon mass-shell is seven-dimensional, $\{x^\alpha, p^i\}$, since p^0 can be determined in terms of the components of the momentum vector by means of equation (5.3),

$$p^0 = p, \quad (5.4)$$

where

$$p^2 \equiv -a^{-2} g_{ij} p^i p^j, \quad (5.5)$$

the metric g_{ij} has the general form (3.1), and the physical photon energy E is related to p^0 through $E = ap^0$.

In terms of $f = f(x^\alpha, p^i)$, Liouville equation (5.1) becomes

$$\frac{df}{d\tau} = \frac{\partial f}{\partial \tau} + \frac{\partial f}{\partial x^i} \frac{dx^i}{d\tau} + \frac{\partial f}{\partial p^i} \frac{dp^i}{d\tau}, \quad (5.6)$$

where we have neglected the dependence on

$$\frac{\partial f}{\partial p^i} \frac{dp^i}{d\tau} \quad (5.7)$$

since it is of second-order in the perturbation series, and here we are only concerned about first-order terms. The second term on the rhs of (5.6) is related to the unit vector along the photon trajectory; to see this, we simply use expressions (5.2) and (5.4), so that

$$\hat{e}^i \equiv \frac{dx^i}{d\tau} = \frac{dx^i}{d\lambda} \frac{d\lambda}{d\tau} = \frac{p^i}{p}. \quad (5.8)$$

Then, the rate of change of the photon distribution function is

$$\frac{df}{d\tau} = \frac{\partial f}{\partial \tau} + \hat{e}^i \frac{\partial f}{\partial x^i} + \frac{\partial f}{\partial p} \frac{dp}{d\tau}. \quad (5.9)$$

In the presence of collisions, particles will be coming in and out of a given volume of the phase space; however, on cosmological scales, the mean free path of the particles is very long, so that we can use the ideal gas approximation to describe this gas of particles. But, in this case, the rate of change of the particle distribution function is no longer zero; instead, it depends on the physical process that describes the collisions, which we call $C[f]$. Then, equation (5.1) becomes

$$\frac{df}{d\tau} = C[f], \quad (5.10)$$

and is called *Boltzmann equation*. Combining expressions (5.9) and (5.10) we find that the Boltzmann equation, in its general form, is given by

$$\boxed{\frac{\partial f}{\partial \tau} + \hat{e}^i \frac{\partial f}{\partial x^i} + \frac{\partial f}{\partial p} \frac{dp}{d\tau} = C[f]}. \quad (5.11)$$

It is important to mention that the Boltzmann equation (5.11) holds for non-relativistic matter as well. In this case, we also have a seven-dimensional phase-space, but the mass-shell condition is determined by the constraint $g_{\alpha\beta} p^\alpha p^\beta = m^2$, where m is the mass of the particle. The final form of the Boltzmann equation is the same as (5.11), but the collision term changes. In Figure 5.1 we present a summary of the interactions among the different species by the time of recombination.

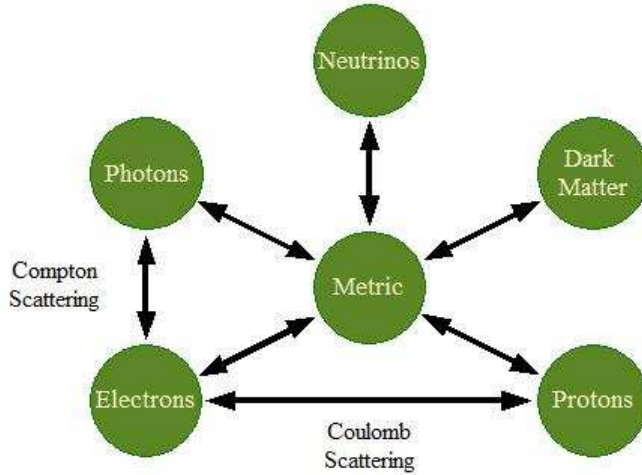


FIGURE 5.1 - Interactions taking place at recombination. Adapted from (DODELSON, 2003).

5.2 Radiative Transfer induced by Tensor Modes

As we have mentioned in Chapter 1, we are primarily interested in the signatures of the tensor modes. In order to study the anisotropies and polarization of CMB generated by such tensor modes, we have to evaluate the respective Boltzmann equation (5.11), first studied in a seminal paper by Polnarev (POLNAREV, 1985). To pursue the task of deriving the Boltzmann equation for the CMB photons interacting with free electrons in the presence of PGWs, we first discuss the collisional term of the Boltzmann equation (5.11).

As we have seen in Section 2.5, the free electrons prior and during recombination scatter the photons tightly coupled to the baryon-photon plasma via Thomson scattering. The collisional term due to Thomson scattering is given by (CHANDRASEKHAR, 1960)

$$\begin{aligned}
 C[\mathbf{f}] &= -\sigma_T N_e a(\tau) \left\{ \hat{\mathbf{f}}(\tau, \mathbf{r}, \nu, \mu, \varphi) \right. \\
 &\quad \left. - \frac{1}{4\pi} \int_{-1}^1 d\mu' d\varphi' P(\mu, \varphi, \mu', \varphi') \hat{\mathbf{f}}(\tau, \mathbf{r}, \nu, \mu', \varphi') \right\}, \quad (5.12)
 \end{aligned}$$

where f is the photon distribution function and $P(\mu, \varphi, \mu', \varphi')$ is the scattering

matrix whose form is

$$P(\mu, \varphi, \mu', \varphi') = Q \left\{ P^0(\mu, \mu') + \sqrt{1 - \mu^2} \sqrt{1 - \mu'^2} P^1(\mu, \varphi, \mu', \varphi') + P^2(\mu, \varphi, \mu', \varphi') \right\}, \quad (5.13)$$

where

$$Q = \begin{pmatrix} 1 & 0 & 0 & 0 \\ 0 & 1 & 0 & 0 \\ 0 & 1 & 0 & 0 \\ 0 & 0 & 0 & 2 \end{pmatrix}, \quad (5.14)$$

$$P^0 = \frac{3}{4} \begin{pmatrix} 2(1 - \mu^2)(1 - \mu'^2) + \mu^2 \mu'^2 & \mu^2 & 0 & 0 \\ \mu'^2 & 1 & 0 & 0 \\ 0 & 0 & 0 & 0 \\ 0 & 0 & 0 & \mu \mu' \end{pmatrix}, \quad (5.15)$$

$$P^1 = \frac{3}{4} \begin{pmatrix} 4\mu \mu' \cos \psi & 0 & -2\mu \sin \psi & 0 \\ 0 & 0 & 0 & 0 \\ 2\mu' \sin \psi & 0 & \cos \psi & 0 \\ 0 & 0 & 0 & \cos \psi \end{pmatrix}, \quad (5.16)$$

$$P^2 = \frac{3}{4} \begin{pmatrix} \mu^2 \mu'^2 \cos 2\psi & -\mu^2 \cos 2\psi & -\mu^2 \mu' \sin 2\psi & 0 \\ -\mu'^2 \cos 2\psi & \cos 2\psi & \mu' \sin 2\psi & 0 \\ \mu \mu'^2 \sin 2\psi & -\mu \sin 2\psi & \mu \mu' \cos 2\psi & 0 \\ 0 & 0 & 0 & 0 \end{pmatrix}, \quad (5.17)$$

σ_T is the Thomson scattering cross-section, $N_e(\tau)$ is the number of free electrons in the unit comoving volume, and we have defined $\mu \equiv \cos \theta$ and $\psi \equiv \varphi - \varphi'$.

Next, let us consider a given beam of radiation characterized by its *Stokes parameters* $\{I, Q, U, V\}$ (CHANDRASEKHAR, 1960), where I is the total intensity of the wave, the parameters Q and U measure the linear polarization of the wave, and V measures its circular polarization. They are integrated over all radiation frequencies, so that there is a set of Stokes parameters for each monochromatic component wave of the radiation beam with frequency ν , $\{I(\nu, \theta, \varphi), Q(\nu, \theta, \varphi), U(\nu, \theta, \varphi), V(\nu, \theta, \varphi)\}$. If the universe were isotropic, the Stokes parameters Q , U and V would be zero, since an isotropic radiation beam does not induce any polarization (CHANDRASEKHAR, 1960); then, CMB would be polarized only in presence of an anisotropic radiation

beam. Such anisotropies and polarization are generated not only by the fluctuations of the geometry, but fundamentally by a "source of handedness" provided by the tensor character of the fluctuations. Therefore, to deal with an anisotropic radiation beam, it is convenient to cast the photon distribution function into a symbolic vector of the form (CHANDRASEKHAR, 1960)

$$\hat{\mathbf{f}}(\tau, \mathbf{r}, \nu, \mu, \varphi) = \begin{pmatrix} \hat{f}_1(\tau, \mathbf{r}, \nu, \mu, \varphi) \\ \hat{f}_2(\tau, \mathbf{r}, \nu, \mu, \varphi) \\ \hat{f}_3(\tau, \mathbf{r}, \nu, \mu, \varphi) \end{pmatrix}, \quad (5.18)$$

where \hat{f}_1 , \hat{f}_2 and $(\hat{f}_1 + \hat{f}_2 + \hat{f}_3)/2$ represent the number of photons with frequency ν and direction $\hat{\mathbf{z}}$ passing through a slit parallel to the directions $\hat{\mathbf{x}}$, $\hat{\mathbf{y}}$ and $\hat{\mathbf{x}} + \hat{\mathbf{y}}$, respectively. The relation between $\hat{\mathbf{f}}$ and the Stokes parameters are given by (CHANDRASEKHAR, 1960), (POLNAREV, 1985),

$$\hat{\mathbf{f}} = \frac{1}{2} \frac{c^2}{h\nu^3} \begin{pmatrix} I + Q \\ I - Q \\ -2U \end{pmatrix}. \quad (5.19)$$

Then, the photon distribution functions \hat{f}_i "encode" the influences of the small fluctuations of the metric, so that they can be also decomposed into its zeroth-order contribution, $\hat{\mathbf{f}}^{(0)}$ *i. e.*, in the absence of the tensor perturbations, and its first-order correction $\hat{\mathbf{f}}^{(1)}$,

$$\hat{\mathbf{f}} = \hat{\mathbf{f}}^{(0)} + \hat{\mathbf{f}}^{(1)}. \quad (5.20)$$

$\hat{\mathbf{f}}^{(0)}$ represents a situation where the radiation field is homogeneous, isotropic and unpolarized, since there is no perturbations caused by the metric fluctuations. In this case, as discussed before, $Q = U = 0$ and, from (5.19), we find that

$$\hat{\mathbf{f}}^{(0)} = \frac{1}{2} \frac{c^2}{h\nu^3} \begin{pmatrix} I \\ I \\ 0 \end{pmatrix}, \quad (5.21)$$

or, by writing $f^{(0)}(\tau, \nu) = c^2 I / 2h\nu^3$,

$$\hat{\mathbf{f}}^{(0)}(\tau, \nu) = f^{(0)}(\tau, \nu) \hat{\mathbf{u}}, \quad (5.22)$$

where

$$\hat{\mathbf{u}} = \begin{pmatrix} 1 \\ 1 \\ 0 \end{pmatrix}. \quad (5.23)$$

Plugging (5.22) into (5.12) with the explicit forms of (5.13), (5.14), (5.15), (5.16) and (5.17), integrating over the angles μ' and φ' , we find that $C[\hat{\mathbf{f}}^{(0)}] = 0$, so that the Boltzmann equation for $\hat{\mathbf{f}}^{(0)}$ is given by

$$\frac{\partial f^{(0)}}{\partial \tau} - \nu \mathcal{H} \frac{\partial f^{(0)}}{\partial \nu} = 0, \quad (5.24)$$

whose solution is $f^{(0)} = f_0(a(\tau)\nu)$, and then equation (5.24) admits the blackbody radiation function as a solution,

$$f_0(\nu) = \frac{1}{e^{h\nu/k_B T} - 1}, \quad (5.25)$$

where the present-time value of T is 2.725 K (KOMATSU et al., 2009).

Once we have discussed the unperturbed case, we can now consider the equation for the perturbations in GR. The third term in equation (5.11) can be evaluated from the geodesic equation for the photon, (A.4), which can be recast into the form

$$\frac{dp_\alpha}{d\lambda} = -\frac{1}{2} g_{\beta\gamma,\alpha} p^\beta p^\gamma; \quad (5.26)$$

next, plugging the the photon mass-shell constraint (5.4) into the definition of tensor perturbations (3.10), we find

$$(p^0)^2 = p^2 \equiv (\delta_{ij} + h_{ij}) p^i p^j. \quad (5.27)$$

Substituting (3.10) and (5.27) into (5.26), it follows that the geodesic equation for tensor perturbations reads

$$\frac{dp^0}{d\lambda} = -\nu \left[\mathcal{H} + \frac{1}{2} \frac{\partial h_{ij}}{\partial \tau} p^i p^j \right] \frac{d\tau}{d\lambda}. \quad (5.28)$$

Before going to the Fourier space to solve this equation, it is convenient to introduce a new parametrization into this model (BOSE; GRISHCHUK, 2002). Let us write down the present-day scale factor $a(\tau_0)$ as a quantity with dimension of length;

then, setting $R_H = c/H_0$ as the present-day Hubble radius, we define $a(\tau_0) = 2R_H$. Now, since the wavenumber of the tensor modes \mathbf{k} is very small (in the frequency range which could produce a signature on CMB), with wavelength comparable to the present-day Hubble radius R_H , we introduce a dimensionless time-independent vector \mathbf{n} which has the same direction of \mathbf{k} , and whose modulus is exactly the proportionality factor between the modulus of \mathbf{k} and R_H :

$$\mathbf{n} = 2R_H \mathbf{k}. \quad (5.29)$$

Bearing these definitions in mind, we expand h_{ij} in an analogous fashion to (4.82),

$$h_{ij}(\tau, x) = \int \frac{d^3n}{(2\pi)^{3/2}} \left[h_n^{(+)}(\tau) \varepsilon_{ij}^{(+)}(\mathbf{n}) + h_n^{(\times)}(\tau) \varepsilon_{ij}^{(\times)}(n) \right] e^{i\mathbf{n}\cdot\mathbf{x}}, \quad (5.30)$$

where $\varepsilon_{ij}^{(+,\times)}$ are the polarization tensors given by (C.33). Then, plugging (5.30) into (5.28), the geodesic equation becomes

$$\frac{dp^0}{d\tau} = -\frac{1}{2} \int \frac{d^3n}{(2\pi)^{3/2}} \left[\frac{\partial h_n^{(+)}(\tau)}{\partial \tau} \varepsilon_{ij}^{(+)} + \frac{\partial h_n^{(\times)}(\tau)}{\partial \tau} \varepsilon_{ij}^{(\times)} \right] p^i p^j e^{i\mathbf{n}\cdot\mathbf{x}}. \quad (5.31)$$

The remaining contribution to be evaluated in (5.31) is related to $\varepsilon_{ij} p^i p^j$; now, defining

$$F^{(+,\times)}(\theta, \varphi) \equiv \varepsilon_{ij}^{(+,\times)} p^i p^j, \quad (5.32)$$

we can evaluate this term precisely by means of the photon angular distribution. This can be constructed as follows: supposing that the modes travel along an arbitrary direction $\hat{\mathbf{k}}$, we introduce the two *polarization vectors* $\{\hat{\varepsilon}_{(1)}^r, \hat{\varepsilon}_{(2)}^r\}$, defined as

$$\varepsilon_{ij}^r \equiv \varepsilon_{(1)i}^r \varepsilon_{(1)j}^r - \varepsilon_{(2)i}^r \varepsilon_{(2)j}^r \quad (5.33)$$

and satisfying

$$\hat{\varepsilon}_{(1)}^r \cdot \hat{\varepsilon}_{(2)}^r = \hat{\varepsilon}_{(1)}^r \cdot \hat{\mathbf{k}} = \hat{\varepsilon}_{(2)}^r \cdot \hat{\mathbf{k}} = 0. \quad (5.34)$$

Hence, the trihedron $\{\hat{\varepsilon}_{(1)}^r, \hat{\varepsilon}_{(2)}^r, \hat{\mathbf{k}}\}$ is orthogonal. Thus, we can use this trihedron as a basis; now, choosing our reference frame such that its axes coincide with the the directions defined by the above trihedron, and decomposing $\mathbf{p} = p \hat{\mathbf{e}}$ in spherical

coordinates in this basis, we have

$$\hat{k} \cdot \hat{\mathbf{e}} = \cos \theta, \quad \hat{\varepsilon}_{(1)} \cdot \hat{\mathbf{e}} = \sin \theta \cos \varphi, \quad (5.35)$$

$$\hat{\varepsilon}_{(2)} \cdot \hat{\mathbf{e}} = \sin \theta \sin \varphi, \quad (5.36)$$

as depicted in Figure 5.2.

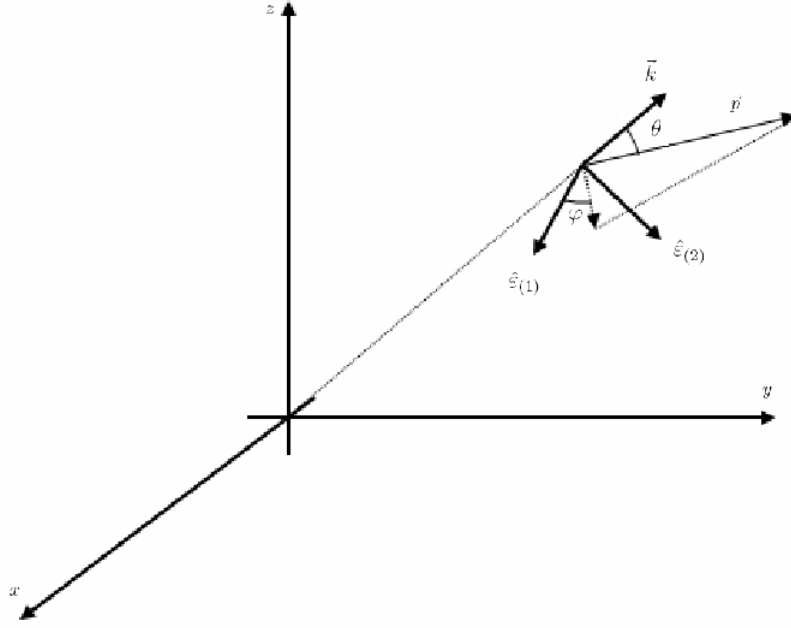


FIGURE 5.2 - Coordinate system for the photon momentum \vec{p} .

With these definitions it follows that

$$\hat{e}_x = \sqrt{1 - \mu^2} \cos \varphi, \quad \hat{e}_y = \sqrt{1 - \mu^2} \sin \varphi. \quad (5.37)$$

Therefore, plugging (C.33) and (5.37) into (5.32), we obtain,

$$F^{(+)}(\theta, \varphi) = \frac{1}{2}(1 - \mu^2) \cos 2\varphi \propto Y_{2,+2}(\mu, \varphi) \quad (5.38)$$

$$F^{(\times)}(\theta, \varphi) = \frac{1}{2}(1 - \mu^2) \sin 2\varphi \propto Y_{2,-2}(\mu, \varphi), \quad (5.39)$$

where $Y_{\ell m}(\mu, \varphi)$ are the usual spherical harmonics (ABRAMOWITZ; STEGUN, 1972). The results (5.38) and (5.39) show us that a GW leaves an imprint on the photon angular distribution in the form of a quadrupole $Y_{2, \pm 2}$ and, as a consequence, shifts the photon frequency along the line of sight. This is the so-called *Sachs-Wolfe* (SW) effect induced by tensor modes (GIOVANNINI, 2005). Note that the SW effect is purely gravitational, and has nothing to do with the details of the interaction between the photons and electrons. Also, there are also the scalar and vector versions of the SW effect, but they will not be considered here.

Now let us address the question of Thomson scattering of the CMB photons by electrons. Prior to Thomson scattering, the photons are unpolarized, and their angular distribution are of the form (5.38) and (5.39) due to the tensor SW effect. Hence, the Stokes parameters are given by (POLNAREV, 1985),

$$\begin{aligned}\hat{a}_{(+)}(\mu, \varphi) &= \frac{1}{2} (1 - \mu^2) \cos 2\varphi \hat{\mathbf{u}}, \\ \hat{a}_{(\times)}(\mu, \varphi) &= \frac{1}{2} (1 - \mu^2) \sin 2\varphi \hat{\mathbf{u}},\end{aligned}\tag{5.40}$$

where we have introduced the vector $\hat{\mathbf{u}}$ in (5.23). Now, defining the operator \hat{P} as

$$\hat{P}\hat{\xi}(\mu, \varphi) = \frac{1}{4\pi} \int_{-1}^1 d\mu' d\varphi' P(\mu, \varphi, \mu', \varphi') \hat{\xi}(\mu', \varphi'),\tag{5.41}$$

where P is the scattering matrix (5.13), it is straightforward to see, for $\hat{\xi} = \hat{a}$ (dropping the polarization index for the moment), that

$$\hat{P}\hat{a} = \alpha\hat{a} + \beta\hat{b},\tag{5.42}$$

where α and β are constants, and \hat{b} is a vector which under \hat{P} behaves as

$$\hat{P}\hat{b} = \alpha'\hat{a} + \beta'\hat{b},\tag{5.43}$$

where α' and β' are constants as well. From (5.13), (5.40), (5.42) and (5.43) we

readily see that

$$\begin{aligned}\hat{b}_{(+)}(\mu, \varphi) &= \frac{1}{2} \begin{pmatrix} (1 + \mu^2) \cos 2\varphi \\ -(1 + \mu^2) \cos 2\varphi \\ 4\mu \sin 2\varphi \end{pmatrix}, \\ \hat{b}_{(\times)}(\mu, \varphi) &= \frac{1}{2} \begin{pmatrix} (1 + \mu^2) \sin 2\varphi \\ -(1 + \mu^2) \sin 2\varphi \\ -4\mu \cos 2\varphi \end{pmatrix}.\end{aligned}\quad (5.44)$$

Therefore, the Thomson interaction changes the angular pattern of the photons from the unpolarized state characterized by (5.40) to the polarized state characterized by the (5.44). In this sense, the PGWs act as ‘‘sources of handedness’’ for the CMB polarization.

The angular distribution functions \hat{a} and \hat{b} are closed under Thomson scattering, so that they can be used as a basis. This fact holds only for linear polarization; for a circular pattern, as it is well known, the polarization vectors are a complex linear combination of the polarization vectors. Then, in this case,

$$\begin{aligned}\hat{a}_r(\mu, \varphi) &= \frac{1}{2} (1 - \mu^2) e^{\pm 2i\varphi} \hat{\mathbf{u}}, \\ \hat{b}_r(\mu, \varphi) &= \frac{1}{2} \begin{pmatrix} (1 + \mu^2) \\ -(1 + \mu^2) \\ \mp 4i\mu \end{pmatrix} e^{\pm 2i\varphi},\end{aligned}\quad (5.45)$$

where $r = 1$ corresponds to a left-hand polarization, and $r = 2$ to the right-hand one. Now, with this general basis (5.45), we may expand the function $\hat{\mathbf{f}}^{(1)}(x, p)$ in terms of it. Since the function $\hat{\mathbf{f}}^{(1)}$ has no dependence on the modulus of photon momenta (remember that we are considering only first-order terms in h), we can simply write this function as depending on the photon direction, $\hat{\mathbf{e}}$; its the p^0 -dependence can be written simply as ν -dependence; therefore, $\hat{\mathbf{f}}^{(1)}(x, p) = \hat{\mathbf{f}}^{(1)}(\tau, \mathbf{r}, \nu, \hat{\mathbf{e}})$. Now, since equation (5.11) is linear, we can expand $\hat{\mathbf{f}}^{(1)}$ in the same way as we did in (5.30),

$$\hat{\mathbf{f}}^{(1)}(\tau, \mathbf{r}, \nu, \hat{\mathbf{e}}) = \int \frac{d^3n}{(2\pi)^{3/2}} \sum_{r=+, \times} \hat{\mathbf{f}}_{\mathbf{n}, r}^{(1)}(\tau, \nu, \hat{\mathbf{e}}) e^{i\mathbf{n}\cdot\mathbf{x}},\quad (5.46)$$

which allows us to rewrite the Boltzmann equation (5.11) in the following way: using the fact that $p^0 = h\nu$, where ν is comoving photon frequency, and the constraint

(5.3), substituting these elements plus (5.31) and (5.46) into (5.11), we get

$$\begin{aligned} \left[\frac{\partial}{\partial \tau} + q(\tau) + i\hat{\mathbf{e}} \cdot \hat{\mathbf{f}} \right] \hat{\mathbf{f}}_{\mathbf{n},r}^{(1)}(\tau, \nu, \hat{\mathbf{e}}) &= \frac{1}{2} \rho(\nu) e^i e^j \varepsilon_{ij}^r(\mathbf{n}) \frac{dh_n^r(\tau)}{d\tau} \hat{\mathbf{u}} \\ &+ \frac{q(\tau)}{4\pi} \int d\Omega' \hat{\mathbf{P}}(\mathbf{e}; \mathbf{e}') \hat{\mathbf{f}}_{\mathbf{n},r}^{(1)}(\tau, \nu, \hat{\mathbf{e}}), \end{aligned} \quad (5.47)$$

where we have defined

$$\rho(\nu) \equiv \nu \frac{dn^{(0)}}{d\nu}, \quad (5.48)$$

and introduced the *scattering rate* $q(\tau)$ by

$$q(\tau) \equiv \sigma_T N_e(\tau) a(\tau). \quad (5.49)$$

Now we have to evaluate the integral on the right-hand side of (5.47). To do so, it is convenient to factor out the angular dependence of $\hat{\mathbf{f}}_{\mathbf{n},r}^{(1)}$, and this can be achieved using the basis (5.45) and the Fourier expansion (5.46),

$$\begin{aligned} \hat{\mathbf{f}}_{\mathbf{n},r}^{(1)}(\tau, \nu, \mu, \varphi) &= \frac{1}{2} \rho(\nu) [\alpha_{\mathbf{n},r}(\tau, \mu) \hat{a}_r(\mu, \varphi) \\ &+ \beta_{\mathbf{n},r}(\tau, \mu) \hat{b}_r(\mu, \varphi)], \end{aligned} \quad (5.50)$$

where $\alpha_{\mathbf{n},r}(\tau, \mu)$ and $\beta_{\mathbf{n},r}(\tau, \mu)$ are functions to be determined by the solutions of the Boltzmann equation. Now, substituting (5.50) into (5.11) and (5.12), using (5.20), (5.31), (5.49) and (5.50), we obtain the Boltzmann equations for the radiative transfer in the presence of weak gravitational fields (dropping the indices \mathbf{n}, r for the sake of simplicity) (POLNAREV, 1985), (BASKARAN et al., 2006),

$$\boxed{\frac{\partial}{\partial \tau} \beta(\tau, \mu) + [q(\tau) + in\mu] \beta(\tau, \mu) = \frac{3}{16} q(\tau) I(\tau)}, \quad (5.51)$$

$$\boxed{\frac{\partial}{\partial \tau} \xi(\tau, \mu) + [q(\tau) + in\mu] \xi(\tau, \mu) = \frac{d}{d\tau} h(\tau)}, \quad (5.52)$$

where we have defined

$$\xi(\tau, \mu) \equiv \alpha(\tau, \mu) + \beta(\tau, \mu), \quad (5.53)$$

and

$$\mathcal{I}(\tau) \equiv \int_{-1}^1 d\mu' \left[(1 + \mu'^2)^2 \beta(\tau, \mu') - \frac{1}{2} (1 - \mu'^2)^2 \xi(\tau, \mu') \right]. \quad (5.54)$$

The solutions to the Boltzmann equations (5.51) and (5.52), given by the functions $\alpha(\tau, \mu)$ and $\beta(\tau, \mu)$, are the essential elements for the computation of the anisotropies and polarization of the CMB, as we sketch in the next section.

5.3 The T, E and B-Modes

In this section we derive the explicit forms of the T, E and B-mode functions and the correlation function C_ℓ for polarization. We follow closely (KAMIONKOWSKI et al., 1997) and (CABELLA; KAMIONKOWSKI, 2004), introducing the harmonic analysis on the full sky.

To begin with, let us first construct the polarization tensor associated with the Stokes parameters $Q(\theta, \varphi)$ and $U(\theta, \varphi)$, where the coordinates (θ, φ) describe the position of a given region of the sky. We consider first the simplest case, associated with a flat 2-dimensional surface. For a radiation beam linearly polarized propagating in the \hat{z} -direction, its polarization vectors lie on the $x - y$ plane; then, rotating the axes by an angle α around \hat{z} , the coordinates transform as

$$\begin{pmatrix} x' \\ y' \end{pmatrix} = \begin{pmatrix} \cos \alpha & \sin \alpha \\ -\sin \alpha & \cos \alpha \end{pmatrix} \begin{pmatrix} x \\ y \end{pmatrix}, \quad (5.55)$$

whereas the Stokes parameters Q and U transform as (CHANDRASEKHAR, 1960)

$$\begin{pmatrix} Q' \\ U' \end{pmatrix} = \begin{pmatrix} \cos 2\alpha & \sin 2\alpha \\ -\sin 2\alpha & \cos 2\alpha \end{pmatrix} \begin{pmatrix} Q \\ U \end{pmatrix}. \quad (5.56)$$

Now, calling A_{ab} the 2×2 matrix in (5.56), it follows that the quantity

$$\mathcal{P}_{ab}(\theta, \varphi) = \frac{1}{2} \begin{pmatrix} Q(\theta, \varphi) & U(\theta, \varphi) \\ U(\theta, \varphi) & -Q(\theta, \varphi) \end{pmatrix} \quad (5.57)$$

transforms as a tensor under rotations of the $x - y$ axes, that is, $\mathcal{P}'_{ab} = A_{ac}A_{bd}\mathcal{P}_{cd}$. Since the tensor (5.57) is built on the two polarization parameters Q and U , we shall denote it as the symmetric-trace-free (STF) part of the *polarization tensor*, for it satisfies the relations $\mathcal{P}_{ab} = \mathcal{P}_{ba}$ and $g^{ab}\mathcal{P}_{ab} = 0$ respectively, where the metric is simply given by $g_{ab} = \text{diag}\{1, 1\}$ on a flat space. The full polarization tensor is composed of a symmetric contribution $P_{(ab)}$ (but not necessarily trace-free) plus the

antisymmetric $P_{[ab]}$ and STF part:

$$P_{ab} = P_{(ab)} + P_{[ab]} + \mathcal{P}_{ab}; \quad (5.58)$$

now, the expressions for $P_{(ab)}$ and $P_{[ab]}$ can be easily implemented as

$$P_{(ab)} \propto g_{ab}, \quad P_{[ab]} \propto \varepsilon_{ab}, \quad (5.59)$$

where ε_{ab} is the completely antisymmetric pseudotensor whose components are $\varepsilon_{12} = -\varepsilon_{21} = 1$.

The polarization tensor (5.58) provides all the information concerning the radiation beam, *i.e.*, it contains the radiation intensity and polarization pattern. From the STF contribution (5.57) we see that it contains the linear polarization information; he have only to include the intensity and the circular polarization patterns into P_{ab} , which are given by the remaining Stokes parameters I and V . Since I is a scalar and V is a pseudoscalar (CHANDRASEKHAR, 1960), we can rewrite (5.59) as

$$P_{(ab)}(\theta, \varphi) = \frac{1}{2}I(\theta, \varphi)g_{ab}, \quad P_{[ab]}(\theta, \varphi) = -\frac{i}{2}V(\theta, \varphi)\varepsilon_{ab}, \quad (5.60)$$

so that the polarization tensor (5.58) is now

$$P_{ab}(\theta, \varphi) = \frac{1}{2}I(\theta, \varphi)g_{ab} - \frac{i}{2}V(\theta, \varphi)\varepsilon_{ab} + \mathcal{P}_{ab}(\theta, \varphi). \quad (5.61)$$

The generalization of the tensor (5.61) to the 2-sphere is straightforward. We have only to specify g_{ab} and ε_{ab} , which are given by (KAMIONKOWSKI et al., 1997), (CABELLA; KAMIONKOWSKI, 2004)

$$g_{ab}(\theta, \varphi) = \begin{pmatrix} 1 & 0 \\ 0 & \sin^2 \theta \end{pmatrix}, \quad \varepsilon_{ab}(\theta, \varphi) = \sin \theta \begin{pmatrix} 0 & -1 \\ 1 & 0 \end{pmatrix}. \quad (5.62)$$

Now, using the properties $\mathcal{P}_{ab} = \mathcal{P}_{ba}$, $g^{ab}\mathcal{P}_{ab} = 0$ and (5.62), we find that the STF part of the polarization tensor is

$$\mathcal{P}_{ab}(\theta, \varphi) = \frac{1}{2} \begin{pmatrix} Q & -U \sin \theta \\ -U \sin \theta & -Q \sin^2 \theta \end{pmatrix}, \quad (5.63)$$

whereas the polarization tensor itself is

$$P_{ab}(\theta, \varphi) = \frac{1}{2} \begin{pmatrix} I + Q & -(U - iV) \sin \theta \\ -(U + iV) \sin \theta & (I - Q) \sin^2 \theta \end{pmatrix}. \quad (5.64)$$

On the two-sphere tensor analysis can be easily implemented; the "divergence" and "curl" of a symmetric rank-2 tensors are respectively given by $T^{ab}{}_{:ab}$ and $T^{ab}{}_{:ac}\varepsilon^c{}_b$, where ":" denotes covariant differentiation. With these elements at hand, we introduce invariants which can be built up from the polarization tensor P_{ab} and its derivatives. The only possible invariants which can be built from P_{ab} solely are

$$I(\theta, \varphi) = g^{ab}P_{ab}(\theta, \varphi), \quad V(\theta, \varphi) = i\varepsilon^{ab}P_{ab}(\theta, \varphi); \quad (5.65)$$

the first derivatives of P_{ab} do not give rise to invariants, but the second derivatives do, in the form of a "divergence" and a "curl" (BASKARAN et al., 2006),

$$E(\theta, \varphi) = -2\mathcal{P}_{ab}{}^{:ab}, \quad B(\theta, \varphi) = -2\mathcal{P}_{ab}{}^{:bc}\varepsilon^a{}_c, \quad (5.66)$$

respectively. With these invariants we get a very convenient way to completely characterize the radiation beam, since they do not depend on the reference frame chosen. We now proceed to expand the invariants (I, E, B, V) in spherical harmonics in order to perform an analysis on the each multipole of the radiation field (BASKARAN et al., 2006)

$$I(\theta, \varphi) = \sum_{\ell=0}^{\infty} \sum_{m=-\ell}^{\ell} a_{\ell m}^T Y_{\ell m}(\theta, \varphi), \quad (5.67)$$

$$E(\theta, \varphi) = \sum_{\ell=2}^{\infty} \sum_{m=-\ell}^{\ell} \left[\frac{(\ell+2)!}{(\ell-2)!} \right]^{\frac{1}{2}} a_{\ell m}^E Y_{\ell m}(\theta, \varphi), \quad (5.68)$$

$$B(\theta, \varphi) = \sum_{\ell=2}^{\infty} \sum_{m=-\ell}^{\ell} \left[\frac{(\ell+2)!}{(\ell-2)!} \right]^{\frac{1}{2}} a_{\ell m}^B Y_{\ell m}(\theta, \varphi), \quad (5.69)$$

$$V(\theta, \varphi) = \sum_{\ell=0}^{\infty} \sum_{m=-\ell}^{\ell} a_{\ell m}^V Y_{\ell m}(\theta, \varphi). \quad (5.70)$$

It is important to stress that these expansions are consistent with the similar definitions in the literature (KAMIONKOWSKI et al., 1997), (ZALDARRIAGA; SELJAK,

1997).

We are now in position to write down the T, E and B-mode functions (5.67), (5.68) and (5.69) in terms of the functions $\alpha(\mu, \varphi)$ and $\beta(\mu, \varphi)$ introduced in (5.50). From (5.18) and (5.19) we obtain for a monochromatic radiation beam

$$\begin{aligned} I(\tau, \nu, \theta, \varphi) &= \frac{h\nu^3}{c^2} [f_1(\tau, \nu, \theta, \varphi) + f_2(\tau, \nu, \theta, \varphi)], \\ Q(\tau, \nu, \theta, \varphi) &= \frac{h\nu^3}{c^2} [(f_1(\tau, \nu, \theta, \varphi) - f_2(\tau, \nu, \theta, \varphi))], \\ U(\tau, \nu, \theta, \varphi) &= -4\frac{h\nu^3}{c^2} f_3(\tau, \nu, \theta, \varphi), \end{aligned} \quad (5.71)$$

so that from (5.45), (5.50) and (5.71) we get (restoring the \mathbf{n} -dependence of the Fourier expansion),

$$I_{\mathbf{n},r}(\tau, \nu, \theta, \varphi) = \frac{h\nu^3}{c^2} [f^{(0)}(\nu) + \rho(\nu)\alpha_{\mathbf{n},r}(\tau, \mu)(1 - \mu^2)e^{\pm 2i\varphi}], \quad (5.72)$$

$$Q_{\mathbf{n},r}(\tau, \nu, \theta, \varphi) = \frac{h\nu^3}{c^2} \rho(\nu)\beta_{\mathbf{n},r}(\tau, \mu)(1 + \mu^2)e^{\pm 2i\varphi}, \quad (5.73)$$

$$U_{\mathbf{n},r}(\tau, \nu, \theta, \varphi) = \mp 2\frac{h\nu^3}{c^2} \rho(\nu)\beta_{\mathbf{n},r}(\tau, \mu)\mu e^{\pm 2i\varphi}. \quad (5.74)$$

From equations (5.73) and (5.74) we may readily evaluate the expressions for E and B , using (5.62), (5.63), (5.66) and (5.72-5.74); then, integrating over photon frequencies, we obtain

$$\begin{aligned} I_{n,r}(\mu, \varphi) &= \gamma [(1 - \mu^2) \alpha_{n,r}(\tau, \mu) e^{\pm 2i\varphi}], \\ E_{n,r}(\mu, \varphi) &= -\gamma \left[(1 - \mu^2) \left((1 + \mu^2) \frac{d^2}{d\mu^2} + 8\mu \frac{d}{d\mu} + 12 \right) \beta_{n,r}(\tau, \mu) e^{\pm 2i\varphi} \right], \\ B_{n,r}(\mu, \varphi) &= \mp \gamma \left[2(1 - \mu^2) \left(i\mu \frac{d^2}{d\mu^2} + 4i \frac{d}{d\mu} \right) \beta_{n,r}(\tau, \mu) e^{\pm 2i\varphi} \right], \end{aligned} \quad (5.75)$$

where we have defined

$$I_0 \equiv \int d\nu \frac{h\nu^3}{c^2} f^{(0)}(\nu), \quad (5.76)$$

and

$$\gamma \equiv \int d\nu \frac{h\nu^3}{c^2} \rho(\nu) = -4I_0. \quad (5.77)$$

Once we have the key expressions for evaluating the power spectrum correlation function all we must do now is solving the Boltzmann equations (5.51) and (5.52), which we handle in the next section.

5.4 The Solutions to the Boltzmann Equations

In the paper (BASKARAN et al., 2006) the authors discuss an analytical method for solving the Volterra equation represented by (5.51) in terms of a series expansion, and compare their results with the exact numerical solutions. Here we follow only their numerical approach, which we sketch below. To do so, we introduce first the functions

$$\Phi(\tau) = \frac{3}{16}g(\tau)\mathcal{I}(\tau), \quad (5.78)$$

$$H(\tau) = e^{-\kappa(\tau)}\frac{dh(\tau)}{d\tau}, \quad (5.79)$$

where the function $\kappa(\tau)$ represents the *optical depth* of the universe, and is defined within a time interval τ' and τ :

$$\kappa(\tau, \tau') \equiv \int_{\tau'}^{\tau} d\tau'' q(\tau''),$$

where $q(\tau)$ is the scattering rate (5.49), $g(\tau)$ is the *visibility function*, written as

$$g(\tau) = q(\tau)e^{-\kappa(\tau)} = \frac{d}{d\tau}e^{-\kappa(\tau)}, \quad (5.80)$$

and satisfying

$$\int_0^{\tau_0} g(\tau)d\tau = 1. \quad (5.81)$$

Taking $\tau' = \tau_0$, we further write the optical depth from a given conformal instant τ to the present as $\kappa(\tau_0, \tau) = \kappa(\tau)$, that is

$$\kappa(\tau) = \int_{\tau}^{\tau_0} d\tau' q(\tau'). \quad (5.82)$$

Next, using these definitions, the formal solutions to the equations (5.51) and (5.52)

are given by the integral relations (BASKARAN et al., 2006)

$$\beta(\tau, \mu) = e^{\kappa(\tau) - in\mu\tau} \int_0^\tau d\tau' \Phi(\tau') e^{in\mu\tau'}, \quad (5.83)$$

$$\xi(\tau, \mu) = e^{\kappa(\tau) - in\mu\tau} \int_0^\tau d\tau' H(\tau') e^{in\mu\tau'}. \quad (5.84)$$

Now, since the function $H(\tau)$ is known, we can obtain a single integral equation for the function (5.78) by plugging (5.83) and (5.84) into (5.54), so that

$$\begin{aligned} \mathcal{I}(\tau) &= e^{\kappa(\tau)} \int_{-1}^1 \int_0^\tau d\mu d\tau' \left\{ (1 + \mu^2)^2 \Phi(\tau') \right. \\ &\quad \left. - \frac{1}{2} (1 - \mu^2)^2 H(\tau') \right\} e^{in\mu(\tau' - \tau)}; \end{aligned} \quad (5.85)$$

such expression can be further simplified by introducing the kernels $K_\pm(\tau - \tau')$, defined as

$$K_\pm(\tau - \tau') = \int_{-1}^1 d\mu (1 \pm \mu^2)^2 e^{in\mu(\tau - \tau')}, \quad (5.86)$$

so that expression (5.85) yields

$$\begin{aligned} \mathcal{I}(\tau) &= e^{\kappa(\tau)} \int_0^\tau d\tau' \left\{ K_+(\tau - \tau') \Phi(\tau') \right. \\ &\quad \left. - \frac{1}{2} K_-(\tau - \tau') H(\tau') \right\}. \end{aligned} \quad (5.87)$$

The final equation for $\Phi(\tau)$ is obtained by multiplying both sides of this equality by $(3/16)q(\tau)e^{-\kappa(\tau)}$ and using the expression (5.78), so that

$$\Phi(\tau) = \frac{3}{16}q(\tau) \int_0^\tau d\tau' \Phi(\tau') K_+(\tau - \tau') + F(\tau), \quad (5.88)$$

where $F(\tau)$ is related to the function (5.79) by

$$F(\tau) = -\frac{3}{32}q(\tau) \int_0^\tau d\tau' H(\tau') K_-(\tau - \tau'). \quad (5.89)$$

The solution to Volterra integral equation (5.88) provides the values of the functions α and β for every conformal instant τ ; in particular, to the present-day τ_0 , the

expressions $\alpha(\tau_0, \mu) = \alpha(\mu)$ and $\beta(\tau_0, \mu) = \beta(\mu)$ are respectively given by

$$\begin{aligned}\alpha_{n,r}(\mu) &= \int_0^{\tau_0} d\tau (H_{n,r}(\tau) - \Phi_{n,r}(\tau)) e^{-i\mu\zeta}, \\ \beta_{n,r}(\mu) &= \int_0^{\tau_0} d\tau \Phi_{n,r}(\tau) e^{-i\mu\zeta},\end{aligned}\tag{5.90}$$

where we have introduced the variable $\zeta = n(\tau_0 - \tau)$.

We are now ready to compute the coefficients $a_{\ell m}^X$: we substitute expressions (5.67-5.69) and (5.90) into (5.75), and integrate over angular variables, so that

$$\begin{aligned}a_{\ell m, nr}^T &= (-i)^{\ell-2} (\delta_{2,m}\delta_{1,r} + \delta_{-2,m}\delta_{2,r}) a_{\ell, nr}^T, \\ a_{\ell m, nr}^E &= (-i)^{\ell-2} (\delta_{2,m}\delta_{1,r} + \delta_{-2,m}\delta_{2,r}) a_{\ell, nr}^E, \\ a_{\ell m, nr}^B &= (-i)^{\ell-2} (\delta_{2,m}\delta_{1,s} - \delta_{-2,m}\delta_{2,s}) a_{\ell, nr}^B,\end{aligned}\tag{5.91}$$

where

$$a_{\ell, nr}^T = \gamma \sqrt{4\pi(2\ell+1)} \int_0^{\eta_0} d\eta (H_{n,r}(\eta) - \Phi_{n,r}(\eta)) T_\ell(\zeta),\tag{5.92}$$

$$a_{\ell, nr}^E = \gamma \sqrt{4\pi(2\ell+1)} \int_0^{\eta_0} d\eta \Phi_{n,r}(\eta) E_\ell(\zeta),\tag{5.93}$$

$$a_{\ell, nr}^B = \gamma \sqrt{4\pi(2\ell+1)} \int_0^{\eta_0} d\eta \Phi_{n,r}(\eta) B_\ell(\zeta),\tag{5.94}$$

and $T_\ell(\zeta)$, $E_\ell(\zeta)$, $B_\ell(\zeta)$ are the multipole projection functions which appear after the integration over the angular variables, whose form are given by

$$\begin{aligned}T_\ell(\zeta) &= \sqrt{\frac{(\ell+2)!}{(\ell-2)!}} \frac{j_\ell(\zeta)}{\zeta^2}, \\ E_\ell(\zeta) &= \left[\left(2 - \frac{l(l-1)}{\zeta^2} \right) j_\ell(\zeta) - \frac{2}{\zeta} j_{\ell-1}(\zeta) \right], \\ B_\ell(\zeta) &= 2 \left[-\frac{(\ell-1)}{\zeta} j_\ell(\zeta) + j_{\ell-1}(\zeta) \right].\end{aligned}\tag{5.95}$$

5.5 Correlation functions

So far we have discussed the theoretical aspects of the interaction between the PGWs and the CMB photons; however, a compelling theory must predict some quantity which can be confronted with observations. In the case of CMB, the most powerful

observable is the *correlation function* $C_\ell^{XX'}$, where $X = T, E, B, V$ represents its temperature fluctuations and the polarization modes. Satellites like COBE, WMAP and Planck and balloon-borne or ground experiments¹ measure the power spectrum $C_\ell^{XX'} \times \ell$ to some extent, and then the arena to the confrontation ‘*theory versus experiment*’ is set. The expression for the correlation functions for anisotropies and polarization are given by (BASKARAN et al., 2006)

$$C_\ell^{XX'} = \frac{\mathcal{C}^2}{4\pi^2(2\ell + 1)} \int ndn \sum_{r=1,2} \sum_{m=-\ell}^{\ell} [a_{\ell m, nr}^X a_{\ell m, nr}^{X'*} + a_{\ell m, nr}^{X*} a_{\ell m, nr}^{X'}]. \quad (5.96)$$

where the amplitudes $a_{\ell m}^X$ come from the expressions (5.95). The evaluation of this integral is not an easy task, and it must be carried out numerically (despite some approximations can lead to analytical results as given in references (PRITCHARD; KAMIONKOWSKI, 2005) and (XIA; ZHANG, 2009)); then, as an application of all the theory we went through so far, and to set the basis for the discussion in the next chapter, we develop a computation of the CMB power spectrum for anisotropies induced by PGWs in GR.

The first step in this computation concerns the numerical solution to the evolution equation of the PGWs, (4.85). Since the events we have been talking about take place at the time of recombination, the scale factor appearing in equation (4.85) must be of a typical universe dominated by matter. However, to be more precise in our calculations, we also include radiation; then, for the parametrization chosen $a(\tau_0) = 2R_H$, the scale factor for a flat universe filled with radiation and matter, is given by (BASKARAN et al., 2006)

$$a(\tau) = 2R_H \left(\frac{1 + z_{eq}}{2 + z_{eq}} \right) \tau \left(\tau + \frac{2\sqrt{2 + z_{eq}}}{1 + z_{eq}} \right), \quad (5.97)$$

where z_{eq} is the redshift associated with the epoch of radiation-matter equality, whose value is $z_{eq} \sim 3 \times 10^3$, and the corresponding conformal instant τ_{eq} is

$$\tau_{eq} = (\sqrt{2} - 1) \frac{\sqrt{2 + z_{eq}}}{1 + z_{eq}} \sim 7.6 \times 10^{-3}. \quad (5.98)$$

¹See (BOCK et al., 2006) and references therein for further details.

Substituting the scale factor (5.97) into (4.85), we obtain exact analytical solutions for the functions $\mu_n(\tau)$ (BOSE; GRISHCHUK, 2002). Following (BASKARAN et al., 2006), we normalize the GW amplitudes $h_n(\tau)$ in terms of its value at $\tau_r = 10^{-6}$ (in terms of redshift, $z_r \sim 3 \times 10^7$); the resulting numerical solutions are displayed in the figure 5.3.

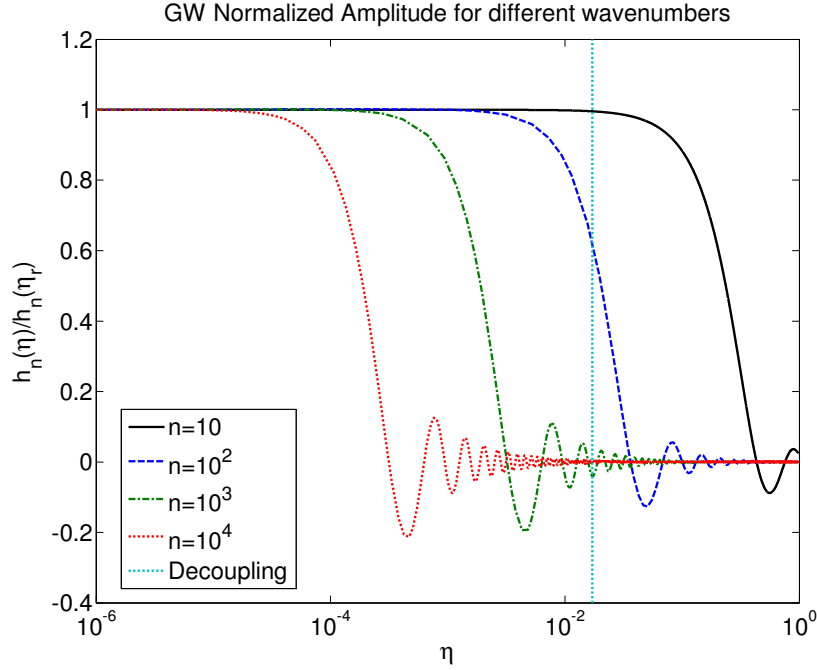


FIGURE 5.3 - The time evolution of the normalized GW amplitudes $h_n(\tau)/h_n(\tau_r)$. Compare with Figure 1 of (BASKARAN et al., 2006).

After having the evolution of the modes, the next steps are the numerical integration of the Volterra equation (5.88). To perform this we have first to derive the expressions for the scattering rate (5.49), which depends on the number of free electrons in the unit comoving volume, $N_e(\tau)$, given by (PEEBLES, 1993)

$$N_e(\tau) = \left(1 - \frac{Y_p}{2}\right) \frac{X_e(\tau)\Omega_b\rho_c}{m_p} \left(\frac{a(\tau_0)}{a(\tau)}\right)^3,$$

where $X_e(\tau)$ can be approximated by the fitting function (HU; SUGIYAMA, 1995)

$$X_e(\tau) = \left(1 - \frac{Y_p}{2}\right)^{-1} \left(\frac{c_2}{1000}\right) \left(\frac{m_p}{2\sigma_T R_H \rho_c}\right) \Omega_b^{c_1-1} \left(\frac{z}{1000}\right)^{c_2-1} \left(\frac{a'}{a}\right) (1+z)^{-1}. \quad (5.99)$$

In these formulae $Y_p \approx 0.23$ is the primordial helium mass fraction, Ω_b is the baryon content, and m_p is the mass of a proton. The constants are given by $c_1 = 0.43$, $c_2 = 16 + 1.8 \ln \Omega_B$, and we take $\Omega_b = 0.046$ (KOMATSU et al., 2009).

Along with the pre-recombination era, there was another epoch in the history of the universe in which ionization played another momentous role. As we have stated in Chapter 2.5, at decoupling the universe underwent a transition from a completely ionized state to a state in which neutral hydrogen and helium atoms were formed. In this process the radiation decoupled from the matter, originating the CMB radiation and a neutral pre-galactic baryonic medium (PGM). Then, at some redshift between $14 < z < 6$ the PGM was ionized again by the UV radiation from the first luminous objects, leaving the intergalactic medium (IGM) ionized (FAN et al., 2006). Such process is called *reionization*, and would leave observable imprints on the CMB polarization spectrum due to the interactions of the CMB photons with the free electrons now available due to the reionized medium. However, the reionization epoch is still not fully understood, and many models have been proposed to shed a light on the physics of this process (see (LEE, 2009) and references therein), which can be homogeneous models with a sudden reionization (*e.g.* as discussed in (XIA; ZHANG, 2009), (GIANNANTONIO; CRITTENDEN, 2007)), or extended models with double reionization (CEN, 2003), among others (see (XIA; ZHANG, 2009) for a more comprehensive list of papers).

Since in this work simplicity is our guiding principle, we shall consider solely the epoch of recombination, whose physical process is very well understood. Despite reionization is fundamental to understand the low-multipole behavior of CMB polarization, it can be neglected in a first-approximation to study temperature anisotropies generated by the tensor modes. Having said that, all we have to do now is to compute numerically the coefficients (5.91), and then integrate expression (5.96) to get the final result, which is depicted in Figure 5.4.

As for the polarization modes, the power spectra look like the one depicted in Figure 5.5.

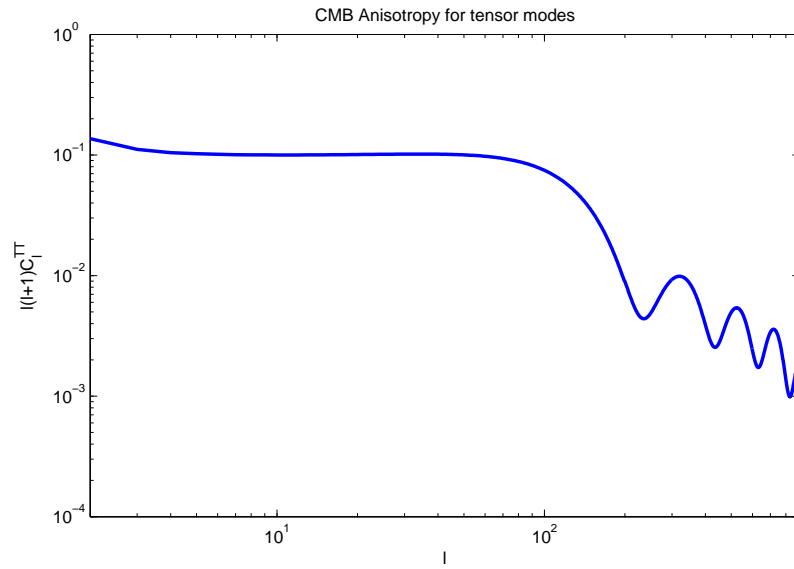


FIGURE 5.4 - Temperature anisotropies induced by GWs in GR.

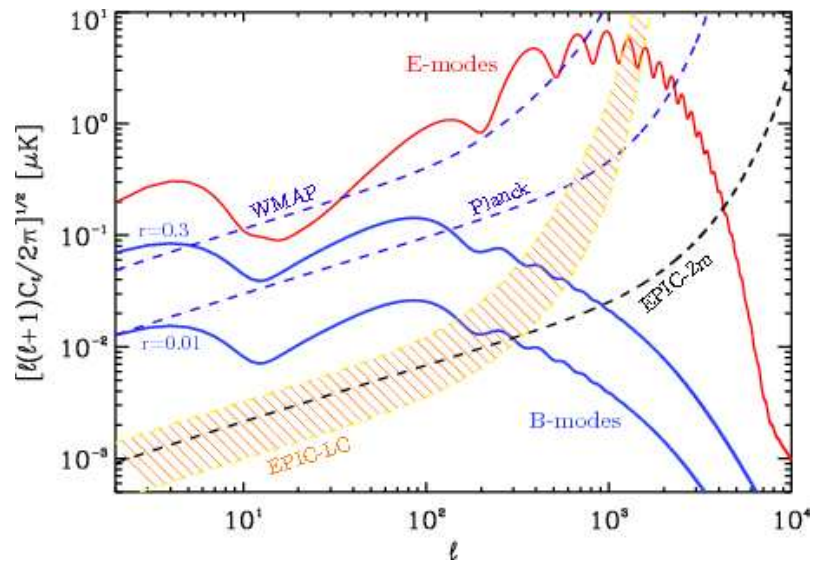


FIGURE 5.5 - CMB polarization power spectra. Figure adapted from (BOCK,2008).

6 SIGNATURES OF MASSIVE GRAVITONS IN THE CMB

In this Chapter we study the signatures of vector and tensor modes of theories with massive gravitons, as an example of the Class 1 of alternative cosmologies in the Table 1.2.

6.1 Theories of Gravity with Massive Gravitons

As we have argued in Section 1.1.1, it seems that the simplest and most natural modification to GR is the introduction of a mass for the gravitons. The study of theories with massive gravitons dates back to 1939 in the pioneering work of M. Fierz and W. Pauli (FIERZ; PAULI, 1939), who investigated a linearized field theory of spin-two massive particles. The Lorentz invariance of the Fierz-Pauli (FP) lagrangian yields a spin-two massive state with six polarization modes (states with helicities ± 2 , ± 1 and 0), differing from GR where one finds only a spin-two state with the two tensor polarization modes (helicities ± 2). Such extra degrees of freedom yield an additional contribution of one vector and one real scalar massless particles with helicities ± 1 and 0, respectively. The scalar particle couples to the trace of the stress energy-momentum tensor, causing a discontinuity in the propagator when one switches from the massive to the massless regime. This is the so-called van Dam-Veltman-Zakharov (vDVZ) discontinuity (DAM; VELTMAN, 1970; ZAKHAROV, 1970), whose net effect for a theory of a massive spin-two graviton is catastrophic (BOULWARE; DESER, 1972): it would not even pass the solar-system tests for a theory of gravity (the prediction of the angle concerning the bending of the light by the Sun, for example).

However, in a full theory of gravity, we must consider nonlinear effects; the FP theory is valid only in the linear approximation. Nonlinear effects eliminate the vDVZ discontinuity in the classical level (VAINSHTEIN, 1972; DEFFAYET et al., 2002), so that classically we may reconcile the massive theory with the GR predictions. Moreover, at the quantum level, the nonlinear interactions appear at the loop diagrams, so that the theory becomes strongly coupled above the energy scale $\Lambda = (m^4 M_P)^{1/5}$, where m is the graviton mass and M_P is the Planck mass (ARKANI-HAMED et al., 2003; AUBERT, 2004). For masses $m \sim H_0$, where H_0 is the present-day value of the Hubble parameter, the energy scale Λ is too small, well below the expected value, $\Lambda = (m M_P)^{1/2}$. In brane-world models (CHARMOUSIS et al., 2000; GREGORY et al., 2000; KOGAN et al., 2000; DVALI et al., 2000) a similar problem occurs: either they

have ghosts (LUTY et al., 2003; DUBOVSKY; LIBANOV, 2003; CHACKO et al., 2004; PILO et al., 2000), or are strong coupled at low energies (LUTY et al., 2003; DUBOVSKY; LIBANOV, 2003; CHACKO et al., 2004; RUBAKOV, 2003).

A great step forward was taken in the works (ARKANI-HAMED et al., 2004) and (RUBAKOV, 2004). In reference (ARKANI-HAMED et al., 2004) the authors proposed a consistent modification of gravity in the infrared as an analog of the Higgs mechanism in GR. In this model, Lorentz invariance is spontaneously broken and the graviton, as a result, acquires a mass. In reference (RUBAKOV, 2004) the author introduces a Lorentz-violating massive gravity model in which the vDVZ discontinuity, ghosts and the low strong coupling scale are absent. In reference (DUBOVSKY, 2004) the author studies the most general Lorentz-violating gravitational theory with massive gravitons, showing that there is a number of different regions in the mass parameter space of this theory in which it can be described by a consistent low-energy effective theory without instabilities and the vDVZ discontinuity.

Therefore, the theory of *Massive Gravity*, as developed in (RUBAKOV, 2004) and (DUBOVSKY, 2004) gives rise to physical propagating modes, and is free of the pathologies mentioned above. Also, there is a version of the FP model - which we call *modified Fierz-Pauli* model (MFP), which neither suffers the vDVZ discontinuity nor is discarded by solar-system measurements (FINN; SUTTON, 2002). Also, GR is recovered in this model when $m \rightarrow 0$. We start our analysis of the signatures of these massive models with the MFP model.

6.1.1 The Modified Fierz-Pauli Model

Let us now analyze how do GWs arise in the case of the MFP model. In this case, the graviton mass lagrangian appears as a quadratic term in the perturbation of the metric tensor $h_{\alpha\beta}$ in the weak-field limit, so that its action is given by (FINN; SUTTON, 2002), (GABADADZE; GRUZINOV, 2005):

$$\begin{aligned}
S &= \frac{M_P^2}{8} \int d^4x \left[h_{\alpha\beta,\gamma} h^{\alpha\beta,\gamma} - 2h_{\alpha\beta}{}^{;\beta} h^{\alpha\gamma}{}_{;\gamma} + 2h_{\alpha\beta}{}^{;\beta} h^{,\alpha} - h^{,\alpha} h_{,\alpha} \right. \\
&\quad \left. - 4M_P^{-2} h_{\alpha\beta} T^{\alpha\beta} - m^2 \left(h_{\alpha\beta} h^{\alpha\beta} - \frac{1}{2} h^2 \right) \right], \tag{6.1}
\end{aligned}$$

where h is given by (B.10). If instead of the contribution $m^2 h^2/2$ to the last term on the right-hand side of (6.1) one had $m^2 h^2$, this model would correspond to the origi-

nal Fierz-Pauli action, which is plagued by the vDVZ discontinuity (DAM; VELTMAN, 1970).

The Einstein equations associated with the action (6.1) follow from (A.10),

$$\begin{aligned} \square h_{\alpha\beta} &- h_{\alpha}{}^{\gamma}{}_{,\gamma\beta} - h_{\beta}{}^{\gamma}{}_{,\gamma\alpha} + h_{,\alpha\beta} + \eta_{\alpha\beta} h^{\gamma\delta}{}_{,\gamma\delta} \\ &- \eta_{\alpha\beta} \square h + m^2 \left(h_{\alpha\beta} - \frac{1}{2} \eta_{\alpha\beta} h \right) = -2M_P^{-2} T_{\alpha\beta}; \end{aligned} \quad (6.2)$$

then, imposing the conservation of the stress energy-momentum tensor, $\nabla_{\alpha} T^{\alpha\beta} = 0$, we get, in a Minkowski background, the same constraint $\bar{h}_{\alpha\beta}{}^{,\alpha} = 0$ found in GR (B.18), where $\bar{h}_{\alpha\beta}$ has the same form as (B.9). However, unlike GR, in the present case it emerges as a constraint from the conservation of the stress energy-momentum tensor rather than a gauge choice. This constraint eliminates four degrees of freedom out of the ten independent components of the space-time metric, leaving then only six independent modes (five coming from the spin-2 and spin-1 modes, and one coming from the spin-0 trace). Since these modes correspond exactly to the polarization states of the GW, we may readily associate the components of $\bar{h}_{\alpha\beta}$ with the corresponding ones of (C.27), so that the only nonzero contributions are the spatial components \bar{h}_{ij} .

Using the arguments above and plugging equation (B.18) into (6.2), we obtain, in the absence of sources,

$$(\square + m^2) \bar{h}_{ij} = 0, \quad (6.3)$$

which is clearly a Klein-Gordon equation for a wave propagating in the direction $\hat{\mathbf{k}} = \hat{\mathbf{z}}$. For the sake of simplicity we henceforth drop the bar over the tensor \bar{h}_{ij} .

Due to the oscillatory character of equation (6.3) we may expand the tensor field h_{ij} into the Fourier modes as we did in (C.28) and (C.29); in particular, for the TTF component of the tensor perturbation to the metric h_{ij} (corresponding to the NP amplitude Ψ_4 mode with $r = 4, 5$), we write

$$\tilde{h}_{ij}^{\perp} = \varepsilon_{ij}^4(k) \tilde{h}^4(k) + \varepsilon_{ij}^5(k) \tilde{h}^5(k), \quad (6.4)$$

whereas for the longitudinal polarization state we extend the definition (6.4) to the

Ψ_3 modes (associated with $r = 2, 3$) as

$$\tilde{h}_{ij}^{\parallel} = \varepsilon_{ij}^2(k)\tilde{h}^2(k) + \varepsilon_{ij}^3(k)\tilde{h}^3(k); \quad (6.5)$$

where $\varepsilon_{ij}^{2,3,4,5}$ are the polarization tensor given in (C.27). Then, by Fourier transforming (6.4) and (6.5) back to the configuration space, we see that both $h_{ij}^{\perp,\parallel}$ satisfies (6.3), that is

$$(\square + m^2) h_{ij}^{\perp,\parallel} = 0, \quad (6.6)$$

which reduces to the GW equation for GR in the limit $m = 0$. The tensor h_{ij}^{\perp} encompasses both transverse polarization modes “+” and “ \times ” characteristic of GR. As for the scalar modes Ψ_2 and Φ_{22} , we will not consider them here, since scalar fluctuations are not “sources of handedness” to excite the CMB B-polarization mode.

6.1.2 Massive Gravity

As we have pointed out at the beginning of this section, the key ingredient to construct a physically-consistent theory of gravitation with massive gravitons lies on the spontaneous violation of the Lorentz symmetry. In what follows we do not go into the technical details of the construction of this model; we just summarize the basic ideas. A more thorough review of these topics can be found in (RUBAKOV; TINYAKOV, 2008) and (BEBRONNE, 2009).

As in the Higgs analog in the Standard Model of electroweak interactions, we introduce, following (DUBOVSKY, 2004) and (DUBOVSKY et al., 2005), a set of four scalar Goldstone fields $\phi^0(x)$, $\phi^i(x)$, such that the action for Massive Gravity is written as

$$S = \int d^4x \sqrt{-g} [-M_P^2 R + \Lambda^4 F(X, V^i, W^{ij}) + \mathcal{L}_{matter}], \quad (6.7)$$

where the first term on the right-hand side represents the usual Einstein-Hilbert action, and F is an arbitrary function of the metric components, their derivatives, and the Goldstone fields. The lagrangian for ordinary matter, \mathcal{L}_{matter} , is assumed to be minimally coupled to the metric. The simplest way to combine the derivatives of the Goldstone fields to enter the argument of F is given by the set of scalar

quantities

$$\begin{aligned} X &= \Lambda^{-4} g^{\alpha\beta} \partial_\alpha \phi^0 \partial_\beta \phi^0, \quad V^i = \Lambda^{-4} g^{\alpha\beta} \partial_\alpha \phi^0 \partial_\beta \phi^i, \\ W^{ij} &= \Lambda^{-4} g^{\alpha\beta} \partial_\alpha \phi^i \partial_\beta \phi^j - \frac{V^i V^j}{X}, \end{aligned} \quad (6.8)$$

where Λ is the parameter which characterizes the cutoff scale of the theory. The second term on the right-hand side of (6.7) is invariant under the spatial reparametrization symmetry $x^i(t) \rightarrow x^i(t) + \xi^i(t)$ and rotations.

We now introduce the ‘‘vacuum’’ solutions for the model (6.7),

$$g_{\alpha\beta} = a^2 \eta_{\alpha\beta}, \quad \phi^0 = \Lambda^2 t, \quad \phi^i = \Lambda^2 x^i, \quad (6.9)$$

which corresponds to the flat FRW space; in the ‘‘unitary gauge’’ described by (6.9) the action will depend solely on the metric components. Now, in order to study linear cosmological perturbations around a flat FRW space, we spontaneously break the Lorentz symmetry of the model by fixing the Goldstone fields to the vacuum (6.9), so that the only remaining perturbations are given by (3.12) supplemented by the constraints (3.9) and (3.11).

Now, in the unitary gauge (6.9) we expand $\sqrt{-g + \delta g}$, $X(g + \delta g)$, $V^i(g + \delta g)$, $W^{ij}(g + \delta g)$ and $F(g + \delta g)$ in powers of the metric perturbation δg , and substitute these results into the massive term in (6.7), so that the lagrangian for the second-order perturbations reads

$$\mathcal{L}_m = \frac{M_P^2}{2} [m_0^2 \delta g_{00}^2 + 2m_1^2 \delta g_{0i}^2 - m_2^2 \delta g_{ij}^2 + m_3^2 \delta g_{ii} \delta g_{jj} - 2m_4^2 \delta g_{00} \delta g_{ii}], \quad (6.10)$$

where m_0 , m_1 , m_2 , m_3 and m_4 are parameters related to the function F and its derivatives,

$$\begin{aligned} m_0^2 &= \frac{\Lambda^4}{M_P^2} [X F_X + 2X^2 F_{XX}], \quad m_1^2 = \frac{2\Lambda^4}{M_P^2} \left[-X F_X - W F_W + \frac{1}{2} X W F_{VV} \right], \\ m_2^2 &= \frac{2\Lambda^4}{M_P^2} [W F_W - 2W^2 F_{WW}], \quad m_3^2 = \frac{\Lambda^4}{M_P^2} [W F_W + 2W^2 F_{WW}], \\ m_4^2 &= -\frac{\Lambda^4}{M_P^2} [X F_X + 2X W F_{XW}], \end{aligned} \quad (6.11)$$

where $W = -1/3\delta_{ij}W^{ij}$ and

$$\begin{aligned}
F_X &= \frac{\partial F}{\partial X}, & F_{XX} &= \frac{\partial^2 F}{\partial X^2}, & F_{VV}\delta_{ij} &= \frac{\partial^2 F}{\partial V^i \partial V^j}, \\
F_W\delta_{ij} &= \frac{\partial F}{\partial W^{ij}}, & F_{XW}\delta_{ij} &= \frac{\partial^2 F}{\partial X \partial W^{ij}}, \\
\frac{\partial^2 F}{\partial W^{ij} \partial W^{kl}} &= F_{WW1}\delta_{ij}\delta_{kl} + F_{WW2}(\delta_{ik}\delta_{jl} + \delta_{il}\delta_{jk}).
\end{aligned} \tag{6.12}$$

(see Appendix A in references (DUBOVSKY et al., 2005) and (BEBRONNE; TINYAKOV, 2007) for details). The spatial indices in (6.10) are summed over and, as argued in the reference (RUBAKOV, 2004), the mass parameters m_i are proportional to some scale denoted by m .

The Einstein equations for the model (6.7), with the Goldstone fields in the unitary gauge (6.9), and metric (3.12) read (for computational details, see Appendix A of the references (DUBOVSKY et al., 2005) and (BEBRONNE; TINYAKOV, 2007)),

$$\begin{aligned}
\mathcal{H}^2 &= \frac{a^2}{3M_{\text{P}}^2}(\rho_m + \rho_\phi + \rho_\Lambda), \\
\mathcal{H}' + \mathcal{H}^2 &= -\frac{a^2}{2M_{\text{P}}^2}(p_m + p_\phi + p_\Lambda), \\
\partial_0(a^3 F_X X^{1/2}) &= 0,
\end{aligned} \tag{6.13}$$

where ρ_m and p_m stand for the density and pressure for the ordinary matter respectively, and

$$\rho_\phi = \Lambda^4 X F_X, \quad p_\phi = \Lambda^4 W F_W, \tag{6.14}$$

$$\rho_\Lambda = -\frac{\Lambda^4}{2}F, \quad p_\Lambda = \frac{\Lambda^4}{2}F. \tag{6.15}$$

6.2 Cosmological Perturbations in Massive Theories of Gravity

Once we have established the dynamical equations for the background, let us now turn our attention to the metric perturbations. The steps toward obtaining the dynamical equations for the massive metric perturbations are the same as followed in Section 3.3, despite of the slight modifications in the perturbed metric of these two distinct massive theories. We start with an analysis of the MFP model.

6.2.1 Cosmological Perturbations in the MFP Model

In Chapter 3 we have discussed the concepts and techniques of the theory of cosmological perturbations. The core of this powerful tool lies on the metric decomposition (3.12), in which the fluctuations are represented by scalars, transverse vectors and TTF tensors. In the case of the modified Fierz-Pauli model the same metric decomposition cannot be performed due to the extra polarization modes; we instead introduce (BESSADA; MIRANDA, 2009b)

$$\delta g_{\alpha\beta} = a(\tau)^2 \begin{pmatrix} 2\phi & X_i - Q_{,i} \\ X_i - Q_{,i} & -h_{ij} \end{pmatrix}, \quad (6.16)$$

where ϕ and Q are scalar fields, X_i is a divergenceless vector field, and h_{ij} is the cosmological version of the tensor given by the solution to equation (6.3), carrying the corresponding six polarization modes spanned in the NP formalism. The two scalar fields, plus the two components of the transverse vector field and the six modes of the tensor field give exactly the required ten degrees of freedom. The mass Lagrangian for this model can be constructed analogously as in (6.1), that is, it appears as a quadratic term in the metric (6.16). The full action is then obtained by adding up this contribution to the usual Einstein-Hilbert one, and the Einstein equations can be derived using the standard tools. Before doing that, it is convenient to decompose the tensor perturbation h_{ij} into its TTF and longitudinal parts in the Fourier space. In (C.28) the whole time-dependence of h_{ij} is contained in the exponential since it is a solution to a wave equation of the form (6.3); now, such time-dependence changes because of the extra temporal function $a(\tau)$ appearing in (6.16), which introduces a damping in the oscillation. Therefore, we Fourier-expand the massive tensor perturbation h_{ij} as

$$h_{ij}(\tau, x) = \sum_{r=1}^6 \int \frac{d^3k}{(2\pi)^{3/2}} \tilde{h}_{\mathbf{k}}^r(\tau) \varepsilon_{ij}^r(\mathbf{k}) e^{i\mathbf{k}\cdot\mathbf{x}}, \quad (6.17)$$

so that the TT and longitudinal components of \tilde{h}_{ij} can be written in the same foot as (6.4) and (6.5), that is

$$\tilde{h}_{ij}^{\perp}(\tau, \mathbf{k}) \equiv \varepsilon_{ij}^4(\mathbf{k}) \tilde{h}^4(\tau, \mathbf{k}) + \varepsilon_{ij}^5(\mathbf{k}) \tilde{h}^5(\tau, \mathbf{k}), \quad (6.18)$$

$$\tilde{h}_{ij}^{\parallel}(\tau, \mathbf{k}) \equiv \varepsilon_{ij}^2(\mathbf{k}) \tilde{h}^2(\tau, \mathbf{k}) + \varepsilon_{ij}^3(\mathbf{k}) \tilde{h}^3(\tau, \mathbf{k}); \quad (6.19)$$

now, deducing the Einstein equations for the cosmological MFP model according to the techniques discussed in Section 3.3, we see that both fields h_{ij}^\perp and h_{ij}^\parallel satisfy the same dynamical equations

$$h_{ij}^{\perp\prime\prime} - \nabla^2 h_{ij}^\perp + 2\mathcal{H}h_{ij}^{\perp\prime} + a^2 m^2 h_{ij}^\perp = 0, \quad (6.20)$$

$$h_{ij}^{\parallel\prime\prime} - \nabla^2 h_{ij}^\parallel + 2\mathcal{H}h_{ij}^{\parallel\prime} + a^2 m^2 h_{ij}^\parallel = 0. \quad (6.21)$$

Therefore, both the transverse tensor modes and the longitudinal vector modes evolve in the same way, unlike GR, in which vector (3.99-3.100) and tensor (3.101) modes behave quite differently. This fact will represent an important signature, as we shall discuss later.

6.2.2 Cosmological Perturbations in Massive Gravity

In the case of Massive Gravity, the cosmological perturbations to the metric are given by (3.12), together the following set of perturbations to the Goldstone fields in the unitary gauge (6.9), (BEBRONNE; TINYAKOV, 2007)

$$\tilde{\phi}^0 = \phi^0 + \Lambda^2 \lambda^0, \quad \tilde{\phi}^i = \phi^i + \Lambda^2 (\lambda^i + \lambda^{,i}), \quad (6.22)$$

where λ^0 e λ are scalar fields and λ^i is a divergenceless vector field. Now, under the infinitesimal coordinate transformations (3.49), we can show that the following vector fields

$$W_i = S_i + F_i', \quad \sigma_i = \lambda_i - F_i, \quad (6.23)$$

are invariant.

The action for Massive Gravity on a flat FRW background is then given by (6.7) with (3.12) and the Goldstone fields set to their vacuum values (6.9); the matter lagrangian \mathcal{L}_{matter} is assumed to be described by a perfect fluid whose perturbations for the fluid four-velocity are the same as in (3.68). With these features, the Einstein equations for the tensor field h_{ij} are given by (BEBRONNE; TINYAKOV, 2007),

$$h_{ij}'' - \nabla^2 h_{ij} + 2\mathcal{H}h_{ij}' + a^2 m_2^2 h_{ij} = 0, \quad (6.24)$$

whereas for the gauge-invariant vector fields defined by (6.23) the Einstein equations

read, in the longitudinal gauge,

$$\begin{aligned} \nabla^2 W_i - 2a^2 \rho_m M_P^{-2} (1+w) \omega_i &= 0, & W_i' + 2\mathcal{H}W_i - a^2 m_2^2 \sigma_i &= 0, \\ m_2^2 \nabla^2 \sigma_i &= 0, \end{aligned} \tag{6.25}$$

where $\delta_\zeta = v - (E' + B)$, and w is the equation of state parameter of the ordinary matter (BEBRONNE; TINYAKOV, 2007).

By solving equations (6.25) we conclude that the only relevant vector field is W_i , whose amplitude decays with a^{-2} as in (3.102), which is exactly the same behavior of vector fields as derived in GR.

To end this section let us discuss an important aspect concerning the mass parameters of Massive Gravity. As we have pointed out at the beginning of this Section, there are regions in the mass parameter space in which this theory is free of ghosts and instabilities; this means that the mass parameters m_0 , m_1 , m_2 , m_3 and m_4 cannot be chosen arbitrarily, but they have to satisfy some constraints (RUBAKOV, 2004), (DUBOVSKY, 2004). Since in this work we deal only with the mass parameter m_2 , there is a number of choices on these parameters in which the model is physically healthy; therefore, any of these choices would produce a physically acceptable theory. We simply assume that the mass parameters in our work are within the region in which the pathologies are absent.

Specific restrictions on the function F are discussed in (DUBOVSKY et al., 2005). In this reference, the authors demonstrate the existence of a wide class of functions F for which expanding cosmological solutions are compatible with constant graviton masses and allow for the effective field theory description. Therefore, we may simply restrict F in such a way the mass m_2 is constant along the story of the universe, which we assume to hold throughout this work.

6.3 Primordial Massive Tensor Modes

It is important to note that both the MFP model and Massive Gravity give rise to the same results for the TTF polarization modes of the tensor perturbations as can be seen from equations (6.20) and (6.24), whereas for vector perturbations the situation changes drastically. Then, the behavior of the tensor modes is the same for both models, which we next analyze.

We first Fourier-expand the massive tensor field h_{ij} as in (5.30), (with the parametrization (5.29)) and then plug into equation (6.24), whose result is

$$h_n^{(m)''} + 2\mathcal{H}h_n^{(m)'} + (n^2 + m^2 a^2) h_n^{(m)} = 0, \quad (6.26)$$

where the superscript (m) stands for massive. In (6.26) we have dropped the GW polarization indices r since they give the same contribution. Defining an analogous variable to (4.84) for the massive case, $\mu_n^{(m)}(\tau) = a(\tau)h_n^{(m)}(\tau)$, and substituting it into equation (6.26), we find (BESSADA; MIRANDA, 2009a)

$$\mu_n^{(m)''} + \left[n^2 + m^2 a^2 - \frac{a''}{a} \right] \mu_n^{(m)} = 0. \quad (6.27)$$

As we have discussed in Section 5.5, the scale factor (5.97) represents very well the periods of the universe relevant to recombination, so that it makes sense to employ it in Massive Gravity as well, since we may expect that the contribution of massive gravitons to the expansion of the universe is negligible in its early epochs; then, as a first approximation, we may neglect the contribution of the components ρ_ϕ , equation (6.14), and ρ_Λ , equation (6.15), in (6.13).

Now, using the above arguments and consequently the scale factor (5.97), we can solve numerically equation (6.27) for different wavenumbers n and masses m . We choose the graviton masses m using the following argument: in GR, only GW with frequencies ν within the range $10^{-15}Hz$ to $10^{-18}Hz$ may leave a signature on CMB polarization; these frequencies correspond to wavenumbers k within the range $10^{-25}cm^{-1}$ ($n \sim 5 \times 10^3$) to $10^{-28}cm^{-1}$ ($n \sim 10$). For Massive Gravity, we use the same values for k , but now we vary the frequencies in order to obtain constant nonzero graviton masses through the dispersion relation

$$\omega^2 = k^2 + m^2, \quad (6.28)$$

which comes straight from (6.24), where now $\omega = 2\pi\nu$. As a result, we find that if the values of the mass m lie within the range $10^{-66} - 10^{-62}g$, the corresponding frequencies have values very close to the expected in GR. In particular, we've found that if the graviton mass is $m = 10^{-66}g \sim 10^{-29}cm^{-1}$, the behavior of the GWs in Massive Gravity is exactly *the same* of GWs in GR. Therefore, if the graviton mass is equal or less than the graviton mass limit $m_l = 10^{-66}g$, *the effects of Massive*

Gravity are indistinguishable from GR (BESSADA; MIRANDA, 2009a).

It is important to mention that there has been a lot of efforts to constrain the masses of the tensor modes over the past few decades: (GOLDHABER; NIETO, 1974) ($m < 2.0 \times 10^{-62}g$), (TALMADGE et al., 1988) ($m < 7.68 \times 10^{-55}g$), (FINN; SUTTON, 2002) ($m < 1.4 \times 10^{-52}g$), and (COORAY; SETO, 2004) ($\sim 10^{-56}g$). A recent and comprehensive review of the methods to determine the bounds for the masses of gravitons and photons can be found in (GOLDHABER; NIETO, 2008), which we refer to for further details.

Since we are interested in investigating signatures of massive gravitons, we shall consider only graviton masses higher than the limit $m = 10^{-66}g$; the numerical solutions to the massive tensor perturbation equations (6.27) are depicted in the Figure 6.1 below. For sake of comparison we depict the general-relativistic GW amplitudes in each graph as well. We have used the same normalization as (BASKARAN et al., 2006), and the plots start at $\tau = \tau_r = 10^{-6}$. The mass $m = 2.843 \times 10^{-28}cm^{-1}$ correspond to $m = 10^{-65}g$, and so forth.

Let us now analyze in detail the behavior of massive gravitons in the light of equation (6.27) (BESSADA; MIRANDA, 2009a). In the very early universe, before the time of equality radiation-matter, the value of $a(\tau)$ is very low, and then the m^2a^2 on the left-hand side of (6.27) can be dropped; therefore, we recover the characteristic tensor mode equation of GR, (4.85), and the behavior of massless and massive gravitons are the same. On superhorizon scales, $n \ll a''/a$, the resulting equation for the tensor modes is

$$\mu_n^{(m)''} - \frac{a''}{a} \mu_n^{(m)} = 0, \quad (6.29)$$

whose solution is given by $\mu_n^{(m)} = f(n)a$, which means that the tensor amplitudes are "frozen", no matter the gravitons are massless or not. This particular behavior can be clearly seen from figures 6.1 - 6.6, where the amplitudes are constant for all the modes considered prior to decoupling.

However, as the universe evolves, the tensor modes "fall" into the horizon, so that their amplitudes are no longer constant; on subhorizon scales, $n \gg a''/a$, we can neglect the effect of the term a''/a , so that we are left with

$$\mu_n^{(m)''} + [n^2 + m^2a^2] \mu_n^{(m)} = 0. \quad (6.30)$$

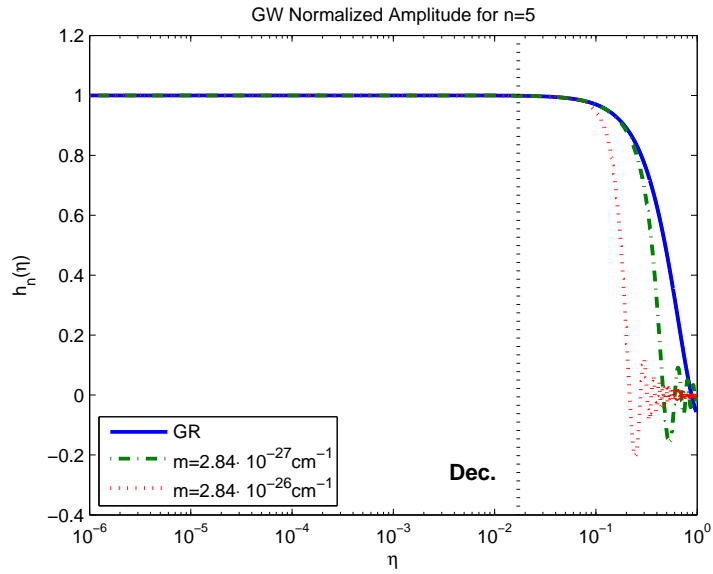


FIGURE 6.1 - The time evolution of the normalized GW amplitudes for $n = 5$.

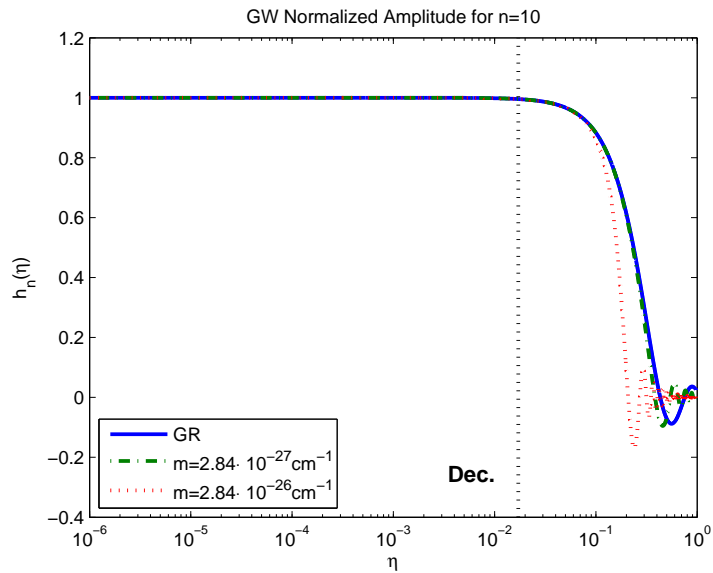


FIGURE 6.2 - For $n = 10$.

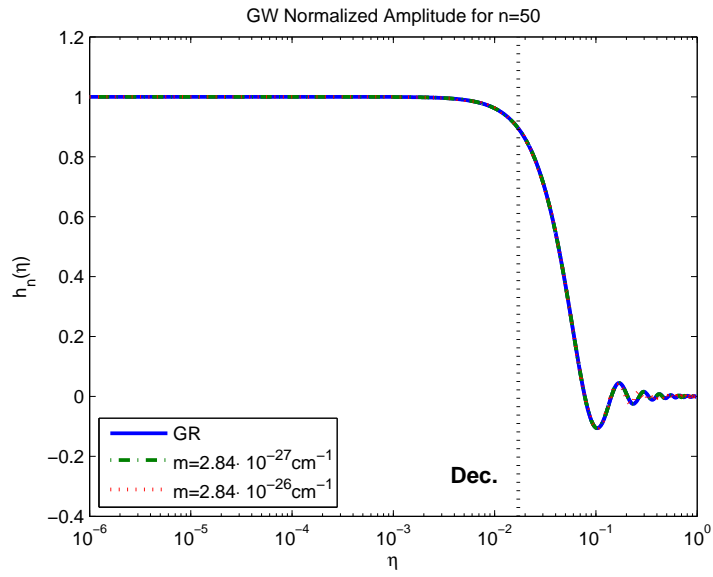


FIGURE 6.3 - For $n = 50$.

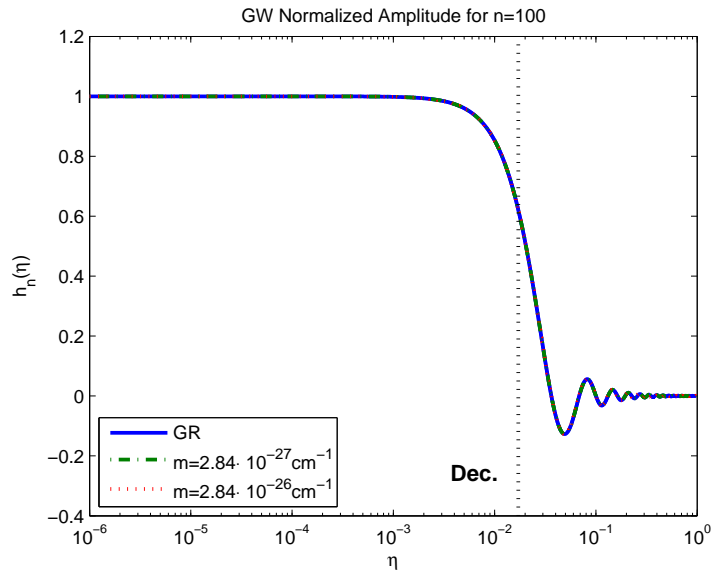


FIGURE 6.4 - For $n = 100$.

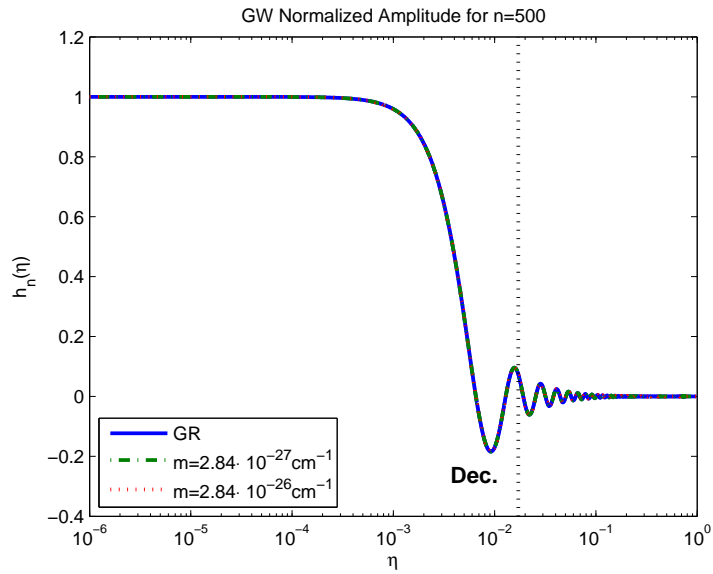


FIGURE 6.5 - For $n = 500$.

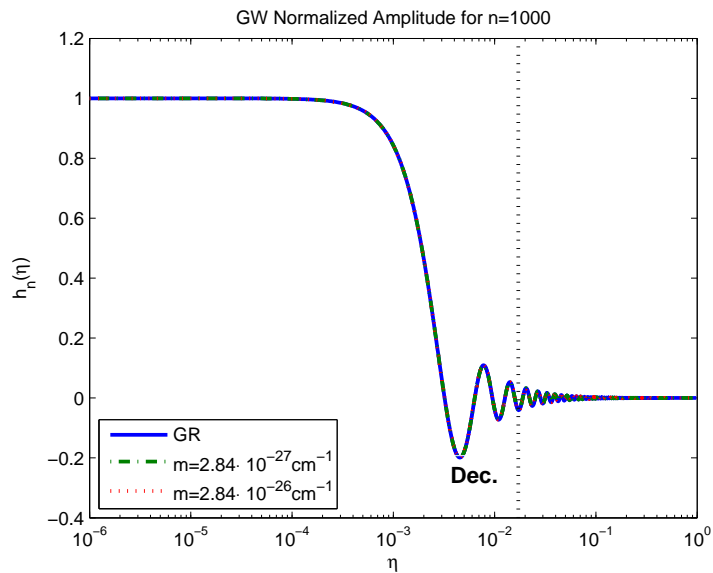


FIGURE 6.6 - For $n = 1000$.

On subhorizon scales the massive term becomes dominant over low values of n , so that it “enforces” the tensor modes to fall into the horizon earlier than in the massless case. It is clear from equation (6.30) that the heavier the gravitons, the earlier their modes fall into the horizon. This effect can be clearly seen in the figures 6.1, 6.2 and 6.4, where the n values are sufficiently low to account for this effect. However, for larger values of n , this effect weakens, since $n^2 \gg m^2 a^2$ in the time of decoupling, and the massive term will be predominant only for low redshifts, as can be seen in figures 6.5, 6.6 and 6.7.

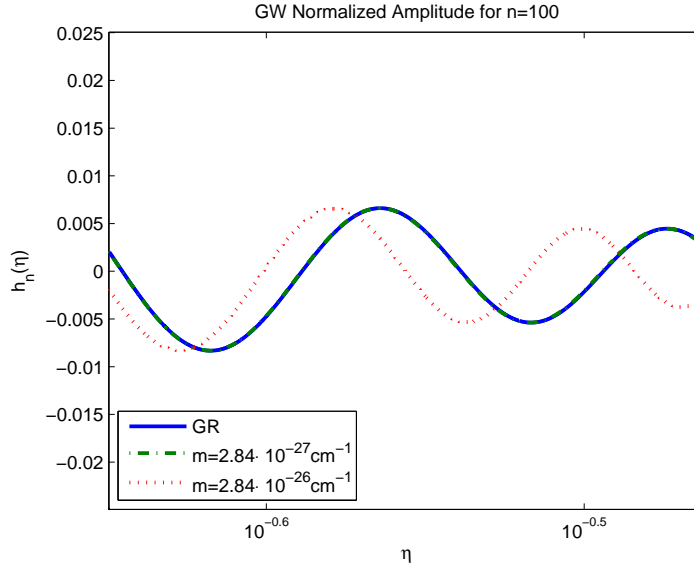


FIGURE 6.7 - The “tail of Figure 6.4 zoomed in, showing the phase difference in the tensor modes at very low redshifts for both massless and massive gravitons.

In particular, for low n (corresponding to tensor modes with long wavelengths), its constant contribution to (6.30) can be completely neglected, so that we are left with

$$\mu_n^{(m)''} + \left[n^2 + m^2 a^2 - \frac{a''}{a} \right] \mu_n^{(m)} = 0, \quad (6.31)$$

and then the oscillatory behavior is strikingly different from the massless case, as shown in figures 6.1, 6.2. For higher n (that is, tensor modes with short wavelengths), though, this effect is not so strong, but induces a slight phase difference in the oscillatory behavior of the tensor modes. Such phase difference is stronger for higher

masses; as an example of it, we have zoomed in the “tail” of figure 6.2 to show this fact. This is presented in figure 6.7.

Hence, from this analysis we may conclude that the tensor modes of Massive Gravity behave similarly to the massless modes of GR, but the heavier the tensor modes are, the more distinct are their physical evolution if compared to the massless modes. Nevertheless, if massive gravitons do exist, they likely have left a signature on some physical observable; then, by comparing the predicted signatures of the massless and the massive modes with the observed ones, one should be able to determine whether they possess or not a nonzero mass. As argued in Chapter 1, the best observable is the CMB, and is in there we will be looking for such signatures.

6.4 Boltzmann Equations for Massive Gravitons

As we have seen in Section 6.2, the MFP model and Massive Gravity are equivalent with respect to the TTF tensor modes, but only the vector modes of the first model may give rise to relevant contributions to CMB polarization and anisotropies. In this Section, using the techniques developed in Chapter 5, we investigate how these contributions modify the radiative transport equations.

6.4.1 The Sachs-Wolfe effect induced by Massive Gravitons

We have discussed in Section 5.2 that the CMB photons are polarized due to the Thomson scattering with the free electrons in the epoch of recombination. Prior to Thomson scattering, the cosmological perturbations imprint a signature on the photon angular pattern, the SW effect. As we have seen, this effect can be computed through the geodesic equation (5.28), thus providing the source of the SW effect given by the product (5.32), $F = \varepsilon_{ij} p^i p^j$. In turn, the angular pattern was calculated according to the polarization vectors defined in (5.33); then, we expressed the photon momentum \mathbf{p} in the basis (5.34), depicted in Figure 5.2. Therefore, using (C.27) and (5.35-5.36), it follows that (BESSADA; MIRANDA, 2009b)

$$\varepsilon_{ij}^2 p^i p^j = \mu \sqrt{1 - \mu^2} \cos \varphi \propto Y_{2,+1}(\mu, \varphi), \quad (6.32)$$

$$\varepsilon_{ij}^3 p^i p^j = \mu \sqrt{1 - \mu^2} \sin \varphi \propto Y_{2,-1}(\mu, \varphi), \quad (6.33)$$

$$\varepsilon_{ij}^4 p^i p^j = (1 - \mu^2) \cos 2\varphi \propto Y_{2,+2}(\mu, \varphi), \quad (6.34)$$

$$\varepsilon_{ij}^5 p^i p^j = (1 - \mu^2) \sin 2\varphi \propto Y_{2,-2}(\mu, \varphi); \quad (6.35)$$

The results (6.32-6.35) show that *theories of gravitation with the Ψ_3 and Ψ_4 modes leave an imprint on the photon angular distribution in the form of a quadrupole*, with $m = \pm 2$ for the Ψ_4 modes ($r = 4, 5$, which coincides with GR), and with $m = \pm 1$ for the Ψ_3 modes ($r = 2, 3$). Since the MFP model has non-decaying vector modes, they will leave an imprint of the form (6.32-6.33). The tensor modes will contribute with the SW effect through relations (6.34-6.35) for both the MFP model and Massive Gravity, and they coincide with the GR result (5.38-5.39) (BESSADA; MIRANDA, 2009b).

6.4.2 The Basis for Thomson Scattering

We now turn to the derivation of the Thomson scattering term (5.12) for massive gravitons. As we have discussed in Section 5.2, CMB polarization is generated by means of Thomson scattering by converting the unpolarized state characterized by (5.40) to the polarized state characterized by the (5.44). In order to find an analog effect in both the MFP and Massive Gravity we must derive first the basis for the Thomson scattering. Following the same steps as taken in Section 5.2, we find (BESSADA; MIRANDA, 2009b)

a) Ψ_3 Modes:

$$\hat{a}^2 = \frac{1}{2}\mu\sqrt{1-\mu^2}\cos\varphi\hat{\mathbf{u}}, \quad \hat{a}^3 = \frac{1}{2}\mu\sqrt{1-\mu^2}\sin\varphi\hat{\mathbf{u}}, \quad (6.36)$$

b) Ψ_4 Modes:

$$\hat{a}^4 = \frac{1}{2}(1-\mu^2)\cos 2\varphi\hat{\mathbf{u}}, \quad \hat{a}^5 = \frac{1}{2}(1-\mu^2)\sin 2\varphi\hat{\mathbf{u}}, \quad (6.37)$$

where the vector $\hat{\mathbf{u}}$ is given by (5.23). Note that the tensor SW effect for massive gravitons (6.37) is the same as for GR, (5.38-5.39). Next, using the operator (5.41), and (5.42-5.43), it follows, for $\hat{\xi} = \hat{a}^r$ ($r = 2, 3, 4, 5$), that (BESSADA; MIRANDA, 2009b)

a) Ψ_3 Modes:

$$\hat{b}^2 = \frac{1}{2}\sqrt{1-\mu^2}\begin{pmatrix} \mu\cos\varphi \\ -\mu\cos\varphi \\ 2\sin\varphi \end{pmatrix}, \quad \hat{b}^3 = \frac{1}{2}\sqrt{1-\mu^2}\begin{pmatrix} \mu\sin\varphi \\ -\mu\sin\varphi \\ -2\cos\varphi \end{pmatrix}, \quad (6.38)$$

b) Ψ_4 Modes:

$$\hat{b}^4 = \frac{1}{2} \begin{bmatrix} (1 + \mu^2) \cos 2\varphi \\ -(1 + \mu^2) \cos 2\varphi \\ 4\mu \sin 2\varphi \end{bmatrix}, \quad \hat{b}^5 = \frac{1}{2} \begin{bmatrix} (1 + \mu^2) \sin 2\varphi \\ -(1 + \mu^2) \sin 2\varphi \\ -4\mu \cos 2\varphi \end{bmatrix}. \quad (6.39)$$

The Thomson basis vectors given by (6.36) and (6.38), (6.37) and (6.39) allows us to factor out the angular dependence of the photon distribution vectors, and they constitute the first-order contribution to $\hat{\mathbf{f}}$, as in (5.20).

6.4.3 The Full Boltzmann Equations

Once we have obtained the form of the photon distribution vector (5.20) for the TTF and longitudinal GW modes, we are able to write down the full Boltzmann equations (5.11). They are given by (BESSADA; MIRANDA, 2009b)

a) Ψ_3 Modes:

$$\chi^r(\tau, \mu)' + [q(\tau) + in\mu] \chi^r(\tau, \mu) = H^r(\tau), \quad (6.40)$$

$$\beta^r(\tau, \mu)' + [q(\tau) + in\mu] \beta^r(\tau, \mu) = \frac{3}{8} q(\tau) \mathcal{J}^r(\tau), \quad (6.41)$$

for $r = 2, 3$, and

$$\mathcal{J}^r(\tau) \equiv \int_{-1}^1 d\mu' [\chi^r(\tau, \mu') \mu'^2 (1 - \mu'^2) + \beta^r(\tau, \mu') (1 + \mu'^2 - 2\mu'^4)] \quad (6.42)$$

b) Ψ_4 Modes:

$$\xi^r(\tau, \mu)' + [q(\tau) + in\mu] \xi^r(\tau, \mu) = H^r(\tau), \quad (6.43)$$

$$\beta^r(\tau, \mu)' + [q(\tau) + in\mu] \beta^r(\tau, \mu) = \frac{3}{16} q(\tau) \mathcal{K}^r(\tau) \quad (6.44)$$

for $r = 4, 5$ and

$$\mathcal{K}^r(\tau) \equiv \int_{-1}^1 d\mu' \left[\beta^r(\tau, \mu') (1 + \mu'^2)^2 - \frac{1}{2} \xi^r(\tau, \mu) (1 - \mu'^2)^2 \right], \quad (6.45)$$

In the equations above, $q(\tau)$ is the scattering rate, defined in (5.49), and the functions $\xi(\tau, \mu)$, $\chi(\tau, \mu)$ and $H^r(\tau)$ are defined as

$$\xi^r \equiv \alpha^r + \beta^r, \quad \chi^r \equiv \alpha^r - \beta^r, \quad (6.46)$$

$$H^r \equiv \frac{1}{2} \frac{\partial h^r(\eta)}{\partial \eta}. \quad (6.47)$$

Equations (6.43) and (6.44) for massive gravitons with Ψ_4 mode are identical in form to the corresponding ones in GR, given by (5.51) and (5.52), as well as the integral term (6.45) to (5.54). However, the terms (6.47), which carry the content of the GW, are different for the massless and massive modes, so that we may expect different signatures for the massive tensor modes as compared to the massless ones.

The Boltzmann equations for the Ψ_3 modes, (6.40) and (6.41), do not appear in GR. Since the vector and tensor modes satisfy the same dynamical equation, and the mathematical form of the equations (6.40) and (6.41) is very different from (6.43) and (6.44), it is clear that the vector polarization modes of massive gravitons leave a characteristic signature distinguishable from the tensor ones, which could, in principle, be probed by measurements on the CMB E and B-modes (BESSADA; MIRANDA, 2009b). Since the experiments in the Planck satellite will improve the WMAP5 results for the E-mode, we may expect that such future measurements might decide whether nontrivial GW signatures - as we showed here through equations (6.40) and (6.41) for Ψ_3 -modes - appear or not in the CMB polarization spectrum. In this case, we conclude that CMB polarization measurements may be decisive to test alternative theories of gravitation - in particular, the massive model as we discussed here.

6.5 CMB Anisotropies induced by Massive Tensor Modes

As an application of the results found in the last Section, here we numerically solve the Boltzmann equations (6.43-6.44) for the tensor massive modes. We use the results found in Section 6.3 and apply the techniques developed in Section 5.5 to evaluate the correlation functions for the massive tensor modes. For the reasons discussed in Section 5.5, we do not consider reionization in the present work, which implies that no signature of massive gravitons can be seen in the polarization spectrum. This

happens because in this case the visibility function (5.80) is zero at this epoch, and then the source functions Φ (5.78) will be zero, since they depend linearly on $g(\tau)$. However, this fact does not affect CMB anisotropies, since the mode coefficients $a_{\ell m}^T$, given by (5.92), depends on $H(\tau)$, defined by (5.79), and (6.47), which is not zero even in the absence of reionization. Since the source function $H(\tau)$ depends on the tensor mode amplitudes, and massive and massless modes are different at late times, we conclude that the massive modes would leave a distinct signature on CMB low multipoles even without reionization.

As we have discussed in Section 6.3, if the mass of the tensor mode is less or equal than m_t , Massive Gravity produces the same results as GR; we choose then masses within the range $m = 10^{-27} \text{cm}^{-1} - m = 10^{-25} \text{cm}^{-1}$, whose associated anisotropies power spectrum is depicted in Figure 6.8 (BESSADA; MIRANDA, 2009a).

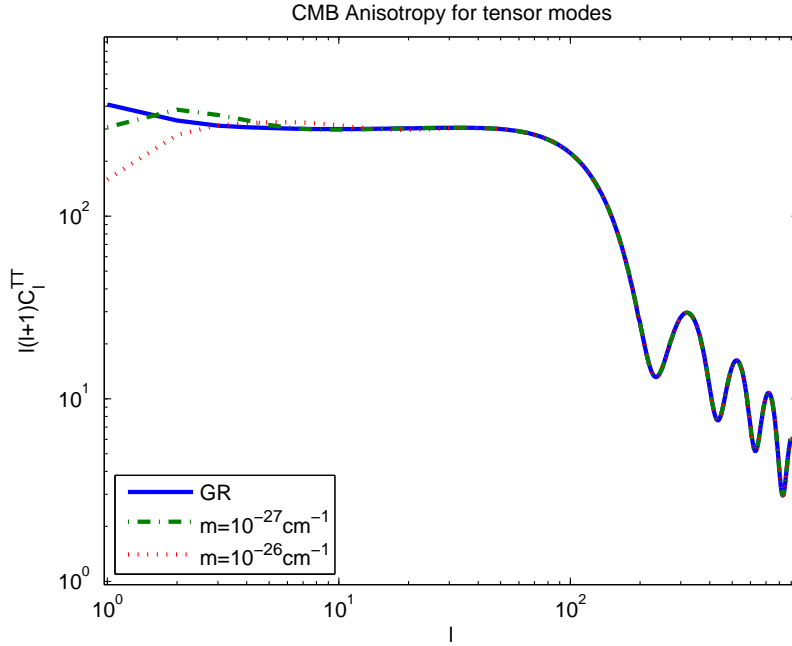


FIGURE 6.8 - The correlation functions C_{ℓ}^{TT} for GR and Massive Gravity. Note that the massive gravitons leave a signature on the spectrum for low multipoles.

This figure show distinct signatures for massless and massive gravitons, as we have argued above. Therefore, for the range of masses selected, massive tensor modes leave a clear signature on low multipoles $\ell < 30$. Figure 6.9 shows the low-multipole

region of the correlation function 6.8 in detail.

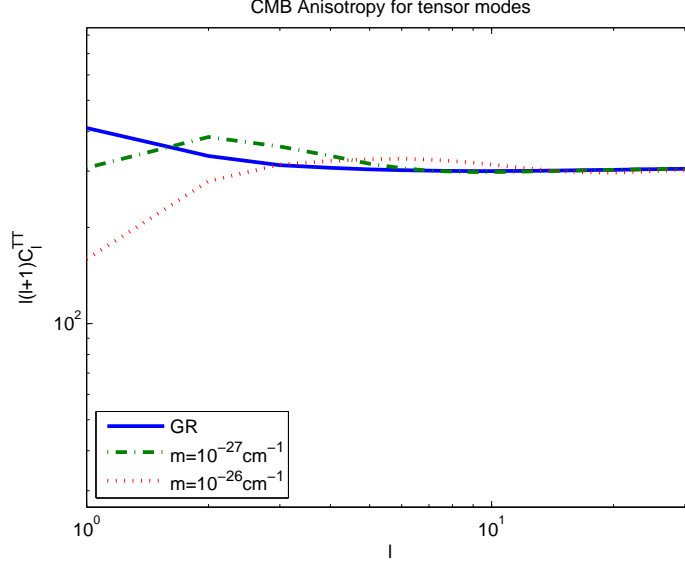


FIGURE 6.9 - The low-multipole “tail” in the TT correlation function. Note the quite distinct signatures for $\ell < 30$ for the mass range selected.

Since the heavier modes fall into the horizon earlier, they have the stronger signature, as shown. If we had chosen a different mass, say $m = 10^{-21} \text{cm}^{-1}$, the signature would be stronger, and possibly would appear for multipoles $\ell > 30$. This can be explained by simply analyzing the trend shown in figures 6.1 and 6.2: the heavier the mass, the earlier the modes fall into the horizon, which correspond to higher multipoles. However, even in this case, as the trend shown in figure 6.9 indicates, the signature will be particularly strong on low multipoles. Therefore, if the tensor modes of the metric fluctuations are massive, they could be detected directly by the CMB anisotropy power spectrum if their mass are greater than the limit $m_l \sim 10^{-29} \text{cm}^{-1}$, and their signatures would be noticeable specially on low multipoles.

Therefore, the results above indicate clearly that the future measurements on the TT correlation might be decisive for probing the existence of massive tensor modes, for the signature left by them could be strong enough to be distinguished from those of the massless modes (BESSADA; MIRANDA, 2009a).

7 SIGNATURES OF DBI INFLATION IN THE CMB

In this Chapter we derive new solutions in the context of DBI inflation and analyze their observational consequences as an example of the Class 2 of alternative cosmologies in the Table 1.2. We change the current notation used so far, so that a prime denotes a derivative with respect to the field ϕ .

7.1 DBI Inflation - An Overview

In warped D-brane inflation (see (MCALLISTER; SILVERSTEIN, 2008) and (CLINE, 2006) for a review), inflation is regarded as the motion of a D3-brane in a six-dimensional “throat” characterized by the metric (KLEBANOV; STRASSLER, 2000)

$$ds_{10}^2 = h^2(r) ds_4^2 + h^{-2}(r) (dr^2 + r^2 ds_{X_5}^2), \quad (7.1)$$

where h is the warp factor, X_5 is a Sasaki-Einstein five-manifold which forms the base of the cone, and r is the radial coordinate along the throat. In this case, the inflaton field ϕ is identified with r as $\phi = \sqrt{T_3}r$, where T_3 is the brane tension. The dynamics of the D3-brane in the warped background (7.1) is then dictated by the DBI Lagrangian

$$\mathcal{L} = -f^{-1}(\phi) \sqrt{1 - 2f(\phi)X} - f^{-1}(\phi) - V(\phi), \quad (7.2)$$

where $f^{-1}(\phi) = T_3 h(\phi)^4$ is the inverse brane tension, $V(\phi)$ is an arbitrary potential, and X is the kinetic term, defined in (D.2). We also assume that the background cosmological model is described by the flat FRW metric (2.6).

A quick inspection of the DBI Lagrangian (7.2) shows that it is a special case of k-inflation, characterized by a varying speed of sound c_s as described in Appendix D. In particular, the speed of sound for DBI models can be calculated from (7.2) and (D.15), whose result is

$$c_s(\phi) = \sqrt{1 - 2f(\phi)X}. \quad (7.3)$$

In those models it is convenient to introduce an analog of the Lorentz factor, related to $c_s(\phi)$ by:

$$\gamma(\phi) = \frac{1}{c_s(\phi)}. \quad (7.4)$$

We next introduce the generalization of the inflationary flow hierarchy for DBI models (PEIRIS et al., 2007). Taking the derivative of (7.2) with respect to X we see that

$$\mathcal{L}_X = \gamma(\phi); \quad (7.5)$$

then, in order to find the analogs of the flow parameters and equations derived in Appendix D, all we have to do is substitute (7.5) into equations (D.23), (D.25) and (D.26),

$$\epsilon(\phi) = \frac{2M_P^2}{\gamma(\phi)} \left(\frac{H'(\phi)}{H(\phi)} \right)^2, \quad (7.6a)$$

$$s(\phi) = \tilde{s}(\phi) = \frac{2M_P^2}{\gamma(\phi)} \frac{H'(\phi)}{H(\phi)} \frac{\gamma'(\phi)}{\gamma(\phi)}, \quad (7.6b)$$

note that in the DBI model $s = \tilde{s}$, which reduces the number of parameters. The η in the DBI model comes from (D.24)

$$\eta(\phi) = \frac{2M_P^2}{\gamma(\phi)} \frac{H''(\phi)}{H(\phi)}, \quad (7.7)$$

which suffices for our present discussion. The remaining flow parameters can be found in (PEIRIS et al., 2007).

From the definition of the number of e-folds, (4.23), and expression (7.6a), we find

$$N = \frac{1}{\sqrt{2M_P^2}} \int_{\phi_e}^{\phi} \sqrt{\frac{\gamma(\phi)}{\epsilon(\phi)}} d\phi. \quad (7.8)$$

In terms of the number of e-folds, the flow parameters (D.28-D.30) become

$$\epsilon = \frac{1}{H} \frac{dH}{dN}, \quad (7.9a)$$

$$s = \frac{1}{\gamma} \frac{d\gamma}{dN}. \quad (7.9b)$$

The dynamics of the inflaton field can be completely described by this hierarchy of equations, which are equivalent to the Hamilton-Jacobi equations (SPALINSKI,

2007b)

$$\dot{\phi} = -\frac{2M_P^2}{\gamma(\phi)}H'(\phi), \quad (7.10a)$$

$$3M_P^2H^2(\phi) - V(\phi) = \frac{\gamma(\phi) - 1}{f(\phi)}, \quad (7.10b)$$

which follows from (7.5) and (D.20-D.21). Using (7.3) and (7.10a-7.10b), we have that

$$\gamma(\phi) = \sqrt{1 + 4M_P^4 f(\phi) [H'(\phi)]^2}. \quad (7.11)$$

In terms of the flow parameter ϵ , the potential, $V(\phi)$, and the inverse brane tension, $f(\phi)$, can be written as

$$V(\phi) = 3M_P^2H^2 \left(1 - \frac{2\epsilon}{3} \frac{\gamma}{\gamma + 1} \right), \quad (7.12)$$

and

$$f(\phi) = \frac{1}{2M_P^2H^2\epsilon} \left(\frac{\gamma^2 - 1}{\gamma} \right), \quad (7.13)$$

respectively.

As for perturbations, the techniques introduced in Section D.3 can be applied to the present case, since the DBI model is a particular case of k-essence. Since for DBI inflation relation $s = \tilde{s}$ (7.6b) holds, it follows, from (D.49) and (D.50) that

$$n_s - 1 = -4\epsilon + 2\eta - 2s, \quad (7.14)$$

and

$$r = 16\epsilon c_s. \quad (7.15)$$

7.2 The Model

7.2.1 The General Setting

The usual approach to the construction of a model of inflation normally starts with a choice of the inflaton potential, $V(\phi)$; then, all the flow parameters are derived, and the dynamical analysis is performed. In this work we adopt the reverse procedure: we first look for the solutions to the differential equation satisfied by the Hubble

parameter $H(\phi)$,

$$\frac{H'(\phi)}{H(\phi)} = \pm \sqrt{\frac{\epsilon(\phi)\gamma(\phi)}{2M_P^2}}, \quad (7.16)$$

and only afterwards derive the form of the potential. Equation (7.16) can be easily derived from the definition of the flow parameter ϵ , given by (7.6a), and the sign ambiguity indicates in which direction the field is rolling. Notice that in order to solve equation (7.16) we must know the form of the functions $\epsilon(\phi)$ and $\gamma(\phi)$; we choose them to be power-law functions of the inflaton field (BESSADA et al., 2009),

$$\epsilon(\phi) = \left(\frac{\phi}{\phi_e}\right)^\alpha, \quad (7.17a)$$

$$\gamma(\phi) = \gamma_e \left(\frac{\phi}{\phi_e}\right)^\beta, \quad (7.17b)$$

where γ_e is the value of the Lorentz factor at the end of inflation¹, and α and β are constants. Another case which is worth studying appears when ϵ is *constant*, so that

$$\epsilon(\phi) = \epsilon = \text{const.}, \quad (7.18)$$

with the same parametrization for γ . We have kept ϕ_e for the following reason: in the *IR* DBI model the inflaton field rolls down from the tip of the throat toward the bulk of the manifold with increasing speed of sound; then, when the field enters the bulk c_s becomes equal to 1, and then inflation “ends”. In the *UV* case the behavior is the opposite, that is, the field evolves away from the bulk and reaches the tip when $c_s = 1$. To reproduce both cases we could have set $\gamma_e = 1$ from the onset, so that $c_s(\phi_e) = 1$, as required; also, $c_s(\phi) = 1$ in the canonical limit, that is, when $\beta = 0$. However, by taking γ_e arbitrary, we also reproduce the non-canonical models with constant speed of sound introduced by Spalinski (SPALINSKI, 2008). It is clear that in the latter case γ_e does not refer necessarily to the end of inflation, so that if we take $\gamma_e \gg 1$ it does not mean a superluminal propagation (as would be the case if $\beta \neq 0$). Bearing this distinction in mind we can use the same notation unambiguously.

When $\alpha \neq 0$, substituting (7.17a) and (7.17b) into (7.16), we see that the Hubble

¹Henceforth all the variables with a subscript e are evaluated at the end of inflation.

parameter takes the form

$$H(\phi) = H_e \exp \left[\sigma \sqrt{\frac{\gamma_e}{2M_P^2 \phi_e^{\alpha+\beta}}} I(\phi) \right], \quad (7.19)$$

where we have defined

$$I(\phi) \equiv \int_{\phi_e}^{\phi} d\phi' \phi'^{(\alpha+\beta)/2}, \quad (7.20)$$

and σ accounts for the sign ambiguity appearing in (7.16). When ϵ is constant, the solution to (7.16) reads

$$H(\phi) = H_e \exp \left[\sigma \sqrt{\frac{\epsilon \gamma_e}{2M_P^{\beta+2}}} I(\phi) \right], \quad (7.21)$$

where the integral $I(\phi)$ is the same as in (7.20).

It is clear that the integral (7.20) admits two distinct solutions: a logarithmic one when $\alpha + \beta = -2$, and power-law for $\alpha + \beta \neq -2$. These two solutions will give rise to different classes of inflationary potentials, which we shall address in the next subsections.

To conclude this section we derive the general formula for the number of e-folds. For $\alpha \neq 0$ this expression can be determined by equations (7.8), (7.17a), and (7.17b), so that

$$N(\phi) = \sigma \sqrt{\frac{\gamma_e \phi_e^{\alpha-\beta}}{2M_P^2}} J(\phi), \quad (7.22)$$

where

$$J(\phi) = \int_{\phi_e}^{\phi} d\phi' \phi'^{(\beta-\alpha)/2}; \quad (7.23)$$

if $\alpha = 0$ we must use the parametrization (7.18), so that expression (7.22) changes to

$$N(\phi) = \sigma \sqrt{\frac{\gamma_e}{2M_P^2 \epsilon \phi_e^\beta}} \tilde{J}(\phi), \quad (7.24)$$

where

$$\tilde{J}(\phi) = \int_{\phi_e}^{\phi} d\phi' \phi'^{\beta/2}. \quad (7.25)$$

In the next section, we discuss particular cases of this general class of solutions.

7.2.2 The Solutions $\alpha + \beta = -2$.

For this class of solutions, the parameters α and β are related by

$$\alpha = -2 - \beta; \quad (7.26)$$

notice that the case $\alpha = 0$ implies $\beta = -2$, which corresponds to the case where the flow parameters ϵ and s are constant (KINNEY; TZIRAKIS, 2008). Evaluating the integral (7.20) and substituting it into (7.19), we find

$$H(\phi) = H_e \left(\frac{\phi}{\phi_e} \right)^{p/2}, \quad (7.27)$$

where the exponent p is determined by

$$p = \sigma \phi_e \sqrt{\frac{2\gamma_e}{M_P^2}}. \quad (7.28)$$

Let us now analyze the sign ambiguity appearing in (7.28). We first write the expression (7.27) as

$$p = 2 \frac{\ln(H(\phi)/H_e)}{\ln(\phi/\phi_e)}; \quad (7.29)$$

then, for $\alpha < 0$, we have, from (7.17a), in the slow-roll limit,

$$\epsilon(\phi) = \left(\frac{\phi}{\phi_e} \right)^{-|\alpha|} \ll 1, \quad (7.30)$$

which implies $\phi \gg \phi_e$ and $\dot{\phi} < 0$ for $\phi > 0$ (the large-field limit, see subsection 4.4.1), so that $\ln(\phi/\phi_e) > 0$. Since the weak-energy condition implies that $\dot{H} < 0$, we have $H(\phi) \geq H_e$, and then $\ln(H(\phi)/H_e) > 0$. Therefore, from (7.29), $\alpha < 0$ implies $p > 0$. From definition (7.28) we see that $p > 0$ implies $\sigma = -1$ if $\phi < 0$, and $\sigma = +1$ if $\phi > 0$.

Conversely, if $\alpha > 0$, we have, from (7.17a), in the slow-roll limit,

$$\epsilon(\phi) = \left(\frac{\phi}{\phi_e} \right)^{+|\alpha|} \ll 1, \quad (7.31)$$

which implies $\phi \ll \phi_e$ and $\dot{\phi} > 0$ for $\phi > 0$ (the small-field limit, see subsection 4.4.2), so that $\ln(\phi/\phi_e) < 0$. Again, $\ln(H(\phi)/H_e) > 0$, so that, from (7.29), $\alpha > 0$

implies $p < 0$. From definition (7.28) we see that $p < 0$ implies $\sigma = -1$ if $\phi > 0$, and $\sigma = +1$ if $\phi < 0$.

Therefore, what really distinguishes the models is the sign of the exponent of α ; the sign of σ simply dictates which direction the field is rolling in, exactly as in canonical inflation. We are left with two distinct models, whose properties are summarized in Table 7.1. (For $\phi < 0$ the sign rule is easily obtained by flipping all the signs of the quantities present in Table 7.1.)

TABLE 7.1 - The sign rule for models with $\alpha + \beta = -2$ and $\phi > 0$ (BESSADA et al., 2009).

Model 1.	$p > 0, \alpha < 0$	$\sigma = +1$	$\phi > 0$	$\dot{\phi} < 0$
Model 2.	$p < 0, \alpha > 0$	$\sigma = +1$	$\phi > 0$	$\dot{\phi} < 0$

7.2.3 The Solutions $\alpha + \beta \neq -2$

Let us first consider the case $\alpha \neq 0$. The solution to the integral (7.20) is

$$H(\phi) = \tilde{H}_e \exp \left[\frac{\sigma K \phi_e}{\alpha + \beta + 2} \bar{\phi}^{(\alpha+\beta+2)/2} \right], \quad (7.32)$$

where we have defined

$$\tilde{H}_e = H_e \exp \left[-\frac{\sigma \sqrt{2\gamma_e} \phi_e}{M_P(\alpha + \beta + 2)} \right], \quad (7.33)$$

$$K = \sqrt{\frac{2\gamma_e}{M_P^2}}, \quad \bar{\phi} = \frac{\phi}{\phi_e}. \quad (7.34)$$

In order to fix the sign ambiguity let us rewrite expression (7.32) as

$$d \ln H = \frac{2\sigma K \phi_e}{\alpha + \beta + 2} d\bar{\phi}^{(\alpha+\beta+2)/2}, \quad (7.35)$$

then, as we have seen in (7.30), the condition $\alpha < 0$ corresponds to the large-field limit, $\phi \gg \phi_e$; so, if $\alpha + \beta + 2 < 0$ and $\phi > 0$, we have $d\bar{\phi}^{(\alpha+\beta+2)/2} > 0$, so that from

(7.35),

$$\underbrace{d \ln H}_{<0} = \frac{2\sigma K \phi_e}{\alpha + \beta + 2} \underbrace{d\bar{\phi}^{(\alpha+\beta+2)/2}}_{>0}$$

$$\implies -\frac{\sigma K |\phi_e|}{|\alpha + \beta + 2|} < 0, \quad (7.36)$$

implying that $\sigma = +1$. Applying the same analysis for $\alpha + \beta + 2 < 0$ and $\phi < 0$, we find $\sigma = -1$. For $\alpha + \beta + 2 > 0$ we find $\sigma = +1$ for $\phi > 0$, and $\sigma = -1$ for $\phi < 0$. The results in the large-field limit are summarized in Table 7.2. The same reasoning also applies for $\alpha > 0$, that is, the small-field limit, given by (7.31); the results are summarized in Table 7.3, where we have four distinct models: As in the previous

TABLE 7.2 - The sign rule for models with $\alpha + \beta \neq -2$, $\alpha < 0$, and $\phi > 0$ (BESSADA et al., 2009).

Model 3.	$\alpha + \beta + 2 > 0$	$\sigma = +1$	$\phi < 0$
Model 4.	$\alpha + \beta + 2 < 0$	$\sigma = +1$	$\phi < 0$

TABLE 7.3 - The sign rule for models with $\alpha + \beta \neq 0$, $\alpha > 0$ and $\phi > 0$ (BESSADA et al., 2009).

Model 5.	$\alpha + \beta + 2 > 0$	$\sigma = -1$	$\phi > 0$
Model 6.	$\alpha + \beta + 2 > 0$	$\sigma = +1$	$\phi < 0$
Model 7.	$\alpha + \beta + 2 < 0$	$\sigma = -1$	$\phi > 0$
Model 8.	$\alpha + \beta + 2 < 0$	$\sigma = +1$	$\phi < 0$

case, the model $\phi < 0$ is easily obtained by flipping all the signs of the quantities present in Tables 7.2 and 7.3.

In the case $\epsilon = const.$, $\beta \neq -2$, the solution to the integral (7.20) is given by

$$H(\phi) = \tilde{H}_e \exp \left[\sigma \sqrt{\frac{2\epsilon\gamma_e}{M_P^2 \phi_e^\beta}} \frac{\phi^{(\beta+2)/2}}{\beta + 2} \right], \quad (7.37)$$

where

$$\tilde{H}_e = H_e \exp \left[-\sigma \sqrt{\frac{2\epsilon\gamma_e}{M_P^2 \phi_e^\beta} \frac{\phi_e^{(\beta+2)/2}}{\alpha + \beta + 2}} \right]. \quad (7.38)$$

It is straightforward to see that the same sign rules shown in Tables 7.2 and 7.3 also apply to this case.

7.3 Classes of inflationary potentials in DBI inflation

In this section we proceed to analyze the solutions obtained in the last section. The key ingredient, in order to understand the physics associated with these classes of solutions, is the study of the form of the inflationary potential, which is obtained from the expressions (7.12), (7.17b), and the corresponding expression for the Hubble parameter, given by either (7.27) or (7.32). Once we have the form of such non-canonical potentials, we can compare these expressions with the usual canonical inflationary potentials discussed in Section 4.4. To do so, we must make some choices for the exponents α and β first, and then on the corresponding dynamics of the field; hence, as we have seen in the Tables 7.1, 7.2 and 7.3, we have eight distinct models altogether. Our main aim is to reproduce the classes of the inflationary potentials found in Section 4.4; then, in doing so, we leave out some interesting solutions, but our emphasis here is on understanding the physics of the non-canonical models, which can be achieved through a close comparison with the well-established potentials found in the literature.

7.3.1 Large-field polynomial potentials

A quick look at expressions (7.12) and (7.27) suggests that the model 1 in Table 7.1, characterized by $p > 0$ and $\alpha < 0$, is the non-canonical counterpart of large-field polynomial models, for its potential also goes like ϕ^p . To check this, let us first analyze the behavior of the speed of sound (7.17b). Since the equality (7.26) implies $\beta > -2$, we see from (7.17b) that $\beta > 0$ corresponds to

$$\gamma(\phi) = \gamma_e \left(\frac{\phi}{\phi_e} \right)^{|\beta|} \implies \gamma \rightarrow \infty \quad \text{as} \quad \phi \rightarrow \infty, \quad (7.39)$$

or, in terms of the speed of sound,

$$c_s \rightarrow 0 \quad \text{as} \quad \phi \rightarrow \infty; \quad (7.40)$$

since in the large-field limit the field strength is very large at early times, we conclude from (7.40) that the speed of sound starts off with a *subluminal* value. Also, from (7.39), we see that $\gamma/(\gamma + 1) \rightarrow 1$; then, using this fact and plugging (7.27) into (7.12), we find (BESSADA et al., 2009)

$$V(\phi) \sim 3M_P^2 H_e^2 \left(\frac{\phi}{\phi_e} \right)^p, \quad (7.41)$$

which behaves exactly as a canonical large-field potential, (4.52). The non-canonical potential (7.41) shows that the inflaton field starts evolving from a value $\phi \sim \mu$ with a very low speed of sound, and then rolls down toward its minimum at origin. Once there, the speed of sound becomes unity as well as the flow parameter ϵ and then inflation ends. The potential evaluated at μ corresponds to the vacuum energy density,

$$V(\mu) = \Lambda^4 \implies \Lambda^4 \sim 3M_P^2 H_e^2, \quad (7.42)$$

so that in terms of these two quantities, the Hubble parameter (7.27) and the inflationary potential (7.41) assume the form

$$H(\phi) = \frac{\Lambda^2}{\sqrt{3M_P^2}} \left(\frac{\phi}{\mu} \right)^{p/2} \quad (7.43)$$

$$V(\phi) = \Lambda^4 \left(\frac{\phi}{\mu} \right)^p, \quad (7.44)$$

respectively.

The end of inflation is achieved when $\phi = \phi_e$, whose value can be determined from (7.28) and the sign rule for the model 1 in Table 7.1:

$$\frac{\phi_e}{M_P} = \frac{p}{\sqrt{2\gamma_e}}; \quad (7.45)$$

then, in terms of the expression (7.45) the flow parameter ϵ takes the form

$$\epsilon(\phi) = \left[\frac{\sqrt{2\gamma_e}}{p} \right]^{-\beta-2} \left(\frac{\phi}{M_P} \right)^{-\beta-2}, \quad (7.46)$$

whereas the two other relevant flow parameters s and η are given by

$$s(\phi) = \frac{2\beta}{p} \epsilon(\phi), \quad (7.47)$$

$$\eta(\phi) = \frac{p-2}{p}\epsilon(\phi), \quad (7.48)$$

where we have used (7.6b), the first expression of (7.7), plus (7.17b), (7.43) and (7.45). The expression for the number of e-folds is obtained from expressions (7.22), (7.23) and (7.26) for $\alpha \neq 0$, so that

$$N(\phi) = \frac{p}{2(\beta+2)} \left[\frac{1}{\epsilon(\phi)} - 1 \right]. \quad (7.49)$$

In the analysis performed above we have considered solely models with $\alpha < 0$ and $\beta > 0$; the case $\alpha = 0$ has been studied in the paper (KINNEY; TZIRAKIS, 2008), and leads to potentials like (7.44) in the UV limit $s < 0$. The case $\beta = 0$, $\gamma_e = 1$, corresponds to canonical large-field models; in this limit, the expressions for the flow parameters ϵ and η , given by (7.46) and (7.48), yield

$$\epsilon(\phi) = \frac{p^2 M_P^2}{2 \phi^2}, \quad (7.50)$$

$$\eta(\phi) = \frac{p(p-2)}{2} \frac{M_P^2}{\phi^2}, \quad (7.51)$$

which coincides with the corresponding canonical expressions (4.53) and (4.54), respectively. Also in this limit, from (7.45) we see that inflation ends when

$$\frac{\phi_e^c}{M_P} = \frac{p}{\sqrt{2}}, \quad (7.52)$$

which coincides with the canonical expression found in (4.55). Hence, *all* large-field polynomial models with $p > 2$ are particular cases of this non-canonical version. Also, if $\gamma_e \neq 1$, we recover the Spalinski model (SPALINSKI, 2008) with a polynomial potential as well. Another particular case of this general class is *isokinetic inflation*, proposed in (TZIRAKIS; KINNEY, 2009). For this model, we can show that by setting $\alpha = -p/2 - 1$ and $\beta = p/2 - 1$, we reproduce all the expressions derived in (KINNEY; TZIRAKIS, 2008) up to a redefinition of the exponent of the potential².

Therefore, we have a completely well-defined D-brane inflationary scenario with large-field potentials like (7.44), a flow parameter ϵ given by (7.17a) with $\alpha < 0$,

²In isokinetic inflation the potential has the form $V(\phi) \propto \phi^{2p_{iso}}$ (TZIRAKIS; KINNEY, 2009), whereas in our model we have defined the exponent p (expression (7.28)) such that $V(\phi) \propto \phi^p$. Then $p = 2p_{iso}$.

and a small speed of sound characterized by (7.17b) with $\beta \geq 0$, reproducing not only the canonical large-field polynomial potentials, but also other models discussed in the literature. For these reasons we will call this class *non-canonical large-field polynomial models*.

In particular, as we will see in section 7.4, these models predict values for the scalar spectral index and tensor-to-scalar ratio which agree very well with WMAP5 observations.

7.3.2 Small-field polynomial potentials

For non-canonical models we can express the small-field limit $\phi \ll \mu$ by choosing $\alpha > 0$; also, as we have derived in section 7.2.3, the condition $\dot{\phi} > 0$ for $\phi > 0$ is satisfied when $\sigma = -1$ and $\alpha + \beta + 2 > 0$, which corresponds to the model 5 in Table 7.3. In this case, the Hubble parameter (7.32) takes the form

$$H(\phi) = \tilde{H}_e \exp \left[-\frac{K\phi_e}{\alpha + \beta + 2} \bar{\phi}^{(\alpha+\beta+2)/2} \right]; \quad (7.53)$$

where K and ϕ_e are given by (7.34); since $\bar{\phi} = \phi/\phi_e$ in the small-field limit, and $\alpha + \beta + 2 > 0$, we can expand expression (7.53) to first-order in $\bar{\phi}$, so that

$$H(\phi) = \tilde{H}_e \exp \left[1 - \frac{K\phi_e}{\alpha + \beta + 2} \bar{\phi}^{(\alpha+\beta+2)/2} \right]. \quad (7.54)$$

Since $\beta > -2 - \alpha$ and $\alpha > 0$, we see that β can take either sign; in particular, for $\beta > 0$, from (7.17b) we have the following relation

$$\gamma(\phi) = \gamma_e \left(\frac{\phi}{\phi_e} \right)^{-|\beta|} \implies \gamma \rightarrow \infty \quad \text{as} \quad \phi \rightarrow 0, \quad (7.55)$$

or, in terms of the speed of sound,

$$c_s \rightarrow 0 \quad \text{as} \quad \phi \rightarrow 0. \quad (7.56)$$

In the small-field limit, we have always $\phi \ll \phi_e$, so that $\phi \rightarrow 0$ corresponds to early times; then, from (7.56) we conclude that the field propagates with subluminal speed of sound at early times. Also, property (7.55) implies that $\gamma/(\gamma + 1) \rightarrow 1$, so that

by using this fact and plugging (7.54) into (7.12), we find

$$V(\phi) \sim 3M_P^2 \tilde{H}_e^2 \left[1 - \frac{2}{3} \bar{\phi}^\alpha - \frac{2K\phi_e}{\alpha + \beta + 2} \bar{\phi}^{(\alpha+\beta+2)/2} \right] \quad (7.57)$$

in the slow-roll limit. It is clear that we can derive out of expression (7.57) different sort of potentials, depending on the relations between the exponents. Let us analyze one of such possible choices; we define first the exponent

$$p = \frac{\alpha + \beta + 2}{2}, \quad (7.58)$$

and we choose α and β such that p is always *integer*. Then, if $\alpha \geq p$, we see that $\alpha \geq \beta + 2$, and the potential (7.57) takes the form

$$V(\phi) \sim 3M_P^2 \tilde{H}_e^2 \left[1 - \frac{K\phi_e}{p} \bar{\phi}^p \right], \quad \alpha \geq \beta + 2. \quad (7.59)$$

In the canonical small-field model, the energy scale of inflation is given by $\Lambda^4 = V(0)$, so that in the non-canonical case, the vacuum energy density is given by

$$\Lambda^4 = 3M_P^2 \tilde{H}_e^2, \quad (7.60)$$

whereas the effective symmetry-breaking scale (4.57) reads

$$\frac{1}{\mu^p} = \sqrt{\frac{2\gamma_e}{M_P^2 \phi_e^{\alpha+\beta}}}; \quad (7.61)$$

then, in terms of these two quantities, the inflationary potential (7.57) becomes, in the small-field limit, (BESSADA et al., 2009)

$$V(\phi) = \Lambda^4 \left[1 - \frac{1}{p} \left(\frac{\phi}{\mu} \right)^p \right], \quad (7.62)$$

which coincides with the canonical small-field potential (4.56), as expected.

Then, in the non-canonical case the field also rolls down from an unstable vacuum state whose energy density is given by (7.60) with very low speed of sound, and evolves toward a minimum characterized by a scale μ given by (7.61) for $\alpha \geq p \geq 2$, and such behavior is exactly the same as the canonical case.

From (7.61) we see that inflation ends when

$$\frac{\phi_e}{\mu} = \left[\frac{\mu}{M_P} \sqrt{2\gamma_e} \right]^{1/(p-1)}, \quad (7.63)$$

so that the flow parameters are given by

$$\epsilon(\phi) = \left[\frac{M_P}{\mu\sqrt{2\gamma_e}} \right]^{(p-1)/\alpha} \left(\frac{\phi}{\mu} \right)^\alpha, \quad (7.64)$$

$$s(\phi) = -\beta \sqrt{\frac{2M_P^2}{\gamma_e\phi_e^2}}, \quad (7.65)$$

$$\eta(\phi) = (\alpha + \beta) \sqrt{\frac{M_P^2}{2\gamma_e\phi_e^2}} \bar{\phi}^{(\alpha-\beta-2)/2} + \epsilon(\phi), \quad (7.66)$$

where we have used (7.6b), the first expression of (7.7), plus (7.17a), (7.17b), (7.53) and (7.63).

In particular, in the canonical limit $\beta = 0$, $\gamma_e = 1$ we have $\alpha \geq 2$, so that for *even* values of α all the potentials with $p \geq 2$ are reproduced. In this limit, from (7.58) we see that $\alpha = 2(p - 1)$; then, from (7.64) the flow parameter ϵ assumes the form

$$\epsilon(\phi) = \frac{M_P}{\mu\sqrt{2}} \left(\frac{\phi}{\mu} \right)^{2(p-1)}, \quad (7.67)$$

whereas from (7.63) we see that inflation ends at

$$\frac{\phi_e}{\mu} = \left[\frac{\mu}{M_P} \sqrt{2} \right]^{1/(p-1)}. \quad (7.68)$$

Expressions (7.67) and (7.68) agree with the corresponding canonical expressions (4.58) and (4.59), respectively.

Therefore, in the slow-roll limit *all* canonical small-field polynomial models with $p \geq 2$ are particular solutions to the non-canonical model described in this section when $\beta = 0$, $\gamma_e = 1$ and α even; hence, we have again a well-defined D-brane inflationary scenario with a small-field potential like (7.62), a flow parameter ϵ given by (7.17a) with $\alpha > 0$, and a small speed of sound characterized by (7.17b) with $\beta \leq 0$, reproducing all the canonical small-field polynomial potentials when $\beta = 0$. For these reasons we will call this class *non-canonical small-field polynomial models*.

7.3.3 Hybrid potentials

In the last two sections we have discussed the small-field models characterized by $\dot{\phi} > 0$ for positive ϕ , given by the model 5 in Table 7.3. Let us now examine a similar model, with $\alpha + \beta + 2 > 0$ but with $\dot{\phi} < 0$ for positive ϕ . In this case, $\sigma = +1$, (model 6 in Table 7.3); then, the Hubble parameter (7.32) takes the form

$$H(\phi) = \tilde{H}_e \exp \left[\frac{K\phi_e}{\alpha + \beta + 2} \bar{\phi}^{(\alpha+\beta+2)/2} \right], \quad (7.69)$$

where the constant K and variable $\bar{\phi}$ are given by the definitions (7.34). Since $\bar{\phi} \ll 0$ and $p > 0$, where p is given by (7.58), we expand expression (7.69) to first-order in $\bar{\phi}$,

$$H(\phi) = \tilde{H}_e \exp \left[1 + \frac{K\phi_e}{2p} \bar{\phi}^p \right]. \quad (7.70)$$

The analysis leading to the sign of β is identical to that made in section 7.3.2 since, as in that case, $\beta > -2 - \alpha$ and $\alpha > 0$; then, using the same arguments we find that the field rolls down the potential with a subluminal speed of sound. Also, since $\gamma/(\gamma + 1) \rightarrow 1$ at early times, we have, plugging (7.70) into (7.12), that

$$V(\phi) \sim 3M_P^2 \tilde{H}_e^2 \left[1 - \frac{2}{3} \bar{\phi}^\alpha + \frac{K\phi_e}{p} \bar{\phi}^p \right] \quad (7.71)$$

in the slow-roll limit. As in the model derived in section 7.3.2, we choose α and β such that p is always integer; then, for $\alpha > p$, the potential (7.71) takes the form

$$V(\phi) \sim 3M_P^2 \tilde{H}_e^2 \left[1 + \frac{K\phi_e}{p} \bar{\phi}^p \right]. \quad (7.72)$$

In this case, the minimum of the potential is at the origin, as in the small-field polynomial case, but now $V(\phi) > V(0)$ around $\phi = 0$. Therefore, the field rolls toward the minimum with nonzero vacuum energy, $\Lambda^4 = V(0)$. This is exactly the behavior of the canonical hybrid potentials (LINDE, 1991; LINDE, 1994). Then, we may write the potential (7.69) as (BESSADA et al., 2009)

$$V(\phi) \sim \Lambda^4 \left[1 + \left(\frac{\phi}{\mu} \right)^p \right], \quad (7.73)$$

where we have defined

$$\frac{1}{\mu^p} = \frac{1}{p} \sqrt{\frac{2\gamma_e}{M_P^2 \phi_e^{2(p-1)}}}, \quad (7.74)$$

which coincides with its canonical counterpart (4.62).

7.3.4 Exponential potentials

Since the general expression for the Hubble parameter derived in section 7.2.3 is of an exponential form, we focus on its large-field limit solution, given by the model 4 in Table 7.2. In this case $\dot{\phi} < 0$ for positive ϕ , so that $\sigma = +1$. The expression for the Hubble parameter (7.32) for $\alpha < 0$, is given by

$$H(\phi) = \tilde{H}_e \exp \left[\sqrt{\frac{1}{2p} \left(\frac{\phi}{M_P} \right)^{\alpha+\beta+2}} \right], \quad (7.75)$$

where we have defined

$$p = \frac{(\alpha + \beta + 2)^2}{4\gamma_e} \left(\frac{\phi_e}{M_P} \right)^{\alpha+\beta}. \quad (7.76)$$

Since $\alpha + \beta + 2 > 0$, the exponent of the speed of sound is restricted to the values $\beta > -\alpha - 2$; then, for $\beta > 0$, we have that $\gamma \rightarrow \infty$ as $\phi \rightarrow \infty$, and then $c_s \rightarrow 0$ at early times since ϕ is in the large-field limit. Hence, the field propagates with a subluminal speed of sound at early times, and $\gamma/(\gamma + 1) \rightarrow 1$. Using this fact and substituting (7.75) into (7.12) we find (BESSADA et al., 2009)

$$V(\phi) \sim 3M_P^2 \tilde{H}_e^2 \exp \left[\sqrt{\frac{2}{p} \left(\frac{\phi}{M_P} \right)^{\alpha+\beta+2}} \right]. \quad (7.77)$$

Then, the field rolls down the potential toward the minimum at origin, characterized by a nonzero vacuum energy $V(0) = \Lambda^4$ with a subluminal speed of sound. This is similar to the behavior of exponential potentials in canonical models, except for the fact that $c_s = 1$. Since $\Lambda^4 = 3M_P^2 \tilde{H}_e^2$, the final form of the non-canonical potential (7.77) is

$$V(\phi) \sim \Lambda^4 \exp \left[\sqrt{\frac{2}{p} \left(\frac{\phi}{M_P} \right)^{\alpha+\beta+2}} \right]. \quad (7.78)$$

Before we study the non-canonical limit of the potential (7.78), let us have a look first at the flow-parameter ϵ . We have used the parametrization associated with $\alpha \neq 0$, given by (7.17a), but we can make it general as follows: substituting and (7.17b) and (7.76) into (7.17a), we find

$$\epsilon(\phi) = \frac{(\alpha + \beta + 2)^2}{4p\gamma(\phi)} \left(\frac{\phi}{M_P} \right)^{\alpha+\beta}. \quad (7.79)$$

which holds even when $\alpha = 0$, for $\epsilon(\phi) = \epsilon = \text{const.}$ in that case. The other two flow parameters s and η are given respectively by

$$s(\phi) = \beta \left(\frac{\phi}{M_P} \right)^{-1} \sqrt{\frac{2\epsilon(\phi)}{\gamma(\phi)}}, \quad (7.80)$$

$$\eta(\phi) = \frac{\alpha + \beta}{\sqrt{2}} \left(\frac{\phi}{M_P} \right)^{-1} \sqrt{\frac{\epsilon(\phi)}{\gamma(\phi)}} + \epsilon(\phi), \quad (7.81)$$

where we have used (7.6b), the first expression of (7.7), plus (7.17b) and (7.75).

Then, with the parametrization defined by (7.79), we see that in the canonical case $\alpha = \beta = 0$, $\gamma_e = 1$, expressions (7.78), (7.79) and (7.81) give

$$V(\phi) = \Lambda^4 \exp \left[\sqrt{\frac{2}{p} \left(\frac{\phi}{M_P} \right)^2} \right]. \quad (7.82)$$

$$\epsilon(\phi) = \eta(\phi) = \frac{1}{p}, \quad (7.83)$$

which matches the results derived for the canonical case given by (4.63) and (4.64) respectively. Expression (7.83) shows that we have to restrict the values of (7.76) to be $p > 1$, so that we get $\epsilon \leq 1$ in the canonical limit.

Therefore, we have a completely well-defined D-brane inflationary scenario with exponential potentials like (7.78), a flow parameter ϵ given by (7.79) with $\alpha \leq 0$, and a small speed of sound characterized by (7.17b) with $\beta \geq 0$, which reproduces the corresponding canonical model. We will call this class *non-canonical exponential models*.

The four distinct non-canonical classes obtained so far are summarized in Table 7.4 below. See also Figures 4.2, 4.3, 4.4 in Chapter 4, since the non-canonical potentials

behave in the same way as in the canonical case.

TABLE 7.4 - A summary of the distinct models discussed in this work.

model	α	β	p	$V(\phi)$
Large-field	$\alpha = -\beta - 2$	$\beta \geq 0$	$\phi_e \sqrt{\frac{2\gamma_e}{M_P^2}}$	$\Lambda^4 \left(\frac{\phi}{\mu}\right)^p$
Small-field	$\alpha \geq p$	$\beta \leq 0$	$\frac{\alpha+\beta+2}{2}$	$\Lambda^4 \left[1 - \frac{1}{p} \left(\frac{\phi}{\mu}\right)^p\right]$
Hybrid	$\alpha \geq p$	$\beta \leq 0$	$\frac{\alpha+\beta+2}{2}$	$\Lambda^4 \left[1 + \left(\frac{\phi}{\mu}\right)^p\right]$
Exponential	$\alpha \leq 0$	$\beta \geq 0$	$\frac{(\alpha+\beta+2)^2}{4\gamma_e} \left(\frac{\phi_e}{M_P}\right)^{\alpha+\beta}$	$\Lambda^4 \exp \left[\sqrt{\frac{2}{p}} \left(\frac{\phi}{M_P}\right)^{\alpha+\beta+2} \right]$

7.4 An Application of Non-Canonical Large-Field Polynomial Models

In this section we study some applications of the large-field models derived in section 7.3.1. We choose this class of non-canonical potentials because the expressions for the scalar spectral index, the tensor/scalar ratio and the level of non-gaussianity are particularly simple, depending on two parameters solely, p and β . Let us first derive an expression for the flow parameter ϵ in terms of N . From (7.46) and (7.49) we find

$$\epsilon(N) = \frac{p}{p + 2(\beta + 2)N}. \quad (7.84)$$

The other two flow parameters s and η are given by

$$s(N) = \frac{2\beta}{p + 2(\beta + 2)N}, \quad (7.85)$$

$$\eta(N) = \frac{p - 2}{p + 2(\beta + 2)N}; \quad (7.86)$$

where we have used (7.6b), the first expression of (7.7), plus (7.17b), (7.43) and (7.84). Inserting (7.84), (7.85) and (7.86) into (7.14), we find, in the slow-roll limit,

$$n_s = 1 - \frac{2(p + 2\beta + 2)}{p + 2(\beta + 2)N}. \quad (7.87)$$

The expression for the speed of sound in terms of N can be calculated in the same way: we use (7.17a), (7.17b) and (7.49), so that

$$c_s(N) = \frac{1}{\gamma_e} \left[\frac{p}{p + 2(\beta + 2)N} \right]^{\beta/(\beta+2)}. \quad (7.88)$$

Next, using (7.15), (7.84) and (7.88) we can derive a general expression for the tensor/scalar ratio, which is given by

$$r(N) = \frac{16}{\gamma_e} \left[\frac{p}{p + 2(\beta + 2)N} \right]^{2(\beta+1)/(\beta+2)}. \quad (7.89)$$

The expression for the level of non-gaussianity f_{NL} is given by (PEIRIS et al., 2007)

$$f_{NL} = -\frac{35}{108} \left(\frac{1}{c_s^2} - 1 \right), \quad (7.90)$$

which can be easily evaluated by using expression (7.88).

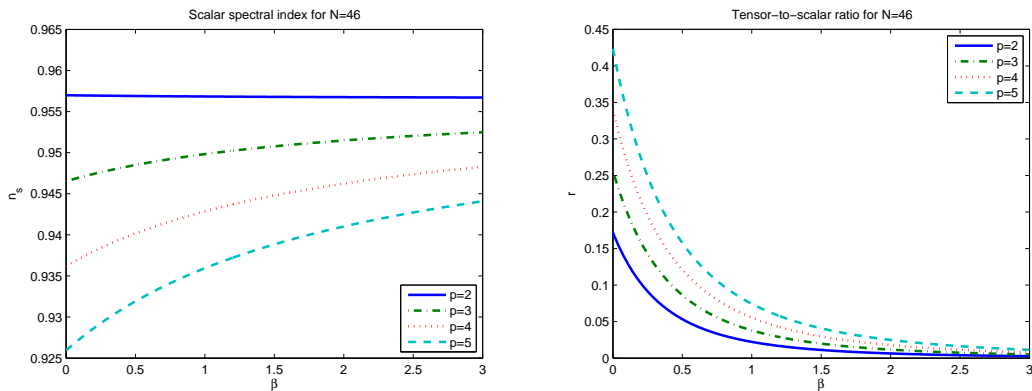


FIGURE 7.1 - The observables n_s (left), r (right) as a function of the exponent of the speed of sound β for each value of p ($V(\phi) \propto \phi^p$) for $N = 46$.

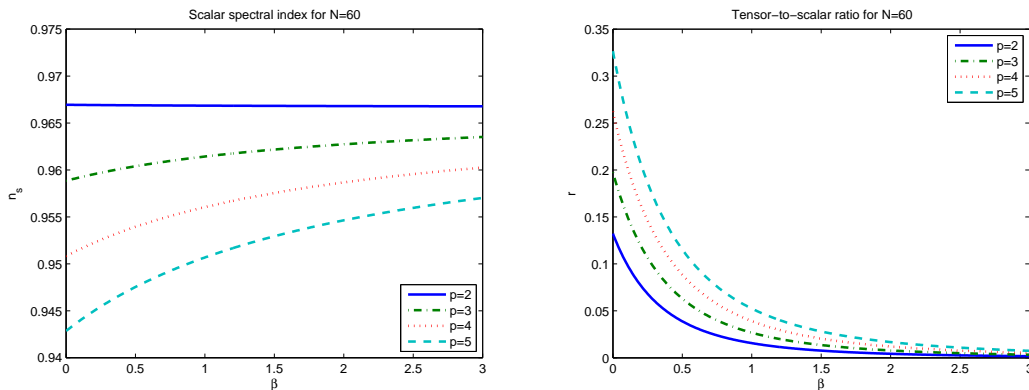


FIGURE 7.2 - The observables n_s (left), r (right) as a function of the exponent of the speed of sound β for each value of p ($V(\phi) \propto \phi^p$) for $N = 60$.

Therefore, the tensor/scalar ratio will have a power-law dependence as well, with exponent $2(\beta + 1)/(\beta + 2)$, which means that, for a given value of p , a larger β corresponds to a smaller r . Since $\beta \geq 0$ for non-canonical large-field models, we have, from (7.4) and (7.17b), that $c_s \propto \phi^{-\beta}$; then, fields rolling with *slower* speed of sound would produce *lower* tensor/scalar ratios. However, from (7.90), we see that f_{NL} depends on c_s^{-2} , and then a low speed of sound would produce a *larger* level of non-gaussianity; then, for large-field models low- r tensor modes are strongly correlated with the amplitude of non-gaussianity, as has been discussed in the reference (TZIRAKIS; KINNEY, 2009) for isokinetic inflation. Then, the suppression of tensor modes by a large amount of non-gaussianity is a feature shared by all non-canonical models with large-field polynomial potentials.

Let us next make some predictions on the values of n_s , r and f_{NL} through expressions (7.87), (7.89) and (7.90) respectively, when the modes cross the horizon 46 or 60 e-folds before the end of inflation. As we have discussed in section 7.2.1, we have set $\gamma_e = 1$, which characterizes the end of inflation; the results are depicted in figures 7.3 and 7.4. In both figures, the left plots refer to the variation of the scalar index in terms of β for each value of p . The right plots in Figs. 7.3 and 7.4 show the corresponding tensor/scalar ratio. In these plots we see that for larger values of p and small β the modes have large values of r (the observable lower bound is $r < 0.22$); then, as β increases, the speed of sound gets lower and, in consequence, the tensor/scalar ratio as well. For f_{NL} (7.90), a field rolling very slowly produces a large amount of non-gaussianity, as can be seen in the left plots of figures 7.3 and 7.4. Therefore, as was first discussed in the particular case of isokinetic inflation

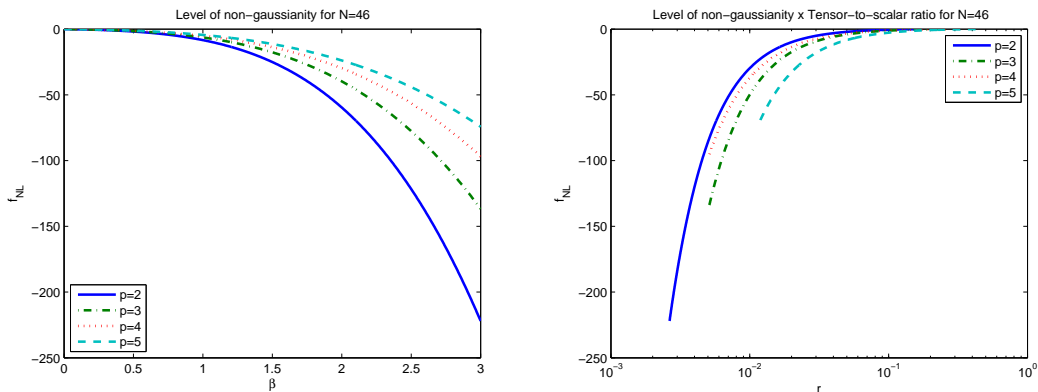


FIGURE 7.3 - The observable f_{NL} as a function of the exponent of the speed of sound β (left) for each value of p ($V(\phi) \propto \phi^p$) for $N = 46$. On right is depicted the behavior of f_{NL} compared to r .

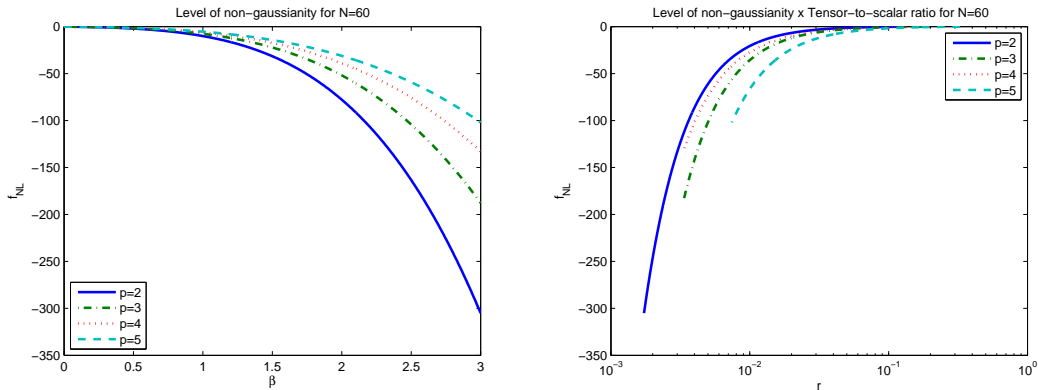


FIGURE 7.4 - The observable f_{NL} as a function of the exponent of the speed of sound β (left) for each value of p ($V(\phi) \propto \phi^p$) for $N = 60$. On right is depicted the behavior of f_{NL} compared to r .

(TZIRAKIS; KINNEY, 2009), the production of large non-gaussianity is strictly correlated with low tensor amplitudes, and this is a feature common to all large-field polynomial potentials. This behavior is shown in the bottom right plots of figures 7.3 and 7.4.

We next compare the results obtained with the current WMAP5 data (KOMATSU et al., 2009), (KINNEY et al., 2008). The results are depicted in Fig. 7.5 for different values of p . Straight lines indicate the different values of β , with the left (right) extremity indicating the value of (n_s, r) evaluated at $N = 46$ ($N = 60$). Green lines correspond to $\beta = 0$ (canonical limit), blue lines to $\beta = 1$, orange lines to $\beta = 2$

and light blue lines to $\beta = 3$. The left (right) extremity of each line correspond to the case where a mode crossed the sound horizon 46 (60) e-folds before the end of inflation.

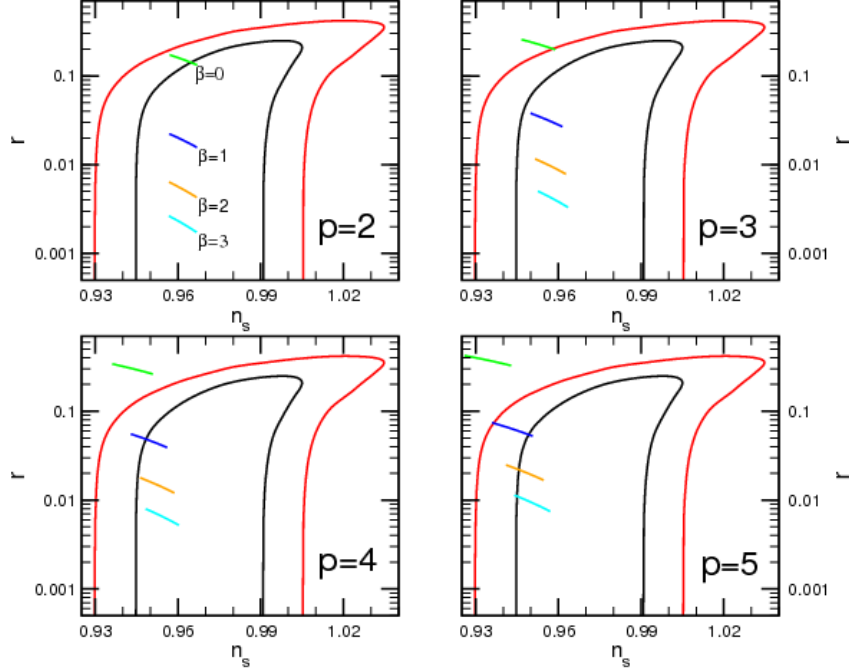


FIGURE 7.5 - 68 % (black) and 95 % C.L. (red) on the n_s and r parameter space for WMAP5 alone. In each panel we plot the values of n_s and r for a specific potential $V(\phi) \propto \phi^p$ according to the exponent β of the speed of sound.

As shown in (KINNEY et al., 2008), all canonical models with $p > 2$ are ruled out by WMAP5 data alone; however, in the non-canonical case, figure 7.5 shows that the models with $p \leq 5$ are also consistent with the observable data. A field evolving with slow-varying speed of sound produces low-amplitude tensors, then pushing the values (n_s, r) inwards the observable region. However, a large amount of non-gaussianity is produced, which is a distinct signature of non-canonical large-field polynomial models and can be a powerful observable to discriminate among inflationary models.

8 SIGNATURES OF TACHYACOUSTIC COSMOLOGY IN THE CMB

In this Chapter we introduce a new mechanism to solve the horizon problem and to generate a nearly scale-invariant spectrum for the fluctuations as an example of the Class 3 of alternative cosmologies in the Table 1.2. As in the former Chapter, here a prime denotes a derivative with respect to the field ϕ .

8.1 Tachyacoustic Cosmology

As we have discussed in Chapter 4, inflaton solves the flatness and horizon problems by means of a fluid with negative pressure, so that $\Omega = 1$ turns to a stable fixed point (that is, the universe evolves toward flatness), and the Hubble horizon shrinks as the universe expands, so that at very early times all the comoving scales were far inside the horizon. These results can be summarized by the expressions in (4.7). Furthermore, the solution to the horizon problem and the flatness problem are linked in inflation via a conservation law,

$$\frac{d}{d \ln a} \frac{|\Omega - 1|}{d_H^2} = 0. \quad (8.1)$$

Through this conservation law, a universe with shrinking comoving horizon size is identical to a universe which is evolving toward flatness, (4.7). Inflation therefore solves the horizon and flatness problems of the standard Big Bang with a *single* mechanism: accelerated expansion.

However, inflation is not the only way to accomplish this goal, as can be seen from the fact that the acceleration \ddot{a} appears nowhere in the conservation law (8.1). To solve both the horizon and flatness problems, it is sufficient to have a *shrinking* comoving Hubble radius. We then propose a method of solving the cosmological horizon problem and seeding scale-invariant primordial perturbations in a cosmology with *decelerating* expansion and a corresponding *growing* comoving Hubble horizon (BESSADA et al., 2009). The key to implementing such a model is the fact that curvature perturbations are not generated at the Hubble horizon, but at the *acoustic horizon* determined by the speed of sound of a scalar field,

$$D_H \simeq \frac{c_s}{aH}. \quad (8.2)$$

For canonical field theories, the two are identical, but for non-canonical field the-

ories, they are not. If one has a decaying, superluminal sound speed, curvature perturbations can be generated outside the Hubble horizon without inflation. We propose the term *tachyacoustic* for such cosmologies, which are closely related to varying speed of light theories. This idea has some history: such cosmologies were first proposed by Armendariz-Picon in the context of modified dispersion relations (ARMENDARIZ-PICON, 2006), and the generation of perturbations in such cosmologies was further considered by Piao (PIAO, 2007). The idea re-emerged in the context of varying speed of light theories by Magueijo (MAGUEIJO, 2008), and non-canonical Lagrangians by Magueijo (MAGUEIJO, 2009) and Piao (PIAO, 2009a).

In this work, we consider a way of generating scale-invariant superhorizon cosmological perturbations based on non-canonical scalar field Lagrangians with a speed of sound faster than the speed of light, $c_s > 1$. If the universe is dominated by a scalar field with speed of sound c_s , the relevant horizon for the generation of density perturbations is not the Hubble horizon d_H but the acoustic horizon, D_H , given by (8.2). Mode freezing at the acoustic horizon is well-known in non-canonical inflation models, for example k-Inflation (ARMENDARIZ-PICON *et al.*, 1999) and DBI inflation (SILVERSTEIN; TONG, 2004). In non-canonical inflation models, the Hubble horizon and the acoustic horizon are *both* shrinking in comoving units, resulting in the generation of density perturbations at the acoustic horizon and gravitational wave perturbations at the Hubble horizon (GARRIGA; MUKHANOV, 1999) (see also Section D.3). However, the comoving Hubble horizon need not be shrinking to generate curvature perturbations: all that is required is that the *acoustic* horizon be shrinking, $dD_H/d\ln a < 0$. In this case, if curvature perturbations are to be generated on scales larger than the Hubble horizon, it is necessary that the acoustic horizon be larger than the Hubble horizon, which requires a speed of sound greater than the speed of light. Such theories were studied recently by Babichev *et al.* (BABICHEV *et al.*, 2006; BABICHEV *et al.*, 2008), who showed that k-essence theories with $c_s > 1$ are causally self-consistent (see Appendix D.4), and can be mapped to bimetric theories with two “light cones”, one given by the Hubble horizon, and the other given by the acoustic horizon, which can be larger than the Hubble horizon without the presence of closed timelike loops. This opens the possibility that one can construct a decelerating cosmology which nonetheless generates perturbations on super-Hubble scales via a superluminal, shrinking acoustic cone.

To explicitly construct such a model, consider a DBI Lagrangian (7.2) as a phe-

nomenological *ansatz*. There is a class of exact solutions (CHIMENTO; LAZKOZ, 2008; KINNEY; TZIRAKIS, 2008) to the equation of motion for the field ϕ where the two flow parameters ϵ (7.9a) and s (7.9b) are *constant*, so that the scale factor evolves as a power-law, $a \propto t^{1/\epsilon}$; then, the expansion is accelerating (*i.e.* inflation) for $\epsilon < 1$. The speed of sound (7.3) evolves as

$$c_s \propto e^{-sN}, \quad (8.3)$$

and the Hubble parameter evolves as

$$H = \frac{\dot{a}}{a} \propto e^{\epsilon N}. \quad (8.4)$$

The parameter ϵ is a positive-definite quantity for $P_\phi \geq -\rho_\phi$, so that the Hubble constant always decreases with expansion. In contrast, the parameter s can take either sign, with $s > 0$ corresponding to a sound speed which increases with expansion, and $s < 0$ corresponding to an decreasing sound speed. (See Ref. (KINNEY; TZIRAKIS, 2008) for a detailed derivation of this solution). The important dynamics for the generation of perturbations is the time evolution of the corresponding horizons in comoving units. The comoving Hubble horizon evolves as

$$d_H \propto (aH)^{-1} \propto e^{(1-\epsilon)N} \propto \tau, \quad (8.5)$$

where τ is the conformal time. The Hubble horizon is shrinking in comoving units for $\epsilon < 1$, which is identical to accelerated expansion, and is the usual condition for inflation. The acoustic horizon behaves as

$$D_H \propto \frac{c_s}{aH} \propto e^{(1-\epsilon-s)N} \propto \tau^{(1-\epsilon-s)/(1-\epsilon)}. \quad (8.6)$$

Therefore the condition for a shrinking acoustic horizon, $1 - \epsilon - s > 0$, is *not* identical to accelerated expansion. For $\epsilon > 1$ and $s < 1 - \epsilon$, the expansion is non-inflationary, the Hubble horizon is growing in comoving units, and the acoustic horizon is shrinking. The initial singularity is at $\tau = 0$, and we see immediately that for the tachyacoustic solution, the speed of sound in the scalar field is *infinite* at the initial singularity, and the acoustic horizon is likewise infinite in size. Therefore, such a cosmology presents no ‘‘horizon problem’’ in the usual sense, since even a spatially infinite spacetime is causally connected on the initial-time boundary (BESSADA et al., 2009). Furthermore, unlike in the case of inflation, there is no period of reheating

necessary, since the cosmological evolution can be radiation-dominated throughout and the cosmic temperature is not driven exponentially to zero.

In the next section, we use the the generalized flow function approach of Bean, *et al.* (BEAN *et al.*, 2008b), introduced in Section D.2 to construct a class of Lagrangians with solutions of the type outlined above, with constant flow parameters.

8.2 Cosmological solutions for constant flow parameters

The simplest way to solve the flow equations (D.31) derived in Section D.2 is to take all of the flow parameters to be constant,

$$\frac{d\epsilon}{dN} = \frac{ds}{dN} = \frac{d\tilde{s}}{dN} = \frac{d^\ell\lambda}{dN} = \frac{d^\ell\alpha}{dN} = \frac{d^\ell\beta}{dN} = 0. \quad (8.7)$$

Then, from (D.28-D.30) we easily find the following relations (BESSADA *et al.*, 2009):

$$\begin{aligned} H &\propto e^{\epsilon N}, \\ c_s &\propto e^{-sN}, \\ \mathcal{L}_X &\propto e^{\tilde{s}N}, \end{aligned} \quad (8.8)$$

The first two are identical to the DBI case, equations (8.3) and (8.4), but in the fully general case \mathcal{L}_X evolves independently of c_s . It is straightforward to verify that the full flow hierarchy (D.32) reduces to an exactly solvable set of algebraic equations, with the higher-order parameters expressed in terms of ϵ , s , and \tilde{s} . We can use the relations (D.23,D.26,D.25) to solve for $H(\phi)$, $c_s(\phi)$, and $\mathcal{L}_X(\phi)$ as follows: from equations (D.23,D.25), we have

$$\tilde{s} = \frac{2M_P^2}{\mathcal{L}_X} \left(\frac{H'}{H} \right) \frac{\mathcal{L}'_X}{\mathcal{L}_X} = M_P \sqrt{2\epsilon} \frac{\mathcal{L}'_X}{\mathcal{L}_X} = \text{const.} \quad (8.9)$$

We then have a differential equation for \mathcal{L}_X ,

$$\frac{\mathcal{L}'_X}{\mathcal{L}_X^{3/2}} = \frac{\tilde{s}}{M_P \sqrt{2\epsilon}} = \text{const.}, \quad (8.10)$$

with solution

$$\mathcal{L}_X(\phi) = \frac{8\epsilon}{\tilde{s}^2} \left(\frac{M_P}{\phi} \right)^2, \quad (8.11)$$

where the integration constant has been absorbed into a field redefinition. From equation (8.8), the field then evolves as

$$\phi^2 \propto e^{-\tilde{s}N}, \quad (8.12)$$

so that the direction of the field evolution depends on the sign of \tilde{s} ,

$$\frac{d\phi}{\phi} = -\frac{\tilde{s}}{2}dN. \quad (8.13)$$

Equation (D.23) then reduces to

$$\left(\frac{H'}{H}\right)^2 = \frac{4\epsilon^2}{\tilde{s}^2\phi^2}, \quad (8.14)$$

with solution

$$H \propto \phi^{\pm 2\epsilon/\tilde{s}}. \quad (8.15)$$

The sign ambiguity can be resolved by requiring that the universe be expanding, $dH/dN > 0$, so that

$$H \propto \phi^{-2\epsilon/\tilde{s}} \propto e^{\epsilon N}. \quad (8.16)$$

Finally, we solve for the speed of sound using equation (D.26), which reduces to

$$\frac{c'_s}{c_s} = \frac{2s}{\tilde{s}} = \text{const.}, \quad (8.17)$$

with solution

$$c_s \propto \phi^{2s/\tilde{s}}. \quad (8.18)$$

Since our choice of $N = 0$ corresponds to an arbitrary renormalization of the scale factor $a \propto e^{-N}$, we can without loss of generality define $c_s = 1$ at $N = 0$, so that the general solution for the background evolution is given by

$$\mathcal{L}_X = \frac{8\epsilon}{\tilde{s}^2} \left(\frac{M_P}{\phi}\right)^2, \quad (8.19)$$

$$H(\phi) = H_0 \left(\frac{\phi}{\phi_0}\right)^{-2\epsilon/\tilde{s}}, \quad (8.20)$$

$$c_s(\phi) = \left(\frac{\phi}{\phi_0}\right)^{2s/\tilde{s}}, \quad (8.21)$$

where the field evolves as

$$\frac{\phi}{\phi_0} = e^{-\tilde{s}N/2}. \quad (8.22)$$

We can derive the time dependence of the scale factor using the Hamilton-Jacobi equation (D.20),

$$\dot{\phi} = \frac{\tilde{s}}{2} H(\phi) \phi = \sqrt{2X}, \quad (8.23)$$

so that the kinetic term can be written as

$$X(\phi) = \frac{\tilde{s}^2}{8} H^2(\phi) \phi^2. \quad (8.24)$$

Integrating expression (8.23) gives

$$H(t) = \frac{1}{\epsilon t}, \quad (8.25)$$

so that the scale factor evolves as a power-law in time, consistent with the fact that $\epsilon = \text{const.}$ and the equation of state $w = P_\phi/\rho_\phi$,

$$a(t) \propto t^{1/\epsilon} = t^{2/3(1+w)}. \quad (8.26)$$

Radiation-dominated evolution therefore corresponds to $\epsilon = 2$, and matter-dominated evolution corresponds to $\epsilon = 3/2$. Inflation corresponds to $\epsilon < 1$. The comoving Hubble horizon evolves proportional to the conformal time,

$$d_H \propto (aH)^{-1} \propto e^{(1-\epsilon)N} \propto \tau, \quad (8.27)$$

and the acoustic horizon evolves as

$$D_H \propto \frac{c_s}{aH} \propto e^{(1-\epsilon-s)N} \propto \tau^{(1-\epsilon-s)/(1-\epsilon)}, \quad (8.28)$$

identically to the DBI case discussed in Section 8.1, equation (8.6). For $\epsilon > 1$, the acoustic horizon is shrinking in comoving units for $s < 1 - \epsilon$. Note that this behavior is independent of the parameter \tilde{s} , which determines the form of the Lagrangian, as we discuss in the next section.

8.3 Reconstructing the Action

In the past two sections we have solved the flow hierarchy for a model characterized by constant flow parameters, which allowed us to solve for $H(\phi)$, $c_s(\phi)$, and $\mathcal{L}_X(\phi)$; only the derivative of the Lagrangian with respect to the kinetic term X is determined. Therefore this solution corresponds not to a single action but a class of actions. In this section we derive a general equation for Lagrangians in this class, and discuss two specific examples.

From equations (8.11) and (8.21), we see that the speed of sound c_s can be written in terms of \mathcal{L}_X

$$c_s^2 = C^{-1} \mathcal{L}_X^{-2s/\tilde{s}} = \left[1 + 2X \frac{\mathcal{L}_{XX}}{\mathcal{L}_X} \right]^{-1}, \quad (8.29)$$

where we have used equation (D.16), and defined

$$C \equiv \left(\frac{\tilde{s}^2 \phi_0^2}{8M_P^2 \epsilon} \right)^{2s/\tilde{s}}. \quad (8.30)$$

The result is a differential equation for the function $\mathcal{L}(X, \phi)$ (BESSADA et al., 2009):

$$2X \mathcal{L}_{XX} + \mathcal{L}_X - C \mathcal{L}_X^n = 0, \quad (8.31)$$

where we have defined

$$n \equiv 1 + \frac{2s}{\tilde{s}}. \quad (8.32)$$

Therefore, by specifying a relationship between the parameters s and \tilde{s} , we can construct a Lagrangian as the solution to the differential equation (8.31). For example, a canonical Lagrangian with speed of sound $c_s = \text{const.} = 1$ is just the case $s = 0$, so that $n = 1$ and $C = 1$, and equation (8.31) becomes

$$\mathcal{L}_{XX} = 0, \quad (8.33)$$

with general solution

$$\mathcal{L} = f(\phi) X - V(\phi). \quad (8.34)$$

Here $f(\phi)$ and $V(\phi)$ are free functions which arise from integration of the second-order equation (8.31). The function $f(\phi)$ can be eliminated by a field redefinition $d\varphi = \sqrt{f(\phi)} d\phi$, resulting in a manifestly canonical Lagrangian for φ , as we would expect from setting $c_s = 1$. We emphasize that equation (8.31) is constructed us-

ing the solution (8.21), and is not a general condition on the Lagrangian. That is, equation (8.31) allows us to construct a Lagrangian which admits solutions of the desired form, but those solutions are not necessarily unique. A canonical Lagrangian can support inflationary solutions, but not tachyacoustic solutions, and is therefore not of interest here. However, other choices of n do yield tachyacoustic solutions, and we focus on two such choices (BESSADA et al., 2009):

- a) $n = 0$: A Cuscuton-like model.
- b) $n = 3$: A DBI model.

We discuss each case separately below.

8.3.1 $n = 0$: A Cuscuton-like model

The case $n = 0$ corresponds to $\tilde{s} = -2s$ in (8.32), with solution

$$\mathcal{L}(X, \phi) = 2f(\phi)\sqrt{X} + CX - V(\phi). \quad (8.35)$$

This Lagrangian is similar to a ‘‘cuscuton’’ Lagrangian (AFSHORDI et al., 2007b), with the addition of a term proportional to X . Unlike the original Cuscuton model, which represents a causal field with infinite speed of sound, the solution obtained here is valid for the general case, in which the speed of sound can be finite. A similar cuscuton-like Lagrangian was considered in Ref. (PIAO, 2009a).

As in the canonical case, the functions $f(\phi)$ and $V(\phi)$ are free functions resulting from integrating equation (8.31). Unlike the canonical case, however, neither can be removed by a field redefinition. However, both functions are fully determined by our choice of solution with ϵ , s , and \tilde{s} constant. Differentiating equation (8.35) with respect to X gives

$$\mathcal{L}_X = \frac{f(\phi)}{\sqrt{X}} + C = \frac{2\epsilon}{s^2} \left(\frac{M_P}{\phi} \right)^2, \quad (8.36)$$

where the right hand side is the solution (8.19). Then

$$\begin{aligned} f(\phi) &= \sqrt{X} \left(\frac{2\epsilon}{s^2} \right) \left(\frac{M_P}{\phi_0} \right)^2 \left[\left(\frac{\phi_0}{\phi} \right)^2 - 1 \right] \\ &= \sqrt{X} \left(\frac{2\epsilon}{s^2} \right) \left(\frac{M_P}{\phi_0} \right)^2 [c_s^2(\phi) - 1] \end{aligned} \quad (8.37)$$

where for $2\tilde{s} = -s$, the expression (8.21) for the speed of sound becomes

$$c_s(\phi) = \left(\frac{\phi_0}{\phi}\right). \quad (8.38)$$

The Lagrangian (8.35) can then be written as

$$\mathcal{L} = X \left(\frac{2\epsilon}{s^2}\right) \left(\frac{M_P}{\phi_0}\right)^2 [2c_s^2(\phi) - 1] - V(\phi). \quad (8.39)$$

The Hubble parameter (8.20) is given by

$$H(\phi) = H_0 \left(\frac{\phi}{\phi_0}\right)^{\epsilon/s}, \quad (8.40)$$

and we can then express the kinetic term as a function of ϕ using equation (8.24):

$$X(\phi) = \frac{s^2}{2} H^2 \phi^2 = \frac{s^2 \phi_0^2 H^2(\phi)}{2 c_s^2(\phi)}, \quad (8.41)$$

The Lagrangian (8.35) can then be written entirely as a function of the field ϕ ,

$$\mathcal{L} = M_P^2 \epsilon H^2(\phi) \left[2 - \frac{1}{c_s^2(\phi)}\right] - V(\phi). \quad (8.42)$$

The Hamilton-Jacobi Equation (D.20) becomes:

$$\begin{aligned} 3M_P^2 H^2 &= 2M_P^2 \epsilon H^2 - \mathcal{L} \\ &= V(\phi) + \frac{M_P^2 \epsilon H^2}{c_s^2}, \end{aligned} \quad (8.43)$$

and we have an expression for the potential $V(\phi)$,

$$V(\phi) = M_P^2 H^2(\phi) \left[3 - \frac{\epsilon}{c_s^2(\phi)}\right]. \quad (8.44)$$

The Hubble parameter $H(\phi)$ and the speed of sound $c_s(\phi)$ are given by equations (8.40) and (8.38), respectively. For $\phi/\phi_0 \ll 1$, the speed of sound is much greater than the speed of light, $c_s \gg 1$, and the potential is approximately

$$V(\phi) \simeq 3M_P^2 H^2(\phi) = 3M_P^2 H_0^2 \left(\frac{\phi}{\phi_0}\right)^{2\epsilon/s}, \quad (8.45)$$

which can be recognized as a slow-roll-like solution dominated by the potential $H^2 \simeq V^2/3M_P^2$. For $s < 0$, the field is rolling away from the origin, and for $s < 1 - \epsilon$ the comoving acoustic horizon is shrinking and the solution is tachyacoustic.

8.3.2 $n = 3$: The DBI model

The case $n = 3$, corresponds to $\tilde{s} = s$; then, from (D.26) and (D.25), we find $\mathcal{L}_X = c_s^{-1}$. Equation (8.32) is then

$$c_s^2 = \frac{1}{C\mathcal{L}_X^2}, \quad (8.46)$$

so that we can take $C = 1$ without loss of generality. Therefore, the Lagrangian assumes the well-known DBI form,

$$\mathcal{L}(X, \phi) = -f^{-1}(\phi) \sqrt{1 - f(\phi)X} + f^{-1}(\phi) - V(\phi). \quad (8.47)$$

The DBI model with constant flow parameters is extensively discussed in Ref. (KINNEY; TZIRAKIS, 2008), and the reader is referred to this paper for further details. For ϵ and s constant, the functions V and f are fully determined and are given by

$$\begin{aligned} V(\phi) &= 3M_P^2 H^2(\phi) \left[1 - \left(\frac{2\epsilon}{3} \right) \frac{1}{1 + c_s(\phi)} \right], \\ f(\phi) &= \left(\frac{1}{2M_P^2 \epsilon} \right) \frac{1 - c_s^2(\phi)}{H^2(\phi) c_s(\phi)}. \end{aligned} \quad (8.48)$$

The Hubble parameter and speed of sound are given by:

$$H(\phi) = H_0 \left(\frac{\phi}{\phi_0} \right)^{-2\epsilon/s}, \quad (8.49)$$

and

$$c_s(\phi) = \left(\frac{\phi}{\phi_0} \right)^2. \quad (8.50)$$

DBI Lagrangians allow for either inflationary or tachyacoustic evolution (MAGUEIJO, 2009), depending on the values of ϵ and s . Note that for $c_s > 1$, the function f is negative, which has consequences for embedding such a model in string theory.

In this section, we have explicitly constructed Lagrangians, including fully determined potentials, for which the flow parameters are constant and the background

evolution can be solved exactly. For suitable choices of the flow parameters, the evolution is tachyacoustic, *i.e.* with a growing comoving Hubble horizon and a shrinking comoving acoustic horizon. In the next section, we discuss the generation of curvature perturbations at the acoustic horizon and show that such perturbations are nearly scale-invariant, consistent with observation.

8.4 Cosmological Perturbations for constant flow parameters

In the case where the flow parameters are constant, we can use the differential equations (D.31) to reduce the number of independent parameters. We have

$$\begin{aligned}\tilde{\eta} &= \frac{1}{2}(2\epsilon + \tilde{s}), & {}^2\lambda &= \frac{1}{2}(2\epsilon + \tilde{s})(\epsilon + \tilde{s}), \\ {}^1\alpha &= \frac{s}{2\epsilon}(2s + \tilde{s}), & {}^1\beta &= \frac{3\tilde{s}^2}{2\epsilon};\end{aligned}\tag{8.51}$$

then, substituting these values into expressions (D.43) and (D.47), we find, respectively,

$$\bar{F} = 2 - \epsilon - 3s + \frac{9}{4}\tilde{s}^2 - \frac{3}{4}s\tilde{s} + \epsilon s - \frac{1}{2}s^2,\tag{8.52}$$

$$\bar{G} = s(-1 + \epsilon + s).\tag{8.53}$$

It is important to notice that \bar{F} is different from the corresponding expression found in the DBI case (KINNEY; TZIRAKIS, 2008), since the gauge-dependent \tilde{s} comes into play. However, \bar{G} is identical to its DBI analog, and it is expected since basically it comes from the change of variables $\tau \rightarrow y$, which depends solely on the parameters c_s and H , and not on \mathcal{L}_X . For constant flow parameters we can solve equation (D.47) exactly, and the solutions are given by

$$\begin{aligned}u_k(y) &= y^{\frac{1-\epsilon}{2(1-\epsilon-s)}} \left[c_1 H_\nu^{(1)} \left(\frac{y}{1-\epsilon-s} \right) \right. \\ &\quad \left. + c_2 H_\nu^{(2)} \left(\frac{y}{1-\epsilon-s} \right) \right],\end{aligned}\tag{8.54}$$

where c_1 and c_2 are constants, and $H_\nu^{(1)}$, $H_\nu^{(2)}$ are Hankel functions of first and second kind, respectively. The order ν of the Hankel function is given by

$$\nu^2 = \frac{9 - 6\epsilon - 12s + 9\tilde{s}^2 - 3s\tilde{s} + 4\epsilon s - 2s^2 + \epsilon^2}{4(1 - \epsilon - s)^2}; \quad (8.55)$$

next, using (4.101), (8.8) and (D.45) we find that

$$c_s \propto y^{s/(\epsilon+s-1)}; \quad (8.56)$$

then, imposing the Bunch-Davies vacuum $c_2 = 0$, and normalizing the mode amplitudes by means of the canonical quantization condition

$$u_k^* \frac{du_k}{dy} - u_k \frac{du_k^*}{dy} = \frac{i}{c_s k (1 - \epsilon - s)}, \quad (8.57)$$

we find

$$u_k(y) = \frac{1}{2} \sqrt{\frac{\pi}{c_s k}} \sqrt{\frac{y}{1 - \epsilon - s}} H_\nu \left(\frac{y}{1 - \epsilon - s} \right), \quad (8.58)$$

which differs from the DBI case only in the order of the Hankel function (8.55). In the small wavelength limit $y \rightarrow \infty$ the early-time behavior of u_k will be identical to DBI (KINNEY; TZIRAKIS, 2008) for constant flow parameters

$$u_k = \frac{1}{\sqrt{2c_s k}} e^{iy/(1-\epsilon-s)}, \quad (8.59)$$

whereas in the late-time behavior $y \rightarrow 0$ the mode function behaves as

$$|u_k(y)| \rightarrow 2^{\nu-3/2} \frac{\Gamma(\nu)}{\Gamma(3/2)} (1 - \epsilon - s)^{\nu-1/2} \frac{y^{1/2-\nu}}{\sqrt{2c_s k}}. \quad (8.60)$$

From (8.60) we can derive the expression for the scalar spectral index n_s . Using the definition of the power spectrum of curvature perturbations (D.48), and substituting expressions (8.60) and (D.41) into (D.48), we find

$$P_{\mathcal{R}} = \frac{|f(\nu)|^2 H^2}{8\pi^2 M_P^2 c_s \epsilon} \quad (8.61)$$

at horizon crossing, where $f(\nu)$ is a constant given by

$$f(\nu) = 2^{\nu-3/2} \frac{\Gamma(\nu)}{\Gamma(3/2)} (1 - \epsilon - s)^{\nu-1/2}; \quad (8.62)$$

then, from the definition of the scalar spectral index (4.135) and using

$$\frac{d}{d \ln k} = - \left(\frac{1}{1 - \epsilon - s} \right) \frac{d}{dN}, \quad (8.63)$$

we see that the spectral index n_s assumes the form (BESSADA et al., 2009)

$$n_s = 1 - \frac{2\epsilon + s}{1 - \epsilon - s}, \quad (8.64)$$

which does not depend on the gauge-dependent parameter \tilde{s} , and is identical to its DBI analog. This is expected since the power spectrum evaluated at the horizon crossing, equation (8.61), depends solely on H and c_s , whose derivatives with respect to N are related to the gauge-invariant flow parameters ϵ and s . The scale-invariant limit is $s = -2\epsilon$.

For radiation-dominated tachyacoustic expansion with $\epsilon = 2$, the spectral index is

$$n = 1 + \frac{4 + s}{1 + s}, \quad (8.65)$$

where we have $s < -3$ for a shrinking comoving acoustic cone. For $s < -4$, the spectral index is blue, $n > 1$, which is ruled out by observation. The WMAP 2σ limit $n = 0.96 \pm 0.026$ (KOMATSU et al., 2009) corresponds to $s = [-3.814, -3.959]$, so that our model also allows for a scalar spectral index in agreement with observations. Since the Hubble horizon is growing in comoving units, no gravitational wave modes are produced. However, it is important to stress that tachyacoustic cosmology is very recent proposal, and some developments are still underway (BESSADA et al., 2010).

We have demonstrated that accelerated expansion or a collapsing universe are not the only ways to dynamically generate a scale-invariant spectrum of superhorizon curvature perturbations. There is a third way: a superluminal acoustic cone which is shrinking in comoving coordinates. Curvature perturbations generated at the acoustic horizon are familiar from inflationary scenarios based on non-canonical Lagrangians such as k -inflation, as discussed in Appendix D, and DBI inflation, Chapter 7. Such non-canonical Lagrangians arise naturally in string theory. However, in these scenarios, *both* the Hubble horizon and the acoustic horizon are shrinking in comoving units, and the acoustic horizon is typically smaller than the Hubble horizon, *i.e.* $c_s < 1$. It is natural to ask whether tachyacoustic models have a similar, natural stringy embedding, especially since the DBI action (7.2) naturally admits tachy-

acoustic solutions. Such an embedding is nontrivial, however, since the frequently considered case of a 3+1 dimension d-brane evolving in a higher-dimensional throat is ill-defined in the $c_s > 1$ limit. To see this, consider the full ten-dimensional metric of throat plus brane (7.1); the Lagrangian for the field ϕ can be shown to be of the DBI form (7.2), where the inverse brane tension $f(\phi)$ is given in terms of the warp factor $h(\phi)$ by $f^{-1}(\phi) = T_3 h(\phi)^4$. The problem is immediately evident: superluminal propagation $c_s > 1$ requires $f < 0$, so that the factor $h^2(\phi)$ appearing in the metric (7.1) is imaginary, and the metric is ill-defined. Therefore, although the DBI action itself admits tachyacoustic solutions, this limit does not correspond to a well-defined string solution. It is not clear whether or not string manifolds exist which self-consistently admit solutions with $c_s > 1$.

8.5 Boundary Action

Despite the tachyacoustic model solves the horizon problem and generates a nearly-invariant perturbation spectrum, and does not require a reheating phase, it does not solve the flatness problem, and inflation solves both at once. However, inflation has initial conditions problems of its own, in particular the fact that the initial inflationary “patch” must be larger than a horizon size for inflation to start (VACHASPATI; TRODDEN, 1999). Furthermore it has been shown that inflationary spacetimes are in general geodesically past-incomplete (BORDE et al., 2003). The initial conditions for tachyacoustic cosmology are quite different than those for inflation due to the presence of a true “Big Bang” singularity at zero time. However, in this limit, the sound speed is *infinite* and the tachyacoustic solution approaches an instanton. To see this, examine the form of the DBI field Lagrangian (7.2) near the $\tau = 0$ boundary of a tachyacoustic spacetime. From equation (8.3), the $c_s \rightarrow \infty$ limit corresponds to $\phi \rightarrow \infty$ and $f(\phi) \dot{\phi}^2 \rightarrow -\infty$, so that

$$\mathcal{L} \rightarrow \frac{\dot{\phi}}{\sqrt{|f|}} - V(\phi). \quad (8.66)$$

From equation (8.48), the asymptotic behavior of $V(\phi)$ and $f(\phi)$ are

$$\begin{aligned} V(\phi) &\rightarrow 3M_P^2 H^2 \propto \phi^{-4\epsilon/s}, \\ f(\phi) &\rightarrow -\frac{1}{2M_P^2 \epsilon H} \frac{c_s}{H} \propto \phi^{2(1+2\epsilon/s)}. \end{aligned} \quad (8.67)$$

The scale-invariant limit $s = -2\epsilon$ is especially interesting, since

$$\frac{1}{\sqrt{|f|}} \rightarrow \mu^2 = \text{const.}, \quad (8.68)$$

and the Lagrangian takes the form

$$\mathcal{L} \rightarrow \mu^2 \dot{\phi} - V(\phi), \quad (8.69)$$

where $V(\phi) \propto \phi^2$. This can be identified as exactly the ‘‘cuscuton’’ Lagrangian, suggested by Afshordi, *et al.* as a candidate for Dark Energy (MUKHANOV; VIKMAN, 2006; AFSHORDI *et al.*, 2007b; AFSHORDI *et al.*, 2007a). Similarly, the $n = 0$ solution considered in Section 8.3 approaches a cuscuton on the initial boundary surface. The cuscuton is a non-dynamical, instanton-like solution with infinite speed of sound. Consider the action for the Lagrangian (8.69),

$$\begin{aligned} S_\phi &= \int d^4x \sqrt{-g} [\mu^2 \dot{\phi} - V(\phi)] \\ &= \mu^2 \int d\phi \Sigma(\phi) - \int d^4x \sqrt{-g} V(\phi), \end{aligned} \quad (8.70)$$

where $\Sigma(\phi)$ is the volume of a constant- ϕ hypersurface in the spacetime. The classical solutions to the cuscuton action are constant mean curvature hypersurfaces, analogous to soap bubbles (AFSHORDI *et al.*, 2007b). It is interesting to speculate that this property of the cuscuton action may provide a self-consistent cosmological boundary condition, or (even more speculatively) be useful as a solution to the cosmological flatness problem. A full analysis, however, would require inclusion of the gravitational action and solution in a Wheeler-De Witt framework, or perhaps an embedding of the model in string theory or an alternate gravity theory such as Horava-Lifshitz (PIAO, 2009b; AFSHORDI, 2009). This is the subject of future work.

9 CONCLUSIONS AND PERSPECTIVES

In this PhD thesis we have studied four alternative cosmologies, namely, the MFP model, Massive Gravity, DBI inflation and the Tachyacoustic model, and investigated their signatures in CMB. MFP model and Massive Gravity were studied as alternatives to the current FRW model, whereas DBI was chosen as an alternative inflationary scenario (keeping FRW model to drive the dynamics of the universe at late times). Tachyacoustic cosmology has been proposed as a non-inflationary scenario, aiming at solving the same problems addressed by canonical inflation, but through a decelerating phase.

We showed that the MFP model and Massive Gravity lead to the same equations for tensor perturbations, and they give rise to the usual tensor SW effect, despite the tensor amplitudes change due to the massive character of the metric fluctuations. We also derived the corresponding Boltzmann equations, whose form is identical to their general-relativistic analogs. We deduced the dynamical equations for the GW vector longitudinal polarization modes (Ψ_3 -modes) in the MFP model and showed that they do not give the same results of Massive Gravity, in which vector perturbations behave as in GR; instead, they give rise, in a cosmological scenario, to a nontrivial SW effect which leaves a vector signature of quadrupolar form $Y_{2,\pm 1}(\mu, \varphi)$ on the CMB polarization.

Analyzing the Einstein equations for such Ψ_3 -modes we concluded that these vector signatures could be present at the recombination epoch, unlike the vector perturbations in GR and Massive Gravity, which would decay too fast and would not leave any signature on CMB polarization. Therefore, we calculated the new basis for the Thomson scattering for such Ψ_3 -modes, and then deduced the appropriate equation for the radiative transport. Based upon these results we have shown qualitatively that Ψ_3 -mode vector signatures could clearly be distinguished on the CMB polarization from the usual Ψ_4 tensor modes if the former do exist; hence, we could look for such signatures in the E-mode performed by Planck satellite in the near future. In this sense we argued that Planck polarization measurements could be decisive to test alternative theories of gravitation.

As for tensor modes, we evaluated numerically the TT power spectrum induced by them, and showed that there is a graviton mass limit, $m_l \sim 10^{-29} cm^{-1}$, such that gravitons with masses $m \leq m_l$ behave indistinguishably from massless gravitons.

The same happens to gravitons with short wavelengths (wavenumbers $n \geq 100$ in our example): their behavior is almost the same as of the massless gravitons for all the masses taken into account here.

We also showed that long wavelength massive tensor modes fall into the horizon earlier than their massless counterparts, whereas short wavelength modes behaves quite similarly as in GR. The net effect of this behavior, as we have shown in the TT correlation function plotted in figures 6.8 and 6.9, is a distinguished signature on low multipoles; the heavier the mass of the mode, the stronger is its signature as compared to that of massless gravitons. For the range of masses considered here, $m = 10^{-27}cm^{-1}$ - $m = 10^{-25}cm^{-1}$, the signatures show up at $\ell < 30$; however, we have argued that such signatures might appear at $\ell > 30$ in the case of masses greater than $m = 10^{-25}cm^{-1}$. Therefore, our results indicate that the future precise measurements of the CMB anisotropies induced by tensor modes might be decisive for probing the existence of massive gravitons, for the signature left by them could be strong enough to be distinguished from those of the massless modes.

We also proposed a general DBI model characterized by a power-law flow parameter $\epsilon(\phi) \propto \phi^\alpha$ and speed of sound $c_s(\phi) \propto \phi^\beta$, where α and β are constants. We showed that this general model has distinct classes of solutions depending on the relation between α and β , and on the time evolution of the inflaton field. These classes of solutions are summarized in tables 7.1, 7.2 and 7.3. In particular, we showed that in the slow-roll limit the four well-known canonical potentials arise naturally in this general DBI model, having similar properties to their canonical counterparts, except that the speed of sound in general varies with time. We also showed that this general DBI model encompasses not only all the canonical models with the mentioned potentials, but other D-brane scenarios as well: the DBI model with constant speed of sound (SPALINSKI, 2008), with constant flow parameters (KINNEY; TZIRAKIS, 2008), and isokinetic inflation (TZIRAKIS; KINNEY, 2009). The four non-canonical models are summarized in table 7.4.

We also derived the expressions for the spectral index, tensor/scalar ratio and the amplitude of non-gaussianity for large-field potentials in the slow-roll limit. We showed that a low speed of sound suppresses the tensor/scalar ratio r and produces a large amount of non-gaussianity, a feature already explored in the case of isokinetic inflation, and shown to be a general property of all large-field DBI models with polynomial potentials. Unlike canonical inflation, where all polynomial models with

$p > 2$ are ruled out, the suppression of tensor modes in the non-canonical version allows for a larger class of polynomial potentials to lie within the observable range; also, the production of large amount of non-gaussianity is a distinct signature of these DBI large-field models, which can be a powerful observable to discriminate among inflationary models.

We proposed also a non-inflationary model based on a k-essence Lagrangian with superluminal speed of sound, called tachyacoustic cosmology. We calculated the scalar spectral index of perturbations for tachyacoustic solutions, and found that if the flow parameter s is within the range $[-3.814, -3.959]$ the result is compatible with WMAP5 data. Unlike inflationary models, radiation-dominated tachyacoustic models do not require a period of explosive entropy production to transition to a “hot” Big Bang cosmology. The early universe must be scalar-field dominated, but the temperature of the universe is not driven exponentially to zero, since the scalar has a radiation equation of state at all times, and entropy density is conserved (for any radiation component with density ρ_γ , the ratio $\rho_\phi/\rho_\gamma = \text{const}$). The scalar field ϕ must eventually decay to Standard Model degrees of freedom, but as long as this happens before primordial nucleosynthesis, the model will match observations. A slow or late decay of ϕ into other degrees of freedom would also suppress the production of unwanted relics such as monopoles or gravitinos.

Then, the tachyacoustic model solves the horizon problem and provides a nearly scale-invariant spectrum of primordial perturbations; however, it does not solve the flatness problem, which inflation does. Nevertheless, it is important to stress that tachyacoustic cosmology is a very recent proposal, still a *terra incognita* in many aspects, and a great deal of work must be performed in order to explore all its consequences. We hope to tackle some of these issues in a work which is being prepared (BESSADA et al., 2010).

We have seen that CMB measurements is quite a fundamental tool to probe the distinct alternative cosmological models, and we are convinced from the studies performed here that Planck data and the next-generation satellites will become decisive to unravel the deepest secrets of the gravitational interaction.

APPENDIX A - BASIC DEFINITIONS OF GR

A.1 Some key tensors in GR

a) **Covariant derivatives for an arbitrary tensor $T_{\kappa\lambda\dots}^{\alpha\beta\dots}$:**

$$\begin{aligned} \nabla_{\rho} T_{\kappa\lambda\dots}^{\alpha\beta\dots} &= \partial_{\rho} T_{\kappa\lambda\dots}^{\alpha\beta\dots} + \Gamma_{\rho\sigma}^{\alpha} T_{\kappa\lambda\dots}^{\sigma\beta\dots} + \Gamma_{\rho\sigma}^{\beta} T_{\kappa\lambda\dots}^{\alpha\sigma\dots} + \dots \\ &- \Gamma_{\rho\kappa}^{\sigma} T_{\sigma\lambda\dots}^{\alpha\beta\dots} - \Gamma_{\rho\lambda}^{\sigma} T_{\kappa\sigma\dots}^{\alpha\beta\dots} - \dots \end{aligned} \quad (\text{A.1})$$

b) **Christoffel symbols of first kind:**

$$\Gamma_{\alpha\beta\gamma} = \frac{1}{2} [\partial_{\gamma} g_{\alpha\beta} + \partial_{\beta} g_{\gamma\alpha} - \partial_{\alpha} g_{\beta\gamma}]. \quad (\text{A.2})$$

c) **Christoffel symbols of second kind:**

$$\Gamma^{\alpha}_{\beta\gamma} = \frac{1}{2} g^{\alpha\delta} [\partial_{\gamma} g_{\delta\beta} + \partial_{\beta} g_{\gamma\delta} - \partial_{\delta} g_{\beta\gamma}]. \quad (\text{A.3})$$

d) **Geodesic equation:**

$$\frac{d^2 x^{\alpha}}{d\lambda^2} = -\Gamma^{\alpha}_{\beta\gamma} \frac{dx^{\beta}}{d\lambda} \frac{dx^{\gamma}}{d\lambda}, \quad (\text{A.4})$$

where λ is an affine parameter.

e) **Riemann tensor:**

$$R^{\alpha}_{\beta\gamma\delta} = \partial_{\gamma} \Gamma^{\alpha}_{\beta\delta} - \partial_{\delta} \Gamma^{\alpha}_{\beta\gamma} + \Gamma^{\epsilon}_{\beta\delta} \Gamma^{\alpha}_{\epsilon\gamma} - \Gamma^{\epsilon}_{\beta\gamma} \Gamma^{\alpha}_{\epsilon\delta}. \quad (\text{A.5})$$

f) **Ricci tensor:**

$$R_{\alpha\beta} = g^{\gamma\delta} R_{\alpha\gamma\beta\delta}, \quad (\text{A.6})$$

$$R_{\alpha\beta} = \partial_{\gamma} \Gamma^{\gamma}_{\alpha\beta} - \partial_{\beta} \Gamma^{\gamma}_{\alpha\gamma} + \Gamma^{\gamma}_{\alpha\beta} \Gamma^{\delta}_{\gamma\delta} - \Gamma^{\gamma}_{\alpha\delta} \Gamma^{\delta}_{\beta\gamma}. \quad (\text{A.7})$$

g) **Scalar Curvature:**

$$R = g^{\alpha\beta} R_{\alpha\beta}. \quad (\text{A.8})$$

h) **Einstein tensor:**

$$G_{\alpha\beta} = R_{\alpha\beta} - \frac{1}{2}g_{\alpha\beta}R. \quad (\text{A.9})$$

i) **Einstein equations:**

$$G_{\alpha\beta} = \frac{1}{M_P^2}T_{\alpha\beta}. \quad (\text{A.10})$$

APPENDIX B - GAUGE TRANSFORMATIONS IN GR

B.1 Infinitesimal Coordinate Transformations in GR

Under a general coordinate transformation, the metric tensor transforms as

$$\tilde{g}_{\alpha\beta}(\tilde{x}) = \frac{\partial x^\kappa}{\partial \tilde{x}^\alpha} \frac{\partial x^\lambda}{\partial \tilde{x}^\beta} g_{\kappa\lambda}(x); \quad (\text{B.1})$$

in particular, considering a simple infinitesimal translation of the coordinates, given by

$$\tilde{x}^\alpha = x^\alpha + \xi^\alpha, \quad (\text{B.2})$$

it is easy to see that (B.1) becomes

$$\tilde{g}_{\alpha\beta}(\tilde{x}) = g_{\alpha\beta} - g_{\alpha\lambda} \xi^\lambda_{,\beta} - g_{\lambda\beta} \xi^\lambda_{,\alpha}. \quad (\text{B.3})$$

Decomposing the metric tensor into a background ${}^{(0)}g_{\alpha\beta}$ and an infinitesimal perturbation $\delta g_{\alpha\beta}$ piece, as in (3.1), we get

$$\tilde{g}_{\alpha\beta}(\tilde{x}) = {}^{(0)}g_{\alpha\beta}(x) + {}^{(0)}g_{\alpha\beta, \kappa}(x) \xi^\kappa + \delta \tilde{g}_{\alpha\beta}(x). \quad (\text{B.4})$$

where we have assumed that the background metric is form-invariant (3.46), that is, ${}^{(0)}\tilde{g}_{\alpha\beta}(\tilde{x}) = {}^{(0)}g_{\alpha\beta}(\tilde{x})$. From expressions (B.3) and (B.4), using the constraint $\nabla_\kappa {}^{(0)}g_{\alpha\beta} = 0$ (satisfied by any metric tensor), and definitions (A.2) and (A.3), we find

$$\delta \tilde{g}_{\alpha\beta} = \delta g_{\alpha\beta} - \nabla_\alpha \xi_\beta - \nabla_\beta \xi_\alpha. \quad (\text{B.5})$$

B.2 Application: Weak Gravitational Fields in GR - Gravity Waves

As an important application of the principles derived above, let us derive the dynamical equations for a weak gravitational field in GR, which leads to the concept of *Gravity Waves* (GW), a key physical element in all this work. We adopt the following decomposition for the metric (3.1),

$${}^{(0)}g_{\alpha\beta} = \eta_{\alpha\beta}, \quad \delta g_{\alpha\beta} = h_{\alpha\beta}, \quad (\text{B.6})$$

where $h_{\alpha\beta}$ is a weak fluctuation on the Minkowski background: $|h_{\alpha\beta}| \ll 1$. The decomposition (B.6) is widely known as the *weak-field approximation*. Due to this property we can express the inverse of (B.6) as

$$g^{\alpha\beta} = \eta^{\alpha\beta} - h^{\alpha\beta}; \quad (\text{B.7})$$

then, using expressions (A.3), (A.7), (A.8) and (A.9) we see that the Einstein tensor for $h_{\alpha\beta}$ is given by

$$G_{\alpha\beta} = \frac{1}{2} [h^\gamma{}_{\beta,\alpha\gamma} + h^\gamma{}_{\alpha,\beta\gamma} - \square h_{\alpha\beta} - h_{,\alpha\beta}] - \frac{1}{2} \eta_{\alpha\beta} [h^{\kappa\lambda}{}_{,\kappa\lambda} - \square h]. \quad (\text{B.8})$$

We can clean up the mess in expression (B.8) by means of the field redefinition

$$\bar{h}_{\alpha\beta} \equiv h_{\alpha\beta} - \frac{1}{2} \eta_{\alpha\beta} h, \quad (\text{B.9})$$

where h is defined by

$$h \equiv \eta_{\alpha\beta} h^{\alpha\beta}, \quad (\text{B.10})$$

so that expression (B.8) becomes

$$G_{\alpha\beta} = \frac{1}{2} [\bar{h}^\gamma{}_{\beta,\alpha\gamma} + \bar{h}^\gamma{}_{\alpha,\beta\gamma} - \square \bar{h}_{\alpha\beta} - \eta_{\alpha\beta} \bar{h}^{\kappa\lambda}{}_{,\kappa\lambda}]. \quad (\text{B.11})$$

Under the infinitesimal transformations (B.5), $h_{\alpha\beta}$ behaves as

$$\tilde{h}_{\alpha\beta} = h_{\alpha\beta} - \xi_{\alpha,\beta} - \xi_{\beta,\alpha}, \quad (\text{B.12})$$

so that from (B.10) and (B.12) $\bar{h}_{\alpha\beta}$ transforms as

$$\tilde{\bar{h}}_{\alpha\beta} = \bar{h}_{\alpha\beta} - \xi_{\alpha,\beta} - \xi_{\beta,\alpha} + \eta_{\alpha\beta} \xi^\kappa{}_{,\kappa}. \quad (\text{B.13})$$

Then, using (B.13) it is easy (despite cumbersome) to see that the Einstein tensor (B.11) is invariant under the infinitesimal metric transformations (B.13). This invariance property has a very important consequence: we can conveniently choose the form of ξ to simplify considerably the form of the Einstein tensor (B.11). To accomplish this, let us write down $\tilde{G}_{\alpha\beta}$ as

$$\tilde{G}_{\alpha\beta} = \frac{1}{2} \left[-\square \tilde{\bar{h}}_{\alpha\beta} + \tilde{\partial}_\gamma \left(\tilde{\partial}_\alpha \tilde{\bar{h}}^\gamma{}_\beta + \tilde{\partial}_\beta \tilde{\bar{h}}^\gamma{}_\alpha - \eta_{\alpha\beta} \tilde{\partial}_\kappa \tilde{\bar{h}}^{\kappa\gamma} \right) \right], \quad (\text{B.14})$$

and choose ξ in such a way that

$$\tilde{\partial}_\gamma \left(\tilde{\partial}_\alpha \tilde{\tilde{h}}^\gamma{}_\beta + \tilde{\partial}_\beta \tilde{\tilde{h}}^\gamma{}_\alpha - \eta_{\alpha\beta} \tilde{\partial}_\kappa \tilde{\tilde{h}}^{\kappa\gamma} \right) = 0; \quad (\text{B.15})$$

then, plugging expression (B.13) into (B.15), we find

$$\square \xi_\alpha - \bar{h}^\gamma{}_{\alpha,\gamma} = 0. \quad (\text{B.16})$$

Equation (B.16) is identically satisfied by choosing

$$\square \xi_\alpha = 0, \quad (\text{B.17})$$

$$\bar{h}_{\alpha\beta}{}^{;\beta} = 0. \quad (\text{B.18})$$

The constraint equation (B.18) makes up the so-called *De Donder-Einstein-Hilbert gauge*. This gauge condition can also be stated in a different form: if we substitute expression (B.9) into (B.18), and take the additional assumptions

$$h_{\alpha\beta}{}^{;\beta} = 0, \quad h^\alpha{}_\alpha = 0, \quad (\text{B.19})$$

equation (B.18) is identically satisfied. A tensor whose components satisfy the conditions (B.19) is called a *transverse, trace-free* (TTF) tensor.

As a consequence of the De Donder-Einstein-Hilbert gauge, the Einstein equations (A.10) for a TTF tensor become

$$\square \bar{h}_{\alpha\beta} = -\frac{2}{M_P^2} T_{\alpha\beta}, \quad (\text{B.20})$$

that is, a wave equation for the field $h_{\alpha\beta}$ - the GWs.

APPENDIX C - POLARIZATION STATES FOR AN ARBITRARY METRIC THEORY OF GRAVITATION

C.1 The Newman-Penrose Formalism

In order to compute its components in an Lorentz-invariant scheme, it is convenient to introduce, following the pioneering work of Newman and Penrose, (NEWMAN; PENROSE, 1962), the quasiorthonormal complex-null basis (k, l, m, \bar{m}) , where k and l are real null-vectors and m and \bar{m} are a pair of complex numbers, satisfying the following orthogonality relations:

$$k \cdot l = 0, \quad m \cdot \bar{m} = -1, \quad k \cdot \bar{m} = k \cdot m = l \cdot \bar{m} = l \cdot m = 0. \quad (\text{C.1})$$

We follow (EARDLEY et al., 1973) and choose the following set of null vectors,

$$k = -\frac{1}{\sqrt{2}}(1, 0, 0, 1), \quad (\text{C.2})$$

$$l = -\frac{1}{\sqrt{2}}(1, 0, 0, -1), \quad (\text{C.3})$$

$$m = -\frac{1}{\sqrt{2}}(0, 1, i, 0), \quad (\text{C.4})$$

$$\bar{m} = -\frac{1}{\sqrt{2}}(0, 1, -i, 0), \quad (\text{C.5})$$

all satisfying (C.1). With the basis given by (C.2) - (C.5) we can split the Riemann tensor into its irreducible parts, namely, the Weyl tensor, whose ten independent components are given by five complex scalars $(\Psi_0, \Psi_1, \Psi_2, \Psi_3, \Psi_4)$, the Ricci tensor, whose nine independent components are given by the scalars $\Phi_{00}, \Phi_{01}, \Phi_{02}, \Phi_{10}, \Phi_{20}, \Phi_{11}, \Phi_{12}, \Phi_{21}, \Phi_{22}$, and the Ricci scalar Λ . In this context, we may prove that the differential and algebraic properties of the Riemann tensor reduce the number of independent components to six (EARDLEY et al., 1973); they are given by

i) *The Weyl tensor:*

$$\Psi_0 = \Psi_1 = 0, \quad (\text{C.6})$$

$$\Psi_2 = -\frac{1}{6}R_{lklk}, \quad (\text{C.7})$$

$$\Psi_3 = -\frac{1}{2}R_{kl\bar{m}}, \quad (\text{C.8})$$

$$\Psi_4 = -R_{l\bar{m}l\bar{m}}; \quad (\text{C.9})$$

ii) *The Ricci tensor:*

$$\Phi_{00} = \Phi_{01} = \Phi_{10} = \Phi_{02} = \Phi_{20} = 0, \quad (\text{C.10})$$

$$\Phi_{22} = -R_{lml\bar{m}}, \quad (\text{C.11})$$

$$\Phi_{11} = \frac{3}{2}\Psi_2, \quad (\text{C.12})$$

$$\Phi_{12} = \bar{\Phi}_{21} = \bar{\Psi}_3; \quad (\text{C.13})$$

ii) *The Ricci scalar:*

$$\Lambda = -\frac{1}{2}\Psi_2. \quad (\text{C.14})$$

We can reduce, therefore, the number of independent components of the Riemann tensor to the set

$$\{\Psi_2, \Psi_3, \bar{\Psi}_3, \Psi_4, \bar{\Psi}_4, \Phi_{22}\}. \quad (\text{C.15})$$

Henceforth, we call (C.15) *Newman-Penrose (NP) amplitudes*. They play the role of definite helicity states $s = (0, \pm 1, \pm 2)$ under rotations around the z axis in a nearly Lorentz coordinate frame.

C.2 Polarization of GWs

The polarization states for a GW in an arbitrary metric theory of gravitation are given by the independent modes of the Riemann tensor. Since the NP formalism provides all its components by means of the amplitudes $\{\Psi_2, \Psi_3, \bar{\Psi}_3, \Psi_4, \bar{\Psi}_4, \Phi_{22}\}$, we see that such formalism is specially useful for studying GW polarization. In what follows, we first set the general theory, and later derive the polarization states of a

GW in GR.

C.2.1 The general setting

In particular, the two real NP amplitudes (Ψ_2, Φ_{22}) correspond to the state $s = 0$ (which defines the scalar modes), whereas the complex NP amplitudes $(\Psi_3, \bar{\Psi}_3)$ correspond to $s = \pm 1$ (vector modes), and $(\Psi_4, \bar{\Psi}_4)$ to $s = \pm 2$ (tensor modes). The polarization modes can be represented on the $x - y$, $y - z$ or $x - z$ plane (see Figure C.1).

In this figure, the solid (dashed) lines represent the displacement that each mode induces on a ring of test particles at $\omega t = 0$ ($\omega t = \pi$). The relative accelerations of the test masses, as measured by an ideal detector in the coordinate system $\{t, x^i\}$, where t is the proper time, and $u = t - z/c$ represents a null “retarded time”, can be represented by the “driving-force matrix” S (EARDLEY et al., 1973):

$$S_{ij}(t) := R_{i0j0}(u). \quad (\text{C.16})$$

The definition of the driving-force matrix allows the introduction of a basis for the GW polarizations (analogous to the polarization basis for photons); for instance, let us represent the NP amplitudes as

$$p_1(\hat{z}, t) = \Psi_2(u), \quad (\text{C.17})$$

$$p_2(\hat{z}, t) = \text{Re } \Psi_3(u), \quad (\text{C.18})$$

$$p_3(\hat{z}, t) = \text{Im } \Psi_3(u), \quad (\text{C.19})$$

$$p_4(\hat{z}, t) = \text{Re } \Psi_4(u), \quad (\text{C.20})$$

$$p_5(\hat{z}, t) = \text{Im } \Psi_4(u), \quad (\text{C.21})$$

$$p_6(\hat{z}, t) = \Phi_{22}(u); \quad (\text{C.22})$$

(from now on, whenever the index r appears, it will always indicate a given NP amplitude according to the sequence given in (C.2.1), so that $r = 1$ stands for Ψ_2 , and so forth. The index r is called the *polarization index*). Now, writing the NP amplitudes (C.7), (C.8), (C.9) and (C.11) in Cartesian coordinates (recall that the NP basis given by (C.2) - (C.5) can be written in terms of the coordinates $\{t, x^i\}$),

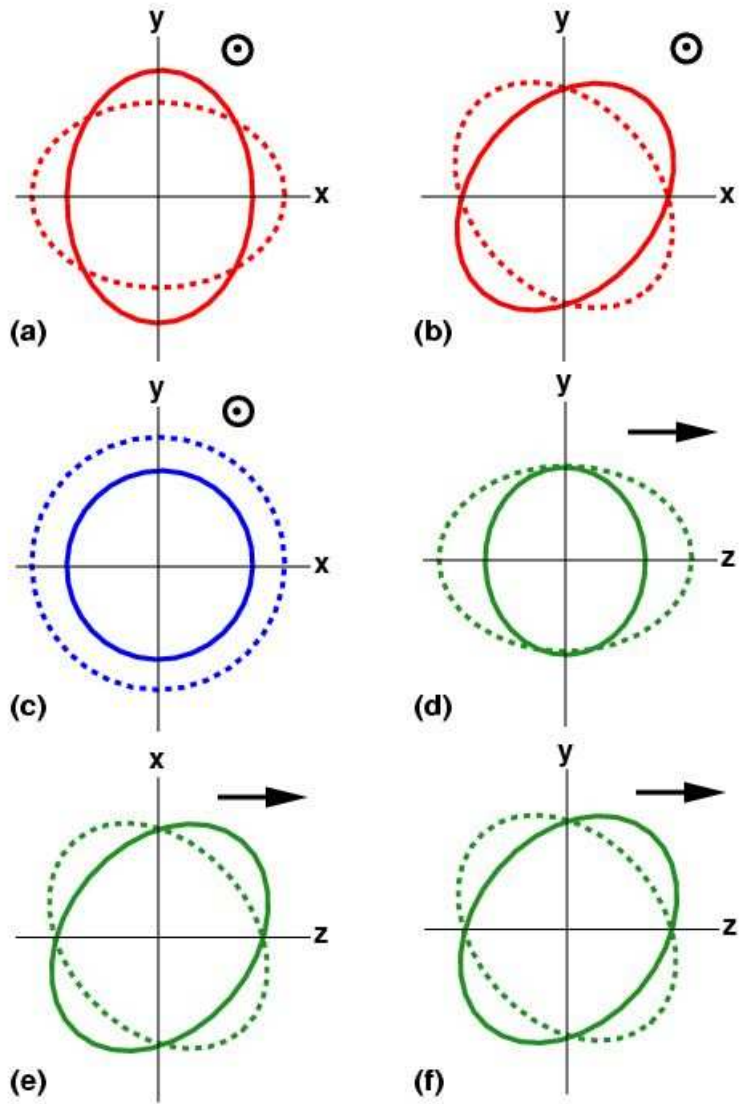


FIGURE C.1 - The six possible polarization modes for an arbitrary metric theory of gravitation. In terms of the NP amplitudes, we have the following: (a) $\text{Re } \Psi_4$; (b) $\text{Im } \Psi_4$; (c) Φ_{22} ; (d) Ψ_2 ; (e) $\text{Re } \Psi_3$; (f) $\text{Im } \Psi_3$. Figure adapted from (WILL, 2005).

we get the following result

$$S = \begin{pmatrix} -\frac{1}{2}(p_4 + p_6) & \frac{1}{2}p_5 & -2p_2 \\ \frac{1}{2}p_5 & \frac{1}{2}(p_4 - p_6) & 2p_3 \\ -2p_2 & 2p_3 & -6p_1 \end{pmatrix} \quad (\text{C.23})$$

or, rearranging the terms,

$$S(t) = \sum_{r=1}^6 p_r(\hat{z}, t) E_r(\hat{z}), \quad (\text{C.24})$$

where $E_r(\hat{z})$ are the *basis polarization matrices*, given by

$$\begin{aligned} E_1 &= -6 \begin{pmatrix} 0 & 0 & 0 \\ 0 & 0 & 0 \\ 0 & 0 & 1 \end{pmatrix}, & E_2 &= -2 \begin{pmatrix} 0 & 0 & 1 \\ 0 & 0 & 0 \\ 1 & 0 & 0 \end{pmatrix} \\ E_3 &= 2 \begin{pmatrix} 0 & 0 & 0 \\ 0 & 0 & 1 \\ 0 & 1 & 0 \end{pmatrix}, & E_4 &= -\frac{1}{2} \begin{pmatrix} 1 & 0 & 0 \\ 0 & -1 & 0 \\ 0 & 0 & 0 \end{pmatrix}, \\ E_5 &= \frac{1}{2} \begin{pmatrix} 0 & 1 & 0 \\ 1 & 0 & 0 \\ 0 & 0 & 0 \end{pmatrix}, & E_6 &= -\frac{1}{2} \begin{pmatrix} 1 & 0 & 0 \\ 0 & 1 & 0 \\ 0 & 0 & 0 \end{pmatrix}. \end{aligned} \quad (\text{C.25})$$

Therefore, the polarization of a GW in an arbitrary metric theory of gravity can be fully described by the basis polarization matrices $E_r(\hat{z})$. However, due to the tensorial character of the space-time metric it is convenient to cast the polarization basis (C.25) into a tensor; hence, along with its spatial components, given by $(E_r)_{ij}(\hat{z})$, there are the 00 and 0*i* components, which are zero by the very definition of the “full driving-force matrix” S (C.16), so that

$$S_{00}(t) = R_{0000}(u) = 0, \quad S_{0i}(t) = R_{0i00}(u) = 0. \quad (\text{C.26})$$

Hence, the *polarization tensor* assumes the form

$$\begin{aligned}
\varepsilon^1 &= \begin{pmatrix} 0 & 0 & 0 & 0 \\ 0 & 0 & 0 & 0 \\ 0 & 0 & 0 & 0 \\ 0 & 0 & 0 & 1 \end{pmatrix}, & \varepsilon^2 &= \begin{pmatrix} 0 & 0 & 0 & 0 \\ 0 & 0 & 0 & 1 \\ 0 & 0 & 0 & 0 \\ 0 & 1 & 0 & 0 \end{pmatrix} \\
\varepsilon^3 &= \begin{pmatrix} 0 & 0 & 0 & 0 \\ 0 & 0 & 0 & 0 \\ 0 & 0 & 0 & 1 \\ 0 & 0 & 1 & 0 \end{pmatrix}, & \varepsilon^4 &= \begin{pmatrix} 0 & 0 & 0 & 0 \\ 0 & 1 & 0 & 0 \\ 0 & 0 & -1 & 0 \\ 0 & 0 & 0 & 0 \end{pmatrix}, \\
\varepsilon^5 &= \begin{pmatrix} 0 & 0 & 0 & 0 \\ 0 & 0 & 1 & 0 \\ 0 & 1 & 0 & 0 \\ 0 & 0 & 0 & 0 \end{pmatrix}, & \varepsilon^6 &= \begin{pmatrix} 0 & 0 & 0 & 0 \\ 0 & 1 & 0 & 0 \\ 0 & 0 & 1 & 0 \\ 0 & 0 & 0 & 0 \end{pmatrix}.
\end{aligned} \tag{C.27}$$

Once we have described the polarization states, let us now connect the formalism described above with GW amplitudes. As we have seen, cosmological GWs are described by equation (3.101), whereas plane GWs of non-cosmological character are given by a Klein-Gordon-like equation (B.20). Due to the oscillatory character of these GW equations, we can expand the tensor field h_{ij} at the classical level into its Fourier modes as follows,

$$h_{ij}(t, x) = \int_{-\infty}^{\infty} \frac{d^3k}{(2\pi)^{3/2}} \tilde{h}_{ij}(t, \mathbf{k}) e^{i\mathbf{k}\cdot\mathbf{x}}, \tag{C.28}$$

where we have considered a wave propagating in the direction $\hat{\mathbf{k}} = \hat{\mathbf{z}}$ and, for the sake of simplicity, we dropped the bar over the tensor on the left-hand side of (B.9) and simply write it as h_{ij} ¹, in the case of GWs described by equation (B.20). Next, we decompose the tensors h_{ij} according to the six polarization tensors ε_{ij}^r derived in (C.27),

$$\tilde{h}_{ij}(t, k) = \sum_{r=1}^6 \varepsilon_{ij}^r(k) \tilde{h}^r(t, k), \tag{C.29}$$

where $\tilde{h}^r(t, k)$ are the GW amplitudes.

¹We neglect the components h_{00} because, as we have discussed above, a GW have at most *six* polarization states, and can be then completely described by the tensor h_{ij} .

The most general form of a GW produced in an alternative theory of gravitation has the form (C.29), with the polarization states given by the polarization tensors (C.27) and depicted in Figure C.1.

C.2.2 Polarization of GWs in GR

Let us now apply the techniques introduced above to the case of tensor modes in GR. As we have seen in the Section B.2, general-relativistic tensor modes possess a large number of symmetries, characterized by the De Donder-Einstein-Hilbert gauge (B.19); then, calculating the NP amplitudes (C.15) and using these constraints, we find that

$$\Psi_2 = \Psi_3 = \bar{\Psi}_3 = \Phi_{22} = 0, \quad (\text{C.30})$$

$$\Psi_4 \neq 0, \quad \bar{\Psi}_4 \neq 0, \quad (\text{C.31})$$

or

$$\tilde{h}^1 = \tilde{h}^2 = \tilde{h}^3 = \tilde{h}^6 = 0. \quad (\text{C.32})$$

Therefore, there are only *two* polarization states for general-relativistic GWs, given by the NP amplitudes Ψ_4 . These two polarization states are transverse, and, as usual in the literature, are denoted by the symbol “+” for the amplitude $\tilde{h}^4 \equiv \tilde{h}_+$, and “×” for the amplitude $\tilde{h}^5 \equiv \tilde{h}_\times$. As can be seen from the structure of ε_{ij}^r for $r = 4, 5$ in (C.27), these modes are also traceless, composing then the TTF modes. The corresponding polarization tensors $\varepsilon_{ij}^{(+, \times)}$ are given by the components $r = 4, 5$ of (C.27),

$$\varepsilon_{ij}^{(+)} = \begin{pmatrix} 1 & 0 & 0 \\ 0 & -1 & 0 \\ 0 & 0 & 0 \end{pmatrix}, \quad \varepsilon_{ij}^{(\times)} = \begin{pmatrix} 0 & 1 & 0 \\ 1 & 0 & 0 \\ 0 & 0 & 0 \end{pmatrix}. \quad (\text{C.33})$$

The corresponding metrics, given by expression (3.1), are

$$g_{\alpha\beta}^{(+)} = a^2 \begin{pmatrix} 1 & 0 & 0 & 0 \\ 0 & -1 - h_+ & 0 & 0 \\ 0 & 0 & -1 + h_+ & 0 \\ 0 & 0 & 0 & -1 \end{pmatrix}, \quad (\text{C.34})$$

$$g_{\alpha\beta}^{(\times)} = a^2 \begin{pmatrix} 1 & 0 & 0 & 0 \\ 0 & -1 & h_{\times} & 0 \\ 0 & h_{\times} & -1 & 0 \\ 0 & 0 & 0 & -1 \end{pmatrix}. \quad (\text{C.35})$$

APPENDIX D - SCALAR FIELD THEORIES - K-ESSENCE

Since throughout this thesis we stumble with scalar fields in almost every chapter, let us summarize here the most important ideas about these field theories. The basic material for Chapters 7 and 8 is also presented in this Appendix.

As a reminder, we changed the notation so that a prime ' indicates a derivative with respect to the field ϕ .

D.1 k-Essence Dynamics

Consider a general Lagrangian density of the form $\mathcal{L} = \mathcal{L}[X, \phi]$, minimally coupled to gravity,

$$S = \int d^4x \sqrt{-g} \{ \mathcal{L}[X, \phi] + \mathcal{L}_{\text{EH}} \}, \quad (\text{D.1})$$

where \mathcal{L}_{EH} is the Einstein-Hilbert Lagrangian density, X is the conventional kinetic term defined in (D.2),

$$X \equiv \frac{1}{2} g^{\alpha\beta} \nabla_\alpha \phi \nabla_\beta \phi, \quad (\text{D.2})$$

($X > 0$ according to our choice of the metric signature) and ϕ is a scalar field. The metric $g_{\alpha\beta}$ is defined on the spacetime characterized by a manifold \mathcal{M} .

In what follows we do not specify the form of the kinetic term, so that we allow the Lagrangian $\mathcal{L}[X, \phi]$ to accommodate an unconventional kinetic term - in better words, a *non-canonical* term - a function of X . These theories are called *k-essence* (ARMENDARIZ-PICON et al., 1999), (ARMENDARIZ-PICON et al., 2001), where k reminds us of the "non-canonicity" of the kinetic term. For this reason we call X canonical kinetic term. The equations of motion for the k-essence comes directly from the variational principle (WEINBERG, 1995)

$$\frac{\delta}{\delta\phi} S[X, \phi] = 0, \quad (\text{D.3})$$

so that the equation of motion for the k-essence field reads (BEAN et al., 2008b),

$$\dot{X} = \frac{\sqrt{2X}}{1 + 2X\mathcal{L}_{XX}} \left(\mathcal{L}_\phi - 2X\mathcal{L}_{X\phi} - 3H\sqrt{2X}\mathcal{L}_X \right), \quad (\text{D.4})$$

where the subscript " X " indicates a derivative with respect to the kinetic term. It

is convenient to rewrite equation (D.4) as (BABICHEV et al., 2008)

$$\tilde{G}^{\mu\nu}\nabla_\mu\nabla_\nu\phi + 2X\mathcal{L}_{X\phi} - \mathcal{L}_\phi = 0, \quad (\text{D.5})$$

where $\tilde{G}^{\mu\nu}$, called “effective” or “acoustic” metric, is given by

$$\tilde{G}^{\mu\nu}(\phi, \nabla\phi) = \mathcal{L}_X g^{\mu\nu} + \mathcal{L}_{XX} \nabla^\mu\phi \nabla^\nu\phi. \quad (\text{D.6})$$

Therefore, the k-essence field *induces* a new metric on \mathcal{M} , which defines a different causal structure for the propagation of the field perturbations, as we discuss in Section D.4 later on. In analogy with hydrodynamics, the k-essence field plays the role of a fluid, whose energy-momentum is given by expression (2.34),

$$T_{\alpha\beta} = (\rho_\phi + P_\phi) u_\alpha u_\beta - P_\phi g_{\alpha\beta}. \quad (\text{D.7})$$

where, as in Section 2.3, u^α is four-velocity of an observer comoving with the fluid, and ρ_ϕ and P_ϕ are the energy density and pressure of the k-essence fluid, respectively. Their expressions can be calculated in terms of the k-essence Lagrangian $\mathcal{L}[X, \phi]$ using the definition of the stress energy-momentum tensor, (WEINBERG, 1995)

$$T_{\alpha\beta} = \frac{2}{\sqrt{-g}} \frac{\delta S_\phi}{\delta g^{\alpha\beta}}, \quad (\text{D.8})$$

whose result is

$$T_{\alpha\beta} = \nabla_\alpha\phi \nabla_\beta\phi \mathcal{L}_X - \mathcal{L} g_{\alpha\beta}; \quad (\text{D.9})$$

then, from expressions (D.8) and (D.9) we immediately deduce that

$$\rho_\phi \equiv u^\alpha u^\beta T_{\alpha\beta} = 2X\mathcal{L}_X - \mathcal{L} \quad (\text{D.10})$$

$$P_\phi \equiv \frac{1}{3}\pi^{\alpha\beta} T_{\alpha\beta} = \mathcal{L}, \quad (\text{D.11})$$

where $\pi^{\alpha\beta} \equiv g_{\alpha\beta} - u_\alpha u_\beta$ is an operator which projects geometric quantities defined on \mathcal{M} onto hypersurfaces orthogonal to the four-velocity u^β , whose expression in terms of ϕ follows from (D.8) and (D.9-D.11),

$$u_\alpha = \frac{\nabla_\alpha\phi}{\sqrt{2X}}. \quad (\text{D.12})$$

For a null-vector n^α , $g_{\alpha\beta}n^\alpha n^\beta = 0$, the Null-energy condition (NEC)

$$T_{\alpha\beta}n^\alpha n^\beta \geq 0 \quad (\text{D.13})$$

applied to (D.9) implies

$$(\text{NEC}) : \quad \mathcal{L}_X \geq 0. \quad (\text{D.14})$$

Hence, k-essence models that fulfils NEC have Hamiltonians bounded from below.

In the fluid approach it is also important to calculate the speed at which small perturbations propagate, the *speed of sound*. The general expression is given by

$$c_s^2 \equiv \left(\frac{\partial P}{\partial \rho} \right)_S, \quad (\text{D.15})$$

where the subscript “S” refers to an adiabatic process. For a k-essence fluid whose energy density and pressure are characterized by expressions (D.10) and (D.11), the expression of the sound velocity (D.15) yields

$$c_s^2 \equiv \frac{P_X}{\rho_X} = \left(1 + 2X \frac{\mathcal{L}_{XX}}{\mathcal{L}_X} \right)^{-1}. \quad (\text{D.16})$$

The Friedmann equation is given by (2.42) and (D.10),

$$H^2 = \frac{1}{3M_P^2} \rho = \frac{1}{3M_P^2} (2X\mathcal{L}_X - \mathcal{L}), \quad (\text{D.17})$$

for a flat FRW metric, and the continuity equation (2.37) is

$$\dot{\rho} = -6HX\mathcal{L}_X. \quad (\text{D.18})$$

As we have seen in Section 4.3, for monotonic field evolution, the field value ϕ can be used as a “clock”, and all other quantities expressed as functions of ϕ , for example $X = X(\phi)$, $\mathcal{L} = \mathcal{L}[X(\phi), \phi]$, and so on. We consider the homogeneous case, so that $\dot{\phi} = \sqrt{2X}$. Using

$$\frac{d}{dt} = \dot{\phi} \frac{d}{d\phi} = \sqrt{2X} \frac{d}{d\phi}, \quad (\text{D.19})$$

we can re-write the Friedmann and continuity equations as the *Hamilton-Jacobi*

equations,

$$\dot{\phi} = \sqrt{2X} = -\frac{2M_P^2}{\mathcal{L}_X} H'(\phi), \quad (\text{D.20})$$

$$3M_P^2 H^2(\phi) = \frac{4M_P^4 H'(\phi)^2}{\mathcal{L}_X} - \mathcal{L}, \quad (\text{D.21})$$

where equations (D.20) and (D.21) are the generalizations of equations (4.28) and (4.29).

D.2 Flow Hierarchy for k-Essence models

Throughout this Section we follow closely (BEAN et al., 2008b), unless otherwise stated. The generalization of the flow parameters (4.32), (4.37), (4.45) and (4.47) are performed as follows. First, from equations (2.49) and (4.31), we see that the flow parameter ϵ can be written alternatively as

$$\epsilon = -\frac{\dot{H}}{H^2}; \quad (\text{D.22})$$

then, taking the time derivative of the Hubble parameter as expressed in equation (D.17), (D.20), we find

$$\epsilon(\phi) = \frac{2M_P^2}{\mathcal{L}_X} \left(\frac{H'(\phi)}{H(\phi)} \right)^2. \quad (\text{D.23})$$

Taking the derivative of (D.23) with respect to ϕ , grouping the terms, and comparing with (4.37), we see that the generalization of the flow parameter η is

$$\tilde{\eta}(\phi) \equiv \frac{2M_P^2}{\mathcal{L}_X} \frac{H''(\phi)}{H(\phi)}. \quad (\text{D.24})$$

However, in doing this derivation, another parameter appears, and it is related to the fact that \mathcal{L}_X is not necessarily constant for a given k-essence model (although in canonical inflation it is). This parameter is

$$\tilde{s}(\phi) \equiv \frac{2M_P^2}{\mathcal{L}_X} \frac{H'(\phi)}{H(\phi)} \frac{\mathcal{L}'_X}{\mathcal{L}_X}. \quad (\text{D.25})$$

Next, taking the derivative of \tilde{s} with respect to ϕ , we also find a second parameter, defined as

$$s(\phi) \equiv -\frac{2M_P^2}{\mathcal{L}_X} \frac{H'(\phi)}{H(\phi)} \frac{c'_S(\phi)}{c_S(\phi)}, \quad (\text{D.26})$$

which measures the variation of the sound speed c_s , which is not necessarily constant.

The number of e-folds dN , equation (4.23), can be re-written in terms of $d\phi$ by:

$$dN = \frac{\mathcal{L}_X}{2M_P^2} \left(\frac{H(\phi)}{H'(\phi)} \right) d\phi, \quad (\text{D.27})$$

then, the general flow parameters (D.23-D.26) can be similarly be re-written in terms of dN ,

$$\epsilon \equiv \frac{1}{H} \frac{dH}{dN}, \quad (\text{D.28})$$

$$s \equiv -\frac{1}{c_s} \frac{dc_s}{dN}, \quad (\text{D.29})$$

$$\tilde{s} \equiv \frac{1}{\mathcal{L}_X} \frac{d\mathcal{L}_X}{dN}. \quad (\text{D.30})$$

Taking successive derivatives d/dN with respect to the number of e-folds yields an infinite hierarchy of flow equations (KINNEY, 2002; BEAN et al., 2008b),

$$\begin{aligned} \frac{d\epsilon}{dN} &= -\epsilon(2\epsilon - 2\tilde{\eta} + \tilde{s}), & \frac{d\tilde{\eta}}{dN} &= -\tilde{\eta}(\epsilon + \tilde{s}) + {}^2\lambda, \\ \frac{ds}{dN} &= -s(\epsilon - \tilde{\eta} + \tilde{s} + s) + \epsilon\rho, & \frac{d\tilde{s}}{dN} &= -\tilde{s}(\epsilon - \tilde{\eta} + 2\tilde{s}) + \epsilon^1\beta, \\ \frac{d^\ell\lambda}{dN} &= -{}^\ell\lambda[\ell(\tilde{s} + \epsilon) - (\ell - 1)\tilde{\eta}] + {}^{\ell+1}\lambda, \\ \frac{d^\ell\alpha}{dN} &= -{}^\ell\alpha[(\ell - 1)(\epsilon - \tilde{\eta}) + \ell\tilde{s} + s] + {}^{\ell+1}\alpha, \\ \frac{d^\ell\beta}{dN} &= -{}^\ell\beta[(\ell - 1)(\epsilon - \tilde{\eta}) + (\ell + 1)\tilde{s}] + {}^{\ell+1}\beta, \end{aligned} \quad (\text{D.31})$$

where the higher-order flow parameters are defined as follows, where $\ell = 1, \dots, \infty$ is an integer parameter:

$$\begin{aligned} {}^\ell\lambda(\phi) &= \left(\frac{2M_P^2}{\mathcal{L}_X} \right)^\ell \left(\frac{H'(\phi)}{H(\phi)} \right)^{\ell-1} \frac{1}{H(\phi)} \frac{d^{\ell+1}H(\phi)}{d\phi^{\ell+1}}, \\ {}^\ell\alpha(\phi) &= \left(\frac{2M_P^2}{\mathcal{L}_X} \right)^\ell \left(\frac{H'(\phi)}{H(\phi)} \right)^{\ell-1} \frac{1}{c_s^{-1}(\phi)} \frac{d^{\ell+1}c_s^{-1}(\phi)}{d\phi^{\ell+1}}, \\ {}^\ell\beta(\phi) &= \left(\frac{2M_P^2}{\mathcal{L}_X} \right)^\ell \left(\frac{H'(\phi)}{H(\phi)} \right)^{\ell-1} \frac{1}{\mathcal{L}_X} \frac{d^{\ell+1}\mathcal{L}_X}{d\phi^{\ell+1}}. \end{aligned} \quad (\text{D.32})$$

D.3 Cosmological Perturbations in k-Essence Models

The introduction of perturbations in k-essence models follows exactly the same steps taken in Section 4.5. For the sake of simplicity we consider the metric in the longitudinal gauge (4.66) with $\Psi = \Phi$ and with a flat FRW as the background metric. The perturbations of the k-essence field $\delta\phi$ induce corresponding fluctuations in the stress energy-momentum tensor (D.9), whose components read (GARRIGA; MUKHANOV, 1999)

$$\delta T^0_0 = \frac{\rho_0 + P_0}{c_s^2} \left[\left(\frac{\delta\phi}{\dot{\phi}} \right)' - \Phi \right] - 3H(\rho_0 + P_0) \frac{\delta\phi}{\dot{\phi}}, \quad (\text{D.33})$$

$$T^0_i = (\rho_0 + P_0) \left(\frac{\delta\phi}{\dot{\phi}} \right)'_{,i}. \quad (\text{D.34})$$

Substituting the Einstein tensors (3.92-3.93) and the components of the tensors (D.33-D.34) into the perturbed Einstein equation (3.91), we find (GARRIGA; MUKHANOV, 1999)

$$\begin{aligned} \frac{d}{dt} \left(\frac{\delta\phi}{\dot{\phi}} \right) &= \Phi + \frac{2M_P^2 c_s^2}{a^2(\rho + p)} \nabla^2 \Phi \\ \frac{d}{dt} (a\Phi) &= \frac{a(\rho + p)}{2M_P^2} \left(\frac{\delta\phi}{\dot{\phi}} \right). \end{aligned} \quad (\text{D.35})$$

Equations (D.35) can be cast into a more convenient form by changing the perturbations Φ and $\delta\phi$ to the new variables ζ and ξ defined by

$$\begin{aligned} \xi &= \frac{2M_P^2 \Phi a}{H} \\ \zeta &= H \frac{\delta\phi}{\dot{\phi}} + \Phi, \end{aligned} \quad (\text{D.36})$$

so that the perturbed Einstein equations (D.35) become

$$\begin{aligned} \dot{\xi} &= \frac{a(\rho + p)}{H^2} \zeta, \\ \dot{\zeta} &= \frac{c_s^2 H^2}{a^3(\rho + p)} \nabla^2 \zeta. \end{aligned} \quad (\text{D.37})$$

As we did in subsection 4.5.2, we define the variable z and the gauge-invariant

Mukhanov-Sasaki potential u as

$$z = \frac{a(\rho + p)^{1/2}}{c_s H}, \quad (\text{D.38})$$

$$u = z\zeta, \quad (\text{D.39})$$

which corresponds to (4.76) and (4.78) respectively. Then, from (D.37) we derive the mode equation for $u(\tau) \propto u_k(\tau) \exp(i\mathbf{k} \cdot \mathbf{x})$, given by (GARRIGA; MUKHANOV, 1999)

$$u_k'' - \left[(c_s k)^2 + \frac{z''}{z} \right] u_k = 0. \quad (\text{D.40})$$

Proceeding analogously as we did in (4.100), the variable (D.38) can be cast into the following form,

$$z = -\frac{aM_P\sqrt{2\epsilon}}{c_s}; \quad (\text{D.41})$$

then, using (4.101), we can evaluate the ratio z''/z in (D.40) in terms of the flow parameters (D.23-D.32); the result is

$$\frac{z''}{z} = a^2 H^2 \bar{F}(\epsilon, \tilde{\eta}, s, \tilde{s}, {}^2\lambda, {}^1\alpha, {}^1\beta), \quad (\text{D.42})$$

where

$$\begin{aligned} \bar{F} \equiv & 2 + 2\epsilon - 3\tilde{\eta} - 3s + \frac{3}{2}\tilde{s} + 2\epsilon^2 + \frac{5}{4}\tilde{s}^2 - 2s\tilde{s} \\ & + \tilde{\eta}^2 + 2\epsilon(\tilde{s} - s) + 3\tilde{\eta}s - \frac{5}{2}\tilde{\eta}\tilde{s} - 4\tilde{\eta}\epsilon + {}^2\lambda \\ & - \frac{1}{2}\epsilon({}^1\alpha) + \epsilon({}^1\beta). \end{aligned} \quad (\text{D.43})$$

Next, we change the conformal time τ to the variable y defined as

$$y \equiv \frac{c_s k}{aH}; \quad (\text{D.44})$$

similarly to what was done in (4.105); then,

$$\frac{d}{d\tau} = -aH(1 - \epsilon - s)y \frac{d}{dy}, \quad (\text{D.45})$$

and

$$\frac{d^2}{d\tau^2} = a^2 H^2 \left[(1 - \epsilon - s)^2 y^2 \frac{d^2}{dy^2} + \bar{G}(\epsilon, \tilde{\eta}, s, \tilde{s}, {}^1\alpha) y \frac{d}{dy} \right], \quad (\text{D.46})$$

where

$$\bar{G} \equiv -s + \epsilon(2s + \tilde{s}) + s(2s + \tilde{s}) + 2\epsilon^2 - 2\epsilon\tilde{\eta} - s\tilde{\eta} - \epsilon(1\alpha).$$

Substituting (D.42) and (D.46) into the mode equation (D.40), we find

$$(1 - \epsilon - s)^2 y^2 \frac{d^2 u_k}{dy^2} + \bar{G} y \frac{du_k}{dy} + [y^2 - \bar{F}] u_k = 0, \quad (\text{D.47})$$

which is an exact equation, without any assumption of slow-roll.

The power spectra for scalar and tensor perturbations are given respectively by similar expressions to (4.130) and (4.133); however, the curvature perturbations must be evaluated when the mode crosses the acoustic horizon, whereas the tensor are evaluated at the Hubble horizon crossing, (GARRIGA; MUKHANOV, 1999)

$$\begin{aligned} P_{\mathcal{R}}^{1/2} &= \frac{1}{8\pi^2} \frac{H^2}{M_P^2 c_s \epsilon} \Big|_{c_s k = aH}, \\ P_T &= \frac{2}{\pi^2} \frac{H^2}{M_P^2} \Big|_{k = aH}. \end{aligned} \quad (\text{D.48})$$

Slow-roll solutions can be worked out following the same steps as in 4.6.1; the values for the scalar spectral index (4.135) and the tensor/scalar ratio are given by (BEAN et al., 2008b)

$$\begin{aligned} n_s - 1 &= -4\epsilon + 2\tilde{\eta} - \tilde{s} - s, \\ n_T &= -2\epsilon, \end{aligned} \quad (\text{D.49})$$

The tensor-to-scalar ratio reads

$$r = 16\epsilon c_s. \quad (\text{D.50})$$

D.4 Causal Structure of k-Essence Models

It is convenient to use the metric (BABICHEV et al., 2008)

$$G^{\mu\nu} \equiv \frac{c_s}{\mathcal{L}_X^2} \tilde{G}^{\mu\nu} \quad (\text{D.51})$$

which is conformally equivalent to $\tilde{G}^{\mu\nu}$, and hence, defines the same causal structure. The inverse metric $G_{\mu\nu}^{-1}$ is given by

$$G_{\mu\nu}^{-1} \equiv \frac{\mathcal{L}_X}{c_s} \left[g_{\mu\nu} - c_s^2 \frac{\mathcal{L}_{XX}}{\mathcal{L}_X} \nabla_\mu \phi \nabla_\nu \phi \right]; \quad (\text{D.52})$$

notice that it has the same form of (D.51), since $\nabla^\mu \phi$ is timelike.

Since tachyacoustic cosmology deals with superluminal propagation of perturbations, it is important to address the issue of *causality* in this model. Babichev *et al.* (BABICHEV *et al.*, 2008) have discussed the conditions that must be fulfilled by a general k-essence model with superluminal propagation in order to avoid causal paradoxes (*i.e.*, the presence of *closed causal curves* - CCC). In this appendix we outline the main ideas of this work and apply to our tachyacoustic model.

To begin with let us introduce some key definitions (WALD, 1984). Let $g_{\mu\nu}$ be a metric with Lorentzian signature defined on a given manifold \mathcal{M} . Given a point $p \in \mathcal{M}$, let t^μ be a timelike vector at p ; then, from this timelike vector we construct a second metric, $\tilde{g}_{\mu\nu}$, related to the background metric $g_{\mu\nu}$ by

$$\tilde{g}_{\mu\nu} \equiv g_{\mu\nu} - t_\mu t_\nu. \quad (\text{D.53})$$

The spacetime $(\mathcal{M}, g_{\mu\nu})$ is defined to be *stably causal* if there is a continuous timelike vector field t^μ such that the spacetime $(\mathcal{M}, \tilde{g}_{\mu\nu})$ possesses no closed timelike curves. The following theorem (8.2.2. in (WALD, 1984)) establishes the necessary and sufficient conditions for a spacetime to be stably causal:

A spacetime $(\mathcal{M}, g_{\mu\nu})$ stably causal if and only if there exists a differentiable function f on \mathcal{M} such that $\nabla^\mu f$ is a past directed timelike vector field.

We can apply this theorem to k-essence models as follows (BABICHEV *et al.*, 2008). First, we must find the analog of the induced metric (D.53) for the case of k-essence models, which can be obtained by means of the equation of motion for a scalar field described by a Lagrangian $\mathcal{L}(X, \phi)$, (D.5); then, using this equation and expression (D.53), we can now apply the theorem stated above and check the stable causality of k-essence models. Let t be time coordinate with respect to the background metric (which is everywhere future directed), which we take to be

FRW. Since $g^{\mu\nu}\nabla_\mu t\nabla_\nu t = 1$, we have, using (D.6) and (D.51),

$$G^{\mu\nu}\nabla_\mu t\nabla_\nu t = \frac{c_s}{\mathcal{L}_X} \left[1 + \frac{\mathcal{L}_{XX}}{\mathcal{L}_X} \dot{\phi}^2 \right]; \quad (\text{D.54})$$

then, since for a *homogeneous* scalar field holds $\dot{\phi}^2 = 2X$, we have, from (D.16) and (D.54) that

$$G^{\mu\nu}\nabla_\mu t\nabla_\nu t = \frac{1}{c_s \mathcal{L}_X} > 0, \quad (\text{D.55})$$

provided the Null Energy Condition (NEC) is satisfied, that is, $\mathcal{L}_X > 0$. Therefore, t plays a role of global time for *both* spacetimes $(\mathcal{M}, g_{\mu\nu})$ and $(\mathcal{M}, G_{\mu\nu}^{-1})$, and then the conditions of the theorem are fulfilled. Then, there is *no* CCC in superluminal k-essence models built from homogeneous scalar fields on a FRW background. Since this is exactly the case of the models introduced in (BESSADA et al., 2009), we conclude that there are no causal paradoxes in tachyacoustic cosmology.

REFERENCES

ABRAMOWITZ, M.; STEGUN, I. A. **Handbook of Mathematical Functions**. New York: Dover, 1972. 63, 75

AFSHORDI, N. Cuscuton and low energy limit of Horava-Lifshitz gravity. **Phys. Rev.**, D80, p. 081502, 2009. 147

AFSHORDI, N.; CHUNG, D. J. H.; DORAN, M.; GESHNIZJANI, G. Cuscuton Cosmology: Dark Energy meets Modified Gravity. **Phys. Rev.**, D75, p. 123509, 2007. 147

AFSHORDI, N.; CHUNG, D. J. H.; GESHNIZJANI, G. Cuscuton: A Causal Field Theory with an Infinite Speed of Sound. **Phys. Rev.**, D75, p. 083513, 2007. 5, 140, 147

ALBRECHT, A. J.; MAGUEIJO, J. A time varying speed of light as a solution to cosmological puzzles. **Phys. Rev.**, D59, p. 043516, 1999. 6

ALBRECHT, A. J.; STEINHARDT, P. J. Cosmology for Grand Unified Theories with Radiatively Induced Symmetry Breaking. **Phys. Rev. Lett.**, v. 48, p. 1220–1223, 1982. 2

ALISHAHIHA, M.; SILVERSTEIN, E.; TONG, D. DBI in the sky. **Phys. Rev.**, D70, p. 123505, 2004. 4, 5

ALPHER, R. A.; BETHE, H.; GAMOW, G. The origin of chemical elements. **Phys. Rev.**, v. 73, p. 803–804, 1948. 1

ARKANI-HAMED, N.; CHENG, H.-C.; LUTY, M. A.; MUKOHYAMA, S. Ghost condensation and a consistent infrared modification of gravity. **JHEP**, v. 05, p. 074, 2004. 90

ARKANI-HAMED, N.; GEORGI, H.; SCHWARTZ, M. D. Effective field theory for massive gravitons and gravity in theory space. **Ann. Phys.**, v. 305, p. 96–118, 2003. 89

ARMENDARIZ-PICON, C. Near scale invariance with modified dispersion relations. **JCAP**, v. 0610, p. 010, 2006. 134

ARMENDARIZ-PICON, C.; DAMOUR, T.; MUKHANOV, V. F. k-Inflation. **Phys. Lett.**, B458, p. 209–218, 1999. 4, 134, 167

- ARMENDARIZ-PICON, C.; MUKHANOV, V. F.; STEINHARDT, P. J. Essentials of k-essence. **Phys. Rev.**, D63, p. 103510, 2001. 167
- AUBERT, A. Strong coupling in massive gravity by direct calculation. **Phys. Rev.**, D69, p. 087502, 2004. 89
- BABICHEV, E.; MUKHANOV, V.; VIKMAN, A. k-Essence, superluminal propagation, causality and emergent geometry. **JHEP**, v. 02, p. 101, 2008. 134, 168, 174, 175
- BABICHEV, E.; MUKHANOV, V. F.; VIKMAN, A. Escaping from the black hole? **JHEP**, v. 09, p. 061, 2006. 134
- BARDEEN, J. M. Gauge Invariant Cosmological Perturbations. **Phys. Rev.**, D22, p. 1882–1905, 1980. 33
- BASKARAN, D.; GRISHCHUK, L. P.; POLNAREV, A. G. Imprints of relic gravitational waves in cosmic microwave background radiation. **Phys. Rev.**, D74, p. 083008, 2006. xiii, 77, 80, 82, 83, 85, 86, 99
- BASSETT, B. A.; TSUJIKAWA, S.; WANDS, D. Inflation dynamics and reheating. **Rev. Mod. Phys.**, v. 78, p. 537–589, 2006. 2
- BAUMANN, D. TASI Lectures on Inflation. 2009. xiii, 9, 21, 39
- BEAN, R.; CHEN, X.; PEIRIS, H.; XU, J. Comparing Infrared Dirac-Born-Infeld Brane Inflation to Observations. **Phys. Rev.**, D77, p. 023527, 2008. 5
- BEAN, R.; CHUNG, D. J. H.; GESHNIZJANI, G. Reconstructing a general inflationary action. **Phys. Rev.**, D78, p. 023517, 2008. 136, 167, 170, 171, 174
- BEBRONNE, M. V. Theoretical and phenomenological aspects of theories with massive gravitons. 2009. 92
- BEBRONNE, M. V.; TINYAKOV, P. G. Massive gravity and structure formation. **Phys. Rev.**, D76, p. 084011, 2007. 94, 96, 97
- BERTONE, G.; HOOPER, D.; SILK, J. Particle dark matter: Evidence, candidates and constraints. **Phys. Rept.**, v. 405, p. 279–390, 2005. 2
- BESSADA, D.; KINNEY, W. H.; STOJKOVIC, D.; WANG, J. Tachyacoustic Cosmology: An Alternative to Inflation, arXiv:0908.3898 (*Accepted for publication in Phys. Rev. D*). 2009. 6, 133, 135, 136, 139, 140, 145, 176

_____. In preparation. 2010. [145](#), [151](#)

BESSADA, D.; KINNEY, W. H.; TZIRAKIS, K. Inflationary potentials in DBI models, arXiv: 0907.1311 . **JCAP**, v. 09, p. 031, 2009. [xv](#), [6](#), [114](#), [117](#), [118](#), [120](#), [123](#), [125](#), [126](#)

BESSADA, D.; MIRANDA, O. D. CMB anisotropies induced by tensor modes in Massive Gravity. **JCAP**, v. 08, p. 033, 2009. [4](#), [98](#), [99](#), [108](#), [109](#)

_____. CMB Polarization and Theories of Gravitation with Massive Gravitons. **Class. Quant. Grav.**, v. 26, p. 045005, 2009. [4](#), [95](#), [104](#), [105](#), [106](#), [107](#)

BLANCO-PILLADO, J. J. et al. Racetrack inflation. **JHEP**, v. 11, p. 063, 2004. [5](#)

BOCK, J. et al. Task Force on Cosmic Microwave Background Research. 2006. [85](#)

_____. The Experimental Probe of Inflationary Cosmology (EPIC): A Mission Concept Study for NASA's Einstein Inflation Probe. 2008.

BOND, J. R.; KOFMAN, L.; PROKUSHKIN, S.; VAUDREVANGE, P. M. Roulette inflation with Kaehler moduli and their axions. **Phys. Rev.**, D75, p. 123511, 2007. [5](#)

BORDE, A.; GUTH, A. H.; VILENKIN, A. Inflationary space-times are incomplete in past directions. **Phys. Rev. Lett.**, v. 90, p. 151301, 2003. [146](#)

BORN, M.; INFELD, L. Foundations of the new field theory. **Proc. Roy. Soc. Lond.**, A144, p. 425–451, 1934. [5](#)

BOSE, S.; GRISHCHUK, L. P. On the observational determination of squeezing in relic gravitational waves and primordial density perturbations. **Phys. Rev.**, D66, p. 043529, 2002. [72](#), [86](#)

BOULWARE, D. G.; DESER, S. Can gravitation have a finite range? **Phys. Rev.**, D6, p. 3368–3382, 1972. [89](#)

BRANDENBERGER, R. H. Alternatives to Cosmological Inflation. 2009. [6](#)

CABELLA, P.; KAMIONKOWSKI, M. Theory of cosmic microwave background polarization. 2004. [78](#), [79](#)

CEN, R. The Universe Was Reionized Twice. **Astrophys. J.**, v. 591, p. 12–37, 2003. [87](#)

- CHACKO, Z.; GRAESSER, M.; GROJEAN, C.; PILO, L. Massive gravity on a brane. **Phys. Rev.**, D70, p. 084028, 2004. 90
- CHANDRASEKHAR, S. **Radiative transfer**. New York: Dover, 1960, 1960. 69, 70, 71, 78, 79
- CHARMOUSIS, C.; GREGORY, R.; RUBAKOV, V. A. Wave function of the radion in a brane world. **Phys. Rev.**, D62, p. 067505, 2000. 89
- CHEN, X.; HUANG, M.-x.; KACHRU, S.; SHIU, G. Observational signatures and non-Gaussianities of general single field inflation. **JCAP**, v. 0701, p. 002, 2007. 5
- CHIMENTO, L. P.; LAZKOZ, R. Bridging geometries and potentials in DBI cosmologies. **Gen. Rel. Grav.**, v. 40, p. 2543–2555, 2008. 5, 135
- CLINE, J. M. String cosmology. 2006. 111
- COORAY, A.; SETO, N. Graviton mass from close white dwarf binaries detectable with LISA. **Phys. Rev.**, D69, p. 103502, 2004. 99
- COPELAND, E. J.; SAMI, M.; TSUJIKAWA, S. Dynamics of dark energy. **Int. J. Mod. Phys.**, D15, p. 1753–1936, 2006. 2
- DAM, H. van; VELTMAN, M. J. G. Massive and massless Yang-Mills and gravitational fields. **Nucl. Phys.**, B22, p. 397–411, 1970. 89, 91
- DEFFAYET, C.; DVALI, G. R.; GABADADZE, G.; VAINSHTEIN, A. I. Nonperturbative continuity in graviton mass versus perturbative discontinuity. **Phys. Rev.**, D65, p. 044026, 2002. 89
- DICKE, R. H.; PEEBLES, P. J. E.; ROLL, P. G.; WILKINSON, D. T. Cosmic Black-Body Radiation. **Astrophys. J.**, v. 142, p. 414–419, 1965. 1
- DIRAC, P. A. M. A Reformulation of the Born-Infeld Electrodynamics. **Royal Society of London Proceedings Series A**, v. 257, p. 32–43, aug. 1960. 5
- DODELSON, S. **Modern cosmology**. Amsterdam: Academic Press, 2003. xiii, 12, 69
- DODELSON, S.; KINNEY, W. H.; KOLB, E. W. Cosmic microwave background measurements can discriminate among inflation models. **Phys. Rev.**, D56, p. 3207–3215, 1997. 4, 50

DUBOVSKY, S. L. Phases of massive gravity. **JHEP**, v. 10, p. 076, 2004. [4](#), [90](#), [92](#), [97](#)

DUBOVSKY, S. L.; LIBANOV, M. V. On brane-induced gravity in warped backgrounds. **JHEP**, v. 11, p. 038, 2003. [90](#)

DUBOVSKY, S. L.; TINYAKOV, P. G.; TKACHEV, I. I. Cosmological attractors in massive gravity. **Phys. Rev.**, D72, p. 084011, 2005. [92](#), [94](#), [97](#)

DUTTA, S. A Classical Treatment of Island Cosmology. **Phys. Rev.**, D73, p. 063524, 2006. [6](#)

DUTTA, S.; VACHASPATI, T. Islands in the Lambda-sea. **Phys. Rev.**, D71, p. 083507, 2005. [6](#)

DVALI, G. R.; GABADADZE, G.; PORRATI, M. 4D gravity on a brane in 5D Minkowski space. **Phys. Lett.**, B485, p. 208–214, 2000. [89](#)

EARDLEY, D. M.; LEE, D. L.; LIGHTMAN, A. P. Gravitational-wave observations as a tool for testing relativistic gravity. **Phys. Rev.**, D8, p. 3308–3321, 1973. [159](#), [161](#)

EINASTO, J. Dark Matter. 2009. [2](#)

FAN, X.-H.; CARILLI, C. L.; KEATING, B. G. Observational constraints on Cosmic Reionization. **Ann. Rev. Astron. Astrophys.**, v. 44, p. 415–462, 2006. [87](#)

FIERZ, M.; PAULI, W. On relativistic wave equations for particles of arbitrary spin in an electromagnetic field. **Proc. Roy. Soc. Lond.**, A173, p. 211–232, 1939. [89](#)

FINN, L. S.; SUTTON, P. J. Bounding the mass of the graviton using binary pulsar observations. **Phys. Rev.**, D65, p. 044022, 2002. [4](#), [90](#), [99](#)

FREESE, K.; FRIEMAN, J. A.; OLINTO, A. V. Natural inflation with pseudo - Nambu-Goldstone bosons. **Phys. Rev. Lett.**, v. 65, p. 3233–3236, 1990. [51](#)

FRIEMAN, J.; TURNER, M.; HUTERER, D. Dark Energy and the Accelerating Universe. **Ann. Rev. Astron. Astrophys.**, v. 46, p. 385–432, 2008. [2](#)

- GABADADZE, G.; GRUZINOV, A. Graviton mass or cosmological constant? **Phys. Rev.**, D72, p. 124007, 2005. [90](#)
- GARRIGA, J.; MUKHANOV, V. F. Perturbations in k-inflation. **Phys. Lett.**, B458, p. 219–225, 1999. [134](#), [172](#), [173](#), [174](#)
- GIANNANTONIO, T.; CRITTENDEN, R. The effect of reionization on the CMB-density correlation. **Mon. Not. Roy. Astron. Soc.**, v. 381, p. 819, 2007. [87](#)
- GIOVANNINI, M. Theoretical tools for the physics of CMB anisotropies. **Int. J. Mod. Phys.**, D14, p. 363–510, 2005. [23](#), [75](#)
- GOLDHABER, A. S.; NIETO, M. M. Mass of the graviton. **Phys. Rev.**, D9, p. 1119–1121, 1974. [99](#)
- _____. Photon and Graviton Mass Limits. 2008. [99](#)
- GRATTON, S.; KHOURY, J.; STEINHARDT, P. J.; TUROK, N. Conditions for generating scale-invariant density perturbations. **Phys. Rev.**, D69, p. 103505, 2004. [6](#)
- GREGORY, R.; RUBAKOV, V. A.; SIBIRYAKOV, S. M. Opening up extra dimensions at ultra-large scales. **Phys. Rev. Lett.**, v. 84, p. 5928–5931, 2000. [89](#)
- GRISHCHUK, L. P. Amplification of gravitational waves in an isotropic universe. **Sov. Phys. JETP**, v. 40, p. 409–415, 1975. [57](#)
- GUTH, A. H. The Inflationary Universe: A Possible Solution to the Horizon and Flatness Problems. **Phys. Rev.**, D23, p. 347–356, 1981. [2](#)
- HU, W.; SUGIYAMA, N. Anisotropies in the Cosmic Microwave Background: An Analytic Approach. **Astrophys. J.**, v. 444, p. 489–506, 1995. [87](#)
- IOCCO, F.; MANGANO, G.; MIELE, G.; PISANTI, O.; SERPICO, P. D. Primordial Nucleosynthesis: from precision cosmology to fundamental physics. **Phys. Rept.**, v. 472, p. 1–76, 2009. [1](#)
- KACHRU, S. et al. Towards inflation in string theory. **JCAP**, v. 0310, p. 013, 2003. [5](#)
- KAMIONKOWSKI, M.; KOSOWSKY, A.; STEBBINS, A. Statistics of Cosmic Microwave Background Polarization. **Phys. Rev.**, D55, p. 7368–7388, 1997. [78](#), [79](#), [80](#)

KHOURY, J.; PIAZZA, F. Rapidly-Varying Speed of Sound, Scale Invariance and Non- Gaussian Signatures. **JCAP**, v. 0907, p. 026, 2009. 6

KINNEY, W. H. Inflation: Flow, fixed points and observables to arbitrary order in slow roll. **Phys. Rev.**, D66, p. 083508, 2002. 49, 60, 171

_____. Cosmology, inflation, and the physics of nothing. 2003. 50

_____. Horizon crossing and inflation with large eta. **Phys. Rev.**, D72, p. 023515, 2005. 60

_____. TASI Lectures on Inflation. 2009. 9, 39, 45

KINNEY, W. H.; KOLB, E. W.; MELCHIORRI, A.; RIOTTO, A. Latest inflation model constraints from cosmic microwave background measurements. **Phys. Rev.**, D78, p. 087302, 2008. 7, 131, 132

KINNEY, W. H.; MAHANTHAPPA, K. T. Inflation at Low Scales: General Analysis and a Detailed Model. **Phys. Rev.**, D53, p. 5455–5467, 1996. 51

KINNEY, W. H.; TZIRAKIS, K. Quantum modes in DBI inflation: exact solutions and constraints from vacuum selection. **Phys. Rev.**, D77, p. 103517, 2008. 5, 116, 121, 135, 142, 143, 144, 150

KLEBANOV, I. R.; STRASSLER, M. J. Supergravity and a confining gauge theory: Duality cascades and chiSB-resolution of naked singularities. **JHEP**, v. 08, p. 052, 2000. 111

KODAMA, H.; SASAKI, M. Cosmological Perturbation Theory. **Prog. Theor. Phys. Suppl.**, v. 78, p. 1–166, 1984. 23

KOGAN, I. I.; MOUSLOPOULOS, S.; PAPAZOGLU, A.; ROSS, G. G.; SANTIAGO, J. A three three-brane universe: New phenomenology for the new millennium? **Nucl. Phys.**, B584, p. 313–328, 2000. 89

KOMATSU, E. et al. Five-Year Wilkinson Microwave Anisotropy Probe (WMAP) Observations:Cosmological Interpretation. **Astrophys. J. Suppl.**, v. 180, p. 330–376, 2009. 2, 19, 72, 87, 131, 145

LEE, K.-G. Constraining Extended Reionization Models Through Arcminute-Scale CMB Measurements. 2009. 87

- LIDDLE, A. R.; LEACH, S. M. How long before the end of inflation were observable perturbations produced? **Phys. Rev.**, D68, p. 103503, 2003. 45
- LINDE, A. D. A New Inflationary Universe Scenario: A Possible Solution of the Horizon, Flatness, Homogeneity, Isotropy and Primordial Monopole Problems. **Phys. Lett.**, B108, p. 389–393, 1982. 2
- _____. Axions in inflationary cosmology. **Phys. Lett.**, B259, p. 38–47, 1991. 52, 125
- _____. Hybrid inflation. **Phys. Rev.**, D49, p. 748–754, 1994. 52, 125
- LOVERDE, M.; MILLER, A.; SHANDERA, S.; VERDE, L. Effects of Scale-Dependent Non-Gaussianity on Cosmological Structures. **JCAP**, v. 0804, p. 014, 2008. 5
- LUCCHIN, F.; MATARRESE, S. Power Law Inflation. **Phys. Rev.**, D32, p. 1316, 1985. 53
- LUTY, M. A.; PORRATI, M.; RATTAZZI, R. Strong interactions and stability in the DGP model. **JHEP**, v. 09, p. 029, 2003. 90
- MAGUEIJO, J. Speedy sound and cosmic structure. **Phys. Rev. Lett.**, v. 100, p. 231302, 2008. 134
- _____. Bimetric varying speed of light theories and primordial fluctuations. **Phys. Rev.**, D79, p. 043525, 2009. 134, 142
- MCALLISTER, L.; SILVERSTEIN, E. String Cosmology: A Review. **Gen. Rel. Grav.**, v. 40, p. 565–605, 2008. 5, 111
- MUKHANOV, V. **Physical Foundations of Cosmology**. Cambridge: Cambridge University Press, 2005. 9, 13, 23, 39
- MUKHANOV, V. F.; FELDMAN, H. A.; BRANDENBERGER, R. H. Theory of cosmological perturbations. **Phys. Rept.**, v. 215, p. 203–333, 1992. 23, 24
- MUKHANOV, V. F.; VIKMAN, A. Enhancing the tensor-to-scalar ratio in simple inflation. **JCAP**, v. 0602, p. 004, 2006. 147
- MUSLIMOV, A. G. ON THE SCALAR FIELD DYNAMICS IN A SPATIALLY FLAT FRIEDMAN UNIVERSE. **Class. Quant. Grav.**, v. 7, p. 231–237, 1990. 46

- NEWMAN, E.; PENROSE, R. An Approach to gravitational radiation by a method of spin coefficients. **J. Math. Phys.**, v. 3, p. 566–578, 1962. [159](#)
- NOVELLO, M.; BERGLIAFFA, S. E. P. Bouncing Cosmologies. **Phys. Rept.**, v. 463, p. 127–213, 2008. [6](#), [39](#)
- PEEBLES, P. J. E. Recombination of the Primeval Plasma. **Astrophys. J.**, v. 153, p. 1, 1968. [1](#)
- _____. **Principles of physical cosmology**. Princeton, NJ: Princeton University Press, 1993. [86](#)
- PEIRIS, H. V.; BAUMANN, D.; FRIEDMAN, B.; COORAY, A. Phenomenology of D-Brane Inflation with General Speed of Sound. **Phys. Rev.**, D76, p. 103517, 2007. [112](#), [129](#)
- PETER, P.; PINHO, E. J. C.; PINTO-NETO, N. A non inflationary model with scale invariant cosmological perturbations. **Phys. Rev.**, D75, p. 023516, 2007. [6](#)
- PIAO, Y.-S. Seeding of Primordial Perturbations During a Decelerated Expansion. **Phys. Rev.**, D75, p. 063517, 2007. [134](#)
- _____. On Primordial Density Perturbation and Decaying Speed of Sound. **Phys. Rev.**, D79, p. 067301, 2009. [134](#), [140](#)
- _____. Primordial Perturbation in Horava-Lifshitz Cosmology. **Phys. Lett.**, B681, p. 1–4, 2009. [147](#)
- PILO, L.; RATTAZZI, R.; ZAFFARONI, A. The fate of the radion in models with metastable graviton. **JHEP**, v. 07, p. 056, 2000. [90](#)
- POLNAREV, A. G. Polarization and Anisotropy Induced in the Microwave Background by Cosmological Gravitational Waves. **Soviet Astronomy**, v. 29, p. 607–+, dec. 1985. [69](#), [71](#), [75](#), [77](#)
- PRITCHARD, J. R.; KAMIONKOWSKI, M. Cosmic microwave background fluctuations from gravitational waves: An analytic approach. **Annals Phys.**, v. 318, p. 2–36, 2005. [85](#)
- RIOTTO, A. Inflation and the theory of cosmological perturbations. 2002. [39](#), [40](#), [42](#)

- RUBAKOV, V. A. Strong coupling in brane-induced gravity in five dimensions. 2003. [90](#)
- _____. Lorentz-violating graviton masses: Getting around ghosts, low strong coupling scale and VDVZ discontinuity. 2004. [4](#), [90](#), [94](#), [97](#)
- RUBAKOV, V. A.; TINYAKOV, P. G. Infrared-modified gravities and massive gravitons. **Phys. Usp.**, v. 51, p. 759–792, 2008. [92](#)
- SALOPEK, D. S.; BOND, J. R. Nonlinear evolution of long wavelength metric fluctuations in inflationary models. **Phys. Rev.**, D42, p. 3936–3962, 1990. [46](#)
- SATHYAPRAKASH, B. S.; SCHUTZ, B. F. Physics, Astrophysics and Cosmology with Gravitational Waves. **Living Rev. Rel.**, v. 12, p. 2, 2009. [7](#)
- SILVERSTEIN, E.; TONG, D. Scalar Speed Limits and Cosmology: Acceleration from D- cceleration. **Phys. Rev.**, D70, p. 103505, 2004. [4](#), [134](#)
- SPALINSKI, M. A consistency relation for power law inflation in DBI models. **Phys. Lett.**, B650, p. 313–316, 2007. [5](#)
- _____. On the Slow Roll Expansion for Brane Inflation. **JCAP**, v. 0704, p. 018, 2007. [113](#)
- _____. Inflation in DBI models with constant gamma. **JCAP**, v. 0804, p. 002, 2008. [5](#), [114](#), [121](#), [150](#)
- STARKMAN, G. D.; STOJKOVIC, D.; TRODDEN, M. Homogeneity, flatness and 'large' extra dimensions. **Phys. Rev. Lett.**, v. 87, p. 231303, 2001. [6](#)
- _____. Large extra dimensions and cosmological problems. **Phys. Rev.**, D63, p. 103511, 2001. [6](#)
- TALMADGE, C.; BERTHIAS, J. P.; HELLINGS, R. W.; STANDISH, E. M. Model Independent Constraints on possible Modifications of Newtonian Gravity. **Phys. Rev. Lett.**, v. 61, p. 1159–1162, 1988. [99](#)
- TAOSO, M.; BERTONE, G.; MASIERO, A. Dark Matter Candidates: A Ten-Point Test. **JCAP**, v. 0803, p. 022, 2008. [2](#)
- TZIRAKIS, K.; KINNEY, W. H. Non-canonical generalizations of slow-roll inflation models. **JCAP**, v. 0901, p. 028, 2009. [5](#), [121](#), [130](#), [131](#), [150](#)

VACHASPATI, T.; TRODDEN, M. Causality and cosmic inflation. **Phys. Rev.**, D61, p. 023502, 1999. 146

VAINSHTEIN, A. I. To the problem of nonvanishing gravitation mass. **Phys. Lett.**, B39, p. 393–394, 1972. 89

WALD, R. M. **General relativity**. Chicago: University of Chicago Press, 1984. 175

WEINBERG, S. **Gravitation and Cosmology: Principles and Applications of the General Theory of Relativity**. New York: Wiley-VCH, 1972. 9, 30

_____. **The Quantum Theory of Fields**. Cambridge: Cambridge University Press, 1995. 167, 168

_____. **Cosmology**. Oxford: Oxford University Press, 2008. 9, 23, 39

WILL, C. M. The confrontation between general relativity and experiment. **Living Rev. Rel.**, v. 9, p. 3, 2005. xiv, 162

XIA, T. Y.; ZHANG, Y. Approximate Analytic Spectra of Reionized CMB Anisotropies and Polarization generated by Relic Gravitational Waves. **Phys. Rev.**, D79, p. 083002, 2009. 85, 87

ZAKHAROV, V. I. Linearized gravitation theory and the graviton mass. **JETP Lett.**, v. 12, p. 312, 1970. 89

ZALDARRIAGA, M.; SELJAK, U. An All-Sky Analysis of Polarization in the Microwave Background. **Phys. Rev.**, D55, p. 1830–1840, 1997. 81

